International Journal of Multidisciplinary Studies and Innovative Technologies

IJMSIT

Year : 2022 | Volume : 6 | Issue : 1

SET TEKNOLOJİ

e-ISSN 2602-4888

International Journal of Multidisciplinary Studies and Innovative Technologies

Year :2022 **Volume : 6** **Issue : 1**

International Journal of Multidisciplinary Studies and Innovative Technologies is online, open access, double blind peer-reviewed, international research journal. Language of the journal is English and Turkish. Authors should only submit original work, which has not been previously published and is not currently considered for publication elsewhere.

An expert editor is assigned to a submitted manuscript. The editor appoints reviewers to evaluate the manuscript. As a result of the evaluation of the manuscript by reviewers, the editor makes a decision about the acceptance, modification or rejection of the manuscript.

IJMSIT is indexed/abstracted in ASOS Index, Google Scholar, Index Copernicus, ResearchBib, DRJI, Eurasian Scientific Journal Index and Sindex.

International Journal of Multidisciplinary Studies and Innovative Technologies

Year: 2022, Volume: 6, Issue: 1

CONTENTS

International Journal of Multidisciplinary Studies and Innovative Technologies

e-ISSN: 2602-4888
dergipark.org.tr/en/pub/ijmsit
Research Article

2022, 6 (1), 01-10
DOI: 10.36287/ijmsit.6.1.1
Received: January 9, 2022; Accepted: May 12, 2022

Display of Zoning Diameter According to the Distance Approach on Separate Organizatiom Zoning Islands

Selim Taşkaya[1*]

[1*] *Artvin Vocational School Department of Architecture and Urban Planning, Artvin Çoruh University*
(e-mail: selim_taskaya@artvin.edu.tr:) (ORCID: 0000-0002-4290-3684)

Abstract – In our country, activities are carried out under the title of zoning studies in order to make an area suitable for holistic living standards. There is a hierarchy in the formation of zoning plans from the upper scale of the country development plans to the lower scale, which are the implementation zoning plans. Along with this hierarchy, in the 1/1000 zoning plans, especially the people living in a region, housing, shopping, social activity, etc. zoning islands are determined within the zoning boundaries determined to meet the needs. Zoning islands can have different building regulations, precedent or building heights. There are possible building regulations within the zoning boundaries, where there may be different types of sitting areas, such as split, block and adjacent basis. On the other hand, the form of a separate zoning island is that the garden-looking building session is given in the middle without being attached to a depth or to the façade. The process of granting construction permits to the existing zoning parcels in the zoning islands, whose identities are determined by this building regulation, is the zoning scale. Zoning diameters, planned areas are given within the framework of type zoning regulations and plan notes. The zoning diameter is given according to the precedent, height and building order of the island. Distance method, on the other hand, is the process of creating the right residential area with the drawing rules of convex shapes, such as square or rectangular, according to the geometric condition of the parcel, in order to be able to give construction permits to the clean zoning parcels in the relevant zoning islands. In our study, it has been tried to show how the settlement areas at the base can be given, which building order, which precedent and how to apply the process to the convex parcels with the distance approach.

Keywords *– Separate Order Reconstruction Island, Distance Approach Method, Zoning Diameter*

Citation: Taşkaya, S. (2022). Display Of Zoning Diameter According To The Distance Approach On Separate Organizatiom Zoning Islands. International Journal of Multidisciplinary Studies and Innovative Technologies, 6(1): 1-10

I. INTRODUCTION

The Zoning Law, which is directly related to fundamental rights and freedoms, brings regulations in areas that are closely related to the society such as the right to property, the right to life and the freedom of settlement [1]. The first of these is the Zoning Law No. 3194. In article 2 of the Zoning Law, the scope of the law is mentioned and it is stated that all buildings to be built within or outside the borders of the municipality and the adjacent area are subject to this law. The Municipal Law No. 5393 covers municipalities according to art.1 and art.2, and regulates their working procedures and principles, duties and authorities [2]. Although the main purpose of planning is livable cities and therefore public benefit, the regulations to be made create some obligations and obligations not only for the institutions authorized to make this regulation, but also for the individuals [4]. Planning, as a concept, is a way of thinking that is thought ahead from a certain moment; It is the sum of the studies aimed at examining the possibilities, possibilities, comparison activities, and establishing regular relations between individuals and their communities and their environment [5]. It is aimed to implement the zoning and urban planning activities in line with the principles of honesty and compliance in the light of laws and regulations by transforming them into implementation plans of 1000 by local governments [6]. Rapid urbanization has brought about unplanned development. This process has revealed an urban texture where social and technical equipment areas are insufficient, transportation planning cannot be done, and industrial facilities are intertwined with living and resting areas [7].

II. MATERIALS AND METHOD

In the material and method section, vector space, affine space, Euclidean space, Euclidean frame, Euclidean coordinate system, line and plane equations, two lines relative to each other, two planes relative to each other, lines and planes relative to each other, basic principles about line and plane. concepts are given [8].

Description 2.1. (Vector Space): Let V be a non-empty set, on which we will call the vector addition, and the product of the scalar (real numbers) is defined. Symbolically, vector addition and scalar multiplication operations [8].

Let x y V be defined as x y V ∂ ∈ for ∈ and rx V∈ for r R x V ∈ ∈ ; that is, let the set V be closed for vector addition and scalar multiplication. If the following conditions are met, the set V is called a vector space on R (set of real numbers) [9]. That is, by adding end-to-end from the length vector, it can be closed, parallel, perpendicular, etc. truth will be obtained.

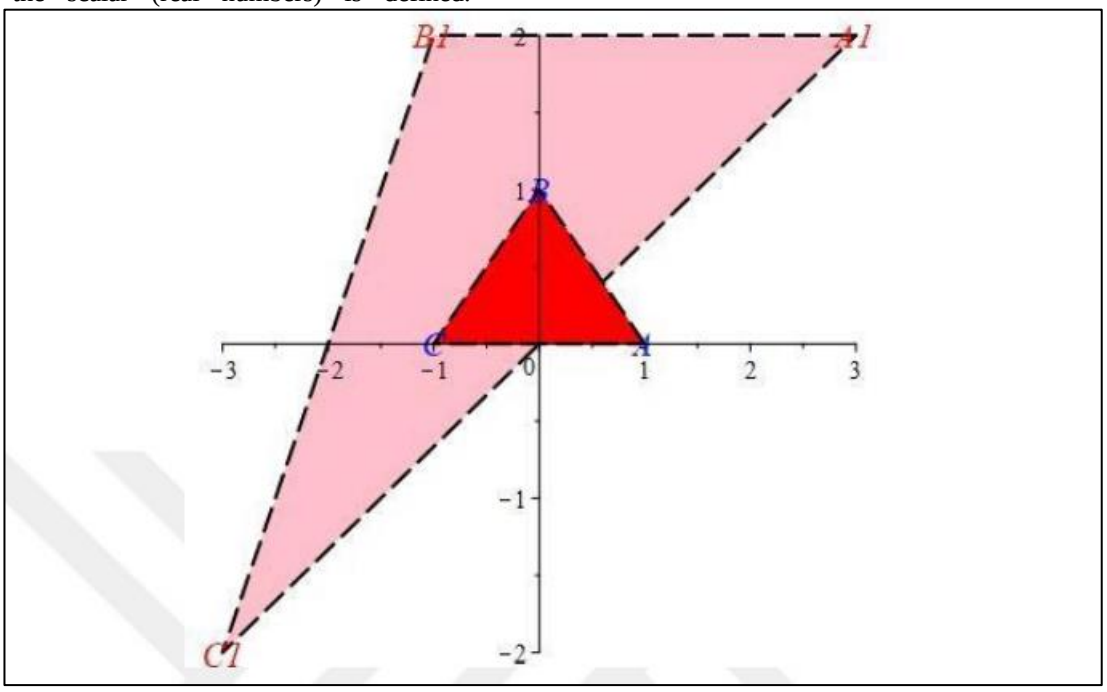

Figure 1. Area Scaling [8].

In Figure 1, when shown graphically, triangle, square, rectangle etc. The method that occurs with the formation of convex fields is the length method in the form of a length vector.

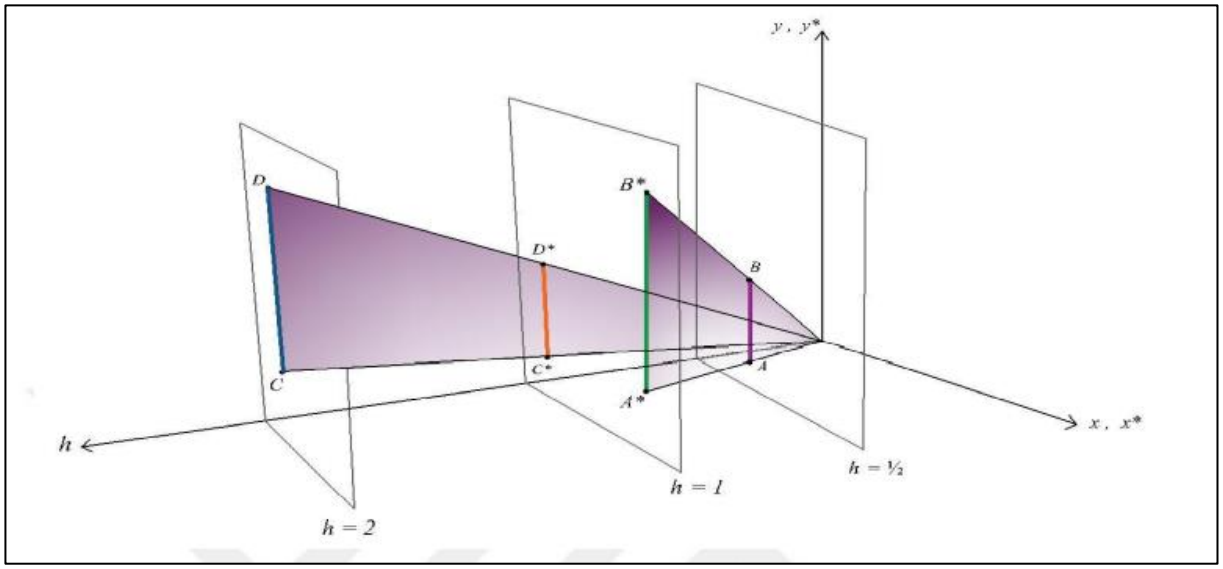

Figure 2. A geometric interpretation of general scaling [8].

Homogeneous coordinates provide a convenient and efficient technique for mapping a set of points from one coordinate system to a corresponding set in an alternate coordinate system.Frequently, an infinite range in one coordinate system matches a finite range in an alternative coordinate system [8]. Parallel lines may not match parallel lines unless pairings are carefully chosen. However, intersection points can be mapped to intersection points. This property is used to specify the homogeneous coordinate representation of a point at

infinity[3],[15],[10].

III. FINDINGS AND DISCUSSION

While making a planning, the most important parameters are the creation of zoning islands with a building order suitable for the regions where the population is dense [12]. In general, the legends that we call island identities are adjacent at the points where the center is located, discrete in the areas to be opened for new settlement and based on a block structure [13]. In addition to these islands that will meet the need for shopping, the building is added to the islands such as religious facilities, social cultural and green areas, and a plan design is made [14]. The arrangement of the parcels that will coincide with these zoning islands is done in line with the provisions of Articles 15, 16 and 18 in the current law, and in line with the plan notes that local governments will receive from their councils [11]. The first action of the residential areas of the buildings is as a result of the display of the zoning status.

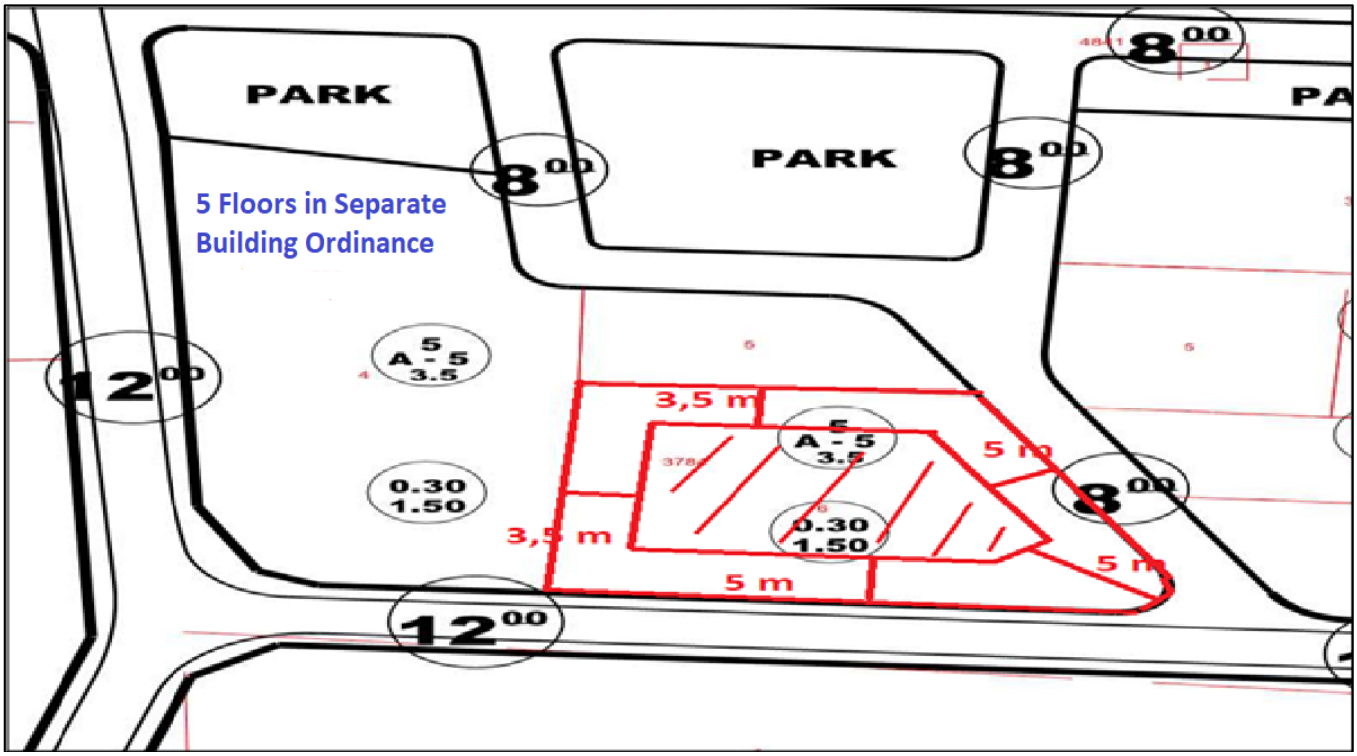

Figure 3. Split Ordinance 5 Floor Zoning Diameter View

In Figure 3., while the zoning diameter is given to the zoning parcel, which is in the form of a separate zoning island, the planned areas will be increased by 5 meters in front drawing distance, 3 meters in places where the distance to the side garden is up to 4 floors, and 0.5 meters per floor after 4 floors. will be given. Since it is a 5-storey zoning, the building stock is given in the middle by taking 3.5 meters from the neighboring parcels facing the road. Since the floor area utilization coefficient is 0.30, the building floor area calculation will be found by multiplying the parcel with this ratio, and the total equivalent will be calculated as 5 floors. Let x y V be defined as x y V $\partial \in$ for $\in$ and rx V$\in$ for r R x V $\in \in$; that is, let the set V be closed for vector addition and scalar multiplication [9]. When the parcel is considered as a universal cluster, such as nested clustering in a parcel with 5 floors, the building's sitting on a parcel with a discrete structure is considered as a subset. After the tensile measurements, it coincides with the same logic, as a mathematical plane, with its narrowing from the origin.

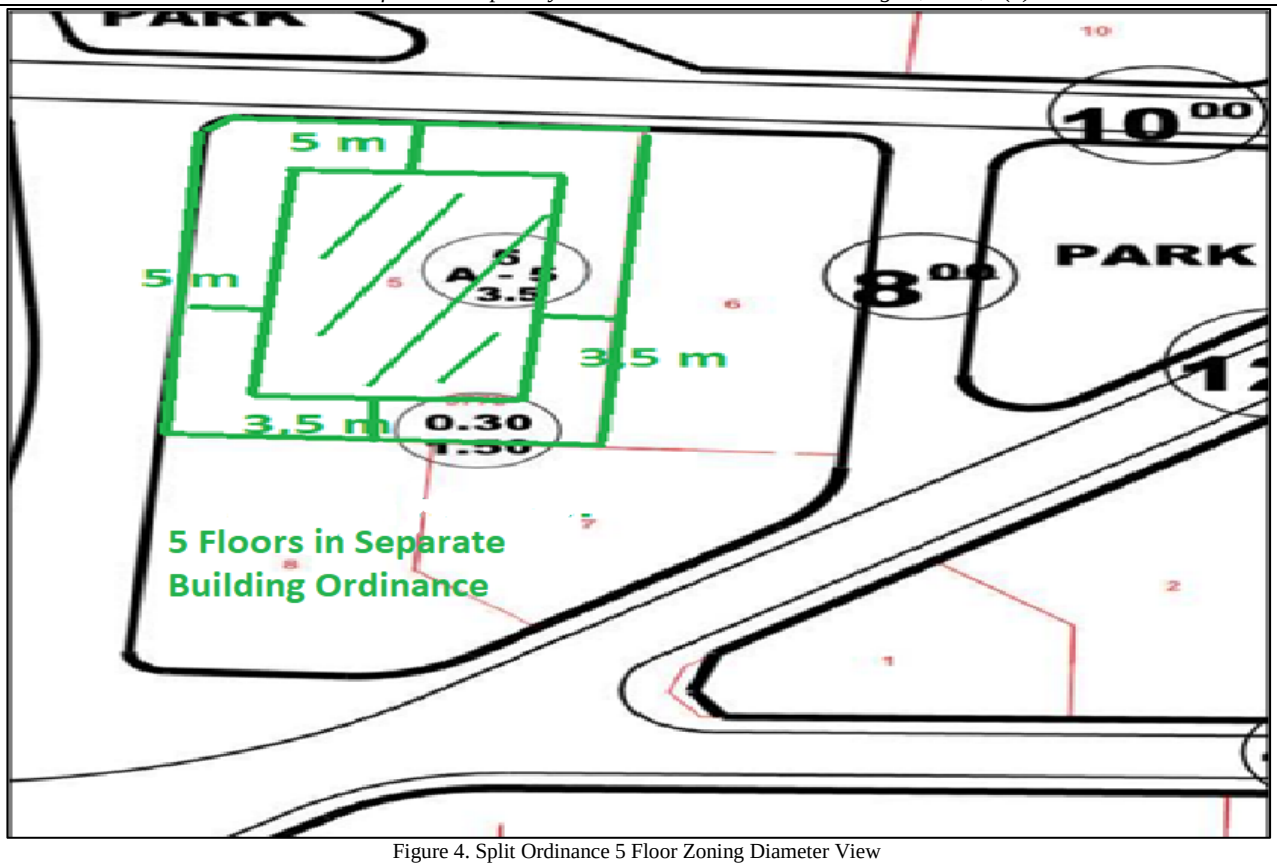

Figure 4. Split Ordinance 5 Floor Zoning Diameter View

In Figure 4., while the zoning diameter is given in a zoning parcel with a separate layout up to 5 floors, the front drawing distance will be 5 meters and the adjacent parcel sides facing the road will be side gardens, so the building residence area will be given by drawing 3.5. Let x y V be defined as x y V ∂ ∈ for ∈ and rx V∈ for r R x V ∈ ∈ ; that is, let the set V be closed for vector addition and scalar multiplication [9]. When the parcel is considered as a universal cluster, such as nested clustering in a parcel with 5 floors, the building's sitting on a parcel with a discrete structure is considered as a subset. After the tensile measurements, it coincides with the same logic, as a mathematical plane, with its narrowing from the origin.

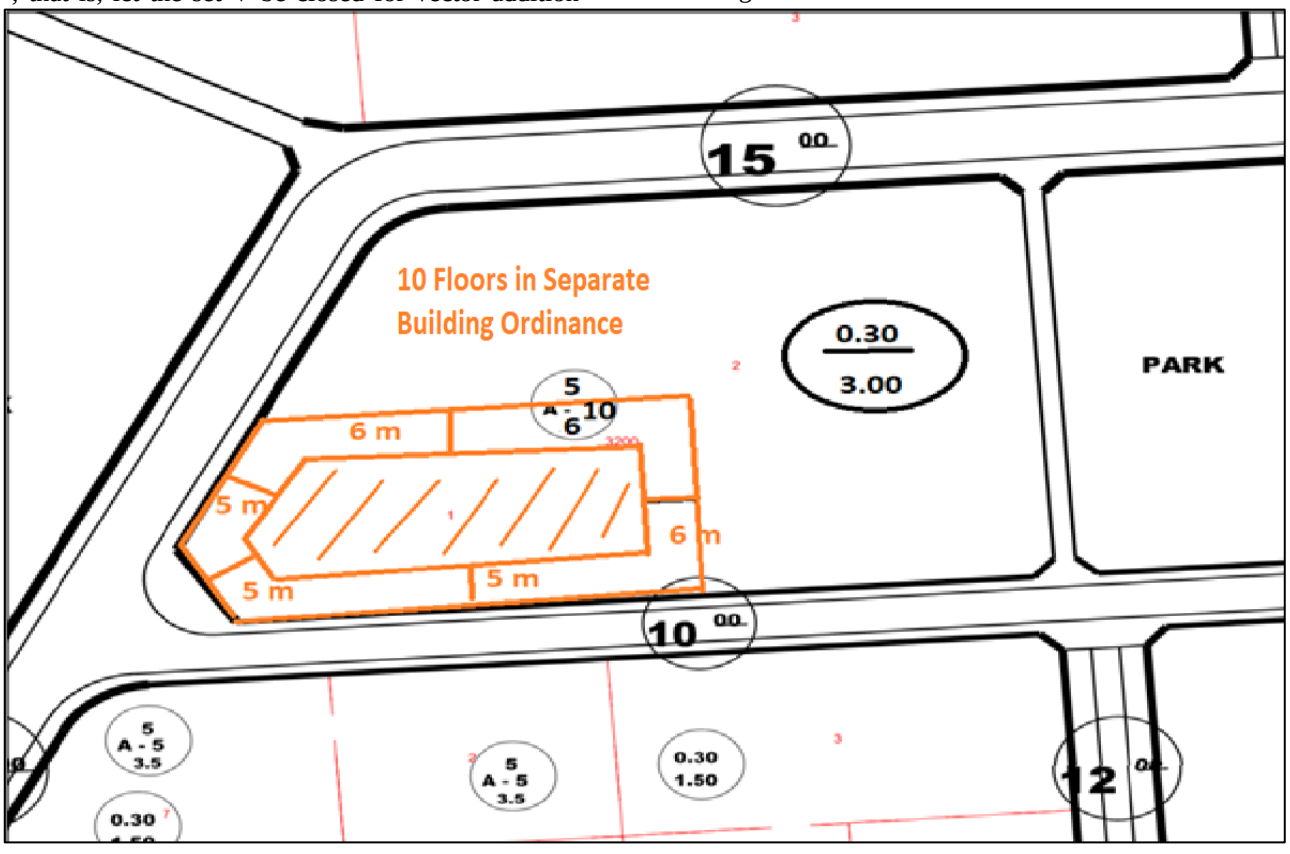

Figure 5. Split Ordinance 10 Floor Zoning Diameter View

In Figure 5, the zoning diameter, front drawing distances of 5 meters and side garden distances of 6 meters are given in the development parcel located on a zoning island in a separate building order. The amount of TKS is shown as 0.30, and the amount of KAKS is shown as 3.00 by multiplying TAKS by 10 times as a total precedent. Let x y V be defined as x y V ∂ ∈ for ∈ and rx V∈ for r R x V ∈ ∈ ; that is, let the set V be closed for vector addition and scalar multiplication [9]. When the parcel is considered as a universal cluster, such as nested clustering in a parcel with 5 floors, the building's sitting on a parcel with a discrete structure is considered as a subset. After the tensile measurements, it coincides with the same logic, as a mathematical plane, with its narrowing from the origin.

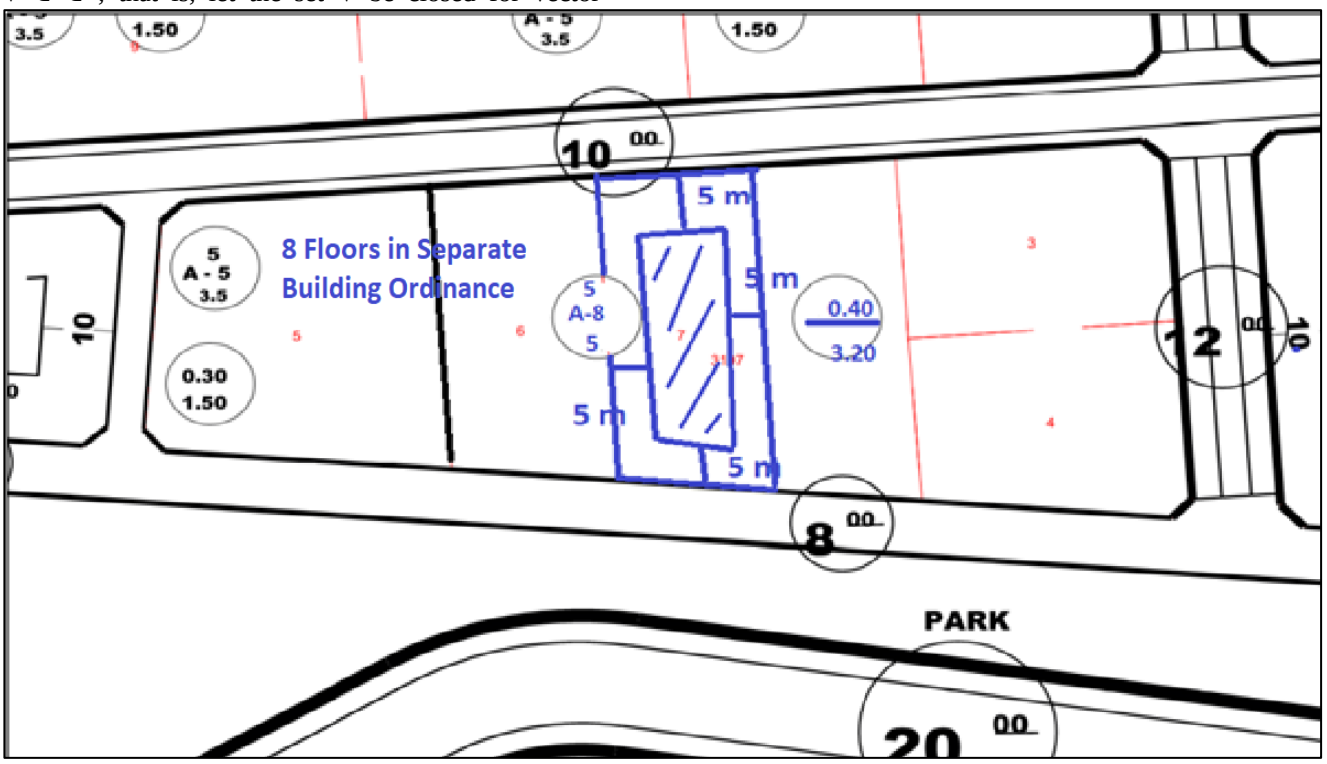

Figure 6. Split Ordinance 8 Floor Zoning Diameter View

In Figure 6., the zoning diameter is given in the middle, since it can be built 5 meters each in the north and south directions, and 8 floors from the side gardens, in a zoning parcel with permission up to 8 floors, in a separate building order, since the parcel can be built in the direction of the maximum precedent. Let x y V be defined as x y V ∂ ∈ for ∈ and rx V∈ for r R x V ∈ ∈ ; that is, let the set V be closed for vector addition and scalar multiplication [9]. When the parcel is considered as a universal cluster, such as nested clustering in a parcel with 5 floors, the building's sitting on a parcel with a discrete structure is considered as a subset. After the tensile measurements, it coincides with the same logic, as a mathematical plane, with its narrowing from the origin.

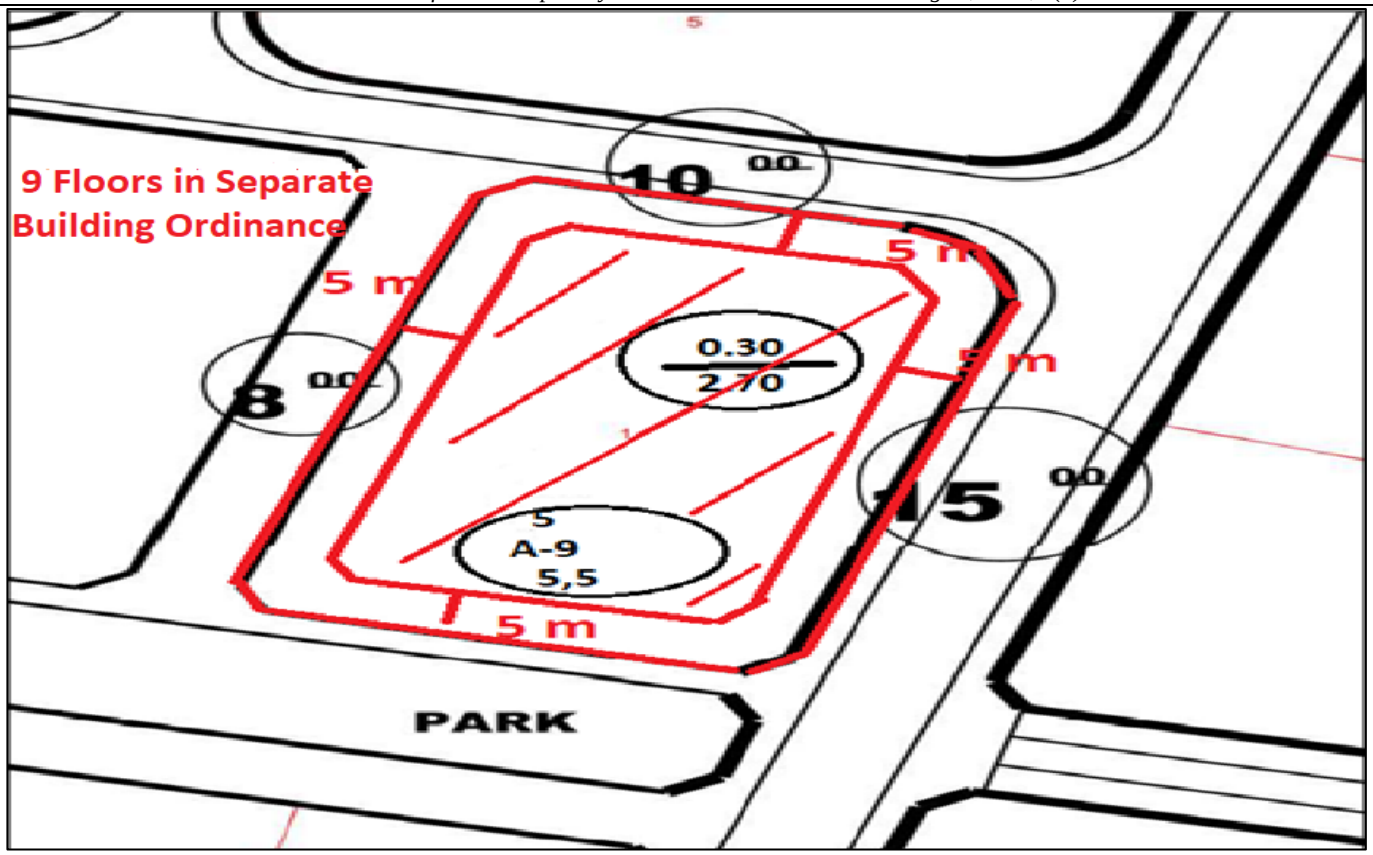

Figure 7. Split Ordinance 9 Floor Zoning Diameter View

In Figure 7., since one side of the parcel will face the road, only the front drawing garden distance will be given and the zoning diameter will be drawn, especially in the zoning islands that have been recorded in the legend as a single zoning. In this zoning plot, 5 meters were drawn each. We see that the floor area of the parcel with permission up to 9 floors is 0.30 and the total equivalent is 2.70 in the separate order. Let x y V be defined as x y V ∂ ∈ for ∈ and rx V∈ for r R x V ∈ ∈ ; that is, let the set V be closed for vector addition and scalar multiplication [9]. When the parcel is considered as a universal cluster, such as nested clustering in a parcel with 9 floors, the building's sitting on a parcel with a discrete structure is considered as a subset. After the tensile measurements, it coincides with the same logic, as a mathematical plane, with its narrowing from the origin.

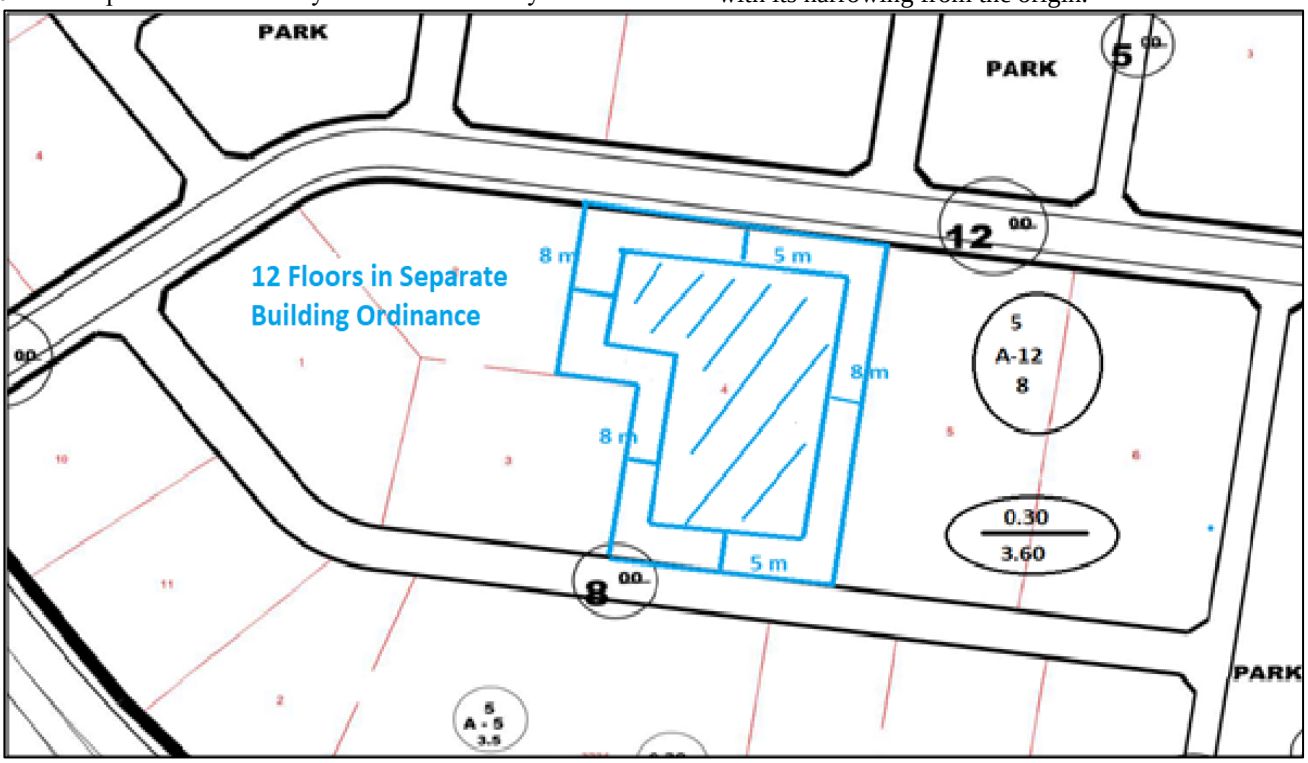

Figure 8. Split Ordinance 12 Floor Zoning Diameter View

In Figure 8., since the parcel on the zoning island, which is in the order of a allowable discrete building up to 12 floors, is a parcel with north and south facades, the front drawing distances are 5 meters, and the side garden distances are 12 floors, and the building residence area is determined by giving 8 meters. It is given that there is a total precedent for 12 floors as E=3.60, that is, it will be understood that title deed area x precedent = total building stock. Let x y V be defined as x y V ∂ ∈ for ∈ and rx V∈ for r R x V ∈ ∈ ; that is, let the set V be closed for vector addition and scalar multiplication [9].When the parcel is considered as a universal cluster, such as nested clustering in a parcel with 12 floors, the building's sitting on a parcel with a discrete structure is considered as a subset. After the tensile measurements, it coincides with the same logic, as a mathematical plane, with its narrowing from the origin.

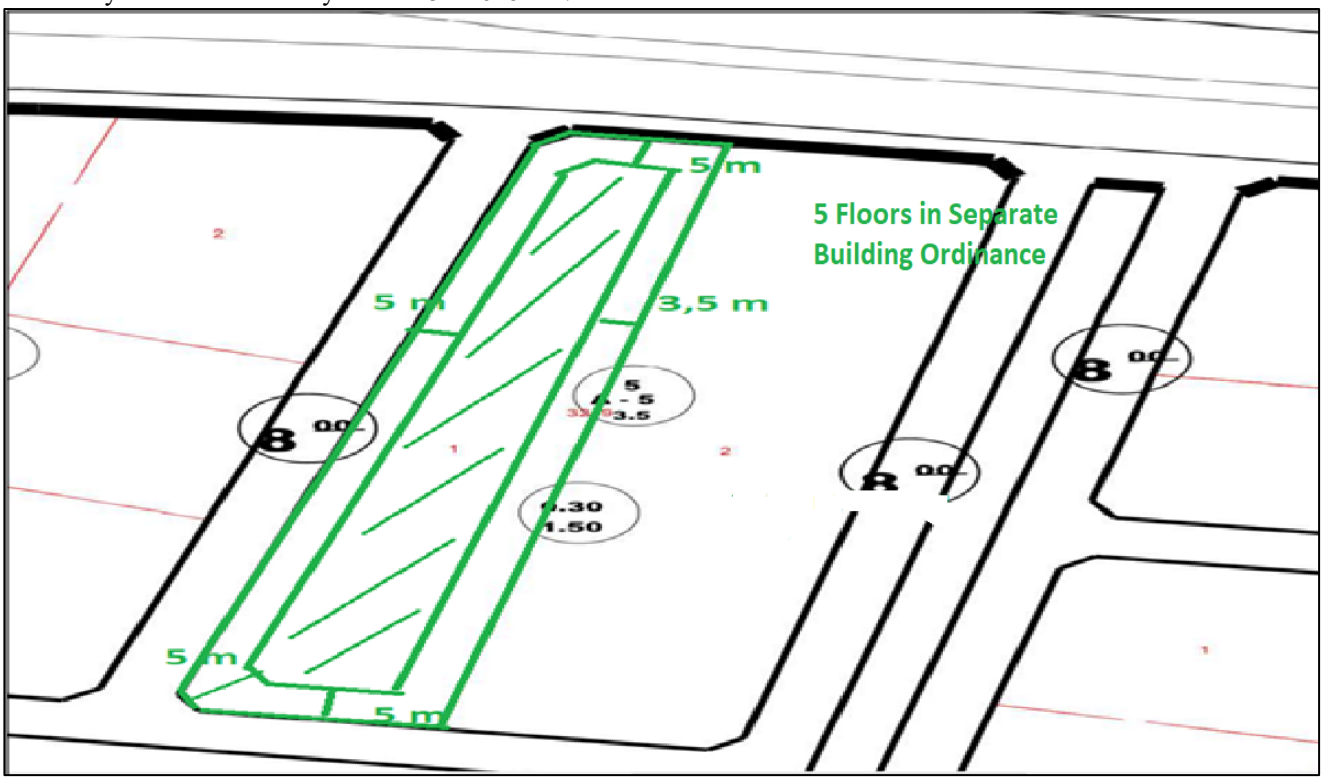

Figure 9. Split Ordinance 5 Floor Zoning Diameter View

In Figure 9., there are 2 zoning parcels on a zoning island with a separate order up to 5 floors. Since 3 sides of the parcel in the west direction face the road, front drawings were made for 5 meters each, and the side garden distance was drawn by 3.5 meters to determine the building's residence area. Let x y V be defined as x y V ∂ ∈ for ∈ and rx V∈ for r R x V ∈ ∈ ; that is, let the set V be closed for vector addition and scalar multiplication [9].When the parcel is considered as a universal cluster, such as nested clustering in a parcel with 5 floors, the building's sitting on a parcel with a discrete structure is considered as a subset. After the tensile measurements, it coincides with the same logic, as a mathematical plane, with its narrowing from the origin.

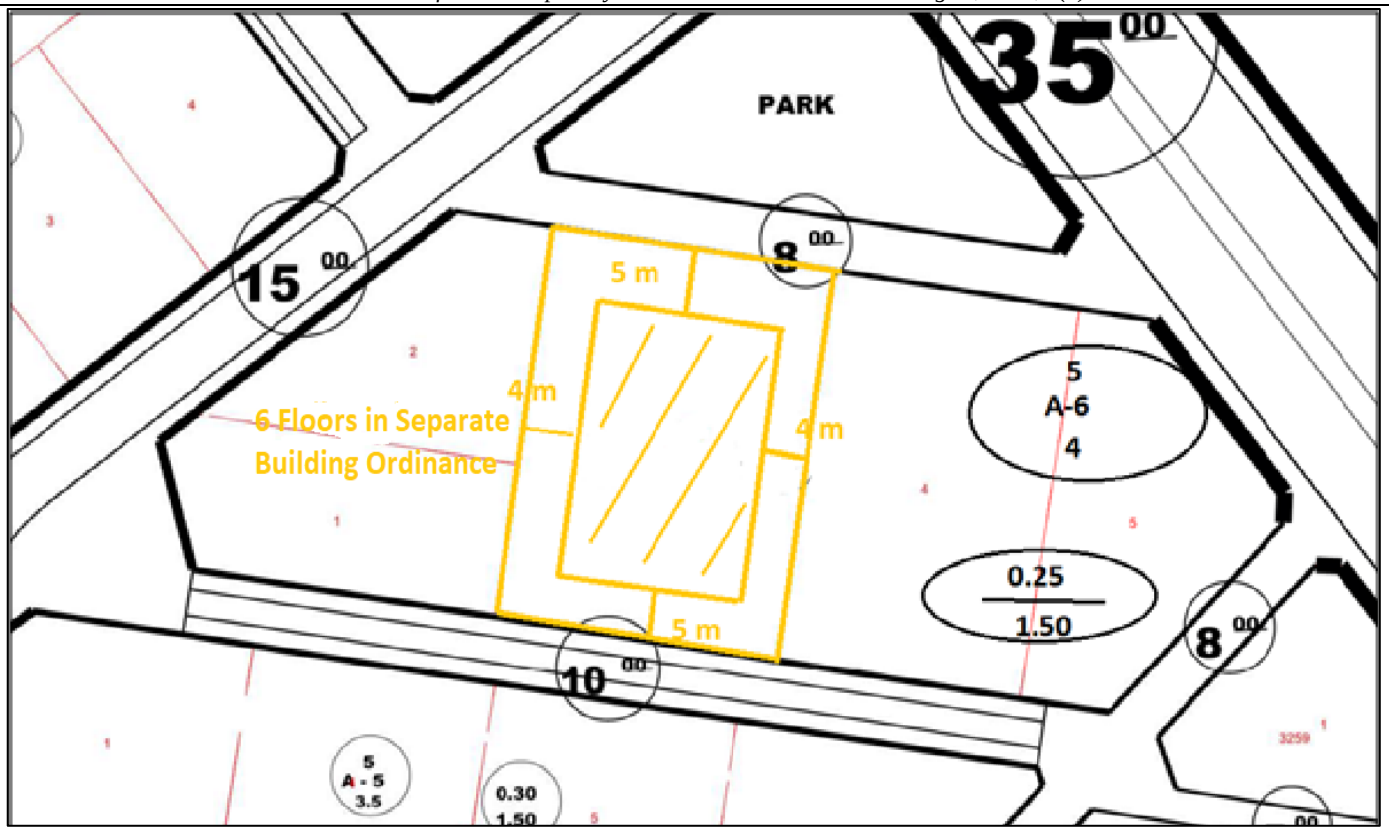

Figure 10. Split Ordinance 6 Floor Zoning Diameter View

In Figure 10., since the relevant parcel is oriented to the north and south, the front draws are given by 5 meters, and the side garden distances are given by drawing 4 meters, since it is 6 floors. Let x y V be defined as x y V ∂ ∈ for ∈ and rx V∈ for r R x V ∈ ∈ ; that is, let the set V be closed for vector addition and scalar multiplication [9].

.

When the parcel is considered as a universal cluster, such as nested clustering in a parcel with 6 floors, the building's sitting on a parcel with a discrete structure is considered as a subset. After the tensile measurements, it coincides with the same logic, as a mathematical plane, with its narrowing from the origin.

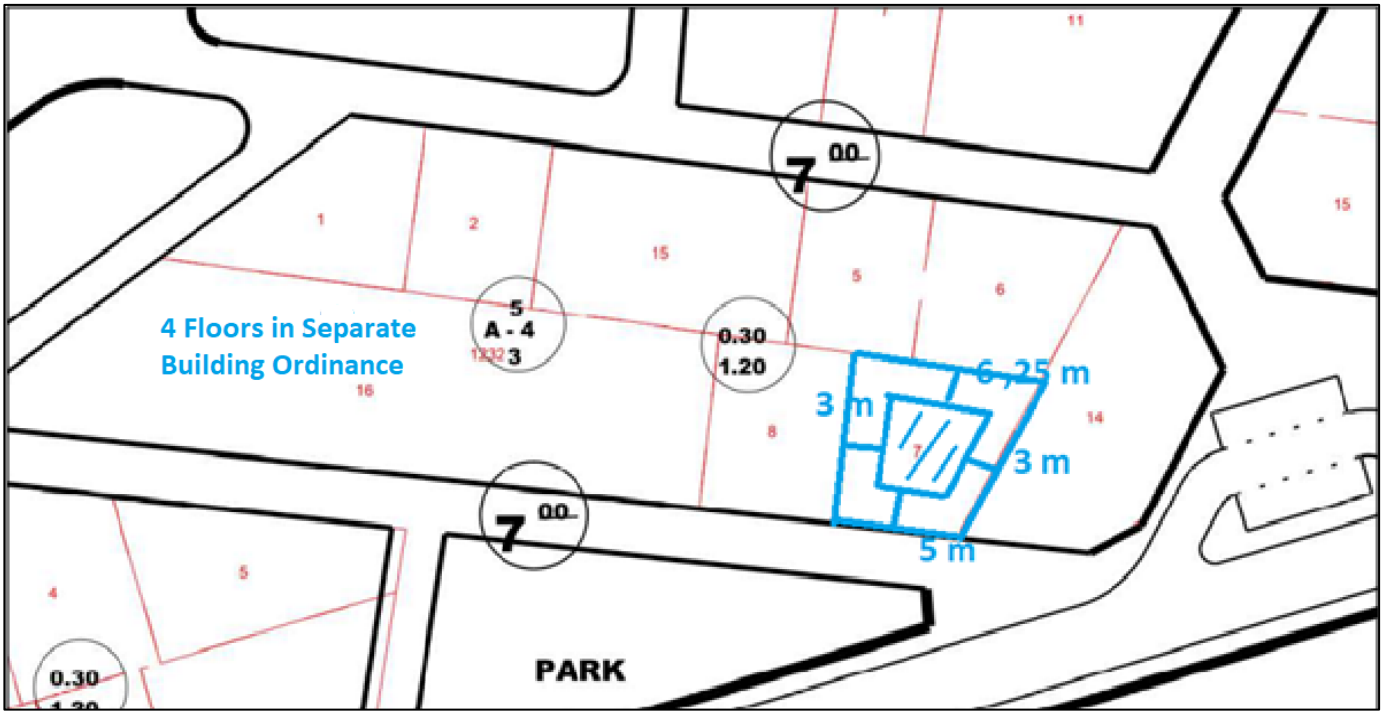

Figure 11. Split Ordinance 4 Floor Zoning Diameter View

In Figure 11, it is shown how zoning distances should be drawn about the front and side gardens in the examples that always face the road with double or triple facades in the other examples. Since only one side of this zoning plot faces the road, the front towing distance is 5 meters and the side is 3 meters, since it is allowed up to 4 floors, and it will be seen that the back garden distance appears. According to the planned type, the rear pulling distance must be in the form of H/2=(3*Number of floors + eave share)/2. If the minimum parcel depth will fall below 10 meters due to the rear pulling to be given, it should be drawn by 3 meters. If this is not the case, the drawing distance will be applied by giving H/2. Therefore, the rear drawing distance of the parcel is given as 6.25 m. Let x y V be defined as x y V $\partial \in$ for $\in$ and rx V$\in$ for r R x V $\in$ $\in$; that is, let the set V be closed for vector addition and scalar multiplication [9].When the parcel is considered as a universal cluster, such as nested clustering in a parcel with 4 floors, the building's sitting on a parcel with a discrete structure is considered as a subset. After the tensile measurements, it coincides with the same logic, as a mathematical plane, with its narrowing from the origin.

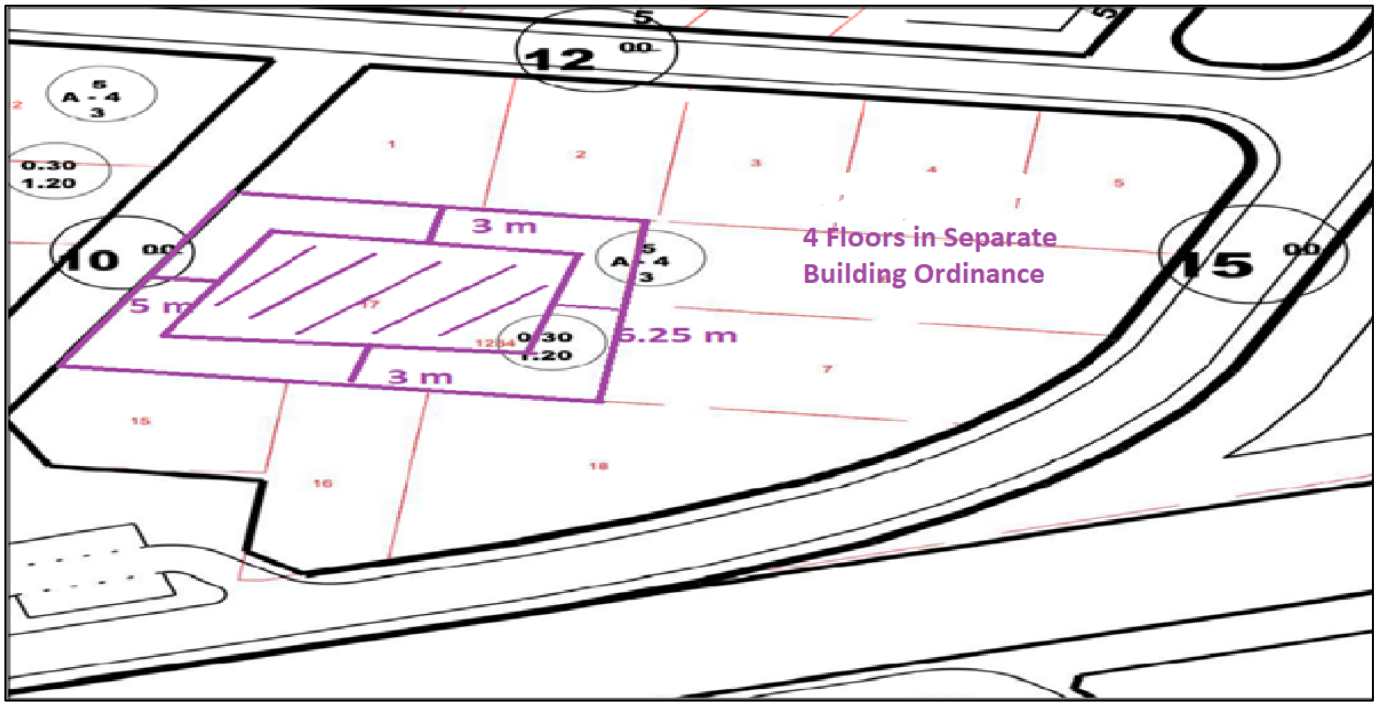

Figure 12. Split Ordinance 4 Floor Zoning Diameter View

In Figure 12., since the immovable property is a zoning parcel with permission up to 4 floors, the front drawing distance is 5 meters, the side garden is 3 meters, and the back garden distance is half of the 6.25 m height, and the zoning diameter is given. Let x y V be defined as x y V ∂ ∈ for ∈ and rx V∈ for r R x V ∈ ∈ ; that is, let the set V be closed for vector addition and scalar multiplication [9]. When the parcel is considered as a universal cluster, such as nested clustering in a parcel with 4 floors, the building's sitting on a parcel with a discrete structure is considered as a subset. After the tensile measurements, it coincides with the same logic, as a mathematical plane, with its narrowing from the origin.

IV. CONCLUSION

The development plans are put into effect in places where there are municipalities such as provinces, districts, towns, according to their scales in the form of master and implementation, and the right understanding of urbanism is tried to be revealed. In these zoning plan legends, zoning islands such as housing, residential trade, trade, socio-cultural, sports facility, DOP areas are created so that cadastral parcels can be converted into zoning parcels by properly dumping them into these islands, and they can get a license for construction. On the islands in the residential areas, the area should be opened from the inside out and the building sessions should be appropriate by giving the distance approximations of these parcels with nested clustering. For this reason, zoning islands are created in adjacent areas in regional centers, and in clear building regulations such as blocks and separate layouts in places to be opened for new settlements. In these islands, it is explained how the zoning diameters should be given according to the planned type zoning regulation and the plan notes approved by the councils of the municipalities. In the examples in the study, the appropriate zoning diameter is shown by showing how the zoning parcels should be given in general in different separate building regulations. TAKS and KAKS calculations and the total equivalent calculations to be used in architectural projects are also tried to be shown and the correct structure formation is examined. Our suggestion is that the zoning diameters should be given in accordance with the convex geometries of the zoning distances and distance approaches specified in the law and regulation, by considering all the parcels in the zoning island, paying attention to the existing structures on the other parcels, without victimizing the neighboring parcels.

ACKNOWLEDGMENT

I would like to thank Semih TAŞKAYA, M.Sc. Metallurgical and Materials Engineer, who did not spare any kind of help in my studies.

Authors' Contributions

The authors' contributions to the paper are equal.

Statement of Conflicts of Interest

There is no conflict of interest between the authors.

Statement of Research and Publication Ethics

The authors declare that this study complies with Research and Publication Ethics

REFERENCES

[1] Aslantas,E; Simsek, G.F.; Berberoglu, O.A. Land and Land Arrangement in Zoning Law. Ankara: Yetkin Publications, p.17, 2006.

[2] Namlı Serin, B., Preparation and Implementation of Zoning Plans, Master's Thesis, Baskent University Institute of Social Sciences, Department of Law, Public Law, 2017.

[3] Applied Geometry for Computer Graphics and CAD. Springer-Verlag, London Berlin Heidelberg.

[4] Onar, Sıddık Sami, General Principles of Administrative Law, C.II. Istanbul, 1966, p.1346; DAY, Text. Administrative law. Ankara: Image Publishing House, 2011, p.492,493; AKYILMAZ, Bahtiyar - SEZGINER, Murat - KAYA, Cemil. Turkish Administrative Law. Seçkin Publications, p.321, 2014.

[5] Crowd, Khalil. Zoning Law Courses. Ankara: Seçkin Publishing, p.43, 2014.

[6] Taşkaya, S., A Research on Reconstruction and Urbanization Activities in Local Governments, Municipality Between 2014-2019, The Case of Elazig Province. International Journal of Eastern Anatolia Science, Engineering and Design, 1(1), 14-28, 2019.

[7] Taşkaya, S., A Research on Zoning Diameters, which are the Basic Points for Construction Permits, International Journal of Eastern Anatolia Science, Engineering and Design, 1(2), 142-153, 2019.

[8] Akagündüz Başköy,D.B., Geometric Transformations and Maple Applications, Mathematics Department Master's Thesis, 2021.

[9] Yüce S, Differential Geometry in Euclidean Space, Pegem Akademi, Ankara. 2017.

[10] Gallier J, Curves and Surfaces in Geometric Modeling, Theory and Algorithms. Morgan, 1999.

[11] Zoning Law, Official Gazette, Vol:24. Pages:1-378, 1999.

[12] Taşkaya, S., Taşkaya, S., Measurement of Multi-Storey Buildings Using Workbench Module in ANSYS Package Software and Analysis of Prototype Analysis, International Journal of Engineering, Design and Technology 1(2): 51-63, 2019.

[13] Taşkaya, S., Taşkaya, S., Measurement of Coordinate Points of Two-Storey Building in Ansys Workbench Software and Investigation of Stress in Beams, International Journal on Mathematics, Engineering and Natural Sciences, 2019, vol:9 page:40-57, 2019.

[14] Taşkaya, S., Sesli, F.A., (2019). Power Test Analysis of Strategic and Local Spatial Data in Noise Pollution, Elazig Province İzzetpaşa Example, International Journal of Eastern Anatolia Science Engineering and Design ISSN: 2667-8764, International Journal of Eastern Anatolia Science Engineering and Design (IJEASED) 1(1):1- 13, 2019.

[15] Adams JA, Rogers DF, Mathematical Elements for Computer Graphics. McGraw Hill, USA, 1990.

International Journal of Multidisciplinary Studies and Innovative Technologies

e-ISSN: 2602-4888
dergipark.org.tr/en/pub/ijmsit
Research Article

2022, 6 (1), 11-18
DOI: DOI: 10.36287/ijmsit.6.1.11
Received: May16, 2022; Accepted: June12, 2022

Comparison of MOEA/D Variants on Benchmark Problems

Tolga Altinoz[1*]

[1*]*Department of Electrical and Electronics Engineering, Ankara University, Ankara, Turkey*
(taltinoz@ankara.edu.tr) (ORCID 0000-0003-1236-7961)

Abstract – Given that the definition of the multi-objective optimization problem is raised when number of objectives is increased in number at the optimization problem, where not only the number of objectives but also the computational resources which are needed to solve the problem, is also more desired. Therefore, novel approaches had required to solve multi-objective optimization problem in a reasonable time. One of this novel approach is utilization of the decomposition method with the evolutionary algorithm/operator. This algorithm was called multi-objective evolutionary algorithm based on decomposition (MOEA/D). Later on, variants have been proposed to improve the performance of the MOEA/D algorithm. However, a general comparison between these variants has needed for demonstrate the performance of these algorithm. For this reason, in this research the variants of MOEA/D algorithms have implemented on benchmark problems (DTLZ and MaF) and the performances has compared with each other. Two metrics had selected to evaluate/compare the performances of the variants. The metrics are IGD and Spread metrics. The results at the end of the implementations suggest that adaptive weighting idea is the most promising idea to increase the performance of the MOEA/D algorithm.

Keywords *– multi-objective optimization, evolutionary algorithm, decomposition, evolutionary algorithms*

Citation: Altinoz, O.T. (2022). Comparison of MOEA/D Variants on Benchmark Problems. International Journal of Multidisciplinary Studies and Innovative Technologies, 6(1): 11-18.

I. INTRODUCTION

The number of objectives in the optimization problem decides the complexity and the title of the problem set. İf the number of objectives is more than one, it is called multiobjective optimization problem. The definition of the multi-objective optimization problem is given as

$$\begin{aligned} \min \quad & F(x) = \left(f_1(x) \dots f_M(x)\right) \\ & subject\ to\ x \in \Omega \\ & \mathrm{g}(x) \leq 0 \\ & \mathrm{h}(x) = 0 \end{aligned} \tag{1}$$

where g(x) and h(x) are constraints with the decision vector $x \epsilon \Omega$ is the decision space and $F{:}\Omega \rightarrow R^M$ is the real valued objective space, where F is the objective function vector of real valued *f*. As the number of objectives is increase in number conventional methods for sorting the solutions with respect to the dominance become computationally costly and since the distance between dimensions on the objective space increase, it is hard to obtain a more diverse solutions on the objective space. Therefore, modern multiobjective optimization algorithms prefer alternative methods like decomposition.

Multi-objective Evolutionary Algorithm based on Decomposition (MOEA/D) [1] is an evolutionary multi objective optimization algorithm which is proposed by Zhang et al. in 2007. The algorithm is based on decomposition (Aggregation function). Decomposition stands for converting the multiobjective problem into many single objective sub-problems. The sub-problems composed from the solutions on the objective space and the pre-defined weight vectors. The diversity of the population is detected explicitly from these weight vectors. MOEA/D is an evolutionary multiobjective optimization algorithm so that the algorithm is built from Genetic operators; crossover, mutation and selection. Instead of the selection operator; other two operators are almost same at MOEA/D. SBX method is selected as the crossover operator at the algorithm. However, parents are selected from neighbouring members of the population. For this reason, two set of vectors are recorded for neighbouring data and weights for the decomposition. Polynomial mutation is selected as the mutation operator. Selection operator differs from evolutionary algorithms. Decomposition is applied to the solutions on the objective space by using a set of weight vectors. Then solutions are converted to the number of sub-problems. The sub-problem values of the offspring and parents are compared in number with respect to the minimization or maximization. Finally, the best members are survived to the next generation.

Even MOEA/D proves itself on many problems, still the performance of the algorithm needs to be improved to get a better distribution of the solutions with a better result with a faster or by using lower computational resources. Therefore, many variants are proposed to increase the performance of the algorithm. To discuss the performance of these variances, in this paper the performance of these variants on 22 benchmark problems with five objectives are compared with each other.

This paper is organized as four sections. After the introduction materials and methods used in this research is given. These are optimization algorithms, benchmark problems and metrics. Then implementation results are given numerically and finally the conclusion of the paper is given as the final section.

Table 1. DTLZ Benchmark Problems

	Mathematical Formulation
DTLZ1	$f_1 = \frac{1}{2}x_1x_2\dots x_{M-1}(1+g(x_M))\dots(1-x_{M-1})(1+g(x_M))\dots f_M = \frac{1}{2}(1-x_1)(1+g(x_M))$ $g(x_M) = 100\left[\lvert x_M\rvert + \sum_{i=1}^{M}\left(\left(x_i-\frac{1}{2}\right)^2 + cos\left(20\pi\left(x_i-\frac{1}{2}\right)\right)\right)\right]$
DTLZ2	$f_1 = (1+g(x_M))cos\left(x_1\frac{\pi}{2}\right)\dots cos\left(x_{M-2}\frac{\pi}{2}\right)cos\left(x_{M-1}\frac{\pi}{2}\right)\dots cos\left(x_{M-2}\frac{\pi}{2}\right)sin\left(x_{M-1}\frac{\pi}{2}\right)\dots$ $f_M = (1+g(x_M))sin\left(x_1\frac{\pi}{2}\right)g(x_M) = \sum_{i=1}^{M}\left(\left(x_i-\frac{1}{2}\right)^2\right)$
DTLZ3	$f_1 = (1+g(x_M))cos\left(x_1\frac{\pi}{2}\right)\dots cos\left(x_{M-2}\frac{\pi}{2}\right)cos\left(x_{M-1}\frac{\pi}{2}\right)\dots cos\left(x_{M-2}\frac{\pi}{2}\right)sin\left(x_{M-1}\frac{\pi}{2}\right)\dots f_M = (1+g(x_M))sin\left(x_1\frac{\pi}{2}\right)$ $g(x_M) = 100\left[\lvert x_M\rvert + \sum_{i=1}^{M}\left(\left(x_i-\frac{1}{2}\right)^2 + cos\left(20\pi\left(x_i-\frac{1}{2}\right)\right)\right)\right]$
DTLZ4	$f_1 = (1+g(x_M))cos\left(x_1^{100}\frac{\pi}{2}\right)\dots cos\left(x^{100}{}_{M-2}\frac{\pi}{2}\right)cos\left(x^{100}{}_{M-1}\frac{\pi}{2}\right)\dots f_M = (1+g(x_M))sin\left(x^{100}{}_1\frac{\pi}{2}\right), g(x_M) = \sum_{i=1}^{M}\left(\left(x_i-\frac{1}{2}\right)^2\right)$
DTLZ5	$f_1 = (1+g(x_M))cos\left(\theta_1\frac{\pi}{2}\right)\dots cos\left(\theta_{M-2}\frac{\pi}{2}\right)cos\left(\theta_{M-1}\frac{\pi}{2}\right)\dots cos\left(\theta_{M-2}\frac{\pi}{2}\right)sin\left(\theta_{M-1}\frac{\pi}{2}\right)\dots f_M = (1+g(x_M))sin\left(\theta_1\frac{\pi}{2}\right)$ $\theta_i = \frac{\pi}{4(1+g(x_M))}(1+2g(x_M)x_i), g(x_M) = \sum_{i=1}^{M}\left(\left(x_i-\frac{1}{2}\right)^2\right)$
DTLZ6	$f_1 = (1+g(x_M))cos\left(\theta_1\frac{\pi}{2}\right)\dots cos\left(\theta_{M-2}\frac{\pi}{2}\right)cos\left(\theta_{M-1}\frac{\pi}{2}\right)$ $\dots f_M = (1+g(x_M))sin\left(\theta_1\frac{\pi}{2}\right)\theta_i = \frac{\pi}{4(1+g(x_M))}(1+2g(x_M)x_i), g(x_M) = \sum_{i=1}^{M}(x_i^{0.1})$
DTLZ7	$f_1 = x_1, f_2 = x_2\dots f_M = (1+g(x_M))hg(x_M) = 1+\frac{9}{\lvert x_M\rvert}\sum x_i, h = M-\sum_{i=1}^{M-1}\left(\frac{f_i}{1+g}(1+sin(3\pi f_i))\right)$

II. MATERIALS AND METHOD

In this section the variants (16) of MOEA/D are briefly given. Then benchmark problems are defined with the metrics that used to compare the performances of the algorithms.

A. Optimization Algorithms

MOEA/D Adaptive Weight Vector Adjustment (MOEA/D-AWA) [2]:

This paper aims at developing a method for weights of the decomposition process. It is stated on the paper that uniformly distributed weights for the decomposition cannot work well on the relatively complex Pareto front. At the problems with complex Pareto front, several sub-problems produce same optimal solution; causes wase of computational sources. Therefore, in this paper, a weight initialization method based on geometric relationship between weight vectors is proposed. For this reason, this variant is a special case solution to address the complex Pareto front problems. The idea behind the method is to find the crowding and sparse area of the objective space. Overpopulated subproblems are deleted and new subproblems are added to the sparse regions.

Covariance Matrix Adaptation-based MOEA/D (MOEA/D-CMA) [3]:

Covariance Matrix Adaptation is a classical method for solving single objective optimization algorithms. In conventional MOEA/D algorithm the operators from Genetic Algorithm like SBX and Polynomial Operator. Generally, instead of SBX, DE is selected as the optimizer however in this variant Covariance Matrix Adaptation method is selected and applied to the MOEA/D algorithm. The results showed that instead of DE, CMA presents better performance than DE.

Multi-objective Evolutionary Algorithm based on Dominance and Decomposition (MOEA/D-DD) [4]:

In this variant both decomposition and dominance ideas are joint to balance the convergence and diversity properties. The idea behind the paper is expending the MOEA/D performance for especially large number of objectives. In this method, widely spread weight vectors for both subproblem and subregion defines. The subregion is considered as niche of the population and the density of the population on this subregion is estimated. Therefore, most of the parents are selected from the neighbouring sub-regions (like in MOEAD-M2M). Instead of all offspring, only one offspring is considered for updating the population.

MOEA/D with Detect-and-Escape Strategy (MOEA/D-DAE) [5]:

This is an improved version of the MOEA/D algorithm especially for the constrained problems. It is stated that the conventional constraint handling method like ϵ-constraint method, is built based on to drag the solution from infeasible region to the feasible region. However, if the population map trap on this new region. Therefore, a new method called detect-and-escape strategy is proposed. Since the proposal is based on only for the constraint problems (even boundaries), it is not expected a better performance than MOEA/D under un-constrained (or boundary) problems.

MOEA/D with Differential Evolution (MOEA/D-DE) [6]:

The conventional MOEA/D algorithm is proposed to use SBX crossover, polynomial mutation, and mostly PBI aggregation function. In this variant instead of SBX crossover operator, Differential Evolution rules are applied to obtain offspring through the algorithm.

MOEA/D with Dynamical Resource Allocation (MOEA/D-DRA) [7]:

In this variant of MOEA/D, tournament selection operator is preferred. To assign different computational effort, the idea of Dynamic Resource Allocation is defined so that for ever fifty

generation the index for determining the number of individuals for selection operator is updated.

Table 2. MaF Benchmark Problems

	Mathematical Formulation
MaF1	$f_1 = (1 - x_1 \dots x_{M-1}) \dots (1 + g(x_M)) \dots f_M = (x_1)(1 + g(x_M)), g(x_M) = \sum_{i=1}^{M} \left(\left(x_i - \frac{1}{2} \right)^2 \right)$
MaF2	$f_1 = (1 + g(x_M)) cos\left(\frac{\pi}{2} \left(\frac{x_1}{2} + \frac{1}{4} \right) \right) \dots cos\left(\frac{\pi}{2} \left(\frac{x_{M-1}}{2} + \frac{1}{4} \right) \right) \dots f_M = (1 + g(x_M)) x_1 sin\left(\frac{\pi}{2} \left(\frac{x_M}{2} + \frac{1}{4} \right) \right)\ g(x_M) = \sum_{i=1}^{M} \left(\left(\frac{\pi}{2} \left(\frac{x_i}{2} + \frac{1}{4} \right) - \frac{1}{2} \right)^2 \right)$
MaF3	$f_1 = \left[(1 + g(x_M)) cos\left(x_1 \frac{\pi}{2} \right) \dots cos\left(x_{M-2} \frac{\pi}{2} \right) cos\left(x_{M-1} \frac{\pi}{2} \right) \dots cos\left(x_{M-2} \frac{\pi}{2} \right) sin\left(x_{M-1} \frac{\pi}{2} \right) \right]^4 \dots f_M = \left[(1 + g(x_M)) sin\left(x_1 \frac{\pi}{2} \right) \right]^2$ $g(x_M) = \left[100 \lvert x_M \rvert + \sum_{i=1}^{M} \left(\left(x_i - \frac{1}{2} \right)^2 + cos\left(20\pi \left(x_i - \frac{1}{2} \right) \right) \right) \right]$
MaF4	$f_1 = a(1 + g(x_M)) \left(1 - cos\left(x_1 \frac{\pi}{2} \right) \dots cos\left(x_{M-2} \frac{\pi}{2} \right) cos\left(x_{M-1} \frac{\pi}{2} \right) \dots cos\left(x_{M-2} \frac{\pi}{2} \right) sin\left(x_{M-1} \frac{\pi}{2} \right) \right) \dots f_M = a(1 + g(x_M)) \left(1 - sin\left(x_1 \frac{\pi}{2} \right) \right)$
MaF5	$f_1 = a^m \left[(1 + g(x_M)) cos\left(x^a{}_1 \frac{\pi}{2} \right) \dots cos\left(x^a{}_{M-2} \frac{\pi}{2} \right) cos\left(x^a{}_{M-1} \frac{\pi}{2} \right) \dots cos\left(x^a{}_{M-2} \frac{\pi}{2} \right) sin\left(x^a{}_{M-1} \frac{\pi}{2} \right) \right]^4 \dots f_M = a \left[(1 + g(x_M)) sin\left(x^a{}_1 \frac{\pi}{2} \right) \right]^4$
MaF6	$f_1 = (1 + g(x_M)) cos(\theta_1) \dots cos(\theta_{M-2}) cos(\theta_{M-1}) \dots cos(\theta_{M-2}) sin(\theta_{M-1}) \dots f_M = (1 + g(x_M)) sin(\theta_1) g(x_M) = \sum_{i=1}^{M} \left(\left(x_i - \frac{1}{2} \right)^2 \right)$ $\theta_i = \begin{cases} \frac{\pi}{2} x_i, i = 1,2, \dots, l-1 \\ \frac{\pi}{4(1 + g(x_M))} (1 + 2g(x_M) x_i), i = l, \dots, M-1 \end{cases}$
MaF7	$f_1 = x_1, f_2 = x_2 \dots f_M = (1 + g(x_M)) h g(x_M) = 1 + \frac{9}{\lvert x_M \rvert} \sum x_i, h = M - \sum_{i=1}^{M-1} \left(\frac{f_i}{1+g} (1 + sin(3\pi f_i)) \right)$
MaF8	Multi-Point Distance Minimization Problem $f_1 = d(x, A_1), f_2 = d(x, A_2), \dots f_M = d(x, A_M)$
MaF9	Multi-Line Distance Minimization Problem $f_1 = d(x, A_1 A_2), f_2 = d(x, A_2 A_3), \dots f_M = d(x, A_1 A_M)$
MaF10	$f_1 = y_M + 2 \left(1 - cos\left(y_1 \frac{\pi}{2} \right) \right) \dots \left(1 - cos\left(y_{M-1} \frac{\pi}{2} \right) \right) f_M = y_M + 2M \left(1 - y_1 - \frac{cos\left(10\pi y_1 + \frac{\pi}{2} \right)}{10\pi} \right), z_i = \frac{x_i}{2i} for\ i = 1, \dots, D$ $t^1{}_i = \begin{cases} z_i\ if\ i = 1, \dots, K \\ \frac{\lvert z_i - 0.35 \rvert}{\lvert 0.35 - z_i \rvert + 0.35} if\ i = K+1, \dots, D \end{cases}, t^2{}_i = \begin{cases} t^1{}_i \\ 0.8 + \frac{0.8(0.75 - t_i^1) min(0, [t_i^1 - 0.75])}{0.75} - \frac{0.2(t_i^1 - 0.85) min(0, [0.85 - t_i^1])}{0.15} \end{cases}$ $t^3{}_i = t^2{}_i{}^{0.02}, t^4{}_i = \begin{cases} \frac{\sum 2j t^3{}_i}{\sum 2j} \\ \frac{\sum 2j t^3{}_i}{\sum 2j} \end{cases}, y_i = \begin{cases} (t^4{}_i - 0.5) max(1, t^4{}_i) + 0.5 \\ t^4{}_M \end{cases}$
MaF11	$f_1 = y_M + 2 \left(1 - cos\left(y_1 \frac{\pi}{2} \right) \right) \dots \left(1 - cos\left(y_{M-1} \frac{\pi}{2} \right) \right) f_M = y_M + 2M(1 - y_1 cos^2(5\pi y_1)), z_i = \frac{x_i}{2i} for\ i = 1, \dots, D$ $t^1{}_i = \begin{cases} z_i\ if\ i = 1, \dots, K \\ \frac{\lvert z_i - 0.35 \rvert}{\lvert 0.35 - z_i \rvert + 0.35} if\ i = K+1, \dots, D \end{cases}, t^2{}_i = \begin{cases} t^1{}_i \\ t^1{}_{K+2(i-K)-1} + t^1{}_{K+2(i-K)} + 2t^1{}_{K+2(i-K)-1} - t^1{}_{K+2(i-K)} \end{cases}$ $t^3{}_i = \begin{cases} \frac{\sum t^2{}_i}{K/M - 1} \\ \frac{\sum t^2{}_i}{D - K/2} \end{cases}, y_i = \begin{cases} (t^3{}_i - 0.5) max(1, t^3{}_i) + 0.5 \\ t^3{}_M \end{cases}$
MaF12	$f_1 = y_M + 2 \left(1 - cos\left(y_1 \frac{\pi}{2} \right) \right) \dots \left(1 - cos\left(y_{M-1} \frac{\pi}{2} \right) \right) f_M = y_M + 2M \left(1 - y_1 cos\left(\frac{\pi}{2} y_1 \right) \right), z_i = \frac{x_i}{2i} for\ i = 1, \dots, D$ $y_i = \begin{cases} (t^3{}_i - 0.5) max(1, t^3{}_i) + 0.5 \\ t^3{}_M \end{cases}$
MaF13	$f_1 = sin\left(\frac{\pi}{2} x_1 \right) + \frac{2}{J_1} \sum y_j^2, \dots, f_M = f_1^2 + f_2^{10} + f_3^{10} + \frac{2}{J_4} \sum y_j^2$
MaF14	$f_1 = x_1^f \dots x_{M-1}^f \left(1 + \sum c_{1,j} g_1 \right), \dots, f_M = \left(1 - x_1^f \right) \left(1 + \sum c_{1,j} g_1 \right)$
MaF15	$f_1 = \left(1 - cos\left(\frac{\pi}{2} x_1^f \right) \dots cos\left(\frac{\pi}{2} x_{M-1}^f \right) \right) \left(1 + \sum c_{1,j} g_1 \right), \dots, f_M = 1 - sin\left(\frac{\pi}{2} x_1^f \right) \left(1 + \sum c_{1,j} g_1 \right)$

MOEA/D with Distance-based Updating Strategy (MOEA/D-DU) [8]:

The motivation of the proposed method is to maintain the desired diversity of the population. For this purpose, the perpendicular distance between solution on the objective space and the weight vector calculate. For the multiobjective problems (three or less objective) the propose idea will fall behind the conventional decomposition algorithm. However, as indicated in the paper, the distance calculation (as a metric) is well suited for many objective optimization problems. Only the updating scheme differs from MOEA/D algorithm. First a new solution is produced (offspring), then perpendicular distance to all weight vectors is calculated. Then, some of these minimum distance solutions are selected. They are compared with neighbourhood solutions and replaced if objective value is smaller.

Dynamic Thompson Sampling for MOEA/D (MOEA/D-DYTS) [9]:

This paper is another variant of the MOEA/D-FRRMAB so that multi-armed bandit problem where the dynamic Thompson sampling (DYTS) is applied to adapt the bandit model. Therefore, to solve Multiarmed Bandit problem an alternative solution algorithm called Thompson sampling is integrated into MOEA/D algorithm.

Table 3. IGD Metric Value for DTLZ1-DTLZ7

Problem	DTLZ1	DTLZ2	DTLZ3	DTLZ4	DTLZ5	DTLZ6	DTLZ7
MOEAD	6.8068e-2 (6.54e-5) =	2.1216e-1 (1.36e-4) =	2.1261e-1 (2.97e-4) =	4.0601e-1 (1.23e-1) -	2.6947e-2 (6.83e-4) +	2.6433e-2 (2.56e-3) +	1.0009e+0 (1.96e-1) +
MOEADDU	6.8935e-2 (3.83e-4) -	2.1578e-1 (8.37e-4) -	2.2094e-1 (1.53e-3) -	2.1772e-1 (1.30e-3) +	1.5516e-1 (1.28e-2) -	1.5026e-1 (2.21e-2) -	9.9328e+0 (3.17e+0) -
MOEADUR	6.9644e-2 (1.25e-3) -	2.1228e-1 (1.42e-3) =	2.3047e-1 (2.02e-3) -	3.2507e-1 (1.75e-1) -	2.8850e-2 (4.84e-3) +	3.1476e-2 (7.68e-3) +	4.8472e-1 (2.62e-2) +
MOEADURAW	6.7862e-2 (9.25e-4) =	2.1213e-1 (1.28e-3) =	2.3258e-1 (6.62e-3) -	3.8249e-1 (1.94e-1) -	6.4273e-2 (1.12e-2) +	7.6124e-2 (2.47e-2) +	3.0985e-1 (1.21e-2) +
MOEADD	6.8082e-2 (1.90e-5)	2.1221e-1 (2.29e-6)	2.1272e-1 (2.08e-4)	2.5670e-1 (9.38e-2)	8.5350e-2 (1.23e-2)	1.0025e-1 (1.49e-2)	3.0005e+0 (1.03e-6)

Table 4. IGD Metric Value for MaF1-MaF8

Problem	MaF1	MaF2	MaF3	MaF4	MaF5	MaF6	MaF7	MaF8
MOEAD	2.2409e-1 (2.62e-3) +	1.3617e-1 (1.40e-3) +	1.2579e-1 (1.84e-3) -	1.0244e+1 (4.70e-1) -	1.0849e+1 (4.26e+0) -	2.0358e-1 (2.93e-1) =	1.0947e+0 (8.50e-2) +	2.9575e-1 (1.15e-2) +
MOEADDU	2.5433e-1 (1.37e-2) =	1.3504e-1 (2.30e-3) +	9.8807e-2 (5.77e-4) +	4.3000e+0 (3.55e-1) +	2.6880e+0 (3.09e-2) +	5.0453e-2 (8.02e-4) +	1.0986e+1 (3.28e+0) -	8.0931e+2 (1.18e+3) =
MOEADUR	1.8549e-1 (4.58e-3) +	1.3334e-1 (2.80e-3) +	9.7018e-2 (1.11e-2) +	2.7576e+0 (6.68e-2) +	3.5005e+0 (1.33e+0) +	9.6127e-3 (6.54e-4) +	4.8641e-1 (3.43e-2) +	1.5651e-1 (7.76e-3) +
MOEADURAW	1.4938e-1 (8.90e-4) +	1.1949e-1 (2.00e-3) +	9.7627e-2 (1.01e-2) +	2.1795e+0 (1.79e-2) +	2.8346e+0 (1.30e+0) +	5.0413e-3 (4.99e-5) +	3.3438e-1 (4.94e-2) +	1.2899e-1 (2.28e-3) +
MOEADD	2.5944e-1 (1.61e-2)	1.5669e-1 (2.78e-3)	1.1565e-1 (3.26e-3)	7.6115e+0 (2.40e-1)	6.6025e+0 (5.30e-1)	8.2438e-2 (5.79e-3)	2.8126e+0 (5.94e-1)	3.7499e-1 (1.23e-2)

Table 5. IGD Metric Value for MaF9-MaF15

Problem	MaF9	MaF10	MaF11	MaF12	MaF13	MaF14	MaF15	+/-/=
MOEAD	1.4732e-1 (1.54e-3) +	7.8067e-1 (7.28e-3) -	7.6132e-1 (6.26e-3) -	1.8090e+0 (1.47e-1) -	1.8624e-1 (3.27e-2) +	6.5899e-1 (2.52e-1) =	6.8952e-1 (7.14e-2) -	9/8/5
MOEADDU	3.5747e-1 (1.36e-2) -	4.9382e-1 (5.72e-3) +	5.2448e-1 (9.48e-3) +	1.4959e+0 (3.57e-2) -	2.0459e-1 (1.30e-2) +	7.6645e-1 (1.04e-1) =	2.8804e+0 (7.90e-1) -	9/10/3
MOEADUR	1.8975e-1 (7.83e-3) +	5.7551e-1 (2.84e-2) =	5.0500e-1 (1.08e-2) +	1.2627e+0 (2.12e-2) +	1.8528e-1 (2.68e-2) +	7.5975e-1 (1.72e-1) =	5.5488e-1 (8.74e-2) =	15/3/4
MOEADURAW	2.0152e-1 (1.36e-2) +	5.0565e-1 (3.29e-2) +	5.5437e-1 (1.11e-2) +	1.1953e+0 (1.59e-2) +	1.5749e-1 (2.30e-2) +	9.0937e-1 (1.10e-1) -	5.8964e-1 (9.34e-2) =	16/3/3
MOEADD	2.9661e-1 (2.86e-3)	5.8604e-1 (3.35e-2)	5.8168e-1 (1.45e-2)	1.3438e+0 (1.31e-2)	2.8767e-1 (5.31e-2)	6.8320e-1 (1.52e-1)	5.1391e-1 (6.54e-2)	

MOEA/D Efficient Global Optimization (MOEA/D-EGO) [10]:

This algorithm is proposed especially solving the expensive optimization problems. This algorithm is based on efficient global optimization algorithm which has been widely accepted as one of the most popular methods using Gaussian Process Model. Through this algorithm, Gaussian model for each subproblem is built based on obtained data from previous generation. In this variation, sampled points select among the decision space. The function value for this sampled data calculates. Decomposed sub-problems and their objective values are collected and predictive model are generated. The idea behind this paper aims at developing a cost-efficient method, hence it is expected to present better performance for expensive optimization problems.

MOEA/D Fitness-rate-rank-based Multiarmed Bandit (MOEA/D-FRRMAB) [11]:

Adaptive operator selection is a method for deciding which operator should be employed in the MOEA/D algorithm. Two stage operator selection is to give reward to the operator, and at the second stage based on the reward operator is selected. The reward mechanism is related to the exploration vs. exploitation dilemma in multiobjective optimization problem similar to a common problem called multiarmed bandit problem. Therefore, upper confidence bound algorithm is employed to address this problem. The overall algorithm is named as Fitness-rate-rank-based Multiarmed Bandit MOEA/D algorithm. As the MOEA/D algorithm, instead of GA operators like SBX crossover and polynomial mutation, in this algorithm Differential Evolution (DE) operators (DE/rand/1, DE/rand/2, DE/current-to-rand/1, and DE/current-to-rand/2) are selected from this proposed method.

Number of Simple Multiobjective Subproblems-based MOEA/D (MOEA/D-M2M) [12]:

The decomposition method at the MOEA/D algorithm aims at developing such a method for obtaining many single-objective optimization problems/sub-problems. In this variant, instead of a many single objective problems (aggregated) number of simple multiobjective problems are considered and algorithm solves these problems in a collaborative way in a single run. In other words, the objective space divide into subregions and considered as multiobjective problems.

MOEA/D with Maximum Relative Diversity Loss (MOEA/D-MRDL) [13]:

At each generation of the MOEA/D algorithm the populations slowly (relatively) converge to the Pareto front. At each generation the direction of the convergency is differs and it causes loss of the diversity. Therefore, in the current algorithm the notion of maximum relative diversity loss. The idea is to compare the parent solution o any other parent solutions since they lead to poor convergence. Similarly, offspring are compared for similarity with respect to the estimated convergence direction.

Table 6. Spread Metric Value for DTLZ1-DTLZ7

Problem	DTLZ1	DTLZ2	DTLZ3	DTLZ4	DTLZ5	DTLZ6	DTLZ7
MOEAD	3.5257e-2 (6.95e-4) -	1.7181e-1 (2.03e-3) +	1.6727e-1 (2.07e-3) +	7.0562e-1 (3.31e-1) =	1.6592e+0 (1.53e-2) =	1.7142e+0 (5.19e-2) -	1.0006e+0 (1.19e-1) -
MOEADDU	6.7552e-2 (1.32e-2) -	2.0470e-1 (5.23e-3) -	2.4238e-1 (1.43e-2) -	2.1815e-1 (8.52e-3) +	5.8727e-1 (4.29e-2) +	9.5654e-1 (7.61e-2) -	1.0005e+0 (9.35e-4) -
MOEADUR	3.1791e-1 (7.88e-2) -	1.8340e-1 (3.02e-2) =	5.4401e-1 (3.54e-2) -	4.8640e-1 (1.44e-1) -	1.3690e+0 (6.60e-2) +	1.4321e+0 (6.69e-2) -	8.3171e-1 (6.39e-2) +
MOEADURAW	2.7893e-1 (5.02e-2) -	1.6652e-1 (2.02e-2) =	6.3180e-1 (8.46e-2) -	2.3389e-1 (1.44e-1) =	3.7914e-1 (5.80e-2) +	6.3333e-1 (1.56e-1) +	3.7629e-1 (6.32e-2) +
MOEADD	3.3831e-2 (8.79e-5)	1.7482e-1 (1.38e-4)	1.7385e-1 (1.39e-3)	3.9945e-1 (4.74e-1)	1.5753e+0 (1.31e-1)	8.0050e-1 (1.16e-1)	1.0000e+0 (2.05e-11)

Table 7. Spread Metric Value for MaF1-MaF8

Problem	MaF1	MaF2	MaF3	MaF4	MaF5	MaF6	MaF7	MaF8
MOEAD	1.7038e+0 (5.77e-2) =	4.0448e-1 (5.82e-3) +	5.0758e-1 (1.81e-2) -	1.0782e+0 (1.20e-1) =	1.0244e+0 (1.92e-1) =	1.4441e+0 (3.09e-1) +	9.4827e-1 (1.67e-2) +	7.9903e-1 (3.85e-2) +
MOEADDU	9.4372e-1 (1.50e-1) +	3.9310e-1 (2.90e-2) +	4.1267e-1 (1.42e-3) +	1.2122e+0 (7.66e-1) =	3.6488e-1 (1.11e-2) +	1.6278e+0 (2.11e-1) +	1.0002e+0 (6.29e-4) +	9.1045e-1 (1.36e-1) +
MOEADUR	6.1989e-1 (4.08e-2) +	5.4407e-1 (4.34e-2) +	5.7743e-1 (8.75e-2) -	6.6258e-1 (7.46e-2) +	6.9546e-1 (6.20e-2) =	1.0101e+0 (6.17e-2) +	8.1426e-1 (5.85e-2) +	6.8274e-1 (6.15e-2) +
MOEADURAW	1.4181e-1 (1.83e-2) +	1.6477e-1 (1.13e-2) +	5.3471e-1 (7.11e-2) -	2.0803e-1 (5.31e-2) +	2.2215e-1 (1.35e-1) +	2.4994e-1 (2.95e-2) +	3.6599e-1 (6.53e-2) +	2.8329e-1 (5.16e-2) +
MOEADD	1.7955e+0 (1.46e-1)	1.2944e+0 (1.03e-1)	4.3287e-1 (1.09e-2)	1.1162e+0 (8.61e-2)	1.0100e+0 (3.44e-1)	2.2488e+0 (4.66e-1)	1.0233e+0 (7.38e-2)	1.0554e+0 (8.10e-2)

Table 8. Spread Metric Value for MaF9-MaF15

Problem	MaF9	MaF10	MaF11	MaF12	MaF13	MaF14	MaF15	+/-/=
MOEAD	5.4185e-1 (1.08e-2) +	6.5211e-1 (1.95e-2) -	5.9811e-1 (1.36e-2) -	5.0025e-1 (4.38e-2) -	1.2917e+0 (6.01e-2) +	1.0217e+0 (2.18e-1) =	8.5327e-1 (5.97e-2) +	9/7/6
MOEADDU	1.6584e+0 (2.05e-1) =	4.6757e-1 (5.27e-3) +	4.8288e-1 (5.41e-2) =	8.9825e-1 (1.09e-1) -	1.4527e+0 (4.53e-1) =	1.3956e+0 (3.46e-1) =	2.1147e+0 (1.64e-1) -	10/7/5
MOEADUR	9.5542e-1 (1.19e-1) +	4.9890e-1 (7.46e-2) =	5.0098e-1 (4.40e-2) =	3.6429e-1 (5.24e-2) =	1.0210e+0 (1.66e-1) +	2.0320e+0 (9.06e-2) -	1.2889e+0 (2.59e-1) =	10/6/6
MOEADURAW	1.5266e+0 (5.60e-1) =	6.6860e-1 (3.46e-2) -	4.3264e-1 (2.83e-2) +	1.4906e-1 (2.51e-2) +	1.3248e+0 (5.89e-1) =	1.5382e+0 (2.78e-1) -	6.9317e-1 (3.19e-1) +	13/5/4
MOEADD	1.6938e+0 (2.28e-1)	5.4218e-1 (4.93e-2)	4.8975e-1 (1.02e-2)	3.8770e-1 (1.32e-2)	1.5086e+0 (1.74e-1)	1.1115e+0 (5.10e-1)	1.1895e+0 (1.35e-1)	

Pareto Adaptive Scalarizing MOEA/D (MOEA/D-PaS) [14]:

In the paper initially all L_p methods for scalarization are evaluated and from the results it is observed that the parameter p is crucial for the performance of the algorithm for different Pareto geometries. The L_p aggregation function is calculated by $1/p$ power of the sum of weighted difference between objective value and ideal points. For four different parameters set of p, the maximum value is selected as the aggregation function (PaS) of the algorithm. From the information at the paper, it is claimed that Pareto adaptive scalarization is a cost-efficient method that avoids the estimation of the Pareto front shape.

Stable Matching Method-based MOEA/D (MOEA/D-STM) [15]:

In this algorithm, the MOEA/D selection operator is considered as an operator for matching the subproblems with the solutions. Therefore, stable marriage problem is selected as a model problem. This stable matching model employ as a selection operator. Each subproblem has one solution in the current population. Subproblems are built based on aggregation functions, and the ranks elated to the objective value and the weight vector is obtained (similar to MOEA/D-DU). The matching algorithm (STM) is applied to these values to assign solutions to each subproblem.

MOEA/D with Updating when Required (MOEA/D-UR) [16]:

Similar to MOEA/D-AWA algorithm, MOEA/D-UR is a method for changing the weights. It is stated that uniformly distributed weights may be failed under complex (geometry of the problem) Pareto front. In the proposed method, a metric is defined and calculated to detect convergency, based on the value of this improvement metric/threshold (rate of offspring and parent vectors obtained from Tchebycheff decompostion), the objective space is divided adaptively to increase diversity.

MOEA/D with Uniformly Randomly Adaptive Weights (MOEA/D-URAW) [17]:

Similarly, also indicated in this variant, the shape and geometry of the Pareto front is the weakness of the MOEA/D algorithm due to the weight vector selection. In the proposed method, based on the sparsity of the population weight vectors are adapted by combining uniform random sampling with the adaptive weight vector selection. The flexible population size allows in this method. Also, the performance of the SBX over DE is indicated and SBX is suggested. Initially, the population sparsity level is calculated. Then external population stores non-dominated solutions during the search. Based on the highest sparsity level of this external population the new weight vector set is constructed.

Table 9. Runtime (sec) for DTLZ1-DTLZ7

Problem	DTLZ1	DTLZ2	DTLZ3	DTLZ4	DTLZ5	DTLZ6	DTLZ7
MOEAD	1.2361e+1 (1.10e-1) +	1.2337e+1 (1.33e-1) +	1.2598e+1 (1.48e-1) +	1.2693e+1 (9.64e-2) +	1.2839e+1 (9.73e-2) +	1.3047e+1 (9.69e-2) +	1.2639e+1 (7.64e-2) +
MOEADDU	1.6550e+1 (3.09e-1) +	1.6541e+1 (1.86e-1) +	1.6457e+1 (1.19e-1) +	1.6807e+1 (8.46e-2) +	1.7224e+1 (2.29e-1) +	1.7547e+1 (1.85e-1) +	1.6883e+1 (1.76e-1) +
MOEADUR	2.6046e+1 (6.46e-1) +	2.6015e+1 (1.73e-1) +	2.4563e+1 (2.00e-1) +	2.8987e+1 (6.07e-1) +	2.7793e+1 (1.71e-1) +	2.8689e+1 (5.25e-1) +	2.8769e+1 (2.87e-1) +
MOEADURAW	2.3460e+1 (2.40e-1) +	3.7011e+1 (8.03e-2) +	1.9754e+1 (2.38e-1) +	3.5192e+1 (1.24e+0) +	2.9633e+1 (5.52e-1) +	2.9077e+1 (5.26e-1) +	3.3074e+1 (1.18e-1) +
MOEADD	4.1776e+1 (3.69e-1)	5.5178e+1 (3.07e+0)	4.9959e+1 (5.22e-1)	5.7491e+1 (3.58e+0)	5.5168e+1 (8.00e-1)	5.7953e+1 (4.83e-1)	5.3916e+1 (4.49e-1)

Table 10. Runtime (sec)for MaF1-MaF8

Problem	MaF1	MaF2	MaF3	MaF4	MaF5	MaF6	MaF7	MaF8
MOEAD	1.2277e+1 (1.34e-1) +	1.2866e+1 (1.18e-1) +	1.2808e+1 (1.54e-1) +	1.3085e+1 (8.25e-2) +	1.4560e+1 (2.43e-1) +	1.4101e+1 (9.21e-2) +	1.7218e+1 (1.57e-1) +	1.9812e+1 (1.35e-1) +
MOEADDU	1.6660e+1 (1.42e-1) +	1.6930e+1 (8.42e-2) +	1.6893e+1 (1.66e-1) +	1.7442e+1 (1.99e-1) +	1.8572e+1 (2.38e-1) +	1.8824e+1 (1.74e-1) +	1.8632e+1 (1.61e-1) +	2.0431e+1 (1.66e-1) +
MOEADUR	2.9304e+1 (2.47e-1) +	3.0985e+1 (4.33e-1) +	2.8182e+1 (4.42e-1) +	2.8489e+1 (4.42e-1) +	3.2310e+1 (2.32e-1) +	3.1842e+1 (3.07e-1) +	3.3762e+1 (4.05e-1) +	3.6927e+1 (2.58e-1) +
MOEADURAW	3.2609e+1 (1.08e-1) +	3.5920e+1 (1.50e-1) +	2.0622e+1 (3.26e-1) +	2.3121e+1 (2.98e-1) +	3.9667e+1 (9.98e-1) +	2.4730e+1 (1.92e-1) +	4.0329e+1 (1.58e-1) +	2.5470e+1 (3.69e-1) +
MOEADD	5.1169e+1 (6.12e-1)	5.8239e+1 (6.23e-1)	4.8092e+1 (2.04e+0)	4.4284e+1 (6.76e-1)	5.8443e+1 (3.09e+0)	5.5572e+1 (2.15e+0)	5.6649e+1 (7.95e-1)	4.7841e+1 (6.17e-1)

Table 11. Runtime (sec)for MaF9-MaF15

Problem	MaF9	MaF10	MaF11	MaF12	MaF13	MaF14	MaF15	+/-/=
MOEAD	1.9057e+1 (1.78e-1) +	1.9914e+1 (1.43e-1) +	2.0716e+1 (1.67e-1) +	2.1227e+1 (1.25e-1) +	1.9136e+1 (1.83e-1) +	2.2750e+1 (1.40e-1) +	2.3080e+1 (2.35e-1) +	22/0/0
MOEADDU	1.9233e+1 (2.06e-1) +	2.3111e+1 (1.33e-1) +	2.4341e+1 (2.40e-1) +	2.4469e+1 (1.78e-1) +	2.3090e+1 (1.13e-1) +	2.6213e+1 (2.67e-1) +	2.6991e+1 (1.62e-1) +	22/0/0
MOEADUR	3.1236e+1 (2.57e-1) +	3.3810e+1 (3.19e-1) +	3.5421e+1 (2.84e-1) +	3.6056e+1 (2.82e-1) +	3.3453e+1 (2.65e-1) +	3.6629e+1 (3.15e-1) +	3.8039e+1 (4.37e-1) +	22/0/0
MOEADURAW	2.1531e+1 (3.28e-1) +	3.3416e+1 (3.58e-1) +	4.0231e+1 (2.55e-1) +	4.3848e+1 (2.43e+0) +	2.5660e+1 (7.51e-1) +	2.8468e+1 (3.12e+0) +	3.8587e+1 (1.21e+0) +	22/0/0
MOEADD	4.8611e+1 (6.66e-1)	6.0058e+1 (5.16e-1)	6.3404e+1 (4.25e-1)	6.3566e+1 (4.18e-1)	5.6062e+1 (9.73e-1)	6.4232e+1 (1.92e+0)	6.4383e+1 (7.30e-1)	

B. Benchmark Problems

In this research in total 22 benchmark problems are considered to implement the MOEA/D variants. These benchmark problems are defined in DTLZ [18] (seven benchmark problems) and MaF [19] (15 benchmark problems). Table 1 and Table 2 gives the test problems respectively.

C. Metrics and Statistical Tests

Unlike single objective optimization problems, a set of solutions are reported from optimization algorithm. The shape of the solutions on the objective space is called Prato approximated solutions. Therefore, some functions needed to extract the feature from this set. These functions are named as metrics. Two important properties are needed to observe for comparison of the algorithms. These properties are accuracy and distribution of the solutions on objective space.

For the accuracy, inverted generalized distance (IGD) metric is proposed in [20] and mathematical description of this metric is given as

$$f_{IGD} = \frac{\sum ds(a,P)}{|P|} \tag{2}$$

The IGD metric is based on computing the average distance between obtained solution candidates and the Pareto Front where $ds(a,P) = \sqrt{\sum(a_i - p_i)^2}$. The second metric is related to the distribution of the solution on the objective space. The spread metric is defined in [21], given as

$$f_{Spread} = \sqrt{\frac{1}{M}\sum\left(\frac{\max(a,PF)-\min(a,PF)}{PF_{max}-PF_{min}}\right)^2} \tag{3}$$

The metric is based on calculation of the normalized squared sum of the distance between maximum and minimum difference between produced solutions and PF.

III. Implementation and Results

In this research the variants of the MOEA/D algorithm are compared with respect to the accuracy and diversity of the solutions. For this purpose, two metrics are selected as IGD and Spread, respectively. Each variant is implemented independently 10 times with the same number of population size (100) and maximum number of function evolution (10^5) for 5 objective benchmark problems.

The variants of MOEA/D [1] algorithms are MOEA/D-AWA [2], MOEA/D-CMA [3], MOEA/D-DD [4], MOEA/D-DAE [5], MOEA/D-DE [6], MOEA/D-DRA [7], MOEA/D-DU [8], MOEA/D-DYTS [9], MOEA/D-EGO [10], MOEA/D-FRRMAB [11], MOEA/D-M2M [12], MOEA/D-MRDL [13], MOEA/D-PaS [14], MOEA/D-STM [15], MOEA/D-UR [16], and MOEA/D-URAW [17]. These algorithms had applied into benchmark problems. Among all these variants only MOEA/D [1], MOEA/D-DD [4], MOEA/D-DU [8], MOEA/D-UR [16], and MOEA/D-URAW [17] had given the comparative results. For this reason, only the results belonging to these five algorithms has reported on the paper. The statistical results for the mean and standard deviation of these independent runs are reported in Tables. Tables 3-5 are given for IGD metric, Tables 6-8 are for Spread metric and Tables 9-11 is presented for runtime of these algorithm.

IGD (Convergence): When all of the algorithms are compared with each other with respect to the number of the benchmark problems; URAW variant presents best performance for 22 benchmark problems. Original MOEA/D algorithm present best performance for 5 benchmark problems, similarly DU, DUR and DD variants present best performance for 3,3, and 1 benchmark problems, respectively. The results support the superior results of the URAW variant.

Spread (Distribution): Spread metric gives the distribution of the solutions on the objective space. Well distributed solutions are desired from the algorithms. Therefore, for the comparison on the spread metric, URAW presents best result of 14 of 22 benchmark problems. MOEAD, DU, DUR and DD variants only present best results from 3, 3, 1 and 1 benchmark problems, respectively.

Runtime: Since it is the main algorithm for the variants, MOEA/D gives the fastest results among all variants. However, if MOEA/D is removed from the results, DU gives the fastest results, meaning that it can be considered to use the lowest computational resources.

IV. Conclusion

The aim of this research is to compare the MOEA/D variants under 22 benchmark problems with five objectives. The results are evaluated on two metrics IGD and Spread. From the results, it is clearly demonstrated that URAW variant gives the best results almost all benchmark problems in both IGD and Spread metrics. In addition, the URAW variant uses relatively less computational resources when it is compared with other variants. The reason behind that is not only the adaptive weight vectors but also flexible population size. Therefore, both convergency and distribution property of the algorithm improves. It is suggested with respect to the results obtained in this paper, weights of the decomposition method and sparce detecting methods will increase the performance of the algorithm. Also, it is suggested to compare the performance of a novel algorithm with URAW variant.

Authors' Contributions

The authors' contributions to the paper are equal.

Statement of Conflicts of Interest

There is no conflict of interest between the authors.

Statement of Research and Publication Ethics

The authors declare that this study complies with Research and Publication Ethics

References

[1] Q. Zhang and H. Li, "MOEA/D: A multiobjective evolutionary algorithm based on decomposition," IEEE Transactions on Evolutionary Computation, vol. 11, no. 6, pp. 712-731, 2007.

[2] Y. Qi, X. Ma, F. Liu, L. Jiao, J. Sun, and J. Wu, "MOEA/D with adaptive weight adjustment," Evolutionary Computation, vol. 22, no. 2, pp. 231-264, 2014.

[3] H. Li, Q. Zhang, and J. Deng, "Biased multiobjective optimization and decomposition algorithm," IEEE Transactions on Cybernetics, vol. 47, no. 1, pp. 52-66, 2017.

[4] K. Li, K. Deb, Q. Zhang, and S. Kwong, "An evolutionary many-objective optimization algorithm based on dominance and decomposition," IEEE Transactions Evolutionary Computation, vol. 19, no. 5, pp. 694-716, 2015.

[5] Q. Zhu, Q. Zhang, and Q. Lin, "A constrained multi-objective evolutionary algorithm with detect-and-escape strategy," IEEE Transactions on Evolutionary Computation, vol. 24, no. 5, pp. 938-947, 2020.

[6] H. Li and Q. Zhang, "Multiobjective optimization problems with complicated Pareto sets, MOEA/D and NSGA-II," IEEE Transactions on Evolutionary Computation, vol. 13, no. 2, pp. 284-302, 2009.

[7] Q. Zhang, W. Liu, and H. Li, "The performance of a new version of MOEA/D on CEC09 unconstrained MOP test instances," Proceedings of the IEEE Congress on Evolutionary Computation, pp. 203-208, 2009.

[8] Y. Yuan, H. Xu, B. Wang, B. Zhang, and X. Yao, "Balancing convergence and diversity in decomposition-based many-objective optimizers," IEEE Transactions on Evolutionary Computation, vol. 20, no. 2, pp. 180-198, 2016.

[9] K. Li, A. Fialho, S. Kwong, and Q. Zhang, "Adaptive operator selection with bandits for a multiobjective evolutionary algorithm based on decomposition," IEEE Transactions on Evolutionary Computation, vol. 18, no. 1, pp. 114-130, 2014.

[10] Q. Zhang, W. Liu, E. Tsang, and B. Virginas, "Expensive multiobjective optimization by MOEA/D with Gaussian process model," IEEE Transactions on Evolutionary Computation, vol. 14, no. 3, pp. 456-474, 2010.

[11] K. Li, A. Fialho, S. Kwong, and Q. Zhang, "Adaptive operator selection with bandits for a multiobjective evolutionary algorithm based on decomposition," IEEE Transactions on Evolutionary Computation, vol. 18, no. 1, pp. 114-130, 2010.

[12] H. Liu, F. Gu, and Q. Zhang, "Decomposition of a multiobjective optimization problem into a number of simple multiobjective subproblems," IEEE Transactions on Evolutionary Computation, vol. 18, no. 3, pp. 450-455, 2014.

[13] S. B. Gee, K. C. Tan, V. A. Shim, and N. R. Pal, "Online diversity assessment in evolutionary multiobjective optimization: A geometrical perspective," IEEE Transactions on Evolutionary Computation, vol. 19, no. 4, pp. 542-559, 2015.

[14] R. Wang, Q. Zhang, and T. Zhang, "Decomposition-based algorithms using Pareto adaptive scalarizing methods," IEEE Transactions on Evolutionary Computation, vol. 20, no. 6, pp. 821-837, 2016.

[15] K. Li, Q. Zhang, S. Kwong, M. Li, and R. Wang, "Stable matching-based selection in evolutionary multiobjective optimization," IEEE Transactions on Evolutionary Computation, vol. 18, no. 6, pp. 909-923, 2014.

[16] L. R. de Farias, A. F. Araujo, "A decomposition-based many-objective evolutionary algorithm updating weights when required," Swarm and Evolutionary Computation, 2021.

[17] L. R. C. Farias and A. F. R. Araujo, "Many-objective evolutionary algorithm based on decomposition with random and adaptive weights," In Proceedings of the IEEE International Conference on Systems, Mans and Cybernetics, 2019.
[18] K. Deb, L. Thiele, M. Laumanns, and E. Zitzler, "Scalable test problems for evolutionary multiobjective optimization," Evolutionary Multiobjective Optimization Theoretical Advances and Applications, pp. 105-145, 2005.
[19] R. Cheng, M. Li, Y. Tian, X. Zhang, S. Yang, Y. Jin, and X. Yao, "A Benchmark Test Suit for Evolutionary Many-objective Optimization," Complex Intell. Syst. Vol. 3, pp. 67–81, 2017.
[20] H. Ishibuchi H. Masuda Y. Tanigaki and Y. Nojima "Modified distance calculation in generational distance and inverted generational distance," in International Conference on Evolutionary Multi-Criterion Optimization. Springer, 2015, pp. 110–125.
[21] M. Ehrgott, "Approximation algorithms for combinatorial multicriteria optimization problems," International Transactions in Operational Research, vol. 7, no. 531, 2000

International Journal of Multidisciplinary Studies and Innovative Technologies

e-ISSN: 2602-4888
dergipark.org.tr/en/pub/ijmsit
Research Article

2022, 6 (1), 19-22
DOI: DOI: 10.36287/ijmsit.6.1.19
Received: May 12, 2022; Accepted: June 12, 2022

Weeds Detection using Deep Learning Methods and Dataset Balancing

Fadıl Arıkan[1*], Şebnem Bora [2] and Aybars Uğur [3]

[1*] *Department of Computer Engineering, Ege University, Izmir, Turkey (fadilarikan19664@gmail.com) (ORCID: 0000-0002-0101-1524)*
[2] *Department of Computer Engineering, Ege University, Izmir, Turkey (sebnem.bora@ege.edu.tr) (ORCID: 0000-0003-0111-4635)*
[3] *Department of Computer Engineering, Ege University, Izmir, Turkey (aybars.ugur@ege.edu.tr) (ORCID: 0000-0003-3622-7672)*

Abstract – Weeds have detrimental effects on agriculture and prove costly for farmers because they can quickly spread to fertile areas and reduce the fertility of the soil. Therefore, weed control is crucial for sustainable agriculture, and by detecting weeds and removing them from agricultural lands, we can transfer the limited resources we have to the plants to be grown, which would be a major step forward in sustainable agriculture. This article explores the feasibility of weed detection methods using deep learning architectures. Architectures used in the research are as follows: ResNet152V2, DenseNet121, MobileNetV2, EfficientNetB1 and EfficientNetB7. The F1-Score of EfficientNetB1 is 94.17\%, which is the highest score among those of all architectures. Among all architectures, EfficientNetB1 has the least number of parameters after MobileNetV2. In this research, data augmentation was done using horizontal flip, rotation, width shift, height shift, and zoom.

Keywords *– deep learning, weeds detection, EfficientNetB1, balanced dataset, sustainable agriculture*

Citation: Arıkan, F., Bora, Ş. and Uğur, A. (2022). Weeds Detection using Deep Learning Methods and Dataset Balancing. International Journal of Multidisciplinary Studies and Innovative Technologies, 6(1): 19-22.

I. INTRODUCTION

Weeds are difficult and expensive to control, and their presence threatens agricultural fields. On the other hand, weeds compete with useful plant species on agricultural lands. They also negatively affect the growers' harvest yields and reduce their incomes. Using herbicides to eliminate weeds is not only costly but also harmful to the environment and human health.

Herbicides are widely used against weeds to minimize their detrimental effects. However, these substances do not easily degrade in nature and their effects under various environmental conditions are still not clearly known (Ustuner, al Sakran, Almhemed[1]).

Deep learning is a type of machine learning that imitates the learning ability of the human brain, and it is one of the most preferred technologies by researchers today. Having led to the emergence of many intelligent systems, deep learning models are frequently used in various fields, especially in smart and sustainable agriculture.

Agriculture is becoming more important with each passing day due to many factors, including global warming, the decrease in freshwater resources, and rapid population growth. Therefore, studies in the field of agriculture are gaining momentum.

In their study, Selvi, Subramanian, and Ramachandran [2] pointed out three key points:

- Accurate classification using CNN for overlapping crops and weeds.
- For real-time classification, the model should be reliable and more robust.
- Reducing the rate of misclassification.

Mowla and Gok [3] studied weed detection with VGG16, VGG19, MobileNetV2, Xception, and DenseNet201 using transfer learning. The architectures used in this study and the relevant statistical information are provided below:

Singh, Rawat, and Ashu [5] used image processing and deep learning methods to detect weeds in agricultural crops. After obtaining the images with FarmBot, they pre-processed and trained them using Artificial Neural Network, and analyzed the results. This study made use of image segmentation, unlike other studies, and a total of 54 photographs. The accuracy is not 100\% according to the results of the study which, although, has shown that the plant species used in architectural education can be distinguished well enough.

- MobileNetV2: 2,257,984 parameters used / 88.27% test accuracy
- VGG16: 14,714,688 parameters used / 89.17% test accuracy
- VGG19: 20,024,384 parameters used / 87% test accuracy
- Xception: 20,861,480 parameters used / 88.27% test accuracy
- DenseNet201: 18,321,984 parameters used / 92.42% test accuracy

- CovWNET (created in the experiment): 3,087,966 parameters used / 90.7% test accuracy

DenseNet201 gave the best results in this study.

Jabir, Noureddine, Sarih and Tannouche [4] investigated the weed status in sugar beet fields. They used 9,260,230 parameters in the CNN architectures they developed, and obtained a validation accuracy value of 73%, which they increased to 82% by optimizing the architecture and increasing the amount of data.

Singh, Rawat, and Ashu [5] used image processing and deep learning methods to detect weeds in agricultural crops. After obtaining the images with FarmBot, they pre-processed and trained them using Artificial Neural Network, and analyzed the results. This study made use of image segmentation, unlike other studies, and a total of 54 photographs. The accuracy is not 100% according to the results of the study which, although, has shown that the plant species used in architectural education can be distinguished well enough.

In a study conducted by Diaz, Castaneda, and Vassallo [6] on plant classification in precision agriculture, accuracy values were compared using deep learning architectures. In the study, pre-trained models such as InceptionV3, VGG16 and Xception were preferred. With a runtime of around 741 seconds and an accuracy score of 86.21%, Xception proved to be more efficient than other models.

Conducted to find an answer to the question "Which pre-trained model is more accurate on the balanced dataset for plant identification?", the research is divided into 5 sections. The section numbers and their contents are as follows:

- Section 2: characteristics of the data set
- Section 3: the method used in the research
- Section 4: results
- Section 5: conclusion

II. MATERIALS AND METHOD

A. Dataset Description

According to the literature review, Giselsson et al. [7] used the "Plant Seedlings Dataset", which is an open data source. This dataset consists of 12 different species and 960 unique weeds found in Denmark. It also contains 5539 photos in total, which are RGB photos with a resolution of 10 pixels per mm. The plants were grown in a laboratory environment and photographed at regular intervals. Styrofoam boxes were used to enlarge the samples, images were created at intervals of 2 to 3 days, starting a few days after the plants emerged, over a total period of 20 days, and a fixed dSLR camera (Canon 600D) was used to photograph the plants.

In this study, the dataset named "Plant Seedlings Dataset" was chosen to be used, and since some images in the first version of the dataset contained more than one plant, the second version was preferred. In order to balance the dataset, we both increased the amount of data using the data augmentation method for the types with missing data, and also reduced the amount of data by deleting the data from the types with large amounts of data. The image shapes of the data created by data augmentation are set to be (66,66,3). The batch size of these photos is 40. Horizontal flip was applied to the photographs in the training and validation dataset created by data augmentation. Rotation range was chosen as 20, width and height shift range and zoom range as 0.2. In addition, photos were reduced by deleting the data from types with a large amount of data.

Table 1. V2 Plant Seedlings Categories[7]

Plants	Original	Balanced
Black-grass	309	500
Charlock	452	500
Cleavers	335	500
Common Chickweed	713	500
Common wheat	253	500
Fat Hen	538	500
Loose Silky-bent	762	500
Maize	257	500
Scentless Mayweed	607	500
Shepherd's Purse	274	525
Small-flowed Cranesbill	576	500
Sugar beet	463	500

B. Method

For our experiment, we used the online community called Kaggle, and chose the aforementioned dataset because it was available for use in the competition and also user friendly. On this website, we first loaded the dataset in our own notebook and subsequently balanced our dataset as shown in Figure 1 and Figure 2, after which the training/testing split ratio was 90:10 and the validation ratio was 10. We divided the dataset into train, test and validation, and we had 5422 data in train set, 485 data in test set and 603 data in validation set. Then, we added the model we plan to use to the system. We used deep learning models such as ResNet152V2, MobileNetV2, DenseNet121, EfficientNetB1, EfficientNetB7. The sizes and parameters of the architectures used are shown in Table 2.

Fig. 1. Dataset before balanced

Shepherd's Purse	525
Sugar beet	500
Charlock	500
Black-grass	500
Loose Silky-bent	500
Cleavers	500
Common wheat	500
Maize	500
Common Chickweed	500
Small-flowered Cranesbill	500
Scentless Mayweed	500
Fat Hen	500

Fig. 2. Dataset after balanced

Table 2. Features of architectures[8]

Model	Size(MB)	Parameters(M)
ResNet152V2	232	60.4
MobileNetV2	14	3.5
DenseNet121	33	8.1
EfficientNetB1	31	7.9
EfficientNetB7	256	66.7

In addition to using many parameters (for optimization purposes) for the models and making sure that these parameters were the same for each model, we also chose the weight used in the models as 'imagenet' and set the models' metric as accuracy. Furthermore, we set the dropout value as 45% and also chose softmax because in this activation function, there is multiple classification in outputs. We initially thought of it as 40 epochs and decided to stop the training when more than 3 epochs fell. We chose the Learning Rate as 0.001 and preferred to reduce it according to the state of the training, during which we observed the loss and accuracy parameters. At the end of the training, we had the values plotted on the chart, and finally prepared the model's confusion matrix and classification report.

III. Results

In Table 3 and Table 4, EfficientNetB1[9] delivered great performance as the 2nd architecture with the lowest size and parameter among the architectures.

In this research, we aimed for maximum f1-score and accuracy among the selected architectures on the balanced dataset. In Table 4, the highest values occurred in the EfficientNetB1 model.

Table 3. Unbalanced Dataset Comparison Based on Accuracy, F1-Score, Precision and Recall

Model	Accuracy	F1-Score	Precision	Recall
ResNet152V2	89.35%	87.83%	88.58%	87.25%
MobileNetV2	88.27%	85.83%	86.92%	85.50%
DenseNet121	92.06%	90.17%	92.08%	89.25%
EfficientNetB1	**93.32%**	**92.17%**	**93.08%**	**91.50%**
EfficientNetB7	90.25%	89.50%	90.83%	88.67%

Table 4. Balanced Dataset Comparison Based on Accuracy, F1-Score, Precision and Recall

Model	Accuracy	F1-Score	Precision	Recall
ResNet152V2	91.34%	90.42%	90.50%	90.42%
MobileNetV2	90.52%	90.08%	90.50%	89.58%
DenseNet121	93.61%	93.17%	93.50%	93.33%
EfficientNetB1	**94.85%**	**94.17%**	**94.42%**	**94.08%**
EfficientNetB7	93.40%	93.42%	94.08%	93.00%

In Table 3 and Table 4, the use of balanced dataset seems to give better results in models. An average of 2% increase can be seen in the EfficientNetB1 model, which has the highest accuracy and f1-score value. There is an increase in other models as well.

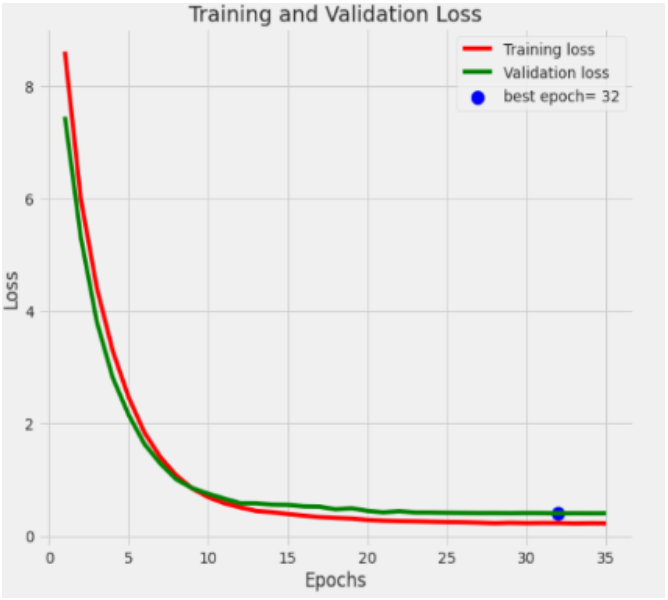

Fig. 3. Train and Validation Loss of EfficientNetB1

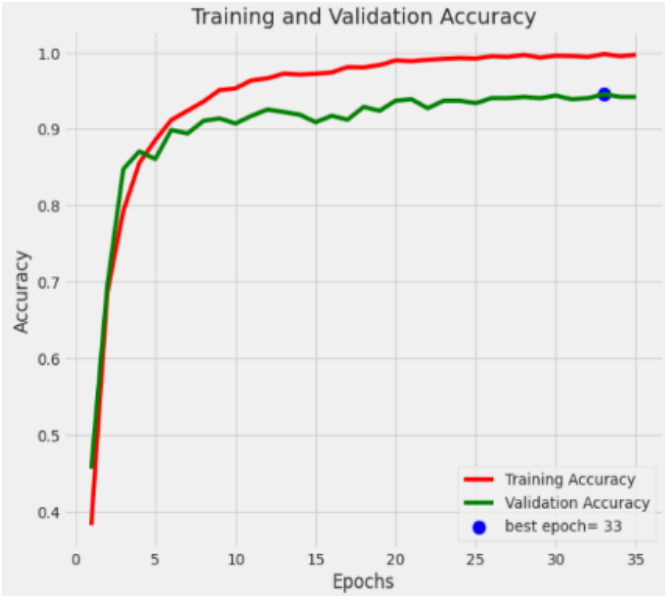

Fig. 4. Train and Validation Accuracy of EfficientNetB1

In Figure 3, the loss value of EfficientNetB1 has decreased continuously and remained at a low value, constantly

approaching zero, while in Figure 4, the accuracy value of EfficientNetB1 has increased continuously despite its fluctuating behaviour. They have reached a balanced state over time without any inconsistency between train and validation accuracy values.

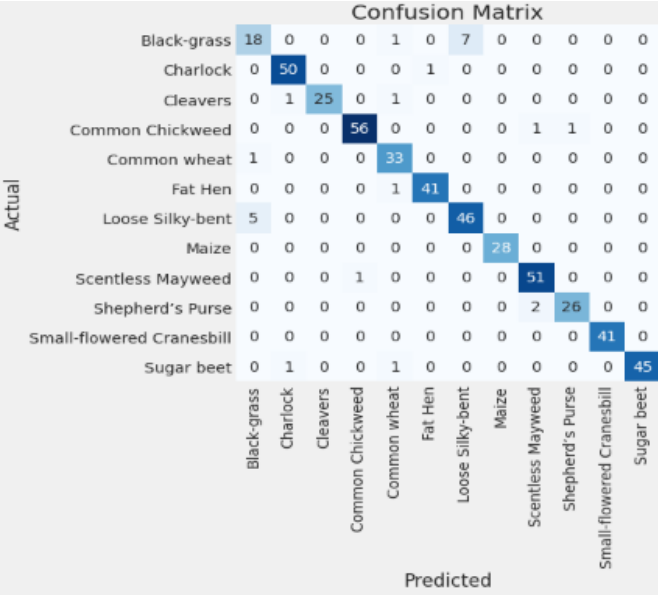

Fig. 5. Confusion Matrix of EfficientNetB1

The values of EfficientNetB1 in the confusion matrix are provided in Figure 5, and it can be observed that Black-Grass is the type with the highest number of errors, and it misclassified 8 photos.

Classification Report:

	precision	recall	f1-score	support
Black-grass	0.75	0.69	0.72	26
Charlock	0.96	0.98	0.97	51
Cleavers	1.00	0.93	0.96	27
Common Chickweed	0.98	0.97	0.97	58
Common wheat	0.89	0.97	0.93	34
Fat Hen	0.98	0.98	0.98	42
Loose Silky-bent	0.87	0.90	0.88	51
Maize	1.00	1.00	1.00	28
Scentless Mayweed	0.94	0.98	0.96	52
Shepherd's Purse	0.96	0.93	0.95	28
Small-flowered Cranesbill	1.00	1.00	1.00	41
Sugar beet	1.00	0.96	0.98	47
accuracy			0.95	485
macro avg	0.94	0.94	0.94	485
weighted avg	0.95	0.95	0.95	485

Fig. 6. Classification Report of EfficientNetB1

In Figure 6, precision, recall and f1-score values of each plant species for the EfficientNetB1 model are shown. Black-grass has the lowest Precision value, and the lowest f1-score.

IV. CONCLUSION

Weed detection is of vital importance to precision agriculture, and our aim in this article was to show that weed detection can be conducted with high accuracy using deep learning architectures on a balanced dataset. The models used in our study are pre-trained models and they are available in the Keras library [8].

Among these models, EfficientNetB1 got the highest results with 94.85% accuracy and 94.17% f1-score. It has not been fully optimized to avoid confusion in comparing models. We think that EfficientNetB1 can be useful for mobile applications due to the number and size of its parameters, and that studies can be conducted on robots working with higher accuracy by using different datasets and models. It is crucial that these datasets are from nature because it is necessary to observe how the model that is used behaves in real-time in the natural environment. Robots can be used for this purpose, and the technical aspects of weed detection methods can be improved. In conclusion, it is our understanding that deep learning applications will increase productivity in agriculture, making it possible to produce more crops using fewer natural resources.

REFERENCES

[1] Ustuner, Tamer \& al Sakran, Muhammad \& Almhemed, Kamal. (2020). Herbisitlerin Ekosistemde Canlı Organizmalar Uzerine Etkisi Ve Alternatif Mucadele Yontemleri. International Journal of Scientific and Research Publications (IJSRP). 10. 633641.

[2] C. T. Selvi, R. S. Sankara Subramanian and R. Ramachandran, "Weed Detection in Agricultural fields using Deep Learning Process," 2021 7th International Conference on Advanced Computing and Communication Systems (ICACCS), 2021, pp. 1470-1473, doi: 10.1109/ICACCS51430.2021.9441683.

[3] M. N. Mowla and M. Gok, "Weeds Detection Networks," 2021 Innovations in Intelligent Systems and Applications Conference (ASYU), 2021, pp. 1-5, doi: 10.1109/ASYU52992.2021.9599046.

[4] Jabir, Brahim \& Noureddine, Falih \& Sarih, Asmaa \& TANNOUCHE, Adil. (2021). A Strategic Analytics Using Convolutional Neural Networks for Weed Identification in Sugar Beet Fields. Agris on-line Papers in Economics and Informatics. 13. 49-57. 10.7160/aol.2021.130104.

[5] K. Singh, R. Rawat, and A. Ashu, "Image Segmentation in Agriculture Crop and Weed Detection Using Image Processing and Deep Learning Techniques", IJRESM, vol. 4, no. 5, pp. 235–238, Jun. 2021.

[6] C. A. Mamani Diaz, E. E. Medina Castaneda and C. A. Mugruza Vassallo, "Deep Learning for Plant Classification in Precision Agriculture," 2019 International Conference on Computer, Control, Informatics and its Applications (IC3INA), 2019, pp. 9-13, doi: 10.1109/IC3INA48034.2019.8949612.

[7] Giselsson, Thomas \& Jørgensen, Rasmus \& Jensen, Peter \& Dyrmann, Mads \& Midtiby, Henrik. (2017). A Public Image Database for Benchmark of Plant Seedling Classification Algorithms.

[8] (2022) Keras Applications. [Online]. Available: https://keras.io/api/applications/

[9] (2022) Balanced Data Coding. [Online]. Available: https://www.kaggle.com/gpiosenka/balance-data-with-augmentation-f1-score-93

International Journal of Multidisciplinary Studies and Innovative Technologies

e-ISSN: 2602-4888
dergipark.org.tr/en/pub/ijmsit
Research Article

2022, 6 (1), 23-28
DOI: 10.36287/ijmsit.6.1.23
Received: May 12, 2022; Accepted: June 12, 2022

Nesnelerin İnterneti Cihazlarına Karşı Yapılan Makine Öğrenmesi Saldırıları

Ahmet Emre ERGÜN[1*] ve Özgü CAN [2]

[1*]*Bartın Üniversitesi, Mühendislik, Mimarlık ve Tasarım Fakültesi, Bilgisayar Mühendisliği Bölümü, Bartın, Türkiye (aergun@bartin.edu.tr) (ORCID: 0000-0002-3025-5640)*
[2] *Ege Üniversitesi, Mühendislik Fakültesi, Bilgisayar Mühendisliği Bölümü, İzmir, Türkiye (ozgu.can@ege.edu.tr) (ORCID: 0000-0002-8064-2905)*

Türkçe Özet – Nesnelerin İnterneti (IoT) cihazlarının sayısının günden güne artmasıyla birlikte bu cihazlara yönelik yapılan saldırılar da artmaktadır. Bu çalışmada, IoT cihazlarında güvenliği sağlama yöntemleri ve IoT cihazlarına yönelik saldırılar ele alınmış, sıfır-güven mimarisinin IoT güvenliğini sağlamadaki önemi açıklanmıştır. Ayrıca, dolgu yöntemlerinin saldırganın kullandığı makine öğrenmesine karşı savunma oranları gösterilmiş ve makine öğrenmesi teknikleriyle kullanılan savunma yöntemleri anlatılmıştır. Bu amaçla, makine öğrenmesi yöntemlerinin etkili olduğu saldırılar, makine öğrenmesi teknikleriyle yapılan saldırılar ve oluşturulan ihlaller belirtilmiştir. Ek olarak, makine öğrenmesi tekniklerinin şifreli trafikte IoT cihazlarını sınıflandırmadaki etkinliği incelenmiştir. Rastgele Orman ve Karar Ağacı sınıflandırma algoritmalarının IoT cihazlarını sınıflandırmadaki etkinliği değerlendirilmiştir. Son olarak, yaygın kullanılan saldırı ve savunma yöntemleri için deneyler gerçekleştirilmiştir. Bu amaçla, IoT cihaz trafiği analiz edilerek dolgulu ve dolgusuz olarak yapılan deneylerin doğruluk oranları karşılaştırılmıştır. Dolgusuz verilere sınıflandırma yapıldığında IoT cihazlarının %84 doğruluk oranı elde edilirken, saldırganın doğru bilgiye erişme oranını düşürmeyi hedefleyen rastgele dolgu yöntemi ile bu doğruluk oranı %19'a düşürülmüştür.

Anahtar Kelimeler – Nesnelerin İnterneti; Makine Öğrenmesi; Dolgu; Şekillendirme; Sıfır-Güven Mimarisi; Sınıflandırma

Atıf: Ergün, A., Can, Ö. (2022). Nesnelerin İnterneti Cihazlarına Karşı Yapılan Makine Öğrenmesi Saldırıları. International Journal of Multidisciplinary Studies and Innovative Technologies, 6(1): 23-28.

Machine Learning Attacks Against Internet of Things Devices

Extended Abstract

As the number of Internet of Things (IoT) devices increases day by day, attacks against these devices are also increasing. In this study, methods of ensuring security in IoT devices and attacks on IoT devices are discussed, and the importance of zero-trust architecture in ensuring IoT security is explained. In addition, the defense rates of padding methods against machine learning used by the attacker are shown and the defense methods used with machine learning techniques are explained. For this purpose, machine learning methods that are effective on attacks, attacks and violations that are achieved by machine learning techniques are specified. In addition, the effectiveness of machine learning techniques in classifying IoT devices in encrypted traffic is examined. The effectiveness of Random Forest and Decision Tree classification algorithms in classifying IoT devices are evaluated. Finally, experiments are carried out for commonly used attack and defense methods. For this purpose, the accuracy rates of the padded and unpadded experiments are compared by analyzing the IoT device traffic. When classifying unpadded data, 84% accuracy rate of IoT devices is achieved, while this accuracy rate has been reduced to 19% with the random padding method that aims to reduce the attacker's rate of accessing correct information.

Keywords – Internet of Things; Machine Learning; Padding; Shaping; Zero-Trust Architecture; Classification

Citation: Ergün, A., Can, Ö. (2022). Machine Learning Attacks Against Internet of Things Devices. International Journal of Multidisciplinary Studies and Innovative Technologies, 6(1): 23-28.

I. GİRİŞ

Nesnelerin İnterneti (*Internet of Things*, IoT), İnternet aracılığıyla diğer cihaz ve sistemlere bağlanarak veri alışverişi yapmak üzere sensörler, yazılımlar ve diğer teknolojilerle oluşturulan fiziksel nesnelerin ağını tanımlar. IoT cihazlarının günümüzde popülerliğinin ve kullanım talebinin artması nedeniyle, bağlantılı IoT cihazlarının toplam sayısının 2030 yılına kadar yaklaşık 80 milyara ulaşacağı tahmin edilmektedir [1].

Teknolojik gelişmelerin ilerlemesi ve IoT cihazlarının gerekliliğinin artmasıyla birlikte ağ ortamına bağlı bu cihazların kullanımının getirdiği güvenlik sorunları mevcuttur.

Verilerin gizliliğini, bütünlüğünü ve kullanılabilirliğini hedef alan saldırıların önlenmesi için güvenlik önlemleri kullanmak önemlidir. Makine öğrenmesi yöntemleri sayesinde önlemler daha etkin bir hale getirilebilmektedir. Makine öğrenmesi yöntemleri güvenliği sağlamakta kullanılabildiği gibi güvenlik sorunlarına yol açan saldırılarda da kullanılabilmektedir.

Bu çalışmada, IoT cihazlarının güvenliğini sağlamaya yönelik önlemler ve IoT cihazlarına karşı yapılan saldırılar değerlendirilmiştir. Makine öğrenmesinin yalnızca güvenliği sağlamada değil saldırılarda da kullanılabileceği belirtilmiştir. Bu çalışmanın hedefi doğrultusunda hangi makine öğrenmesi tekniğinin hangi güvenlik önlemini sağlamada ve hangi makine öğrenmesi tekniğinin hangi saldırıda daha etkin olduğu açıklanmıştır.

Öncelikle, IoT saldırılarına karşı yaygın kullanılan güvenlik önlemleri anlatılmıştır. Bir sonraki bölümde, makine öğrenmesi temelinde kullanılan güvenlik önlemleri açıklanmıştır. Daha sonra, Makine öğrenmesi ile IoT'ye yönelik yapılan saldırılar ve hedef aldığı ihlaller ele alınmıştır. Son olarak, makine öğrenmesi algoritmalarının saldırı ve güvenlik yönünden etkinliği değerlendirilmiştir.

Bu çalışmanın organizasyonu şu şekildedir: ikinci bölümde sıfır-güven (*zero-trust*) mimarisi, dolgu (*padding*) ve şekillendirme (*shaping*) yöntemleri, güvenliği sağlamaya yönelik olarak kullanılan makine öğrenmesi yöntemleri ve makine öğrenmesi tabanlı IoT saldırıları açıklanmış, üçüncü bölümde Rastgele Orman ve Karar Ağacı sınıflandırıcı algoritmalarının dolgulu ve dolgusuz doğruluk performansları değerlendirilmiş ve dördüncü bölümde tartışma ve sonuç sunulmuştur.

II. MATERYAL VE METOTLAR

A. *Yaygın Kullanılan Güvenlik Önlemleri*

IoT cihazlarında güvenliği artırmak için sıfır-güven ilkesini temel alan sıfır-güven mimarisi ve paket boyutlarını değiştirerek makine öğrenmesi modellerini yanıltmayı amaçlayan dolgu ve şekillendirme yöntemleri kullanılabilmektedir.

1. Sıfır-Güven Mimarisi

IoT güvenliğini sağlamak için tüm ağ altyapısı boyunca görünürlük, segmentasyon ve kesintisiz koruma sağlayabilen entegre çözümler gereklidir. Her zaman doğrulamayı ve hiçbir zaman güvenmemeyi esas alan sıfır-güven modelinde, içerideki veya dışarıdaki ağdan gelebilecek verilerin hiçbirine güvenilmemektedir [2]. Ağlara uzaktan erişimin artmasıyla birlikte, IoT cihazlarını korumak için sıfır-güven yaklaşımı önem kazanmaktadır. Sıfır-güven mimarisinde, sıfır-güven erişim ilkesini kullanan Rol Tabanlı Erişim Denetimi, kullanıcılara görevleri için gereken minimum ağ erişimi düzeyini sunarken ağın diğer bölümlerine erişmelerini veya bunları görmelerini engellemek için en az erişim ilkesini kullanan sıfır-güven erişimi, ağ erişim yönetiminin kritik bir bileşenidir. Sıfır-güven mimarisi ayrıca tüm ağ bileşenlerinin kapsamlı yönetim kontrolünü ve görünürlüğünü geliştirmek ve sürdürmek için birbirine bağlı akıllı cihazların kimlik doğrulamasını sağlayabilmektedir [3].

2. Dolgu

IoT trafiği şifreli olsa da ağdaki pasif trafik izleyicilerinin ağı gözetleyerek ağdan elde ettiği verilerle makine öğrenmesi yöntemleri kullanarak ağ trafiğinin gizliliğini ihlal etmesi mümkündür. Saldırganın, IoT cihazları tarafından oluşturulan trafiği makine öğrenmesi yöntemleriyle sınıflandırmasını mümkün olduğunca yanıltmak ve aynı zamanda trafiği sekteye uğratmamak için bantgenişliğini ayarlamak önemlidir. Bu nedenle, mahremiyet ve fayda arasındaki dengeyi sağlamak için saldırganı yanıltırken, mümkün olan en düşük dolgu yöntemini uygulamak gerekmektedir. Dolgu yöntemi, trafikteki paketlerin boyutuna ekstra boyut ekleyerek, saldırganın cihazlar hakkında bilgi sahibi olmak üzere makine öğrenme modeline girmek üzere ele geçirdiği trafiğin, öğrenmeyi yanıltmak için değiştirilmesidir. Rastgele Orman (*Random Forest,* RF) makine öğrenmesi tekniği kullanılarak ağın içindeki ve dışındaki saldırgan tarafından IoT cihazının doğru bir şekilde tespit edilmesine yönelik gerçekleştirilen çalışmanın [4] sonuçları Tablo 1'de sunulmaktadır.

TABLO 1. Rastgele Orman modeli için doğruluk oranları [4]

	Ağ dışındaki saldırgan	**Ağ içindeki saldırgan**
Dolgusuz	%96	-
Seviye-100 Dolgu	%32,77	%66,03
Seviye-500 Dolgu	%14,28	%52,18
Seviye-700 Dolgu	%5,94	%50,38
Seviye-900 Dolgu	%4,96	%49,83

Tablo 1'de sunulan sonuçlar için 21 cihazın 20 günlük trafikten oluşturduğu veri seti [5] kullanılmıştır. İlgili çalışmada [4], ağ dışındaki saldırgan bir ağ içindeki etkinlikleri izlemekte, ağ içindeki saldırgan dolgu yönteminin sağlayıcısı olup, sahip olduğu ağın kullanıcılarını izlemektedir. Bir saniyelik zaman pencerelerinde gruplanmış şifreli trafiğin standart sapma, ortalama ve toplam büyüklüklerini kullanan saldırganın bir IoT cihazını tanımlama doğruluk oranı dolgudan önce %96 iken seviye-900 dolgudan sonra %4,96'ya düşmektedir. Böylelikle, gerçek paket uzunluğuna dolgu eklenerek oluşturulan sahte paket boyutu ile saldırganın öğrenme modeli yanıltılabilmektedir.

3. Şekillendirme

IoT trafiğinin trafik analizi saldırısına karşı korunması için trafiği şekillendirmek etkili bir yöntemdir. Trafik şekillendirmesi, trafiğe sahte paketler ekleyerek kullanıcı etkinliğinin çıkarımının yapılmasını önlemeyi sağlamaktadır. [6] çalışmasında Stokastik Trafik Dolgusu (*Stochastic Traffic Padding, STP*) algoritmasına dayalı trafik şekillendirme yöntemi önerilmektedir. Böylelikle, kullanıcı aktivitesi olmadığında bile trafik periyotlarını belirli aralıklarla dolgulayarak saldırganın hangi zaman periyotlarında gerçek trafik etkinliğinin olduğunu algılaması önlenmektedir. STP, farklı cihazlar ve kullanıcı etkinliği frekansları için trafik bant genişliği yükü ve saldırganın kendinden eminliği arasında ayarlanabilir bir denge sağlamaktadır. Bant genişliği yükü artırılarak saldırganın IoT cihaz tespit doğruluk oranı %50'den %10'a düşürülmüştür.

B. *Makine Öğrenmesi Temelinde Kullanılan Güvenlik Yöntemleri*

Teknolojik gelişmeler sayesinde IoT cihazlarının ağ güvenliğini sağlama olanakları artmaktadır. Yaygın kullanılan IoT saldırılarına karşı makine öğrenmesi yöntemlerinin

kullanılması IoT güvenliğini sağlamak için önemlidir. Doğrulama, erişim kontrolü ve kötü amaçlı yazılım algılama gibi işlemlerin öğrenme tabanlı yapılması ile IoT güvenliği sağlanabilmektedir [7,8]. Bu kapsamda, [7] çalışmasında öğrenme temelli kimlik doğrulama, güvenli yük boşaltma (*secure offloading*), kötü amaçlı yazılım tespiti ve erişim kontrolü yöntemlerinin kullanımına yönelik detaylı bir karşılaştırma sunulmaktadır. Saldırganın makine öğrenmesi olanağına sahip olduğu durum dikkate alındığında, saldırgan makine öğrenmesine yönelik alınabilecek çeşitli önlemler bulunmaktadır [9].

Makine öğrenmesi temelli güvenlik önlemleri aşağıda belirtilmiştir:

- *Öğrenme Tabanlı Kimlik Doğrulama:* Sahtecilik (*spoofing*) ve Dinleme (*eavesdropping*) gibi saldırılara karşı etkilidir. Q-öğrenme tabanlı kimlik doğrulama, önceden bir eğitim veri seti gerektirmeden buluttaki ortamdan öğrenerek IoT cihazlarının kimlik doğrulama başarısını geliştirmesini sağlamaktadır [10].
- *Öğrenme Tabanlı Güvenli Yük Boşaltma:* Hizmet Reddi (*Denial of Service*, DoS) ve Karıştırma (*Jamming*) gibi saldırılara karşı etkilidir. Yük boşaltma, verilerin cihaz veya bulut gibi farklı platforma aktarılması işlemidir. IoT cihazları, Karıştırma ve Sahtecilik saldırılarına karşı yük boşaltma veri değerlerini seçmek için Q-öğrenme tabanlı güvenli yük boşaltmayı kullanmaktadır [11].
- *Öğrenme Tabanlı Kötü Amaçlı Yazılım Tespiti:* Virüs ve Trojan gibi kötü amaçlı yazılım saldırılarına karşı etkilidir. K-en yakın komşu algoritması (*K-Nearest Neighbors*, K-NN) ve Rastgele Orman algoritmaları kullanılarak kötü amaçlı yazılımların tespit edilmesine yönelik bir değerlendirmenin sunulduğu [12] çalışmasında, makine öğrenmesi sınıflandırıcılarının güncel en son kötü amaçlı yazılımları tespit edebildiği kanıtlanmaktadır.
- *Öğrenme Tabanlı Erişim Kontrolü:* DoS, Mahremiyet Sızıntısı ve Kötü amaçlı yazılım saldırılarına karşı etkilidir. Liteartürde, sızma tespiti için Destek Vektör Makinesi (*Support Vector Machine*, SVM) ve K-NN gibi makine öğrenmesi tekniklerinin kullanıldığı çalışmalar yer almaktadır [13].
- *Çekişmeli Eğitim Gradyanı (Adversarial Training Gradient):* Amaç, modelin dayanıklılığını artırmak için eğitim setine yanıltıcı veriler eklemektir. Ancak, kara-kutu (*black-box*) saldırısına karşı bu savunma stratejisi etkisizdir [9].
- *Aktarılabilirliği Engelleme (Blocking the Transferability):* Bu strateji, aktarılabilirlik özelliğini ortadan kaldırmayı ve bir saldırganın yanıltıcı eğitim verileri oluşturmasını önlemeyi amaçlamaktadır. Bu amaçla, eğitim kümesinin girişine bir "NULL" etiket sınıfı eklenmektedir. Sonuç olarak, sınıflandırıcı orijinal etikete daha az güvenir ve yanıltıcı verileri NULL olarak kategorize ederek reddeder [9].
- *Savunma-Üretici Çekişmeli Ağ (Defense-GAN):* Bu mekanizma, kara-kutu (*black-box)* ve beyaz-kutu (*white-box*) saldırılarında çalışmaktadır ve derin sinir ağlarını bozulmalara karşı korumaktadır Amaç, bir üretici çekişmeli ağ yardımıyla yanıltıcı örnekleri engellemektir [9].

C. Makine Öğrenmesi ile Yapılan IoT'ye Yönelik Saldırılar

Makine öğrenmesi teknikleri kullanarak IoT cihazlarındaki trafiğin manipüle edilmesi veya trafik şifreli olsada trafikteki bilgilerin ele geçirilip mahremiyete tehdit olarak kullanılması mümkündür. Saldırganların, makine öğrenmesi tekniklerini IoT ortamlarında yaygın olarak kullanmalarında mahremiyeti ihlal etmeye, sistemi aksatmaya veya yanıltmaya yönelik amaçları bulunmaktadır. Makine öğrenmesi algoritmaları üç kategoride incelenmektedir. Bu kategorilerden, IoT saldırılarında yaygın kullanılan makine öğrenmesi algoritmaları aşağıda belirtilmiştir:

- *K-En Yakın Komşu (K-NN):* Gözetimli öğrenme (*supervised learning*) algoritmasıdır. Bir veri noktasının, kendisine en yakın veri noktalarının hangi gruba ait olduğuna bağlı olarak bir grubun veya diğerinin üyesi olma olasılığını tahmin etmeye yarayan bir veri sınıflandırma yöntemidir.
- *K-Ortalama (K-Means):* Gözetimsiz öğrenme (*unsupervised learning*) algoritmasıdır. Temel amacı, gözlemler ile küme ağırlık merkezi arasındaki mesafelerin toplamını minimize etmek olan bir kümeleme algoritmasıdır.
- *Q-Öğrenmesi (Q-Learning):* Pekiştirmeli öğrenme (*reinforcement learning*) algoritmasıdır. Mevcut durum göz önüne alındığında yapılacak en iyi eylemi bulmaya çalışan bir algoritmadır.

Makine öğrenmesi kategorilerine ait saldırıların oluşturduğu ihlaller ve saldırı türleri Tablo 2'de gösterilmiştir [9]. Gizlilik, Bütünlük ve Kullanılabilirlik ihlallerine yol açan saldırılar ve bu saldırıların hangi makine öğrenmesi kategorisi yoluyla yapıldığı Tablo 2'de sunulmaktadır.

TABLO 2. Makine Öğrenmesi Kategorilerine Göre Saldırı Örnekleri

	Gözetimli Öğrenme	**Gözetimsiz Öğrenme**	**Pekiştirmeli Öğrenme**
İhlaller	Gizlilik ve Mahremiyet İhlali	Bütünlük İhlali	Kullanılabilirlik İhlali
Saldırılar	Trafik Analizi Kriptanaliz Yan Kanal Sosyal Ağ	Kaçınma (*Evasion*) Nedensel (*Causative*) Keşif (*Exploratory*) Sahte Enjeksiyon Kod Enjeksiyonu	Sahtecilik (*Spoofing*) Karıştırma (*Jamming*) Kara Delik (*Blackhole*)

1. Mahremiyet İhlali

Kullanıcıların hassas bilgilerini kötüye kullanım ile ciddi sonuçlara yol açabilecek mahremiyete yönelik saldırılarda mümkündür [14]. Şifrelenmiş IoT trafiğindeki şifrelenmiş paketlerin boyutları makine öğrenmesi teknikleri kullanılarak IoT cihazları ve trafiği hakkında bilgilere erişilebilmektedir [4,15,16].

Makine öğrenmesi teknikleriyle şifrelenmiş verileri sınıflandırmaya karşı dolgu ve şekillendirme yöntemleri kullanılsa da saldırıya uğrayan bir ağdaki cihazlar ve etkinlikler tanımlanabilmektedir. [17]'de sunulan çalışmada,

saldırganın dolgulu ve şekillendirilmiş trafiğe eriştiğinde K-NN algoritmasıyla %81 doğruluk oranında IoT cihazlarını bir saniyelik zaman penceresi düzeyinde ayırt edebildiği gösterilmektedir. Tablo 3'de [17] çalışmasında cihaz sayılarına göre gerçekleştirilen sınıflandırmaların doğruluk oranları gösterilmektedir. Elde edilen sonuçlar doğrultusunda, cihaz sayısı arttıkça doğruluk oranının azaldığı görülmektedir.

TABLO 3. Cihaz sayılarına göre doğruluk oranları [17]

Cihaz Sayısı	Doğruluk Oranı
5	%81
10	%77
14	%75

2. *Bütünlük ve Kullanılabilirlik İhlali*

IoT cihazlarının kullanımı yaygınlaştıkça yeni güvenlik riskleri ortaya çıkmaktadır. Saldırgan, IoT trafiğini izleyerek elde ettiği veriler doğrultusunda cihazların taklit edilmesini veya ağın akışını bozacak şekilde manipüle edilmesini makine öğrenmesi yöntemleri ile sağlayabilmektedir. Böylece saldırgan IoT cihazlarındaki trafiğin bütünlüğünü ve kullanılabilirliğini ihlal etmiş olmaktadır. Sosyal mühendislik saldırıları, keşif saldırısı, Hizmet Reddi (*Denial of Service, DoS*) ve Ortadaki Adam Saldırısı (*Man in the Middle Attack*) gibi saldırıların yanında makine öğrenmesini kullanarak bir saldırgan, bir kullanıcıyı veya sistemi taklit ederek IoT cihazlarını yanıltabilir, sekteye uğratabilir veya hassas bilgileri ele geçirebilir [3,19-22].

Saldırganın IoT cihazlarının yalnızca küçük bir bölümünü kontrol ederek veri füzyonunda karar vermeyi etkilediği çekişmeli makine öğrenmesi (*adversarial machine learning)* tabanlı kısmi model (*partial-model*) saldırısı [21] çalışmasında sunulmaktadır. [22] çalışmasında sunulan çekişmeli makine öğrenmesi üzerine oluşturulan yeni teknikler, karıştırma (*jamming*), spektrum zehirlemesi (*spectrum poisoning*), ve öncelik ihlali (*priority violation*) saldırılarına uygulanmıştır. Saldırgan derin yapay sinir ağı sınıflandırıcı kullanarak bir IoT veri aktarıcısının kanal erişim algoritmasını çıkarmak için keşif (*exploratory*) saldırısını ve bu tahmin sonuçlarına dayanarak veri aktarıcısını test aşamasında yanıltmak için kaçınma (*evasion*) saldırısını kullanmaktadır. IoT aktarıcısı kanal erişim algoritmasını yeniden öğrenme işlemi için eğittiği sırada saldırgan nedensel (*causative*) saldırısıyla aktarıcıya giden verileri manipüle etmektedir.

III. BULGULAR

Bu bölümde, makine öğrenmesi yöntemleri kullanarak mahremiyet ihlaline yol açan saldırgan ve bu ihlali dolgu yöntemi ile önlemeye çalışan kurban ele alınmaktadır. Bu doğrultuda, [5] çalışmasında yer alan veri seti kullanılarak Rastgele Orman ve Karar Ağacı algoritmalarına karşı dolgu yöntemlerinden biri olan rastgele dolgunun etkinliği gösterilmiştir. Rastgele Orman ve Karar Ağacı sınıflandırıcı algoritmalarının dolgu olmadan performansı ve rastgele dolgu olduktan sonraki doğruluk oranları Tablo 4'de verilmiştir. Test verilerinin her bir paketinin uzunluğu kendi uzunluğu ve 1600 bayt arasında rastgele bir değere atandığı rastgele dolgu yöntemine karşı alınan doğruluk oranları ve eğitim(*train*)-test verilerine dolgu yapılmayan dolgusuz yönteme karşı alınan doğruluk oranları gösterilmiştir [23].

TABLO 4. Algoritmalara göre doğruluk oranları.

	Dolgusuz	Rastgele Dolgulu
Rastgele Orman	%83,3	%23
Karar Ağacı	%84,2	%19,8

Bu çalışmada gerçekleştirilen deneylerde, [5] çalışmasında oluşturulan veri seti kullanılmıştır ve bu veri setlerinden beş cihazın trafik analizi yapılmıştır. Eğitim ve test dosyalarındaki cihazların sayısal dağılımı Şekil 1 ve Şekil 2'deki grafiklerde gösterilmektedir.

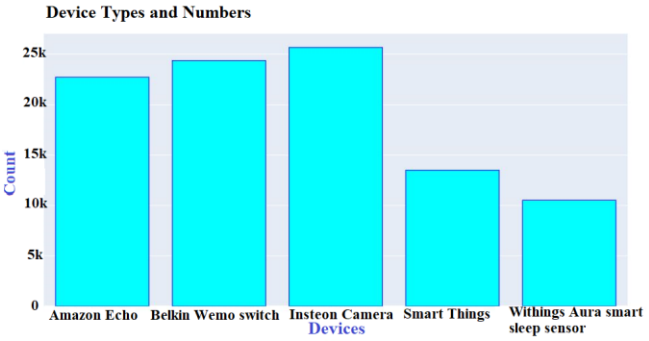

Şekil 1.Train Cihazları ve Sayıları

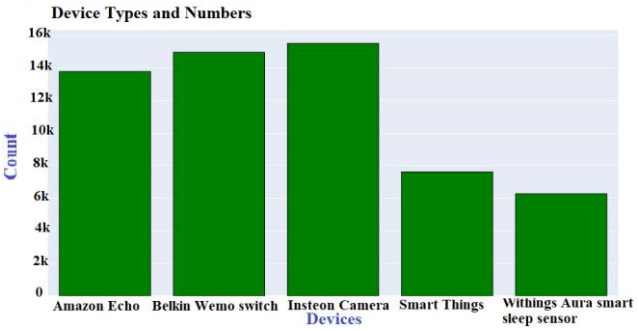

Şekil 2. Test Cihazları ve Sayıları

Rastgele Orman algoritmasıyla yapılan analizdeki karışıklık matrisleri (*confusion matrix*) Şekil 3 ve Şekil 4'de gösterilmektedir.

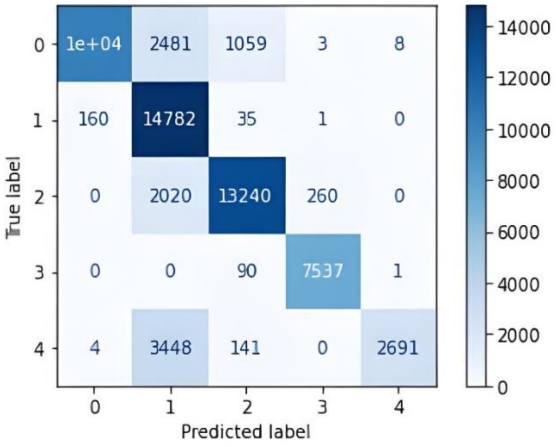

Şekil 3. Dolgusuz Rastgele Orman Karışıklık Matrisi

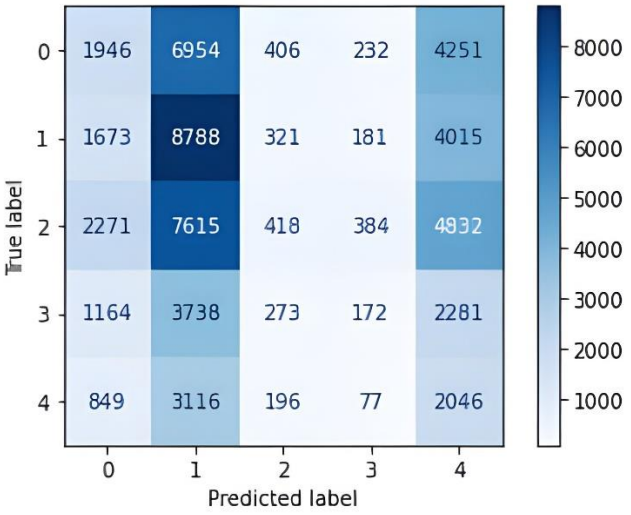

Şekil 4. Rastgele Dolgulu Rastgele Orman Karışıklık Matrisi

Karar Ağacı algoritmasıyla yapılan analizdeki karışıklık matrisleri Şekil 5 ve Şekil 6'da gösterilmektedir.

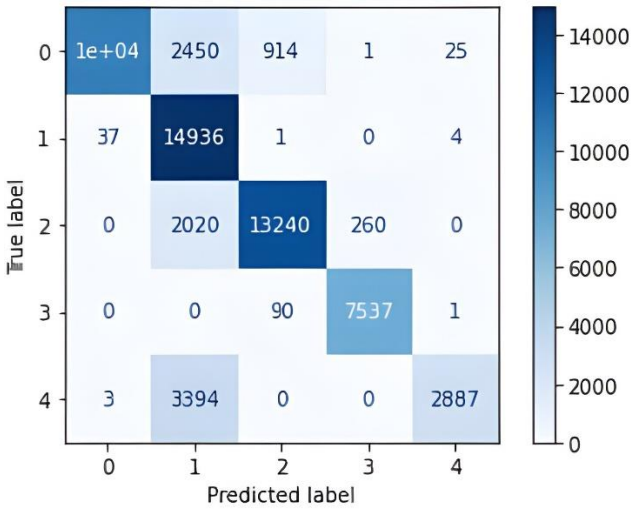

Şekil 5. Dolgusuz Karar Ağacı Karışıklık Matrisi

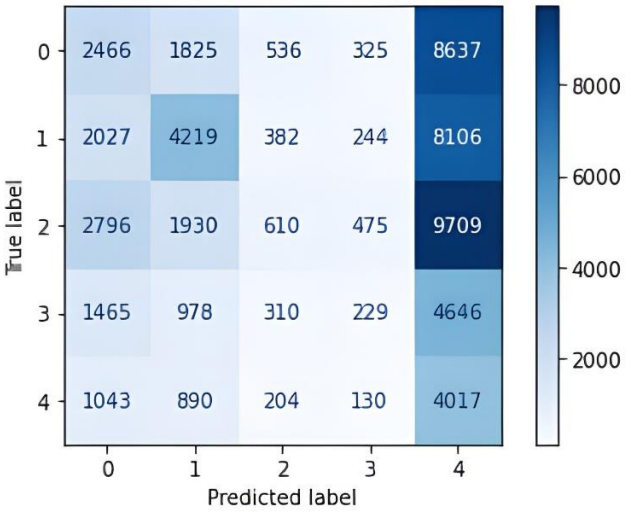

Şekil 6. Rastgele Dolgulu Karar Ağacı Karışıklık Matrisi

Rastgele dolgu ile saldırganın doğruluk oranının her iki sınıflandırıcı için azaldığı gözlemlenmiştir. Dolgusuz yapılan analizlerde Karar Ağacı sınıflandırma algoritması %84,2 doğruluk oranına sahipken Rastgele Orman sınıflandırma algoritması %83,3 doğruluk oranına sahiptir. Rastgele Orman algoritması rastgele dolgu %23 doğruluk oranı ile Karar Ağacı'nın %19,8 doğruluk oranından daha etkili olduğu görülmüştür.

IV. SONUÇ

Makine öğrenmesi yöntemleri saldırılara karşı savunma amacı ile de kullanılmaktadır. Bu çalışmada, IoT'ye yönelik yapılan saldırıların makine öğrenmesiyle daha etkili hale geleceği ve uygulanabilecek saldırıların hangi amaçla kullanılabileceği belirtilmiş ve bu saldırılara karşı alınabilecek önlemler açıklanmıştır. Ek olarak, hangi makine öğrenmesi tekniğinin hangi saldırılarda daha etkili olduğu ve hangisinin saldırılara karşı savunmada daha etkili olduğuna yönelik bir değerlendirme sunulmuştur.

Bu çalışmada ayrıca, IoT cihazlarında mahremiyete yönelik makine öğrenmesi ile yapılan sınıflandırma ve buna karşı alınabilecek dolgu yöntemlerinden biri olan rastgele dolgu yöntemi kullanılarak bir deney gerçekleştirilmiştir. Yaygın kullanılan bir sınıflandırıcı algoritması olan ve içinde çokça Karar Ağacı bulunduran Rastgele Orman algoritmasının dolgulu verilerdeki etkinliği gözlemlenmiştir. Rastgele dolgu yöntemine karşı Rastgele Orman algoritmasının %23 doğruluk oranı ile Karar Ağacı'nın %19,8 doğruluk oranından daha etkili olduğu görülmüştür. Rastgele Orman algoritması eğitim aşamasında çok sayıda Karar Ağacı kullanması nedeni ile Karar Ağacı algoritmasına göre daha iyi sonuç vermiştir.

Gelecek çalışmalar kapsamında, IoT cihaz trafiğinde mahremiyet, bütünlük ve kullanılabilirlik ihlallerine karşı optimal ve güvenilir bir savunma yöntemi geliştirilmesi hedeflenmektedir.

KAYNAKLAR

[1] Chettri, L., & Bera, R. (2019). A comprehensive survey on Internet of Things (IoT) toward 5G wireless systems. *IEEE Internet of Things Journal*, *7*(1), 16-32.

[2] Samaniego, M., & Deters, R. (2018, July). Zero-trust hierarchical management in IoT. In *2018 IEEE international congress on Internet of Things (ICIOT)* (pp. 88-95). IEEE.

[3] Lakhani, A. (2019, June 17). *Examining Top IoT Security Threats and Attack Vectors.* Fortinet. https://www.fortinet.com/blog/industry-trends/examining-top-iot-security-threats-and-attack-vectors

[4] Pinheiro, A. J., de Araujo-Filho, P. F., Bezerra, J. D. M., & Campelo, D. R. (2020). Adaptive Packet Padding Approach for Smart Home Networks: A Tradeoff Between Privacy and Performance. *IEEE Internet of Things Journal*, *8*(5), 3930-3938.

[5] Sivanathan, A., Gharakheili, H. H., Loi, F., Radford, A., Wijenayake, C., Vishwanath, A., & Sivaraman, V. (2018). Classifying IoT devices in smart environments using network traffic characteristics. *IEEE Transactions on Mobile Computing*, *18*(8), 1745-1759.

[6] Apthorpe, N., Huang, D. Y., Reisman, D., Narayanan, A., & Feamster, N. (2019). Keeping the smart home private with smart (er) iot traffic shaping. *Proceedings on Privacy Enhancing Technologies*, *2019*(3), 128-148.

[7] Xiao, L., Wan, X., Lu, X., Zhang, Y., & Wu, D. (2018). IoT security techniques based on machine learning: How do IoT devices use AI to enhance security?. *IEEE Signal Processing Magazine*, *35*(5), 41-49.

[8] Mohamed Shakeel, P., Baskar, S., Sarma Dhulipala, V. R., Mishra, S., & Jaber, M. M. (2018). Maintaining security and privacy in health care system using learning based deep-Q-networks. *Journal of medical systems*, *42*(10), 1-10.

[9] Bout, E., Loscri, V., & Gallais, A. (2021). How Machine Learning changes the nature of cyberattacks on IoT networks: A survey. *IEEE Communications Surveys & Tutorials*.

[10] Xiao, L., Li, Y., Han, G., Liu, G., & Zhuang, W. (2016). PHY-layer system using learning spoofing detection with reinforcement learning in wireless networks. *IEEE Transactions on Vehicular Technology*, *65*(12), 10037-10047.

[11] Xiao, L., Xie, C., Chen, T., Dai, H., & Poor, H. V. (2016). A mobile offloading game against smart attacks. *IEEE Access*, *4*, 2281-2291.

[12] Narudin, F. A., Feizollah, A., Anuar, N. B., & Gani, A. (2016). Evaluation of machine learning classifiers for mobile malware detection. *Soft Computing*, *20*(1), 343-357.

[13] Buczak, A. L., & Guven, E. (2015). A survey of data mining and machine learning methods for cyber security intrusion detection. *IEEE Communications surveys & tutorials*, *18*(2), 1153-1176.

[14] Zhang, Z. K., Cho, M. C. Y., Wang, C. W., Hsu, C. W., Chen, C. K., & Shieh, S. (2014, November). IoT security: ongoing challenges and research opportunities. In *2014 IEEE 7th international conference on service-oriented computing and applications* (pp. 230-234). IEEE.

[15] Sivanathan, A., Sherratt, D., Gharakheili, H. H., Radford, A., Wijenayake, C., Vishwanath, A., & Sivaraman, V. (2017, May). Characterizing and classifying IoT traffic in smart cities and campuses. In *2017 IEEE Conference on Computer Communications Workshops (INFOCOM WKSHPS)* (pp. 559-564). IEEE.

[16] Apthorpe, N., Reisman, D., Sundaresan, S., Narayanan, A., & Feamster, N. (2017). Spying on the smart home: Privacy attacks and defenses on encrypted iot traffic. *arXiv preprint arXiv:1708.05044*.

[17] Engelberg, A., & Wool, A. (2021). Classification of Encrypted IoT Traffic Despite Padding and Shaping. *arXiv preprint arXiv:2110.11188*.

[18] Trimananda, R., Varmarken, J., Markopoulou, A., & Demsky, B. (2020, February). Packet-level signatures for smart home devices. In *Network and Distributed Systems Security (NDSS) Symposium* (Vol. 2020).

[19] Ghasemi, M., Saadaat, M., & Ghollasi, O. (2019). Threats of social engineering attacks against security of Internet of Things (IoT). In *Fundamental research in electrical engineering* (pp. 957-968). Springer, Singapore.

[20] Yekkehkhany, A., Feng, H., & Lavaei, J. (2021, December). Adversarial Attacks on Computation of the Modified Policy Iteration Method. In *2021 60th IEEE Conference on Decision and Control (CDC)* (pp. 49-56). IEEE.

[21] Sagduyu, Y. E., Shi, Y., & Erpek, T. (2019, June). IoT network security from the perspective of adversarial deep learning. In *2019 16th Annual IEEE International Conference on Sensing, Communication, and Networking (SECON)* (pp. 1-9). IEEE.

[22] Luo, Z., Zhao, S., Lu, Z., Sagduyu, Y. E., & Xu, J. (2020, July). Adversarial machine learning based partial-model attack in IoT. In *Proceedings of the 2nd ACM Workshop on Wireless Security and Machine Learning* (pp. 13-18).

[23] Winter, P., Pulls, T., & Fuss, J. (2013, November). ScrambleSuit: A polymorphic network protocol to circumvent censorship. In *Proceedings of the 12th ACM workshop on Workshop on privacy in the electronic society* (pp. 213-224).

International Journal of Multidisciplinary Studies and Innovative Technologies

e-ISSN: 2602-4888
dergipark.org.tr/en/pub/ijmsit
Research Article

2022, 6 (1), 29-37
DOI: DOI: 10.36287/ijmsit.6.1.29
Received: March 31, 2022; Accepted: June 12, 2022

A Novel Student Performance Evaluation Model Based on Fuzzy Logic for Distance Learning

Beyza Esin Özseven[1*] and Naim Çağman[2]

[1*] *Tokat Gaziosmanpaşa University, Institute of Graduate Studies, Department of Mathematics, Tokat, Turkey (beyza_esin@hotmail.com) (ORCID: 0000-0003-4888-8259)*
[2] *Tokat Gaziosmanpaşa University, Institute of Graduate Studies, Department of Mathematics, Tokat, Turkey (naim.cagman@gop.edu.tr) (ORCID: 0000-0003-3037-1868*

Abstract – Distance learning is an education model in which the educator and the student come together independently of time and place and the learning process is continued. Although it has positive aspects in terms of time and space, it has limitations such as weak interaction and poor functioning of evaluation processes. Assessment systems often include multiple-choice or open-ended questions. In other words, the result is evaluated in solving a given problem, and the student's actions can be ignored until the result is reached. In this study, while evaluating student performance, the student's behavior during the semester and the distractor weight coefficient for multiple-choice exams were added, and a performance evaluation was made on the student's incorrect answers. The proposed model was created based on fuzzy logic, and the uncertainties in the evaluation were attempted to be eliminated.

Keywords *– distance learning, fuzzy logic, performance evaluation, e-learning, e-evaluation*

Citation: Esin Özseven, B., Çağman, B. (2022). A Novel Student Performance Evaluation Model Based on Fuzzy Logic for Distance Learning. International Journal of Multidisciplinary Studies and Innovative Technologies, 6(1): 29-37.

I. INTRODUCTION

Education is defined as the process of creating desired change in people's behavior intentionally and through their own experiences [1]. To ensure that the individual learns for life, first must be taught. Lifelong learning, on the other hand, can be achieved with developments in information and communication technologies and advances in educational technologies.

Distance learning is an education system in which the educator and the student do not share the same physical environment, without time constraints, synchronously or asynchronously with the help of information technologies, and which provides the opportunity for retrospective repetition [2]. Although distance learning has existed for many years, it has come to the fore and is used more due to the pandemic in 2020. According to UNESCO data, 91.3% of students at all educational levels worldwide were directly or indirectly affected by the pandemic. Some problems have also emerged with the widespread use of distance learning systems. The choice of the educational system to be used, performance evaluation, academic ethics, and attendance are the main educational problems. In addition to these, the inadequacy of technological infrastructures has emerged as a technical problem [3].

With the spread of artificial intelligence methods and their application in every field, they have also found application in educational sciences. Especially since fuzzy logic and inference systems achieve successful results in cases of uncertainty, they are used effectively in educational sciences and their use is increasing [4]. Different cognitive and affective structures of students, uncertainties in assessment and evaluation, and the development of educational technologies form the basis of the increase in artificial intelligence-based applications [5].

One of the important problems in distance learning is how to evaluate student success in problem-solving courses [6]. Current assessment systems often include multiple-choice or open-ended questions. That is, in solving a given problem, the result is evaluated, and the student's actions can be ignored until he reaches the result. When the purpose of the exams is to determine the learning level of the student and to evaluate only successful or unsuccessful lessons that include problem-solving, it will create uncertainty in the determination of the learning level. In such exams, the learning level of the student should be interpreted with more than two results. Fuzzy logic is one of the methods that can be used to provide this kind of evaluation and to remove uncertainty.

In this study, a fuzzy logic-based performance and exam evaluation model that interacts with students is presented to handle these uncertainties more effectively and to measure interaction. The presented model includes a fuzzy logic-based approach to determine the student's subject-based and end-of-term performance.

In the next section of the study, the situation in the literature was examined. In the third section, the materials and methods used for the proposed model are explained. In the fourth section, the obtained results are given. In the last section, the results and discussion are given.

II. Related Works

Distance learning, which started with the shorthand lesson in the Boston newspaper in 1728, was continued in 1833 with the letter composition lessons given to women by the Swedish University, and schools providing education by letter were established [7]. Then, in 1898, language education was given in Sweden [7]. Later, radio stations related to primary education and education by correspondence were established. With the development of technology, there has been a transition to the web-based distance learning model used today [7].

Currently, there are many studies on software used in distance learning [8]–[13]. In these studies, many software such as Big Blue Button, Openmeetings, Adobe Connect, Electa Live, Blackboard Collaborate, GoToTraning, Perculus, VMukti and WizIQ have been compared.

All the methods that an educator uses to get feedback during or after the learning process can be expressed as assessment and evaluation. Although assessment and evaluation are generally seen as the last stages of education, since learning involves a process, they are needed at every stage of the learning process [14]. For this reason, the evaluation carried out throughout the teaching process is for formative purposes and is aimed at determining the learning level of the student at the end-of-term or at the end-of-chapter. Final exams, assignments, or projects are included in the assessment for level determination [14].

In the literature, in studies for assessment and evaluation and student performance evaluation, artificial neural networks, deep learning, random forest, logistic regression, multilayer perceptron, naive bayes, support vector machines, C4.5, decision trees, k-means, JRIP, J48, k-NN, image processing, and fuzzy inference methods were used [4], [6], [15]–[46]. Since fuzzy logic-based work was done within the scope of the study, the studies carried out with this method are detailed below.

In the studies on performance evaluation, the effects of the educator [15], the exam software [17], [47], the student's movements on the system [20], the attendance status [48], the analysis of the question paper [18], the project evaluation [31], and the expression of the marginal scores with fuzzy inference [36] were mentioned.

Two membership functions and subject-based student scores were used in the study in which student performance was evaluated with fuzzy inference [19]. The fuzzy neural network was used in the study, which takes into account factors such as age, gender, education, past performance, working status, and working environment for the prediction of student performance [49]. In another fuzzy inference-based study, student answers were represented by 7 linguistic expressions as unanswered, very bad, bad, moderate, not bad, good, very good. The linguistic expressions of very good, good, not bad, moderate, bad, and very bad were used in the output of the fuzzy inference system [22]. In studies where fuzzy logic-based performance evaluation was conducted, performance evaluation was conducted using homework, quizzes, midterms, finals, watching videos, reading books, personal development, communication skills, and participation information [25], [26], [50]. While evaluating student performance, there are studies in which past learning levels are used together with the current situation [51], [52]. In these studies, back propagation fuzzy inference [51] and a combination of two fuzzy inference systems were used [52], [53]. In the study, which uses 4-valued feedback fuzzy logic to evaluate student achievement, each value represents the months of the educational process. The output of the system has four values: “more effort required”, “as expected”, “good” and “very good” [6]. In studies using fuzzy logic in order to eliminate the uncertainty in students' passing scores, the student's success or failure was graded using linguistic expressions [6], [36]. In another study, exam score, participation in forums, absenteeism were used as input parameters for fuzzy inference, and student performance was used as output parameter [45]. According to the results of the study, which examined the effects on the student's final exam performance with fuzzy logic, students with high online assessment grades and self-learning processes showed high performance on the final exam [40], [54]. Nor et al. (2021) compared the mathematics course achievement of students in two rural and urban schools with fuzzy logic. The fuzzy decision maker's inputs include midterm and trial exam grades, and the output includes 5 linguistic values (very weak, weak, moderate, good, and very good). A triangular membership function is used as a membership function [55]. Laksana et al. (2021) used fuzzy logic to determine the final grade of university students. The passing grade was evaluated not only according to the exam grade, but also by including form, quiz, and discipline level, with weak, good, and average linguistic expressions [56].

III. Materials and Methods

A. Fuzzy Logic

The basis of fuzzy logic is based on the fuzzy sets study published by Zadeh (1965). In a classical set, an element is either an element of the set or it is not. Therefore, it is shown whether the elements of a classical set belong to the set with values of 0 or 1. In the fuzzy set, the generalization of the classical set is made and the belonging of an element to the set is expressed with a real number in the range of membership degrees [0, 1] [57].

Definition 1. (Fuzzy set) *Let X be a universe. Then a fuzzy set A over X is a function defined as follows:*

$$A = \{x/\mu_A(x) | x \in X, \mu_A(x) \in [0,1]\} \quad (1)$$

where, $\mu_A: X \rightarrow [0,1]$ is defined as the membership function, and $\mu_A(x)$ is defined as the membership value of the x element in the A fuzzy set.

Since fuzzy sets cannot be represented with exact lines, venn diagram representations cannot be mentioned and are instead represented by graphs of membership functions. The x-axis of the membership function graph shows the members, and the y-axis shows the degree of membership [57]. Membership functions that are commonly used include the triangle, trapezoid, gaussian, and bell curve. Since the triangle membership function is used in the proposed model, the details of the triangle membership function are given below.

The triangle membership function is expressed with three members on the x-axis. For example, the triangle membership function for the values 2, 4, and 6 is given in Equation 2 and its graph is given in Figure 1.

$$\mu_A(x;2,4,6) = \begin{cases} \dfrac{x-2}{4-2}, & 2 \le x \le 4 \\ \dfrac{6-x}{6-4}, & 4 \le x \le 6 \\ 0, & x > 6 \; or \; x < 2 \end{cases} \quad (2)$$

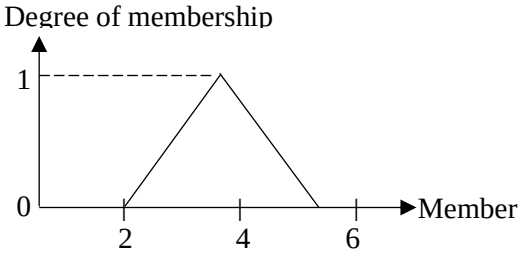

Fig. 1. Example of triangle membership function graph

B. Fuzzy Logic Based Systems

Fuzzy logic was made more flexible by starting from the thought of the inability to express a proposition as true or false, and the proposition was evaluated with fuzzy verbal variables such as some true, some false, very false. Concepts related to fuzzy logic are used in many areas of daily life. For example, in classical logic, 65 exam grades are considered successful and 64 unsuccessful, while in fuzzy logic, this situation can be expressed as 64 less successful. The block diagram of a fuzzy logic-based system is given in Figure 2.

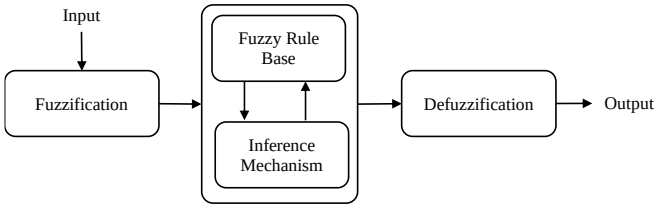

Fig. 2. Block diagram for fuzzy logic based systems [58]

Fuzzification is the conversion of the values used in the input of the system into fuzzy values. The fuzzy rule base contains the table of rules that will be used for the system, expressed as IF-THEN. While writing these rules, all outputs to be obtained depending on the input are used. Thus, each rule logically connects a part of the input space to the output space. All these contexts form the rule base. On the other hand, the inference mechanism ensures that the system behaves with an output by bringing together all the relations established between the input and output fuzzy sets in the fuzzy rule base. The Mamdani and Takagi-Sugeno methods are commonly used for the inference mechanism. In the Mamdani method, “min” is used if the rules are connected with “and” and “max” is used if they are connected with “or” [23]. The output of the inference mechanism will also be the fuzzy set. Defuzzification is the conversion of fuzzy expressions obtained after inference into expressions used in the real world. [58]. There are various methods in the literature that can be used for defuzzification [59].

IV. A PROPOSED MODEL FOR ASSESSING STUDENT ACHIEVEMENT

The proposed model has been divided into 2 categories: activities during the semester and performance evaluation at the end of the term. The activities during the semester include multiple choice exams, classical exams, projects, research, and homework methods. In addition to the activities during the semester, the end-of-term performance includes materials, end-of- chapter evaluations, and attendance at classes during the semester.

The method of Chen and Lee (1999) was used for the classical exam, project, research, and homework, among other activities during the semester [60]. A new model has been proposed by adding the distractor weight, which allows the student to be evaluated on wrong answers in multiple-choice exams.

A. Performance Evaluation During the Semester

Two different approaches based on fuzzy decision-making were used to evaluate activities during the semester, such as the e-exam. The first of these is the evaluation of students' work with classical exams, projects, research, and homework. In this approach, linguistic expressions from Chen and Lee (1999) were used [60]. These expressions are of eleven levels: extremely good (EG), very very good (VVG), very good (VG), good (G), not bad (NB), medium (M), slightly bad (SB), bad (B), very bad (VB), very very bad (VVB), and extremely bad (EB). For these levels, EG=1, VVG=0.99, VG=0.9, G=0.8, NB=0.7, M=0.6, SB=0.5, B=0.4, VB=0.24, VVB=0.09, EB=0 satisfaction levels were specified [60]. The question score and the total exam score are calculated by using these satisfaction levels and the values given by the educator in the range of 0–1 for each level.

The other proposed method for assessing students' exams is for multiple-choice exams. Especially in lessons involving numerical operations, very small mistakes can change the answer to the question. For this reason, a more objective evaluation of such courses can be obtained by examining the student's question-solving stages. However, the applicability of this in distance learning systems is not very possible. Therefore, unlike the literature, in our proposed method, Question Based Response Time (QBRT), Question Difficulty Level (QDL), Distractor Weight (DW), and Question Type (QT) data were used. The method of Chen and Lee (1999) was used to calculate the effect of the output of the fuzzy system on the exam score. QBRT is the time taken to answer each question. QDL is the difficulty level set by the trainer for each question. In lessons with numerical content, very small errors can change the result and cause the result to be incorrect even if all operations are correct. Since the test exams are evaluated only as true or false, the student may fail in this case. To prevent this negativity, the DW expression has been determined. With DW, a weight between 0 and 1 is determined for each option, and this situation is included in the evaluation. For example, if the student can identify the entire map for a concept map-based question, a weight of 1 can be used for the correct answer, and a weight of 0.5 can be used for the relevant option if they know 70% of it. QT, on the other hand, was used to determine the multiple choice (MC) or true/false (TF) question type. In the proposed method, QBRT, QDL, and QT are used as inputs to the fuzzy inference system. DW was taken into consideration while calculating the weights of the question scores.

The linguistic expressions used for QBRT are very fast (VF), fast (F), moderately fast (MF), slow (S), and very slow (VS). The membership functions of the QBRT parameter of the set $x=[0,t]$, with the number of questions n, the duration of

the exam t_{total}, and the average response time $t = \frac{t_{total}}{n}$, are given below.

$$\mu_{VF}(x) = \begin{cases} 1, & 0 \le x \le t * 0.25 \\ \dfrac{t * 0.5 - x}{t * 0.25}, & t * 0.25 \le x \le t * 0.5 \end{cases} \quad (3)$$

$$\mu_{F}(x) = \begin{cases} \dfrac{x - t * 0.25}{t * 0.25}, & t * 0.25 \le x \le t * 0.5 \\ \dfrac{t - x}{t * 0.5}, & t * 0.5 \le x \le t \end{cases} \quad (4)$$

$$\mu_{MF}(x) = \begin{cases} \dfrac{x - t * 0.5}{t * 0.5}, & t * 0.5 \le x \le t \\ \dfrac{t * 1.5 - x}{t * 0.5}, & t \le x \le t * 1.5 \end{cases} \quad (5)$$

$$\mu_{S}(x) = \begin{cases} \dfrac{x - t}{t * 0.5}, & t \le x \le t * 1.5 \\ \dfrac{t * 2.25 - x}{t * 0.75}, & t * 1.5 \le x \le t * 2.25 \end{cases} \quad (6)$$

$$\mu_{VS}(x) = \begin{cases} \dfrac{x - t * 1.5}{t * 0.75}, & t * 1.5 \le x \le t * 2.25 \\ 1, & t * 2.25 \le x \le t_{toplam} \end{cases} \quad (7)$$

For example, since the average time for each question in a 12-minute exam consisting of 4 questions will be 3 minutes, the membership function graph of the question-based response time of the set *x=[0.180]* is given in Figure 3.

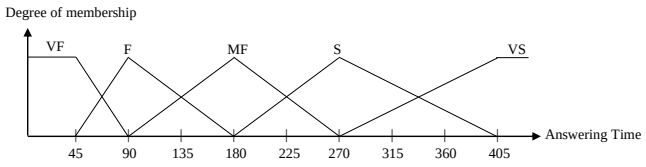

Fig. 3. Example membership function for question-based answering time

Linguistic expressions used for the QDL are very difficult (VD), difficult (D), medium easy (ME), easy (E), and very easy (VE). The membership function graph for the QDL is given in Figure 4.

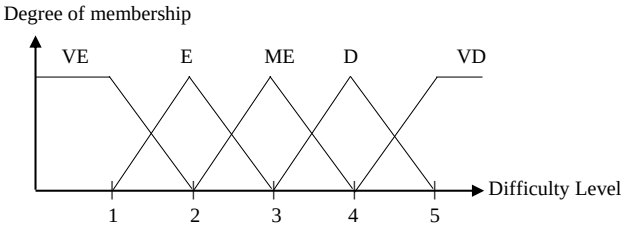

Fig. 4. Membership function used for question difficulty level

The linguistic expressions of Chen and Lee (1999) were used in the output of the created fuzzy model [60]. The membership function graph used for the question result (QR), which expresses the output of the fuzzy model, is given in Figure 5.

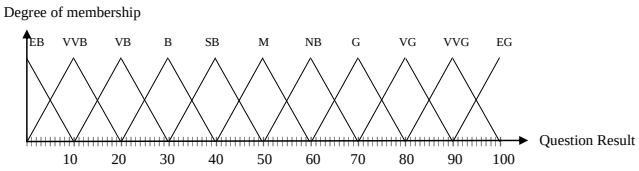

Fig. 5. Membership function used for the question result

B. End of Term Performance Evaluation

To evaluate the end-of-term student performance, e-exam, material usage, end-of-chapter evaluations and attendance to classes were considered. A student can have more than one grade related to the relevant course. The impact rates of these exams will vary according to the relevant institution. For this reason, it is recommended to use a single exam grade obtained after the calculation according to the impact rates of the relevant institution in performance evaluation. In the material usage part, the completion rate of each training material, the difficulty level, and the importance level of the relevant material were used. The success of the student after each chapter is evaluated by the end-of-chapter evaluations. These evaluations are also effective at assessing end-of-term performance. If there is no end-of-term evaluation for the relevant course, this parameter will be ineffective in the performance evaluation. Another evaluation criterion is the student's attendance at classes. This parameter will also be used as a factor in performance evaluation.

The end-of-term performance evaluation is based on fuzzy inference, and the diagram of the relevant module is given in Figure 6.

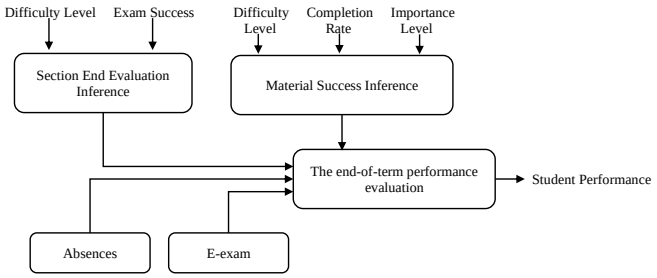

Fig. 6. Fuzzy inference module for performance evaluation

Inference at the end-of-chapter includes the evaluation of the exams at the end of the relevant courses. While making this evaluation, the difficulty level of the department and the success of the exam were used. While calculating the exam success, the fuzzy evaluation system used in the e-exam module was used, and the eleven levels given in Figure 5 were used as output. For the difficulty level, VD, D, ME, E, and VE levels were used. These values are used as the input of the fuzzy inference system and the output of the end-of-chapter evaluation result as eleven levels.

The material success inference includes the use of the educational materials defined for the relevant course by the student. While making this evaluation, the completion rate, difficulty level, and importance level of the material were used as the inputs of the inference system, and the material success

was used as the output. The levels of all completed (AC), three-quarters completed (TQC), half completed (HC), quarter completed (QC), and never done (ND) levels were used for the completion rate. For the difficulty level VD, D, ME, E, and VE levels were used. The very important (VI), important (I), moderate (M), low important (LI), and very low important (VLI) were used for the importance levels. Eleven-level linguistic expressions in Figure 5 were used as output. [60].

The effect of course attendance on performance is subjective and depends on the instructor of the course. Absences of 30% or more are expressed as absentee (AS), absences between 20% and 29% are expressed as less continuous (LC), absences between 10% and 19% are expressed as continuous (C), and absences below 10% are expressed as very continuous (VC).

V. Results for the Proposed Model

A. Results for Evaluation During the Semester

Two different approaches based on fuzzy inference were used to evaluate student performance during the semester. The first of these is the evaluation method that students will present in written form in the form of classical exams, projects, research, and assignments. In this approach, linguistic expressions from Chen and Lee (1999) are used [60]. An example of the application of this method is given in Example 1.

Example 1. Let's evaluate according to the method of Chen and Lee (1999) for a classical exam consisting of 3 questions or criteria.

Table 1. Dataset for Example 1

Questions or Criteria	Score	Satisfaction Levels (SL)										
		EG	VVG	VG	G	NB	M	SB	B	VB	VVB	EB
1	30	0.0	0.0	0.2	0.5	0.9	0.0	0.0	0.0	0.0	0.0	0.0
2	30	0.0	0.0	0.0	0.0	0.0	0.8	0.5	0.0	0.3	0.0	0.0
3	40	0.0	0.0	0.0	0.0	0.7	0.6	0.0	0.2	0.0	0.0	0.0

The satisfaction levels given in Table 1 were given by the trainer for each question/criterion. Using this information, the satisfaction level for each question is calculated as follows.

$$SL(1) = \frac{0.2 * VG + 0.5 * G + 0.9 * NB}{0.2 + 0.5 + 0.9} = \frac{0.2 * 0.9 + 0.5 * 0.8 + 0.9 * 0.7}{0.2 + 0.5 + 0.9} = 0.75625$$

$$SL(2) = \frac{0.8 * M + 0.5 * SB + 0.3 * VB}{0.8 + 0.5 + 0.3} = \frac{0.8 * 0.6 + 0.5 * 0.5 + 0.3 * 0.24}{0.8 + 0.5 + 0.3} = 0.50125$$

$$SL(3) = \frac{0.7 * NB + 0.6 * M + 0.2 * B}{0.7 + 0.6 + 0.2} = \frac{0.7 * 0.7 + 0.6 * 0.6 + 0.2 * 0.4}{0.7 + 0.6 + 0.2} = 0.62$$

The satisfaction level of each question is multiplied by the score of the relevant question and the total score is calculated by summing them.

$$Exam\ Result = SL(1) * 30 + SL(2) * 30 + SL(3) * 40 = 62.525$$

In the other approach, QBRT, QDL, DW and QT data were used to evaluate exams containing multiple choice questions. A rule base containing 51 rules belonging to the fuzzy model created for the evaluation of multiple-choice questions was created. The output of the rule base includes eleven linguistic statements by Chen and Lee (1999). After the output of the fuzzy inference system was obtained, the question scores were calculated using satisfaction levels and DW. In this proposed method, since the correct answers are included in the fuzzy inference system, depending on the QBRT and QDL of the correct answer, a decrease may be observed in the exam success compared to the classical assessment. For this reason, 2-option evaluation is recommended for exam success. In the first method, all questions are included in the fuzzy inference system. The second method is to insert only the wrong answers into the fuzzy inference system.

Example 2. Information for an exam consisting of 5 MC questions, 20 points per question and 20 minutes in duration, is given below. Let's calculate student success in line with this information.

Table 2. Dataset for Example 2

Question	QDL	Correct Answer	DW for each choice					Student Answer	QBRT
			A	B	C	D	E		
1	1	A	1.0	0.0	0.4	0.0	0.2	E	110 sec
2	3	C	0.0	0.2	1.0	0.0	0.0	C	400 sec
3	2	B	0.0	1.0	0.2	0.5	0.3	B	65 sec
4	5	E	0.0	0.0	0.0	0.0	1.0	E	230 sec
5	1	D	0.2	0.0	0.0	1.0	0.0	A	195 sec

According to the information given, since the average time for each question will be 4 minutes, the membership functions of the set *x=[0,240]* and the QBRT membership function graph are given below.

$$\mu_{VF}(x) = \begin{cases} 1, & 0 < x \le 60 \\ \frac{120 - x}{60}, & 60 \le x \le 120 \end{cases}$$

$$\mu_{F}(x) = \begin{cases} \frac{x - 60}{60}, & 60 \le x \le 120 \\ \frac{240 - x}{120}, & 120 \le x \le 240 \end{cases}$$

$$\mu_{MF}(x) = \begin{cases} \frac{x - 120}{120}, & 120 \le x \le 240 \\ \frac{360 - x}{120}, & 240 \le x \le 360 \end{cases}$$

$$\mu_{S}(x) = \begin{cases} \frac{x - 240}{120}, & 240 \le x \le 360 \\ \frac{540 - x}{180}, & 360 \le x \le 540 \end{cases}$$

$$\mu_{VS}(x) = \begin{cases} \frac{x - 360}{180}, & 360 \le x \le 540 \\ 1, & 540 \le x \le 1200 \end{cases}$$

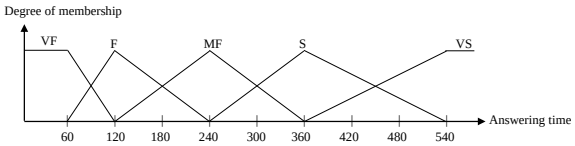

Fig. 7. QBRT membership function

After fuzzification, the values given in the table below were obtained for each question. The rules triggered by each question were determined, and the Mamdani inference method was used.

Table 3. Data obtained after fuzzification for Example 2

	QBRT	QDL	Rule	QR	DW	Question Score
1	0.17 VF and 0.83 F	VE	NB, M	0.17 NB or 0.83 M	0.2	(0.17*0.7+0.83*0.6)*0.2*20=2.468
2	0.78 S and 0.22 VS	ME	M, SB	0.78 M or 0.22 SB	1.0	(0.78*0.6+0.22*0.5)*1*20=11.56
3	0.92 VF and 0.08 F	E	G, NB	0.92 G or 0.08 NB	1.0	(0.92*0.8+0.08*0.7)*1*20=15.84
4	0.083 F and 0.917 MF	VD	VVG, VG	0.083 VVG or 0.917 VG	1.0	(0.083*0.99+0.917*0.9)*1*20=18.15
5	0.38 F and 0.62 MF	VE	M, SB	0.38 M or 0.62 SB	0.2	(0.38*0.6+0.62*0.5)*0.2*20=2.152
Exam Score						50.17

When the classical evaluation is made with these values given as an example, the exam score is 60. When the evaluation was made according to the question type, response time, distractor weight, and difficulty level, and when all the questions were put into the fuzzy inference system, the result was calculated as 50.17. If only wrong answers are inserted into the fuzzy inference system, the result will be 64.62.

B. Results for End of Term Evaluation

The end-of-chapter evaluation inference includes the evaluation of the exams at the end of the relevant courses. While making this evaluation, the difficulty level of the chapter and the success of the exam were used. While calculating the success of the exam, the fuzzy evaluation system used in the e-exam module was used, and eleven levels were used as output: EG, VVG, VG, G, NB, M, SB, B, VB, VVB and EB. For the difficulty level, VD, D, ME, E, and VE levels were used. These values are used as the input of the fuzzy inference system and the output of the end-of-chapter evaluation result as eleven levels. This model was applied to each chapter, and output was obtained for as many as the number of chapters. The average of these outputs is used as an input for performance evaluation. A rule base consisting of 55 rules was created for the end-of-chapter evaluation.

The material achievement inference includes the use of the educational materials defined for the relevant course by the student. While making this evaluation, the completion rate, difficulty level, and importance level of the material were used as the inputs of the inference system, and the material success was used as the output. AC, TQC, HC, QC, and ND levels were used for the completion rate. For the difficulty level, VD, D, ME, E, and VE levels were used. For the importance level, the levels of VI, I, M, LI, and VLI were used. Eleven levels were used as outputs: EG, VVG, VG, G, NB, M, SB, B, VB, VVB, and EB rule base consisting of 120 rules for material success inference was created.

The effect of course attendance on performance is subjective and depends on the instructor of the course. Absences of 30% and above are expressed as AS, between 20% and 29% as LC, between 10% and 19% as C, and below 10% as VC.

After defining the inputs for performance evaluation, the output is determined according to the rule base consisting of 4236 rules. In the light of this information regarding performance evaluation, a sample evaluation is given below.

Example 3. The student statuses for a course with two chapters are given below. Let's evaluate student achievements with the performance evaluation system recommended for these situations.

Table 4. Data set for Example 3

	Chapter 1							
	The end-of-chapter			Material Success				
	Exam Score			Difficulty Level		Completion Rate	Difficulty Level	Importance Level
Student 1	86			D		75%	ME	I
Student 2	62			D		50%	ME	I
Student 3	52			D		25%	ME	I
	Chapter 2					E-exam		Absences
	The end-of-chapter		Material Success					
	Exam Score	Difficulty Level	Completion Rate	Difficulty Level	Importance Level	Exam 1	Exam 2	
Student 1	77	VD	25%	D	VI	74	62	10%
Student 2	84	VD	100%	D	VI	92	97	5%
Student 3	58	VD	50%	D	VI	83	84	25%

The fuzzification of the student data given in Table 4 is given in Table 5. The defuzzification result is given in Table 6. The midpoint method of greatest membership was used when performing the defuzzification and for the end-of-chapter and material success of the 2 units.

Table 5. Fuzzification for Example 2

	Chapter 1						
	The end-of-chapter			Material Success			
	Exam Result	Difficulty Level	Rule	Completion Rate	Difficulty Level	Importance Level	Rule
Student 1	0.4 VG and 0.6 VVG	D	0.4 VG or 0.6 VVG	TQC	ME	I	VG
Student 2	0.8 FD and 0.2 G	D	0.8 NB or 0.2 G	HC	ME	I	G
Student 3	0.8 M and 0.2 NB	D	0.8 NB or 0.2 NB	QC	ME	I	NB
	Chapter 2						
	The end-of-chapter			Material Success			
	Exam Result	Difficulty Level	Rule	Completion Rate	Difficulty Level	Importance Level	Rule
Student 1	0.3 G and 0.7 VG	VD	0.3 VG or 0.7 VG	QC	D	VI	G
Student 2	0.6 VG and 0.4 VVG	VD	0.6 VG or 0.4 EG	AC	D	VI	EG
Student 3	0.2 M and 0.8 NB	VD	0.2 NB or 0.8 G	HC	D	VI	VG

E-exam			Absences
Exam 1	Exam 2	Result	
max(0.6 G, 0.4 VG)=G	max(0.8 NB, 0.2 G)=NB	G	C
max(0.8 VVG, 0.2 EG)=VVG	max(0.3 VVG, 0.7 EG)=EG	EG	VC
max(0.7 VG, 0.3 VVG)=VG	max(0.6 VG, 0.4 VVG)=VG	VG	LC

Based on the information given in the table above and the rule tables, the performance evaluation results are given in the table below.

Table 6. Defuzzification for Example 2

	Chapter 1			Chapter 2			The end-of-chapters	Materials Success
	The end-of-chapter		Mat. Baş	The end-of-chapter		Mat. Baş		
	Fuzzification expression	Result	Rule	Fuzzification expression	Result	Rule		
Student 1	VVG	90	VG	VG	80	G	85 (0.5 VG and 0.5 VVG)	VG
Student 2	NB	60	G	VG	80	EG	70 (İ)	VVG
Student 3	NB	60	NB	G	70	VG	65 (0.5 NB and 0.5 G)	G

	The end-of-chapters	Materials Success	E-exam	Absences	Triggered Rule	RESULT
Student 1	85 (0.5 VG and 0.5 VVG)	VG	G	C	NB	60
Student 2	70 (G)	VVG	EG	VC	VVG	90
Student 3	65 (0.5 NB and 0.5 G)	G	VG	LC	0.5 SB or 0.5 M	50

VI. Conclusion and Discussion

As a result of the reflection of the developments in information technologies on education, distance learning studies focus on many subjects, especially increasing teacher-student interaction, focusing on student-centered education, building academic confidence, and objective evaluation.

An important issue for distance learning systems is the objective and student-centered evaluation of student performance. In the studies, not only exam scores but also student movements within the system, material use, and class participation factors were taken into account in order to evaluate student performance [6].

Student success is planned to be realized through end-of-chapter evaluation, course attendance, and e-exams. For multiple-choice questions, the distractor weight was added to the answer choices and the evaluation was made accordingly. Thus, scoring was not done on exact true and false, but also on incorrect answers according to the distractor weight. In addition, the time the student spent on the questions was also included in the assessment. As a result, a model that offers a very valuable evaluation opportunity for distance learning has been proposed. The proposed model can be used for all distance education courses, especially applied courses. In addition, since the e-exam evaluation module can work on a question-based basis, it can also be used for project and application-based evaluations.

Authors' Contributions

The authors' contributions to the paper are equal.

Statement of Conflicts of Interest

There is no conflict of interest between the authors.

Statement of Research and Publication Ethics

The authors declare that this study complies with Research and Publication Ethics

References

[1] S. Ertürk, 'Eğitimde program geliştirme (4. Baskı) Ankara: Yelken Yayınları', 1974.

[2] F. Ulutaş and B. Ubuz, 'Research and Trends in Mathematics Education: 2000 to 2006.', *Elementary Education Online*, vol. 7, no. 3, 2008.

[3] M. F. Doğ, 'Usability metrics on e-learning systems', Master Thesis, Bahçeşehir University, 2012.

[4] K. Khawar, S. Munawar, and N. Naveed, 'Fuzzy Logic-based Expert System for Assessing Programming Course Performance of E-Learning Students', *Journal of Information Communication Technologies and Robotic Applications*, pp. 54–64, Jun. 2020.

[5] B. Tütmez, 'Bulanık Mantık ve Eğitim Bilimlerinde Kullanılabilirliği', *Eğitim Dergisi*, no. 18, 2018.

[6] M. Annabestani, A. Rowhanimanesh, A. Mizani, and A. Rezaei, 'Descriptive evaluation of students using fuzzy approximate reasoning', *arXiv:1905.02549 [cs]*, May 2019, Accessed: Jan. 10, 2021. [Online]. Available: http://arxiv.org/abs/1905.02549

[7] Y. Altun Türker, 'Selection of distance education learning management system with fuzzy multi-criteria decision making methods', Master's Thesis, Kocaeli University, 2012.

[8] D. Herand and Z. A. Hatipoğlu, 'E-learning and Comparison of Commonly Used E-learning Platforms', *Çukurova Üniversitesi İktisadi ve İdari Bilimler Fakültesi Dergisi*, vol. 18, no. 1, 2014.

[9] A. H. Işık, A. Karacı, O. Özkaraca, and S. Biroğul, 'Web tabanlı eş zamanlı (senkron) uzaktan eğitim sistemlerinin karşılaştırmalı analizi', *Akademik Bilişim*, pp. 10–12, 2010.

[10] S. İzmirli and H. İ. Akyüz, 'Examining synchronous virtual classroom software', *Journal of Theory and Practice in Education*, vol. 13, no. 4, pp. 788–810, 2017.

[11] E. Lavolette, M. A. Venable, E. Gose, and E. Huang, 'Comparing synchronous virtual classrooms: Student, instructor and course designer perspectives', *TechTrends*, vol. 54, no. 5, pp. 54–61, 2010.

[12] S. Schullo, A. Hilbelink, M. Venable, and A. E. Barron, 'Selecting a virtual classroom system: Elluminate live vs. Macromedia breeze (adobe acrobat connect professional)', *MERLOT Journal of Online Learning and Teaching*, vol. 3, no. 4, pp. 331–345, 2007.

[13] D. Yıldırım, H. Tüzün, M. Çınar, A. Akıncı, E. Kalaycı, and H. G. Bilgiç, 'Comparison of Synchronous Virtual Classroom Tools Used In Distance Learning', *Akademik Bilişim*, pp. 451–456, 2011.

[14] H. Baran, 'Measurement and evaluation in open and distance education', *Açıköğretim Uygulamaları ve Araştırmaları Dergisi*, vol. 6, no. 1, pp. 28–40, 2020.

[15] J. R. Echauz and G. J. Vachtsevanos, 'Fuzzy Grading System', *IEEE Transactions on Education*, vol. 38, no. 2, pp. 158–165, May 1995.

[16] S. Kotsiantis, C. Pierrakeas, and P. Pintelas, 'Predicting Students' Performance in Distance Learning Using Machine Learning Techniques', *Applied Artificial Intelligence*, vol. 18, no. 5, pp. 411–426, May 2004.

[17] Ç. Ölmez, 'Analysis of question banks in distance learning with fuzzy logic method', Master Thesis, Afyon Kocatepe University, 2010.

[18] S. N. Ingoley and J. W. Bakal, 'Students' performance evaluation using fuzzy logic', in *2012 Nirma University International Conference on Engineering (NUiCONE)*, Dec. 2012, pp. 1–6.

[19] S. S. Jamsandekar and R. R. Mudholkar, 'Performance Evaluation by Fuzzy Inference Technique', *International Journal of Soft Computing and Engineering*, vol. 3, no. 7, 2013.

[20] O. Yildiz, A. Bal, and S. Gulsecen, 'Improved fuzzy modelling to predict the academic performance of distance education students', *The International Review of Research in Open and Distributed Learning*, vol. 14, no. 5, Dec. 2013.

[21] G. Jyothi, M. C. Parvathi, M. P. Srinivas, and M. S. Althaf, 'Fuzzy Expert Model for Evaluation of Faculty Performance in Technical Educational Institutions', vol. 4, no. 5, p. 10, 2014.

[22] K. Salmi, H. Magrez, and A. Ziyyat, 'A fuzzy expert system in evaluation for E-learning', in *2014 Third IEEE International Colloquium in Information Science and Technology (CIST)*, Oct. 2014, pp. 225–229.

[23] O. Yıldız, 'Evaluating distance learning students' performance by machine learning', PhD Thesis, Istanbul University, 2014.

[24] N. Ghatasheh, 'Knowledge Level Assessment in e-Learning Systems Using Machine Learning and User Activity Analysis', *ijacsa*, vol. 6, no. 4, 2015, doi: 10.14569/IJACSA.2015.060415.

[25] J. Azimjonov, İ. H. Selvi, and U. Özbek, 'Evaluation of distance learning students performance using fuzzy logic', *Yönetim Bilişim Sistemleri Dergisi*, vol. 2, no. 2, Art. no. 2, Oct. 2016.

[26] A. Barlybayev, A. Sharipbay, G. Ulyukova, T. Sabyrov, and B. Kuzenbayev, 'Student's Performance Evaluation by Fuzzy Logic', *Procedia Computer Science*, vol. 102, pp. 98–105, Jan. 2016.

[27] T. Mahboob, S. Irfan, and A. Karamat, 'A machine learning approach for student assessment in E-learning using Quinlan's C4.5, Naive Bayes and Random Forest algorithms', in *2016 19th International Multi-Topic Conference (INMIC)*, Dec. 2016, pp. 1–8.

[28] J. C. S. Silva, J. L. C. Ramos, R. L. Rodrigues, A. S. Gomes, F. D. F. D. Souza, and A. M. A. Maciel, 'An EDM Approach to the Analysis of Students' Engagement in Online Courses from Constructs of the Transactional Distance', in *2016 IEEE 16th International Conference on Advanced Learning Technologies (ICALT)*, Jul. 2016, pp. 230–231.

[29] S. Sisovic, M. Matetic, and M. B. Bakaric, 'Clustering of imbalanced moodle data for early alert of student failure', in *2016 IEEE 14th International Symposium on Applied Machine Intelligence and Informatics (SAMI)*, Jan. 2016, pp. 165–170.

[30] Y. Abubakar and N. B. H. Ahmad, 'Prediction of Students' Performance in E-Learning Environment Using Random Forest', *International Journal of Innovative Computing*, vol. 7, no. 2, Art. no. 2, Dec. 2017.

[31] A. Cebi and H. Karal, 'An application of fuzzy analytic hierarchy process (FAHP) for evaluating students project', *Educ. Res. Rev.*, vol. 12, no. 3, pp. 120–132, Feb. 2017.

[32] R. Umer, T. Susnjak, A. Mathrani, and S. Suriadi, 'On predicting academic performance with process mining in learning analytics', *Journal of Research in Innovative Teaching & Learning*, vol. 10, no. 2, pp. 160–176, Jan. 2017.

[33] M. Hussain, W. Zhu, W. Zhang, and S. M. R. Abidi, 'Student Engagement Predictions in an e-Learning System and Their Impact on Student Course Assessment Scores', *Computational Intelligence and Neuroscience*, Vol. 2018, Oct. 02, 2018. https://www.hindawi.com/journals/cin/2018/6347186/ (accessed Jan. 10, 2021).

[34] C. Turan, Z. A. Reis, and S. Gülseçen, 'Bakış Takibi ile E-Öğrenme Materyalinde Konu Odağı ve Öğrenci Bakış Reflekslerinin İlgisini Değerlendirme', in 2018 5th International Management Information Systems Conference, pp. 34-37 Dec. 2018.

[35] S.-U. Hassan, H. Waheed, N. R. Aljohani, M. Ali, S. Ventura, and F. Herrera, 'Virtual learning environment to predict withdrawal by leveraging deep learning', *International Journal of Intelligent Systems*, vol. 34, no. 8, pp. 1935–1952, 2019.

[36] V. Ivanova and B. Zlatanov, 'Implementation of Fuzzy Functions Aimed at Fairer Grading of Students' Tests', *Education Sciences*, vol. 9, no. 3, p. 214, Aug. 2019.

[37] I. G. Ndukwe, B. K. Daniel, and C. E. Amadi, 'A Machine Learning Grading System Using Chatbots', in *Artificial Intelligence in Education*, Cham, 2019, pp. 365–368.

[38] S. Slater and R. Baker, 'Forecasting future student mastery', *Distance Education*, vol. 40, no. 3, pp. 380–394, Jul. 2019.

[39] P. Sokkhey and T. Okazaki, 'Comparative Study of Prediction Models on High School Student Performance in Mathematics', in *2019 34th International Technical Conference on Circuits/Systems, Computers and Communications (ITC-CSCC)*, Jun. 2019, pp. 1–4.

[40] N. Abu Bakar, S. Rosbi, and A. A. Bakar, 'Robust Estimation of Student Performance in Massive Open Online Course using Fuzzy Logic Approach', *International Journal of Engineering Trends and Technology*, pp. 143–152, Oct. 2020.

[41] Y. Dashko, O. Vitchenko, and M. Kadomtsev, 'Soft models of competence assessment in professional education', *E3S Web Conf.*, vol. 210, p. 18011, 2020.

[42] S. Raval and B. Tailor, 'Mathematical Modelling of Students' Academic Performance Evaluation Using Fuzzy Logic', *International Journal of Statistics and Reliability Engineering*, vol. 7, no. 1, Art. no. 1, Jul. 2020.

[43] H. M. Ünver, 'Design of a Fuzzy Logic Based Custom Exam Production System for High Performance', *International Journal of Engineering Research and Development*, vol. 12, no. 2, pp. 745–752, Jun. 2020.

[44] H. Waheed, S.-U. Hassan, N. R. Aljohani, J. Hardman, S. Alelyani, and R. Nawaz, 'Predicting academic performance of students from VLE big data using deep learning models', *Computers in Human Behavior*, vol. 104, p. 106189, Mar. 2020.

[45] R. Wardoyo and W. D. Yuniarti, 'Analysis of Fuzzy Logic Modification for Student Assessment in e-Learning', *IJID (International Journal on Informatics for Development)*, vol. 9, no. 1, Art. no. 1, Nov. 2020.

[46] S. Gocheva-Ilieva, H. Kulina, and A. Ivanov, 'Assessment of Students' Achievements and Competencies in Mathematics Using

CART and CART Ensembles and Bagging with Combined Model Improvement by MARS', *Mathematics*, vol. 9, no. 1, Art. no. 1, Jan. 2021.

[47] Ö. Bursalıoğlu, 'Uzaktan eğitime uygun mobil destekli çevirimiçi sınav sistemi', Master's Thesis, Kırıkkale Üniversitesi, 2016.

[48] K. Almohammadi, H. Hagras, B. Yao, A. Alzahrani, D. Alghazzawi, and G. Aldabbagh, 'A type-2 fuzzy logic recommendation system for adaptive teaching', *Soft Comput*, vol. 21, no. 4, pp. 965–979, Feb. 2017, doi: 10.1007/s00500-015-1826-y.

[49] N. Arora and J. R. Saini, 'A fuzzy probabilistic neural network for student's academic performance prediction', *International Journal of Innovative Research in Science, Engineering and Technology*, vol. 2, no. 9, pp. 4425–4432, 2013.

[50] N. A. Kumari, D. N. Rao, and M. S. Reddy, 'Indexing student performance with fuzzy logics evaluation in engineering education', *International Journal of Engineering Technology Science and Research*, vol. 4, no. 9, pp. 514–522, 2017.

[51] S. Maitra, S. Madan, and P. Mahajan, 'An Adaptive Neural Fuzzy Inference System for prediction of student performance in Higher Education', in *2018 International Conference on Advances in Computing, Communication Control and Networking (ICACCCN)*, 2018, pp. 1158–1163.

[52] H. Salvi Akansha, M. Khairnar Medha, R. Shaikh Samina, and T. Kokani Shital, 'Prediction and Evaluation of Students Academic Performance using Fuzzy Logic', *International Research Journal of Engineering and Technology (IRJET), e-ISSN*, vol. 5, no. 2, pp. 2395–0056, 2018.

[53] T. Kim, E. Sotirova, A. Shannon, V. Atanassova, K. Atanassov, and L.-C. Jang, 'Interval valued intuitionistic fuzzy evaluations for analysis of a student's knowledge in university e-learning courses', *International Journal of Fuzzy Logic and Intelligent Systems*, vol. 18, no. 3, pp. 190–195, 2018.

[54] N. A. Bakar, S. Rosbi, and A. A. Bakar, 'Evaluation of Students Performance using Fuzzy Set Theory in Online Learning of Islamic Finance Course.', *International Journal of Interactive Mobile Technologies*, vol. 15, no. 7, 2021.

[55] N. A. M. Nor, A. Azizan, B. Moktar, A. A. Aziz, and D. S. M. Nasir, 'Modeling Mathematics Performance Between Rural and Urban School Using a Fuzzy Logic Approach', *Journal of Computing Research and Innovation*, vol. 6, no. 1, pp. 77–87, 2021.

[56] E. A. Laksana, B. T. Munajat, K. Permana, S. Aisyah, S. F. Wijawanto, and T. R. Soleh, 'Student Grade 0Using Fuzzy Logic', *Review of International Geographical Education Online*, vol. 11, no. 5, pp. 1073–1081, 2021.

[57] H. J. Zimmermann, 'Fuzzy set theory-and its applications', *Kluwer*, 1991.

[58] Ö. Mehmet Nuri, *Bulanık Mantık Yöntem ve Uygulamaları*. Türkiye: İKSAD, 2019.

[59] İ. Gültaş, 'A fuzzy AHP solution approach to the determination of the mathematics courses syllabuses in the industrial engineering education', Master's Thesis, Istanbul Technical University, 2007. Accessed: Jan. 10, 2021. [Online]. Available: https://polen.itu.edu.tr/handle/11527/5845

[60] Shyi-Ming Chen and Chia-Hoang Lee, 'New methods for students' evaluation using fuzzy sets', *Fuzzy Sets and Systems*, vol. 104, no. 2, pp. 209–218, Jun. 1999, doi: 10.1016/S0165-0114(97)00208-X.

International Journal of Multidisciplinary Studies and Innovative Technologies

e-ISSN: 2602-4888
dergipark.org.tr/en/pub/ijmsit
Research Article

2022, 6 (1), 38-44
DOI: DOI: 10.36287/ijmsit.6.1.38
Received: April 25, 2022; Accepted: June 20, 2022

Efficient Hardware Optimization for CNN

Seda GUZEL AYDIN[1*] and Hasan Sakir BILGE [2]

[1*]*Electrical and Electronics Engineering, Bingol University, Bingol, Turkey (sgaydin@bingol.edu.tr) (ORCID: 0000-0001-8875-9705)*
[2] *Electrical and Electronics Engineering, Gazi University, Ankara, Turkey (bilge@gazi.edu.tr) (ORCID: 0000-0002-4945-0884)*

Abstract **–** Convolutional Neural Networks (CNN) architectures have been increasingly well-known for image processing applications such as object detection, and remote sensing. Some applications like these systems need to adopt CNN methods for real-time implementation. Embedded devices like Field Programmable Gate Arrays (FPGA) technologies are a favorable alternative to implementing CNN-based algorithms. However, FPGA has some drawbacks such as limited resources and bottlenecks, it is difficult and so crucial to map the whole CNN that has a high number of layers, on FPGA without any optimization. Therefore, hardware optimization techniques are compulsory. In this study, an FPGA-based CNN architecture using high-level synthesis (HLS) is demonstrated, and a synthesis report is created for Xilinx Zynq-7000 xc7z020-clg484-1 target FPGAs. By implementing the CNN architecture on an FPGA platform, the implemented architecture has been fastened. To improve the throughput, the proposed design is optimized for convolutional layers. The most important contribution of this study is to perform optimization on the convolution layer by unrolling kernels and input feature maps and examine the effects on throughput, latency, and hardware resources. In this study, throughput is 15.6 GOP/s for the first convolution layer. With the proposed method in the study, approximately x2.6 acceleration in terms of latency and throughput was achieved compared to the baseline design.

Keywords *– FPGA, Deep learning, Convolutional neural networks, Hardware optimization, HLS*

Citation: Guzel Aydin, S. and Bilge, H. Ş. (2022). Efficient Hardware Optimization for CNN, International Journal of Multidisciplinary Studies and Innovative Technologies, 6(1): 38-44.

I. INTRODUCTION

Because CNN-based methods have presented successful results over traditional methods, these networks consider a powerful tool in many areas, especially in image processing applications. They are just adapted to address numerous problems. Starting with the 7-layer Lenet-5 [1], the deep learning (DL) approaches now continue with more than a hundred layers. In the early days of deep learning networks, researchers aimed to design deeper and wider networks to increase the accuracy of the network [2,3]. By increasing the number of layers and establishing larger networks, it was possible to design networks with high accuracy. However, increasing the number of layers and designing larger networks has increased the workload of the platform used to run the network. In addition, the number of parameters in the used network has increased, which has increased the training and inference stages. This, in addition to the success of CNN's in solving problems, caused an increase in the workload of the undesirable platforms and caused the general-purpose platforms to be insufficient to operate such deep networks. As a consequence of the large number of parameters and the computational burden of CNNs, researchers began to explore ways to design sparse and smaller networks using more compact and fewer parameters [4].

For some applications such as vehicle tracking systems, mobile applications, and object tracking, networks designed for real-time operation are required. CNN-based networks require a high volume of parameters and lots of calculation processes. However, central processing units (CPU) are not much preferred for real-time applications. To address these challenges, new solutions for efficient hardware implementations have been researched recently. To meet this requirement, numerous research tries to CNN to adopt high-performance devices such as Graphics Processing Unit (GPU), and FPGA [5-7]. It is so hard to reveal the parallelism feature in CNN for real-time applications in the CPU. In recent years, DL-based algorithms have been implemented and accelerated on GPU platforms so that notable parallel computing capability and high memory bandwidth. Nevertheless, studies on GPU show that GPU usually consumes more power than FPGA which makes it inefficient and difficult to use in battery-powered devices. In conclusion, it can be said that the computing performance of GPU is noticeable but on the other hand power consumption is high [7]. Therefore, FPGA could be addressed as a potential solution approach for optimizing and accelerating CNNs.

In recent years, significant research has investigated the utilization of accelerated CNN employment on FPGA. The FPGA implementation for CNNs has concerned much regarded a consequence of its reconfigurability, high performance, and energy efficiency. However, CNNs networks are computation-intensive and memory-intensive algorithms so, these features have brought many challenges to CNN implementations on hardware. FPGA has some disadvantages such as limited resources and limited bandwidth. Therefore, implementing complex structures like DL algorithms on FPGA is so challenge problem. To address

these problems, hardware optimization methods can be applied to network design on the platforms.

In the last few years, researchers have been investigating different optimization methods for the development of efficient acceleration of CNN systems on FPGAs. Studies are generally carried out for increasing parallelism, reducing power consumption, and reducing the number of resources used. The majority of the CNN application accelerators are intended on optimizing computation processing engines. Researchers in [8] used implemented YOLO2 on FPGA for optical remote sensing. They used a uniform module to implement multiple types of convolutions for the network. Researchers in [9] proposed a Roofline model to improve throughput for CNN. The Roofline model tries to determine the maximum performance the hardware can achieve for implemented algorithm according to two bounds. They investigate architecture for throughput and required memory bandwidth using unrolling and tilling techniques for optimizing design. They implement an accelerator using Vivado HLS with uniform loop unroll factors for different convolutional layers. The architecture purposed by [10] implemented a deep convolutional neural network accelerator on FPGA to run in real-time. Their platform consists of programmable logic and a programmable system. Both platforms shared the same memory (DDR3). They stated that the FPGA-based accelerator system they designed allows ~25x faster execution faster than the CPU-based implemented architecture. They focused on computation engine optimization; they were not optimized memory access problems. More recently, researchers in [11] used the operation chaining between the layer for data processing architecture for implementing CNN on De2i-150 board that received x18.04 acceleration rate than the baseline design. DSE was explored by different parameters such as processing time, and power consumption. In [12], researchers have employed loop optimization techniques for speeding up convolution operation to design CNN accelerator. They present the quantitative analysis for many design variables to optimize the design. In [13], researchers optimized their design by implementing multiple convolutional layer processors (CLP) to meet different conv layers for better resource utilization. In [14], researchers recommend two types of dedicated hardware structures. The first structure is suitable for the small-size CNN implementation that is designed with specific hardware for each layer. The second structure is one hardware model for each layer that is used multiple times for different layers. This approach uses low resource consumption; however, the throughput is low. There is a control block determining to use which operation. They reported that this structure can be modified for large networks because many layers use the same resources. In [15], researchers recommended an end-to-end CNN accelerator implementation based on FPGA. Their architecture maps the whole layer on one chip. In these model different layers can work concurrently in a pipelined structure therefore throughput can be increased. Streaming design architecture could reach the best throughput through a high parallelism strategy for each layer however this approach uses high resource-consuming In [16], researchers used the tilling technique to accelerate their deep neural network. The tilling technique is employed for reducing the memory bandwidth requirement at the inference state. Their proposed approaches reduce the memory bandwidth by 46.7% at the inference state.

FPGA-based CNN accelerator designs have some limitations that cause considerable challenges in performance and flexibility. The first of them is the limited number of resources such as Look up tables (LUTs), flip flops (FFs), Block Random Access Memory (BRAM), and Digital signal processing (DSP). CNNs have several computations that need a great number of hardware resources. Another challenge is the bandwidth. Limited bandwidth will cause a bottleneck during data exchange between off-chip memory and FPGA, preventing the system from operating at high performance. These challenges motivate researchers to design more optimal systems through a series of hardware optimization approaches considering accelerated CNN on FPGA for designing the high-performance inference phase of CNN. The main contribution of this paper is to perform optimization on the convolution layer by unrolling kernels and input feature maps and examine the effects on throughput, latency, and hardware resources. In this study, throughput is 15.6 GOP/s for the first convolution layer. With the proposed method in the study, approximately x2.6 acceleration in terms of latency and throughput was achieved compared to the baseline design. The rest of this paper is organized as follows. In section 2, brief information about CNN is given. Parallelism methods that can be used for hardware designs are explained in section 3. Section 4 shows the details of the methods used in the study, the hardware implementation, and the results. Section 5 deals with the conclusions.

II. BACKGROUND

In this section, a typical CNN architecture is briefly described.

A. The architecture of Convolutional Neural Networks

A classical CNN is a multi-layer pattern that contains the convolutional layer (Conv layer), activation layer, pooling layer (PL), and fully connected (FC) layer.

1) Convolutional layer

Conv layer is the layer where the convolution process takes place, so this layer is the most important layer of the CNN. The convolution operation performed on the image takes different kernel filters, shifts them on the input feature maps (IFM) and creates an output feature map (OFM). OFM data resulting from the operations performed in this layer form IFMs for the next layer.

```
for(int no=0; no<M; no++) {
   for (int y = 0; y < R; y++){
      for (int x = 0; x <C; x++){
         for (int ni = 0; ni <N; ni++){
            for(int ky=0;ky<k;ky++) {
               for(int kx=0;kx<k;kx++){

                  OBRAM[no][x][y]+=IBRAM[ni][S1*x+kx][S1*y+ky]*WBRAM[ni][no][kx][ky];


               }
            }
         }
      }
   }
}
```

Fig. 1. Pseudo-code of convolution operation for CNN

The filter values used here are determined during the training. Fig. 1 shows the pseudo-code of convolution operation for

CNN. Fig. 2 is demonstrated convolution operation with multiple channel input and multiple kernels. The number of convolution filters is denoted by M, equivalent to the number of output feature maps. The size of the kernels is demonstrated by kxk. The number of channels, height, and width for IFM are denoted by $N, H, and\ W$ respectively. The height and width for OFM are denoted by $C, and\ R$ respectively.

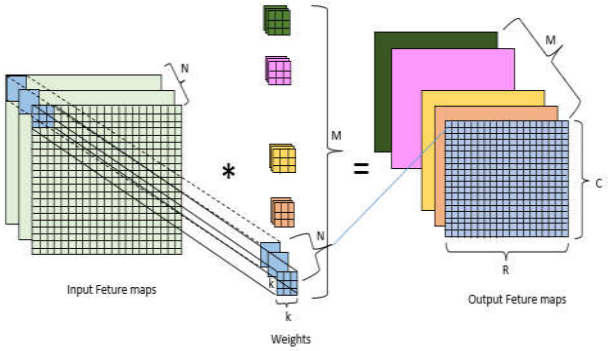

Fig. 2. Convolution operation with multiple channel input

Stride operation enables a dimension reduction of the convolution result by avoiding filters implemented in the whole of the IFMs. Stride (s) parameter defined how many steps are moved in each step-in convolution operation. The padding (p) operation allows remaining the same dimension of the resulting image through the process of adding zeros to the input matrix. The following OFM dimension can be calculated in (1):

$$OFM_{R,C} = \frac{W,H+(2\ x\ p)-k}{s} + 1 \quad (1)$$

The computational complexity (CC) can be denoted by #OP for each convolutional layer of the network could be measured based (2).

$$\#\mathrm{OP}^l = M^l x N^l x R^l x C^l x k^l x k^l \quad (2)$$

2) Activation layer

After the convolution process is finished, the results obtained are passed through the activation function. In the convolution layer, the inputs are multiplied by the weights, and then added together with the bias values. The output signal generated as a result of this process is a simple linear function. This result is converted into a non-linear structure by applying the activation function. Usually, nonlinear and differentiable activation functions are preferred, such as step function, sigmoid, hyperbolic tangent (Tanh), Rectified Linear Unit (ReLU), Softmax etc. The sigmoid function is one of the most commonly used activation functions. It is differentiable. However, due to the gradient vanish problem, the maximum performance of the network using this function could not be achieved so, an alternative activation function was sought to find a solution to this problem. The Tanh converts the input value to the hyperbolic tangent of the angle it. The interval of this function, which has a very similar structure to the sigmoid function, is defined as (-1,+1). However, since the problem of gradients dying at the ends of this function continues, different functions are preferred as an alternative solution. In addition, since the constant Euler's number (e) is used in these two functions, it causes computational complexity in hardware designs and this is a problem in hardware implementations. The ReLU is the most used activation function in accelerating hardware. It rectifies the linear unit, and activating some neurons. The computational load is less than the sigmoid and hyperbolic tangent functions, making it more preferred in multilayer networks.

3) Pooling layer

Usually used after the convolution layer, the purpose of this layer is to reduce the input size for the next convolution layer to reduce the complexity of further layers. The depth (channel) of the input data does not affect the pooling process. The pooling operation occurs as follows: The input feature map is partitioned into smaller rectangles and transformed the defined function value inside that small rectangle [23]. Frequently, max-pooling and average pooling methods are used for pooling operations. Max-pooling returns the max value of the sub-region, and average pooling returns the average of values in the sub-region.

4) Fully connected layer

Like the layers in classical neural networks, each neuron in the FC layer is connected to all the neurons after it. Therefore, these layers are also referred to as densely connected layers. Since there are too many parameters in these layers, they are the layers that consume the most memory for storing these parameters [24].

III.ACCELERATION METHODS FOR CNN

A. Different parallelism structures

CNN architecture has streaming structures. That is, architecture consists of interconnected layers that work one after the other. Therefore, different parallelism methods can be applied to these architectures. [18-20] have exploited several levels of parallelism methods that can be applied to CNN architecture. These are task-level parallelism (batch parallelism), layer-level parallelism, and loop-level parallelism. Task-level parallelism can be defined as the simultaneous execution of two or more inference prediction tasks during the inference phase of the designed model by using efficiently on-chip memory. Layer-level parallelism (Inter-layer) can be achieved depending on the pipeline strategy. In the inference phase, each layer receives data from the previous layer as input. Because the layers are data-dependent on each other, the layers can't run completely in parallel. The model can be accelerated by using the pipeline structure instead of parallelism through launching layer (l) before ending the execution of $(l-1)$. Loop-level parallelism can be defined as kernel-level parallelism. To implement convolution operation MxN kernels are employed. Each of the kernels operate can be executed in parallel ways theoretically because all the convolutions' operations are independent. However, practically, limited computation resources and memory bandwidth does not allow all processes to be performed in parallel on FPGA. On account of this, loop-level parallelism can be implemented in many different ways according to different loop unrolling strategies. Loop-level parallelism is explored in detail in the next section.

The implementation of convolution operation enables numerous techniques for parallelism. However, due to the FPGA resource limitation, exploiting a full parallelism pattern for overall CNN is impossible. In some cases, even just one convolution layer can't run completely in parallel. Therefore, partial parallelism is employed by using the *unrolling* factor and *tilling* factor.

Due to the fact that convolution operations take occur in the convolution layer, most operations, about 90% of all

operations are performed in the convolutional layers. Convolution operation involves multiple multiplies and accumulates (MAC) operations with six nested loops. Therefore, an effective convolution acceleration optimization approaches considerably affects the performance of a hardware-based CNN accelerator. Nested loop optimization techniques, e.g. loop unrolling, tiling, and interchange, or only tune some of the design variables after the accelerator architecture and dataflow are already fixed. Without fully studying the convolution loop optimization before the hardware design phase, the resulting accelerator can hardly exploit the data reuse and manage data movement efficiently.

IV. IMPLEMENTATION OF ACCELERATED CNN

In this study, optimization in the Conv layer is done by unrolling kernel and IFM to decrease latency and increase throughput. Baseline design is used to compare the result of the suggested design in RTL syntheses. Comparison is made by means of latency, throughput, and resource utilization.

The framework of created accelerator system (AC) is shown in Fig. 3. AC system consists of two parts that are Input layer and Conv layer. The input layer is the layer responsible for storing data in BRAM units. The conv layer is the unit where the calculations are made. The Conv layer consists of Processing Elements (PEs) units, buffers, and OFMs. PE is the basic computation unit to perform convolution operations. The number of PE can be determined by unrolling factor N. Unrolling kernels determine the multiplication and adder units.

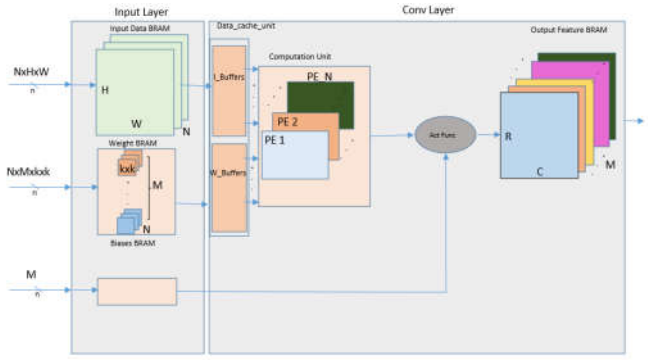

Fig. 3. Proposed accelerator framework

The convolution operation for a three-dimensional image consists of six nested for loops. All of these loops can be unrolled individually or together. Unrolling separately or together causes different parallelism operations. Loop-level parallelism can be implemented in many ways according to different loop unrolling strategies. In this section, the unroll operation performed in different ways for the convolution operation and the hardware equivalent of these operations are examined.

A. Data cache structure

During the inference state of a CNN, it is often necessary to read a large amount of data. The limitation of bandwidth and on-chip memory capacity makes it hard to obtain all data simultaneously. Modern FPGA provides large amounts of on-chip memory which of it is implemented as block RAM (BRAM) where embedded within the fabric. For the inference stage, CNN required memory required for parameters and data which are input data, bias, weight data, and the output of intermediate layers data. The required memory (RM) for the input data can be calculated

$$RM\_IFM = HxWxNxdata\_bit\_widht$$
$$RM\_OFM = RxCxMxdata\_bit\_widht$$
$$RM\_W = kxkxMxNxdata\_bit\_widht$$

The block RAM in Xilinx Zynq-7000 target FPGAs store up to 36 Kbits of data and each 36 Kb block RAM can be constructed as a 64K x 1 (when cascaded with an adjacent 36 Kb block RAM), 32K x 1, 16K x 2, 8K x 4, 4K x 9, 2K x 18, 1K x 36, or 512 x 72 in simple dual-port mode.

Data access time is one of the main challenges in FPGA implementation, therefore, data access pattern is crucial. The data feeding the parallel processing units should also come to these units in parallel. BRAM partitioning method is used for the parallel reception of data on BRAM [22,23]. In order to cache required data in parallel, the BRAMs must be completely partitioned and all data must be recorded in registers. By means of partitioning BRAM completely, the data can be fed to the computation unit in parallel and at the same time the use of BRAM will be reduced, but there may not be enough resources to save this much data to the registers. Therefore, using this method is not suitable for large networks. Using a temporal memory storage controller provides using low resource and low latency. In this study, the data are given to the computational units in parallel using the buffer structure. Data cache structure consists of three units as shown in Fig. 4. The first is the BRAMs where all acquired data are stored on. The second unit is the line buffer (LB) unit. The last is the window buffer (WB) unit. This unit is used to temporarily store data needed for convolution operation in the PE units or computation units. PE units access the same data multiple times because the convolution operation is the iterative algorithm. To avoid reading the same data multiple times the WB could shift all data and replaces the used data which are not required anymore with new data [21]. WB has a kxk register for kernel data and kxk register for the IFM data. It stores the data coming from the LB. LBs are temporary memory storage buffers that can cache rows or columns of IFM data. LB units are created based on shift register logic which shifts all data via WB.

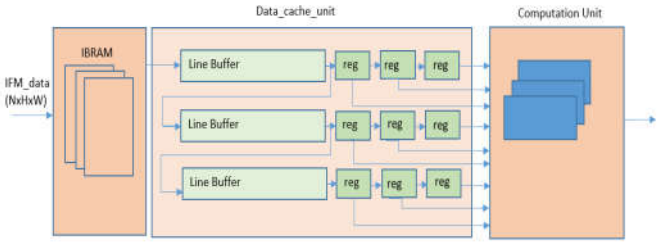

Fig. 4. Data cache structure

B. Baseline design

In the baseline design loops are rolled. That means that one copy of the loop body is synthesized for iterations and re-used for each iteration. This causes all operations to occur in a sequential manner. Sequencing of processes will ensure that the number of resources used is less than designs with parallel processing that are made by unrolling loops. However, latency will be very high than in unrolled loop architecture because the operations are done sequentially. Through the unrolling nested loops, new hardware resources will be assigned for all operations that can be done in parallel, so that operations can be performed faster and in parallel.

Table 1. Parameters for first conv layer

N	M	R	C	kxk
3	6	25	25	5x5

The baseline design process and hardware structure corresponding to baseline design are shown in Fig. 5 and Fig. 6 respectively. In the study, the baseline model represents the situation in which no optimization has been made yet. Table 1 shows the parameters for implemented convolution layer. Only one module is used, and this module is used sequentially for all MAC operations to be made. In this design, the latency is very high, but the number of resources used is very low.

Trip count (TC) is used to define a minimum number of times a loop executes.

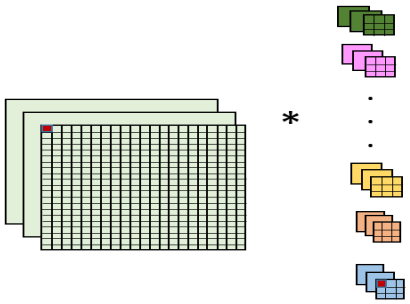

Fig. 5. Baseline design process

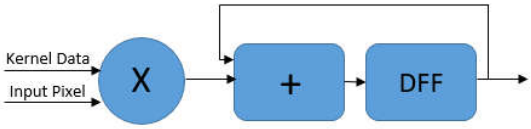

Fig. 6. Corresponding hardware architecture for the baseline design

Summary

Latency (cycles)		Latency (absolute)		Interval (cycles)		
min	max	min	max	min	max	Type
4767857	4768309	47.679 ms	47.683 ms	4767857	4768309	none

Detail

Instance

Loop

	Latency (cycles)			Initiation Interval			
Loop Name	min	max	Iteration Latency	achieved	target	Trip Count	Pipelined
- Loop 1	2353	2353	3	1	1	2352	yes
- Loop 2	451	451	3	1	1	450	yes
- Loop_for_M	4765500	4765500	794250	-	-	6	no
+ Loop_for_RxC	794248	794248	28366	-	-	28	no
++ Loop_for_RxC.1	28364	28364	1013	-	-	28	no
+++ Loop_for_N	1011	1011	337	-	-	3	no
++++ Loop_for_kxk	335	335	67	-	-	5	no
+++++ Loop_for_kxk.1	65	65	13	-	-	5	no

Fig. 7. A part of the synthesis report for the baseline design

In the baseline model, operations are performed sequentially. There is only one multiplication that can perform this structure therefore, it processes by taking one pixel from IFM set and one data from kernel sets at a time. It takes Nxkxk trip count to generate one pixel of one OFM. It takes NxRxkxk TC to generate one row of one OFM and NxRxCxkxk TC to generate one OFM. To generate all OFM it takes MxNxRxCxkxk TC.

#PE=1, #multipliers=1, #adders=1

$$Throughput = \frac{MxNxRxCxkxk}{latency}$$

The latency for baseline design is 47.683 ms. The baseline design uses 25 BRAMs and 5 DSP resources. Throughput is calculated 5.9GOP/s for baseline design. Fig. 7 shows the part of the synthesis report for baseline design.

C. Proposed Design: Unrolling kernels and IFM channels

In this case, operations are performed partially parallel to result in one pixel of OFM sets. The proposed design process and hardware structure corresponding to it are shown in Fig. 8 and Fig. 9 respectively.

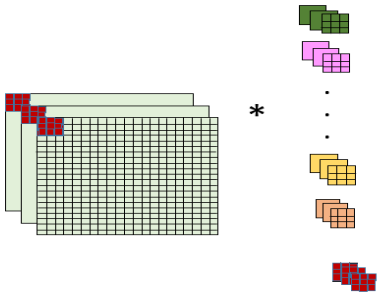

Fig. 8. Proposed design process

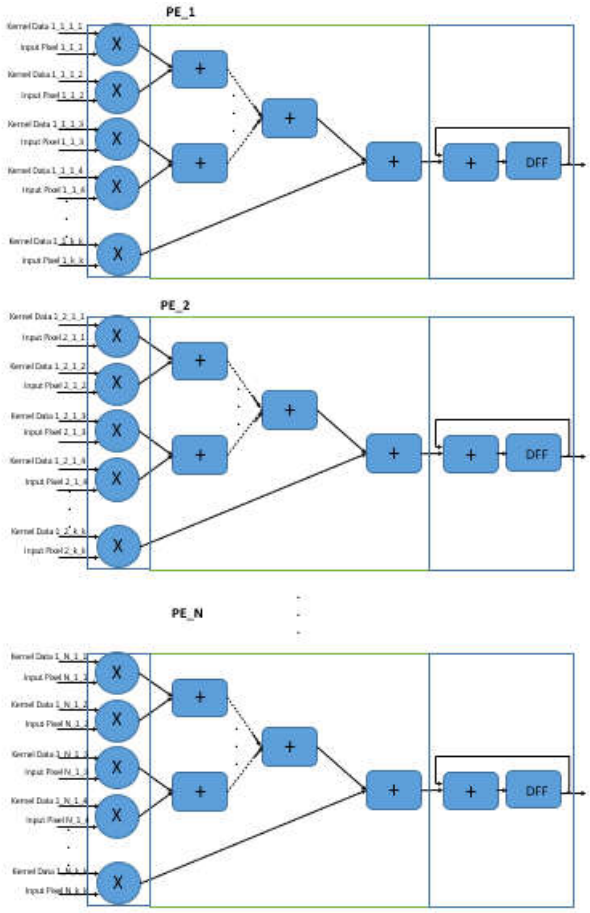

Fig. 9. Corresponding hardware architecture for the proposed design

In the proposed method, input data channels and kernels are unrolled. As a result of this process, N PE units are created for hardware implementation. In each PE unit, kxk multiplication is performed. Fig. 10 shows the part of the synthesis report for the proposed design.

Summary

Latency (cycles)		Latency (absolute)		Interval (cycles)		
min	max	min	max	min	max	Type
1799861	1800313	17.999 ms	18.003 ms	1799861	1800313	none

Detail

Instance

Loop

	Latency (cycles)			Initiation Interval			
Loop Name	min	max	Iteration Latency	achieved	target	Trip Count	Pipelined
- Loop 1	2353	2353	3	1	1	2352	yes
- Loop 2	451	451	3	1	1	450	yes
- Loop_for_M	1797504	1797504	299584	-	-	6	no
+ Loop_for_RxC	299544	299544	10698	-	-	28	no
++ Loop_for_RxC.1	10696	10696	382	-	-	28	no

Fig. 10. A part of the synthesis report for the proposed design

There are Nxkxk multiplication can perform this structure therefore, it processes by taking Nxkxk pixel from IFM set and Nxkxk data from kernel sets at a time. It takes 1 TC to generate one pixel of one OFM. It takes R TC to generate one row of one OFM and RxC TC to generate one OFM. To generate all OFM it takes MxRxC TC.

#PE=N=3, #multipliers=kxkxN#adders=(kxk-1)xN

The latency for the proposed design is 18 ms. Proposed design use 26 BRAMs and 8 DSP resources. Throughput is calculated 15.6 GOP/s for the first convolution layer in proposed design.

V. CONCLUSION

FPGA technologies are a favorable alternative to implementing CNN-based algorithms due to their reconfigurability, high performance, and low energy usage characteristics. However, it is difficult to implement the whole CNN architecture on FPGA without any optimization because of limitations in terms of resources and bottlenecks. In this paper, an FPGA-based CNN architecture using high-level synthesis (HLS) is demonstrated and the implemented architecture has been fastened. To improve the throughput, the proposed design is optimized for convolutional layers by unrolling the kernel and IFM channel. The most important contribution of this study is to perform optimization on the convolution layer by unrolling kernels and input feature maps and examine the effects on throughput, latency, and hardware resources.

ACKNOWLEDGMENT

This research was supported by a grant from (121E393) TUBITAK (Türkiye Bilimsel ve Teknolojik Araştirma Kurumu). We thank the TUBITAK for their support of our research.

Authors' Contributions

The authors' contributions to the paper are equal.

Statement of Conflicts of Interest

There is no conflict of interest between the authors.

Statement of Research and Publication Ethics

The authors declare that this study complies with Research and Publication Ethics

REFERENCES

[1] Y. Lecun, L. Bottou, Y. Bengio, and P. Haffner, "Gradient-based learning applied to document recognition," *Proceedings of the IEEE*, vol. 86, no. 11, pp. 2278–2324, 1998.

[2] K. Simonyan and A. Zisserman, "Very Deep Convolutional Networks for Large-Scale Image Recognition," *arXiv.org*, 2014, doi: 10.48550/arXiv.1409.1556.

[3] A. Krizhevsky, I. Sutskever, and G. E. Hinton, "ImageNet classification with deep convolutional neural networks," *Communications of the ACM*, vol. 60, no. 6, pp. 84–90, May 2017, doi: 10.1145/3065386.

[4] M. Mikaeili and H. S. Bilge, "Estimating Rotation Angle and Transformation Matrix Between Consecutive Ultrasound Images Using Deep Learning," 2020 Medical Technologies Congress (TIPTEKNO), Nov. 2020, doi: 10.1109/tiptekno50054.2020.9299237.

[5] C. Huang, S. Ni and G. Chen, "A layer-based structured design of CNN on FPGA," *2017 IEEE 12th International Conference on ASIC (ASICON), 2017*, pp. 1037-1040, doi: 10.1109/ASICON.2017.8252656.

[6] W. A. Haque, S. Arefin, A. S. M. Shihavuddin, and M. A. Hasan, "DeepThin: A novel lightweight CNN architecture for traffic sign recognition without GPU requirements," *Expert Systems with Applications,* vol. 168, p. 114481, Apr. 2021, doi: 10.1016/j.eswa.2020.114481.

[7] Y. Hu, Y. Liu, and Z. Liu, "A Survey on Convolutional Neural Network Accelerators: GPU, FPGA and ASIC," *2022 14th International Conference on Computer Research and Development (ICCRD),* Jan. 2022, doi: 10.1109/iccrd54409.2022.9730377.

[8] N. Zhang, X. Wei, H. Chen, and W. Liu, "FPGA Implementation for CNN-Based Optical Remote Sensing Object Detection," *Electronics*, vol. 10, no. 3, p. 282, Jan. 2021, doi: 10.3390/electronics10030282.

[9] C, Zhang, P. Li, G. Sun, Y. Guan, B. Xiao, J. Cong, "Optimizing fpga-based accelerator design for deep convolutional neural networks." *In Proceedings of the 2015 ACM/SIGDA International Symposium on Field-Programmable Gate Arrays,* Monterey, CA, USA, 22–24 February 2015; pp. 161–170.

[10] A. Dundar, J. Jin, V. Gokhale, B. Krishnamurthy, A. Canziani, B. Martini, & E. Culurciello," Accelerating deep neural networks on mobile processor with embedded programmable logic*." In Neural information processing systems conference (NIPS).* 2013

[11] M. Arredondo-Velázquez, J. Diaz-Carmona, C. Torres-Huitzil, A. Padilla-Medina, and J. Prado-Olivarez, "A streaming architecture for Convolutional Neural Networks based on layer operations chaining," *Journal of Real-Time Image Processing,* vol. 17, no. 5, pp. 1715–1733, Jan. 2020, doi: 10.1007/s11554-019-00938-y.

[12] Y. Ma, Y. Cao, S. Vrudhula, and J. Seo, "Optimizing the Convolution Operation to Accelerate Deep Neural Networks on FPGA*," IEEE Transactions on Very Large Scale Integration (VLSI) Systems,* vol. 26, no. 7, pp. 1354–1367, Jul. 2018, doi: 10.1109/tvlsi.2018.2815603.

[13] Y. Shen, M. Ferdman and P. Milder, "Maximizing CNN accelerator efficiency through resource partitioning," *2017 ACM/IEEE 44th Annual International Symposium on Computer Architecture (ISCA),* 2017, pp. 535-547, doi: 10.1145/3079856.3080221.

[14] S. Ghaffari and S. Sharifian, "FPGA-based convolutional neural network accelerator design using high level synthesize," *2016 2nd International Conference of Signal Processing and Intelligent Systems (ICSPIS),* 2016, pp. 1-6, doi: 10.1109/ICSPIS.2016.7869873.

[15] Huimin Li, Xitian Fan, Li Jiao, Wei Cao, Xuegong Zhou and Lingli Wang, "A high performance FPGA-based accelerator for large-scale convolutional neural networks*," 2016 26th International Conference on Field Programmable Logic and Applications (FPL),* 2016, pp. 1-9, doi: 10.1109/FPL.2016.7577308.

[16] Z. Liu, Y. Dou, J. Jiang, J. Xu, S. Li, Y. Zhou, Y. Xu, "Throughput-optimized fpga accelerator for deep convolutional neural networks." *ACM Trans. Reconfgurable Technol. Syst. (TRETS)* 10(3), 17, 2017

[17] Y. Zhou, J. Jiang, " An FPGA-based accelerator implementation for deep convolutional neural networks." *In Proceedings of the 2015 4th International Conference on Computer Science and Network Technology, ICCSNT 2015*, Harbin, China, 19–20 December2015; Volume 1, pp. 829–832.

[18] K. Abdelouahab, M. Pelcat, J. Serot, & F. Berry, "Accelerating CNN inference on FPGAs: A survey." arXiv preprint arXiv:1806.01683. 2018.

[19] K. Guo, S. Zeng, J. Yu, Y. Wang, & H. Yang" [DL] A survey of FPGA-based neural network inference accelerators." *ACM Transactions on Reconfigurable Technology and Systems (TRETS),* 12(1), 1-26.2019.

[20] R. Ayachi, Y. Said, & A. Abdelali, "Optimizing Neural Networks for Efficient FPGA Implementation: A Survey." *Archives of Computational Methods in Engineering,* 28(7), 4537–4547. 2021.

[21] G. Muhsin "A Comparative Study between RTL and HLS for Image Processing Applications with FPGAs" thesis, University of California, San Diego, Master of Science.

[22] Vivado Design Suite User Guide High-Level Synthesis Documentation Portal. (2022). Retrieved May 17, 2022, from Xilinx.com website: https://docs.xilinx.com/v/u/2018.3-English/ug902-vivado-high-level-synthesis

[23] S. Guzel Aydin and H. S. Bilge, "FPGA -Based Implementation of Convolutional Layer Accelerator Part for CNN," *2021 Innovations in Intelligent Systems and Applications Conference (ASYU), 2021*, pp. 1-6, doi: 10.1109/ASYU52992.2021.9599029.

[24] F. Uysal, F. Hardalaç, O. Peker, T. Tolunay, and N. Tokgöz, "Classification of Shoulder X-ray Images with Deep Learning Ensemble Models," Applied Sciences, vol. 11, no. 6, p. 2723, Mar. 2021, doi: 10.3390/app11062723.

International Journal of Multidisciplinary Studies and Innovative Technologies

e-ISSN: 2602-4888
dergipark.org.tr/en/pub/ijmsit
Research Article

2022, 6 (1), 45-50
DOI: DOI: 10.36287/ijmsit.6.1.45
Received: May 20, 2022; Accepted: June 20, 2022

Author Identification with Machine Learning Algorithms

İbrahim Yülüce[1*,2], Feriştah Dalkılıç[3]

[1*]*The Graduate School of Natural and Applied Sciences, Dokuz Eylul University, İzmir, Turkey (ibrahim.yuluce@ceng.deu.edu.tr) (ORCID: 0000-0002-3652-7184)*
[2]*Department of Computer Engineering, Ege University, İzmir, Turkey (ibrahim.yuluce@ege.edu.tr) (ORCID: 0000-0002-3652-7184)*
[3]*Department of Computer Engineering, Dokuz Eylul University, İzmir, Turkey (feristah.orucu@deu.edu.tr) (ORCID: 0000-0001-7528-5109)*

Abstract – Author identification is one of the application areas of text mining. It deals with the automatic prediction of the potential author of an electronic text among predefined author candidates by using author specific writing styles. In this study, we conducted an experiment for the identification of the author of a Turkish language text by using classical machine learning methods including Support Vector Machines (SVM), Gaussian Naive Bayes (GaussianNB), Multi Layer Perceptron (MLP), Logistic Regression (LR), Stochastic Gradient Descent (SGD) and ensemble learning methods including Extremely Randomized Trees (ExtraTrees), and eXtreme Gradient Boosting (XGBoost). The proposed method was applied on three different sizes of author groups including 10, 15 and 20 authors obtained from a new dataset of newspaper articles. Term frequency-inverse document frequency (TF-IDF) vectors were created by using 1-gram and 2-gram word tokens. Our results show that the most successful method is the SGD with a classification performance accuracy of 0.976% by using word unigrams and most successful method is the LR with a classification performance accuracy of 0.935% by using word bigrams.

Keywords *– Author identification, Natural Language Processing, Tf-Idf, Text Mining, Machine Learning*

Citation: Yülüce, İ., Dalkılıç, F. (2022). Author Identification with Machine Learning Algorithms. International Journal of Multidisciplinary Studies and Innovative Technologies, 6(1): 45-50.

I. INTRODUCTION

Author profiling, authorship verification, and author identification are the applications of text mining. Author profiling is the examination of authors' texts to determine their class, including gender, age group, etc. Authorship verification is the task of determining whether two or more texts were written by the same author by analyzing linguistic patterns. Author identification deals with estimating the author of an anonymous text from a predefined set of candidate authors.

In this study, we deal with the authorship identification task that is used in many areas including literary studies, history and forensic linguistics. The need to identify the content creator on the internet, detect plagiarism and prevent copyright infringement has increased the interest in authorship identification. In the identification process, stylometric features expose the patterns that appear in the texts belonging to a specific author. Various number of features have been presented including vocabulary richness measures, syntactical features, function words frequencies, character n-gram frequencies, latent semantic analysis (LSA), and Bag-of-Words (BOW) [1, 2, 3] in many previous studies. In addition, deep learning and machine learning based methods have been employed for the feature extraction and author identification tasks in recent studies [4].

In the scope of this study, we collected the newspaper articles of the top three online news portals of Turkey from 2005 to the present. We created a novel dataset to use in the task of identifying the author of a Turkish language text. By using this dataset, we created sub-datasets of different sizes, including 10, 15 and 20 authors with the highest number of articles. Author identification is a multi-class classification problem that deals with labeling an anonymous text with one of the potential authors. We tested some classical machine learning methods including Support Vector Machines (SVM), Gaussian Naive Bayes (GaussianNB), Multi-Layer Perceptron (MLP), Logistic Regression (LR), Stochastic Gradient Descent (SGD) and ensemble learning methods including Extremely Randomized Trees (ExtraTrees), and eXtreme Gradient Boosting (XGBoost) by python implementations using scikit-learn library. Additionally, we used the JPype python module to provide full access to Zemberek Java Library and the matplotlib and seaborn libraries for data visualization. The contributions of our work are comparison of classical machine learning methods with the new generation ensemble learning methods and reveal the effect of working with different sizes of the author candidate pool and n-grams.

The rest of this paper is structured as follows: In section 2, we give some important studies performed in this topic. Section 3 gives an overview about the dataset, preprocessing tasks and classification algorithms used in our experiments. In section 4, we present the experimental results obtained by the proposed method under different cases. Finally, the last section concludes the paper and presents the relevant future work.

II. Literature Review

The task of identifying authors has been studied in different languages for different purposes since 2000. An important part of the literature consists of studies on English language [4, 5, 6, 7, 8]. There are also many studies done in many different languages including Japanese [9], Mongolian [10], Persian [11], Albanian [12], Indian [13, 14], Brazilian [15], Russian [16, 17], German [18], and Arabic [19]. When the existing studies were examined, it was seen that different types of data sets were used for author identification tasks. Some studies have been carried out on newspaper articles [4, 15, 18, 19], while others were carried out on poems [13], novels [11, 12, 16], email content [20], song lyrics [21], source codes [22], or tweets, blog posts, and forums [8, 9, 23]. In some cases, different types of data sources were combined or compared [17, 25]

Early studies in author identification focused on different stylometric techniques. These techniques are based on identification of style markers including lexical and character features or syntactic and semantic features that quantify writing style [9, 26]. The style markers can be exemplified as sentence length, function word and character n-gram frequencies, the number of verbs and punctuation marks in the sentences, vocabulary richness measures etc. With the development and widespread use of machine learning models over the last decade, machine learning-based author identification has become a promising solution for author identification. Mohsen et al. [4] applied a deep learning method with name Stacked Denoising Auto-Encoder for extracting document features and then used the SVM classifier. They used a subset of RCV1 dataset, which contains 100 documents from each of the top 50 authors and reached classification accuracy up to 95.12% under different settings. In [5] authorship attribution experiments were carried out using a Feedforward Neural Network model (FNN) and LR and 95.93% of accuracy was achieved on one of the four widely used datasets. In another recent study [6], pre-trained language models were applied in the field of author identification. They demonstrated that BERT and ELMo pre-trained models achieve the best results (as 92.86%) on a cross-domain dataset. Ramezani [7] employed seven well-known classifiers by using the TF_IDF scheme on two English and Persian datasets and obtained 0.902 and 0.931 accuracy, respectively. Fourkioti et al. [8] combined the three language models based on characters, words, and POS trigrams and achieved the best generalization accuracy of 96% on movie reviews.

A few research on author identification have been carried out in Turkish language. Some studies are based on NLP techniques, while others are based on machine learning techniques. One of the first studies in this field was [26]. Diri and Amasyalı extracted 22 style markers for the 18 different authors to determine the author of an anonymous text. They obtained a success rate of %84 on average. Örücü and Dalkılıç [27] proposed two methods for determining the corresponding author of an anonymous text. Author-specific N-gram Method and Support Vector Machine (SVM) were applied to newspaper columns of 16 authors. The first method reached a success ratio of 87% with 1-grams while SVM had a success ratio of 77% with 2-grams.

Atar et al. [25] collected the columns from the electronic archives of two different newspapers and created a dataset containing 100 training and 20 test articles for each of the 237 authors. They trained the Word2vFisher and Doc2Vec models using a large corpus in Turkish and used the SVM classifier to classify the columns. They stated that the Skip-Gram approach is more successful when compared to the CBOW approach. Kuyumcu et al. [28] used the same dataset in [25] and applied the Tf-Idf weighting method for the vector space that was a combination of word 1-3-n grams and character 2-6-ngrams. They used Ridge Regression as a classifier and achieved an accuracy of 89.6%.

Karaman et al. [29] used a total of 1295 news articles of 10 different authors to predict unknown authors of an articles by using TF-IDF technique and Random Forest, Decision Tree, Naive Bayes and SVM algorithms. They achieved success rates 80%, 69%, 94% and 97% of F-measure, respectively.

It can be noticed from the above examples that the author identification studies in Turkish language are open to development. In this paper, we introduced an author identification method using some classical machine learning and ensemble learning techniques. We also investigated the classification performance of the selected techniques on three different sized author groups and two distinct n-gram profiles.

III. Materials and Methods

A. Dataset

In this study, the dataset was gathered by us from plenty of Turkish News Websites. The collected articles include independent topics written by the authors and it includes articles written from 2005 to the present. Dataset contains 86,852 articles, 49 authors and an average of 1772 texts per author. While the maximum number of articles written by an author is 3,495, the minimum number of articles is 106. The information about the top 20 authors is given in Table 2. One of our authors has a total of 2,391 articles and the average number of words she/he used in these articles is 849.54. Additionally, we also see the minimum average word count per article is 335.11. While the maximum total word count for an author is 2,031,274, the average word count per article is approximately 445. No pre-processing or filtering was applied to the original corpus. Some of the texts have large spaces, url links, special characters and full capital words.

Since there is a great difference in the number of articles collected between the authors, 10-15-20 authors with the most articles were studied. The statistics about the generated three datasets are given in Table 1. The largest dataset with 20 authors, contains 55,108 articles and 24,218,293 total words.

Table 1. Article, word and average word

Dataset	Total Article	Total Word Count
Dataset-10	30,372	12,770,000
Dataset-15	43,451	17,861,840
Dataset-20	55,108	24,218,293

B. Pre-Processing

The original data cannot be sent to a machine learning model without pre-processing. Because real-world data is often noisy, inconsistent and incomplete. If we sent the data to the machine learning algorithm without pre-processing, we may encounter undesirable low scores. So, the below mentioned steps were applied to clean up the texts:

- Removing url links
- Normalizing text to lowercase
- Filtering stop-words

Table 2. Article, word and average word count per article of the top 20 authors

Author	Article Count	Total Word Count	Average Word Count per Article
Author 1	3,494	1,349,874	386,34
Author 2	3,386	1,161,662	343,07
Author 3	3,369	1,093,380	324,54
Author 4	3,084	1,562,320	506,58
Author 5	2,966	1,101,166	371,26
Author 6	2,933	1,274,944	434,68
Author 7	2,864	1,733,088	605,12
Author 8	2,777	1,273,953	458,75
Author 9	2,754	951,911	345,64
Author 10	2,745	1,267,702	461,82
Author 11	2,742	953,534	347,75
Author 12	2,670	1,017,759	381,18
Author 13	2,663	960,657	360,74
Author 14	2,553	1,338,523	524,29
Author 15	2,451	821,367	335,11
Author 16	2,391	2,031,274	849,54
Author 17	2,377	1,086,461	457,07
Author 18	2,362	989,805	419,05
Author 19	2,281	974,750	427,33
Author 20	2,246	1,274,163	567,30

- Filtering special characters
- Removing digits
- White space formatting

After completing these steps, we used the Zemberek library [24]. Zemberek is a natural language processing library that can be used for open-source Turkish languages, developed by using the Java programming language. By using this library, we did lemmatization for words, corrected spelling mistakes, and checked whether a word is Turkish. We compared the Zemberek and NLTK TurkishStemmer, and prefered using the Zemberek library.

C. Tf-Idf Vectorizer

In this paper, The TF-IDF vectorizer has been used to explore similarity between text documents. This is a very common algorithm for converting text to a meaningful representation of numbers, also known as vector representation to feed into machine learning algorithms. It is easy to implement and works fast. TF-IDF was used in the early 1970s to solve an information retrieval problem and then has been successfully used in document classification, topic modelling etc. TF represents the number of times each word occurs in text, article or any kind of datasets. For example, if the word “save” occurs 20 times in a text and the entire text has 1000 words, the TF value is 0,02 (20/1000). IDF shows the importance of the word “save” for a text. It is obtained by dividing the total number of texts by the number of texts containing the term. A score closer to zero indicates that the word is used more often.

TF-IDF Vectorizer in scikit-learn library takes ngram_range (1,1) as default parameter. The parameter (1,1) means only unigrams, (2,2) means only bigrams are used to create TF-IDF vectors. The larger n value indicates a larger probability pool. As the number of n_grams increase, we will see the decrease in the accuracy score in the experimental studies section.

D. Classification Models

In this study, machine learning and ensemble learning algorithms that have been applied to different fields and have shown successful performances were preferred and performance comparisons were made by applying them on three different data sets. The techniques used are briefly described below.

1. SVM (Support Vector Machine)

SVM is one of the supervised learning methods generally used in classification problems. Basically, it tries to separate two classes with a line or plane. It also makes this separation according to the elements at the boundary.

2. Gaussian NB (Naïve Bayes)

Naive Bayes is a probabilistic machine learning model used for classification problems. It can do good work with small data. Naive Bayes assumes that each class follows a Gaussian distribution and NB is a generative model.

3. MLP (Multi Layer Perceptron)

MLP has emerged as a result of the studies done to solve the XOR Problem. It works effectively especially in classification problems.

4. LR (Linear Regression)

LR is a popular, uncomplicated and a supervised learning algorithm. It is the simplest form of regression that is also used to examine the mathematical relationship between variables.

5. SGD (Stochastic Gradient Descent)

SGD is a linear classifier such as SVM or Linear Regression and has been successfully applied to large scale machine learning problems frequently encountered in text classification and natural language processing. It is easy to implement and has many possibilities in code tuning

6. Extra Trees

Extra Trees is an ensemble machine learning algorithm that combines the predictions from many decision trees. It is also easy to use and set various hyperparameters. It gives better

Table 3. Author Identification accuracies of the classifiers

N-gram	Classifier	Dataset-10	Dataset-15	Dataset-20
Unigrams	XgBoost	0.968	0.956	0.946
	SGD	**0.975**	**0.976**	**0.971**
	LR	0.962	0.956	0.954
	SVC-1	0.873	0.840	0.815
	SVC-2	0.945	0.932	0.926
	MLP	0.915	0.846	0.710
	Gaussian NB	0.832	0.775	0.746
	Extra Trees	0.936	0.904	0.871
Bigrams	XgBoost	0.831	0.855	0.822
	SGD	0.932	0.918	**0.900**
	LR	**0.935**	**0.920**	**0.900**
	SVC-1	0.812	0.707	0.633
	SVC-2	0.913	0.886	0.863
	MLP	0.896	0.765	0.607
	Gaussian NB	0.793	0.712	0.668
	Extra Trees	0.875	0.820	0.768
Average		0.900	0.861	0.819

performance than the Random Forest (RF) algorithm.

7. XgBoost (eXtreme Gradient Boosting)

XgBoost is a high-performance version of the Gradient Boosting algorithm optimized with various arrangements. The most important features of the algorithm are that it can achieve high predictive power, prevent overfitting, manage empty data and do them quickly. It is one of the popular algorithms preferred recently.

IV. Experimental Studies

We tested several combinations of hyperparameters' values by using Exhaustive Grid Search technique supplied by scikit-learn library and selected combinations with maximal classification accuracy. Final classification experiments were performed using selected hyperparameters for each classifier as given in Table 4. We used XgBoost and GaussianNB algorithms with default hyperparameters. We got the best results at default parameters even though we tried a wide variety of parameters. Two different settings of the SVC classifier are employed to see performance comparison of different kernel functions.

Table 4. HyperParameters of Classifier Methods

Classifier	HyperParameters
XgBoost	Default
SGD	Alpha=1e-05, max_iter=50, penalty=elasticnet
LR	Max_iter=1000, solver=lbfgs
SVC-1	Kernel=linear, gamma=scale, c=0.025
SVC-2	Kernel=rbf,gamma=2,c=1
MLP	Alpha=1,max_iter=1000
Gaussian NB	Default
Extra Trees	n_estimators=100,max_depth=1000, min_samples_split=2

Author identification performance of the classifiers are shown in Table 3. Accuracy was used as the evaluation metric to measure authorship identification performance. When the performances of the classifiers are evaluated, it is seen that the most successful method for unigrams is SGD. This is followed by the XgBoost and LR methods with almost similar performance. SVC-2 (with rbf kernel) and Extra Trees classifier were also successful by showing over 90% performance. Considering the bigrams, LR and SGD performed better than other classifiers.

The accuracy score is going down with the increasing author count in experiments. Because it is getting harder to predict the right author in a larger pool of authors. Increase in the number of authors also increases the number of tags to be predicted and causes a performance decrease of approximately 4%.

We worked with 1-grams and 2-grams separately for comparison purposes. As the results show us, 1-grams produce better accuracy scores than 2-grams considering all the classifiers. There is a significant difference in accuracy scores of XgBoost and SVC-1 (with linear kernel) classifiers (approximately %12) for different n-gram settings. On average, classifiers performed 5%, 8%, 10% better in unigrams compared to bigrams for Dataset-10, Dataset-15, and Dataset-20, respectively.

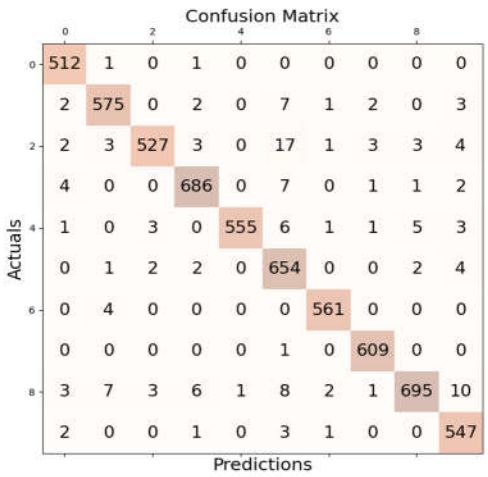

Fig. 1. Confusion Matrix of the SGD classifier by using unigrams for Dataset-10

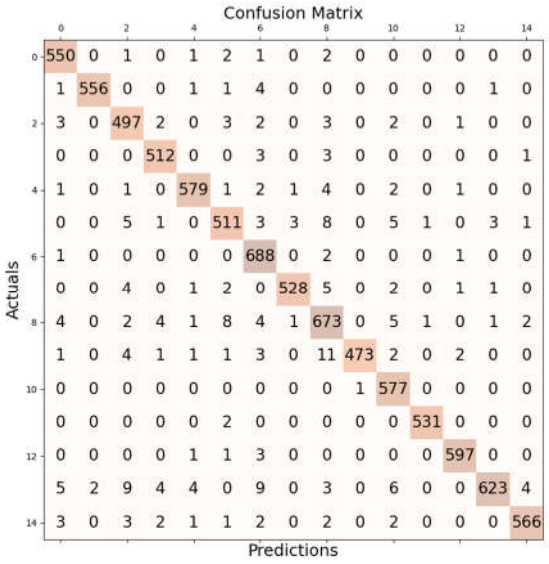

Fig. 2. Confusion Matrix of the SGD classifier by using unigrams for Dataset-15

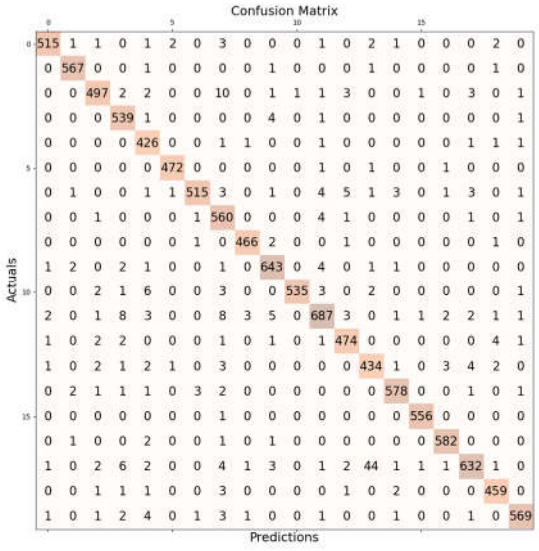

Fig. 3. Confusion Matrix of the SGD classifier by using unigrams for Dataset-20

As shown as in Figure 1, Figure 2 and Figure 3. SGD classifier has a state-of-the-art performance by using unigrams.

V. Conclusion

In this paper, we experimented with the author identification task for Turkish articles. A large amount of news articles has been collected and various text cleaning and pre-processing operations have been applied on it. Three different sizes of the author datasets have been created and unigram and bigram features have been investigated on these datasets. We also used TF-IDF to expose the author's specific ngram features. We set up the maximum features parameter of TFidfVectorizer as 3000 to build a vocabulary that only considers the top 3000 features ordered by term frequency across the particular datasets. Some important machine learning and ensemble learning algorithms that have been applied to different fields and have shown successful performances were trained on the author datasets. The GridSearchCV exhaustive search technique has been employed in the hyperparameter selection process. For all combination of values in the specified range, the network is trained and selected with the best hyperparameter for best accuracy rate.

It has been found that the most successful method for unigrams is SGD according to performance evaluation metrics. It is followed by the XgBoost and LR methods with almost similar performance. LR and SGD performed better than other classifiers in terms of bigrams. Another fact observed is that the prediction accuracy of classifiers is going down approximately 4% with the increasing author count of successive datasets. In addition to that, unigrams produce better accuracy scores than bigrams considering all the classifiers.

As a future work, a number of studies are planned with hybrid models based on BERT and deep neural networks to achieve more efficient models. Additionally, we are going to set up a different model instead of the TF-IDF model, such as Word2Vec word embedding method.

References

[1] Stamatatos, Efstathios. "A survey of modern authorship attribution methods." *Journal of the American Society for information Science and Technology* 60.3 (2009): 538-556.

[2] Alhuqail, Noura Khalid, Author Identification Based on NLP (April 6, 2021). European Journal of Computer Science and Information Technology, Vol.9, No.1, pp.1-26, 2021, Available at SSRN: https://ssrn.com/abstract=3820262

[3] Maël Fabien, Esau Villatoro-Tello, Petr Motlicek, and Shantipriya Parida. 2020. "BertAA : BERT fine-tuning for Authorship Attribution." *In Proceedings of the 17th International Conference on Natural Language Processing (ICON)*, pages 127–137, Indian Institute of Technology Patna, Patna, India. NLP Association of India (NLPAI).

[4] A. M. Mohsen, N. M. El-Makky and N. Ghanem, "Author Identification Using Deep Learning," 2016 15th IEEE International Conference on Machine Learning and Applications (ICMLA), 2016, pp. 898-903, doi: 10.1109/ICMLA.2016.0161.

[5] Yunita Sari, Mark Stevenson, and Andreas Vlachos. 2018. Topic or Style? Exploring the Most Useful Features for Authorship Attribution. *In Proceedings of the 27th International Conference on Computational Linguistics*, pages 343–353, Santa Fe, New Mexico, USA. Association for Computational Linguistics.

[6] Barlas, G., Stamatatos, E. (2020). Cross-Domain Authorship Attribution Using Pre-trained Language Models. In: Maglogiannis, I., Iliadis, L., Pimenidis, E. (eds) Artificial Intelligence Applications and Innovations. AIAI 2020. IFIP Advances in Information and Communication Technology, vol 583. Springer, Cham. https://doi.org/10.1007/978-3-030-49161-1_22

[7] Ramezani, Reza. "A language-independent authorship attribution approach for author identification of text documents." *Expert Systems with Applications* 180 (2021): 115139.

[8] Olga Fourkioti, Symeon Symeonidis, Avi Arampatzis, Language models and fusion for authorship attribution, Information Processing & Management, Volume 56, Issue 6, 2019, 102061, ISSN 0306-4573, https://doi.org/10.1016/j.ipm.2019.102061.

[9] S. Okuno, H. Asai and H. Yamana, "A challenge of authorship identification for ten-thousand-scale microblog users," 2014 IEEE International Conference on Big Data (Big Data), 2014, pp. 52-54, doi: 10.1109/BigData.2014.7004491.

[10] Z. Damiran and K. Altangerel, "Author Identification-An Experiment Based on Mongolian Literature Using Decision Trees." *2014 7th International Conference on Ubi-Media Computing and Workshops*. IEEE, 2014. pp. 186-189.

[11] Ramezani, Reza, Navid Sheydaei, and Mohsen Kahani. "Evaluating the effects of textual features on authorship attribution accuracy." *ICCKE 2013*. IEEE, 2013.

[12] H. Paci, E. Kajo, E. Trandafili, I. Tafa and D. Salillari, "Author Identification in Albanian Language," *2011 14th International Conference on Network-Based Information Systems*, pp. 425-430.

[13] Pandian, A., V. V. Ramalingam, and R. V. Preet. "Authorship identification for Tamil classical poem (Mukkoodar Pallu) using C4. 5 algorithm." *Indian Journal of Science and Technology* 9.46 (2016).

[14] Kale Sunil Digamberrao, Rajesh S. Prasad, Author Identification using Sequential Minimal Optimization with rule-based Decision Tree on Indian Literature in Marathi, Procedia Computer Science, Volume 132, 2018, Pages 1086-1101, ISSN 1877-0509, https://doi.org/10.1016/j.procs.2018.05.024.

[15] Oliveira W Jr, Justino E, Oliveira LS. Comparing compression models for authorship attribution. Forensic Sci Int. 2013 May 10;228(1-3):100-4. doi: 10.1016/j.forsciint.2013.02.025. Epub 2013 Mar 24. PMID: 23597746.

[16] Romanov, Aleksandr & Kurtukova, Anna & Shelupanov, Alexander & Fedotova, Anastasia & Goncharov, Valery. (2020). Authorship Identification of a Russian-Language Text Using Support Vector Machine and Deep Neural Networks. Future Internet. 13. 3. 10.3390/fi13010003.

[17] Fedotova, A.; Romanov, A.; Kurtukova, A.; Shelupanov, A. Authorship Attribution of Social Media and Literary Russian-Language Texts Using Machine Learning Methods and Feature Selection. *Future Internet* 2022, 14, 4. https://doi.org/10.3390/fi14010004

[18] Sage, M., Cruciata, P., Abdo, R., Cheung, J.C., & Zhao, Y.F. (2020). Investigating the Influence of Selected Linguistic Features on Authorship Attribution using German News Articles. *SwissText/KONVENS.*

[19] Otoom, Ahmed & Abdallah, Emad & Jaafer, Shifaa & Hamdallh, Aseel & Amer, Dana. (2014). Towards author identification of Arabic text articles. 2014 5th International Conference on Information and Communication Systems, ICICS 2014. 1-4. 10.1109/IACS.2014.6841971.

[20] O. de Vel, A. Anderson, M. Corney, and G. Mohay. 2001. Mining e-mail content for author identification forensics. *SIGMOD Rec*. 30, 4 (December 2001), 55–64. https://doi.org/10.1145/604264.604272

[21] B. Kırmacı and H. Oğul, "Evaluating text features for lyrics-based songwriter prediction," 2015 IEEE 19th International Conference on Intelligent Engineering Systems (INES), 2015, pp. 405-409, doi: 10.1109/INES.2015.7329743.

[22] Upul Bandara, Gamini Wijayarathna, Source code author identification with unsupervised feature learning, Pattern Recognition Letters, Volume 34, Issue 3, 2013, Pages 330-334, ISSN 0167-8655, https://doi.org/10.1016/j.patrec.2012.10.027.

[23] Alonso-Fernandez, Fernando & Belvisi, Nicole & Hernandez-Diaz, Kevin & Muhammad, Naveed & Bigun, Josef. (2021). Writer Identification Using Microblogging Texts for Social Media Forensics. IEEE Transactions on Biometrics, Behavior, and Identity Science. PP. 1-1. 10.1109/TBIOM.2021.3078073.

[24] Akın, Ahmet Afsin, and Mehmet Dündar Akın. "Zemberek, an open source NLP framework for Turkic languages." *Structure* 10.2007 (2007): 1-5.

[25] M. S. Atar, E. Esen and M. A. Arabaci, "Supervised author recognition with aggregated word embeddings," 2018 26th Signal Processing and Communications Applications Conference (SIU), 2018, pp. 1-4, doi: 10.1109/SIU.2018.8404464.

[26] Diri, B., and Amasyalı, M. F. (2003, June). "Automatic author detection for Turkish texts." In Artificial Neural Networks and Neural Information Processing (ICANN/ICONIP) (pp. 138-141).

[27] Örücü F., Dalkılıç G., "Author Identification Using N-grams and SVM", The 1. International Symposium on Computing in Science & Engineering, ISBN:978-605-61394-0-6 P:130, Kuşadası, 3-5 Haziran 2010

[28] B. Kuyumcu, B. Buluz and Y. Kömeçoğlu, "Author Identification in Turkish Documents with Ridge Regression Analysis," 2019 27th Signal Processing and Communications Applications Conference (SIU), 2019, pp. 1-4, doi: 10.1109/SIU.2019.8806242.

[29] Burcu İlkay KARAMAN, Feriştah DALKILIÇ, Emine Eda ÇAM EKER, "Author Recognition In Modern Turkish For Forensic Linguistic Cases Using Machine Learning", 1st International, 17th National Forensic Science Congress, 12-15 November 2020, Online.

International Journal of Multidisciplinary Studies and Innovative Technologies

e-ISSN: 2602-4888
dergipark.org.tr/en/pub/ijmsit
Research Article

2022, 6 (1), 51-57
DOI: 10.36287/ijmsit.6.1.51
Received: May 20, 2022; Accepted: June 20, 2022

Roblox Studio ile Mühendislik Eğitimi İçin Deneyim Geliştirme

Onur Yolal [1*]

[1*]*Elektronik Teknolojisi Programı, Başkent Üniversitesi Kahramankazan Meslek Yüksekokulu, Ankara, Türkiye*
onuryolal@baskent.edu.tr (ORCID: 0000-0003-4609-0454)

Türkçe Özet – Gerilim kaynağı, ayarlı direnç, kablolar ve bir ampermetre düzeneği ile basit bir elektronik devre çalışmasını temel düzeyde öğrencilere anlatmalıyız. Günümüzde öğrencilerin bilgisayar, telefon, tablet gibi teknolojik cihazlar çağına doğmuş olmaları gerçeği ile başbaşayız. Gün içerisinde vaktinin büyük bir çoğunluğunu sürekli bu cihazların başında geçiren öğrencilerin değerli vakitlerini verimli geçirmedikleri düşüncesiyle endişe ediyoruz. Sadece mühendislik eğitimi için değil, matematik, fen bilgisi (fizik, kimya, biyoloji, coğrafya, geometri gibi pozitif bilimler) veya uygulamalı bilimlere ait temel dersleri öğrencilere öğretirken ne gibi modern ve güncel araçlardan faydalanabiliriz sorusunun cevabı olarak Roblox platformunu kullanmak bu çalışmada esas alınmıştır. Bugün geliştiriciler, dünya çapında yaygın olarak bilinen Roblox platformunu kullanarak kendi oyun deneyimlerini Lua dilinde kodlayıp dünyaya yayınlayabiliyorlar. Günümüzde Roblox Studio ile birlikte mühendislik bilgilerinden yola çıkarak oyun simülasyonu deneyimi geliştirmek mümkün olabilir gibi görünüyor. Bu çalışma ile elektrikte yaygın olarak bilinen Ohm kanunu örnek alınmıştır. Roblox evreninde örnek bir deneyim (Game Experience) geliştirerek basit bir elektrik devresi analizi gerçekleştirmek üzere bir devre simülasyonu geliştirme çalışması yapılmıştır. Bu yaklaşımı ilginç kılan taraf ise Roblox oynamak yerine Roblox Studio ile oyun geliştirme yapılabileceğini öğrenciye göstermektir. Bu çalışmada amaçlanan, Mühendislik eğitimde sıklıkla kullanılan formülleri Roblox platformunda bir oyun deneyimi halinde Lua dilini kullanarak sunma imkanını göstermektir. Mühendislikteki yaklaşımların Roblox Studio'nun sunduğu deneyim geliştirme ortamında üç boyutlu benzetimin gerçekleştirilebilmesi adına bu çalışmanın sunumunun uygun olacağı düşünülmüştür.

Anahtar Kelimeler *– Roblox, Roblox Studio, Metaverse, Oyun Deneyimi, Devre Analizi, Lua programlama dili, Oyun Programlama*

Atıf: Yolal, O. (2022). Roblox Studio İle Mühendislik Eğitimi İçin Deneyim Geliştirme. International Journal of Multidisciplinary Studies and Innovative Technologies, 6(1): 51-57.

Experience Development of Roblox Studio for Engineering Education

Abstract

Explaining a simple electronic circuit analysis with a voltage source, a resistor, cables and an ampermeter assembly to the students at a basic level. Today, we withness the fact that students are born into the age of technological devices such as computers, phones and tablets. We are concerned that kids who spend the majority of their daytime hours using these devices are wasting their important time. This study mostly based on using the Roblox platform as a response to the query, what modern and up-to-date tools can we use while teaching students not only for engineering education, but also mathematics, science (positive sciences such as physics, chemistry, biology, geography, geometry e.t.c.) or applied sciences to students. Today, developers can code their own game experiences in Lua language and publish them to the world using the widely known Roblox platform worldwide. Today, it seems possible to develop a game simulation experience with Roblox Studio based on engineering knowledge. In this study, Ohm's law, which is widely known in electricity, is taken as an example. A circuit simulation development study was conducted to perform a simple electrical circuit analysis by developing an exemplary experience (Game Experience) in the Roblox universe. What makes this approach interesting is to show the student that game development can be done with Roblox Studio instead of playing Roblox. This study's objective is to demonstrate the viability of giving the formulas that are frequently used in Engineering education as a game experience on the Roblox platform by using the Lua language. It was thought that the presentation of this study would be appropriate in order to perform three-dimensional simulation in the experience development environment offered by Roblox Studio of approaches in engineering.

Keywords *– Roblox, Roblox Studio, Metaverse, Game Experience, Circuit Analysis, Lua programming language, Game Programming*

Citation: Yolal, O. (2022). Experience Development Of Roblox Studio For Engineering Education. International Journal of Multidisciplinary Studies and Innovative Technologies, 6(1): 51-57.

I. GİRİŞ

Elektrik-elektronik mühendisliğine ilgi duyan, bu alanda yeni yapılan çalışmaları merakla takip eden, teknolojik gelişmeler ışığında bilgi birikimi doğrultusunda günceli öğrenmeye heves eden başta teknik, endüstri ve Anadolu liseleri öğrencileri, 2 yıllık meslek yüksekokulu öğrencileri, 4 yıllık lisans öğrenimi gören üniversite öğrencileri vardır. Hem teknik bilimlere ilgi duyanlar hem de öğrencilerin eğitimlerinde bilgiyi pekiştirmek üzere birtakım laboratuvar deneyleri yapılması önem taşımaktadır. Laboratuvar imkânı olmayan öğrencilerin bu noktada eksiklik yaşamaması için bilgisayar destekli elektronik devre tasarımı ve çizim programlarından faydalanmaları önerilebilir. Bu noktada bir bilgisayar programının geliştirilmesi bu ihtiyacı karşılamak adına bir gereklilik olarak açığa çıkmaktadır.

2020 yılının Mart ayı itibari ile gündemde yer edinen Covid-19 pandemisi dolayısıyla lise ve üniversite düzeyinde verilen laboratuvar dersleri eğitimlerinde aksaklıklar yaşanmış, birçok laboratuvar öğrenci çalışmasına geçici olarak kapatılmıştı veya uygulama dersleri yapılamamıştı. Küresel anlamda yaşanan bu aksaklık mühendislik eğitimi açısından öğrenciler için telafi edilmesi gereken bir eksiklik olarak ortaya çıkmıştır. Lise ve üniversitelerde uygulama dersi veren öğretmenler ve akademisyenlerin uzaktan ders anlatma programları (Örneğin; Zoom, Microsoft Teams, Skype, Google Classroom gibi) eşliğinde laboratuvarlarda tek başlarına çevirim içi internet bağlantısı ile öğrencilere ders anlatımı yaparak pandemi süreci minimum aksaklıkla atlatılmaya çalışılmıştır. Bir öğrencinin henüz staj yapmadan ve mezun olmadan sektörel deneyiminin bulunması için bir çalışma yaparak elektrik ve elektronik mühendisliği başta olmak üzere mühendislikte kullanılan temel denklem, formül, kanun ve yasaların deneyimlenebileceği bir bilgisayar programına ihtiyaç vardır. Bu ihtiyacı eğitim kurumları nezdinde giderebilmek için okullarda anlatılan derslerin müfredatını takip ederek yapılan elektronik devre deneylerinin Fritzing (EDA Software – Electronic Design Automation) gibi C++ ve Qt tabanlı bir bilgisayar programında da gerçekleştirilmesi kolaylık sağlamıştır. Benzer şekilde Proteus (ISIS ve ARES) adıyla bilinen elektronik devre kurma ve analizi programı kullanılabilmektedir. Bu şekilde önemli olan programlardan bazılarının isimleri: MultiSIM – Electroworkbench, LabView, LT-Spice, Cadence OrCAD Capture ve PSpice, Spice (UC Berkeley) programlarıdır.

Burada sözü edilen bu bilgisayar programlarının birçoğu ücretli ve kapalı kaynak yapıya sahiptir. Her ne kadar Fritzing programı başlangıçta ücretsiz kullanıma izin veriliyorken (freeware) 2021 yılı içerisinde program kullanımı için ücret talep etmeye başladığını duyurulmuştur. [1]

Son dönemde meydana gelen bu gibi gelişmelerin sonucunda ve küresel anlamda meydana gelen enflasyon neticesinde maddi açıdan erişilebilir lisans ücretlerinin giderek maliyetli bir hal alması, açık kaynaklı programların eğitim-öğretim çerçevesinde yapılmaya devam edilmesi gerekliliği, öğrencilere en güncel ve kaliteli bir eğitim materyalinin derslerde kullanılabilmesi, açık kaynaklı programların gelecekte lisans talep edebilecek şekilde karar değişikliğine gitmesi gibi nedenlerden dolayı teknik bilimlere ilgi duyan bir öğrencinin eğitime, bilime ve deney yapabilme ortamına ulaşması giderek daha maliyetli olmakta ve zorlaşmaktadır.

Ülkemizde nicelik anlamında çoğalan eğitim kurumlarının teknik bölümlerde kullanılmak adına laboratuvar imkânı sağlamalarının zaman ilerledikçe ciddi anlamda masraflı olması ve dövize olan baz fiyat hesaplaması sonucunda laboratuvar teçhizatlarının günümüz teknolojik şartları karşılaması zorlaşmakta ve eğitim için sunulan imkanların daraldığı gerçeği akademik birimler tarafından da yaşanılmaktadır. Bu gibi maddi kısıtlamalar zaman zaman meydana gelebilir. Fakat maddi kaynak yaratılmasına olan ihtiyaç laboratuvar şartlarında her zaman en önde gelen gereklilik olarak ortada duruyor olacaktır çünkü birtakım sarf malzemelerin yerine yenilerinin satın alınması başta olmak üzere sıklıkla laboratuvar imkanlarının geliştirilmesine ihtiyaç duyulmaktadır.

Eğitim kurumları, yukarıda sözü edilen maddi zorluklarla baş edebilmek ve öğrencinin bilgi birikimini gelişen teknoloji ile arttırabilmek için Roblox platformundaki Roblox Studio programının buna dolaylı yoldan bir çözüm olabileceği sonucu fikrini akla getirmiştir. Roblox Studio ile uygulamalı dersler arasındaki bağlantıyı kurarken öncesinde YouTube Gaming internet sitesi [2] incelenmiştir. Dünya çapında ve anlık olarak bilgisayar, konsol oyun cihazları, sanal gerçeklik gözlükleri ile desteklenen oyunlar ve cep telefonu, tabletler gibi mobil cihazlar dahil oynanan oyunların canlı yayınlarının anlık izleyici sayısına dikkat edilmiştir. YouTube Gaming haricinde Twitch, Vimeo, Dailymotion, izlesene, dlive gibi bilinen canlı yayın platformlarındaki oyun canlı yayınları anlık izleyici sayısına odaklanılmıştır. [3]

Her bilgisayar, konsol veya mobil oyunun programlamaya imkân sunmaması sebebiyle bazı oyunlar araştırma dışında tutularak kapsam daraltılmıştır. Burada en öne çıkan kıstas dünya çapında popüler olarak oynanan ve canlı yayını çok sayıda kişi tarafından izlenen ilgili oyların kendi içerisinde ve oyun firması sınırları dahilinde (Dışarıdan tersine mühendislik gibi bir uygulama veya bilgisayar programı gerektirmeyecek şekilde resmi bir geliştirici dağıtımı izin ve yetkisi ile) ilgili oyunun yazılım geliştirmeye olanak verecek bir yapıya sahip olup olmaması olmuştur.

Minecraft, dünya çapında genç oyunlar tarafından bilinirliği yüksek, anlık oyuncu sayısı yüksek ve kullanımı kolay oyun arayüzü ve yüksek performans gerektirmeyen oyun içeriği dolayısıyla ilk akla gelen seçenek olmuştur. Ancak Minecraft'ın hikaye oyun modunun oynanabilmesi için kayıt ücretinin ödenmesinin gerekliliği ve Code Builder gibi hazır bloklar ile sürükle-bırak (Drag & Drop) mantığıyla çalışan [4] yapısı arka planda yazılan kodların geliştiriciden gizleniyor oluşu (No-Code consepti) Minecraft'ı lise'den ziyade ilkokul 1. ve 8. sınıflar arası öğrenciler için eğitim amaçlı kullanılmasına daha yatkın olabileceği düşündürtmüştür. Bu sebeplerden dolayı Minecraft ile programlama bu çalışmanın dışında tutulmuştur çünkü lise ve üniversite düzeyinde yazılım geliştirme metoduyla mühendislik eğitimi çalışmalarının yapılması isteği vardır. Sürükle-bırak mantığı ile arka planda meydana gelen işlemlerin mühendisliği nispeten gizlendiği ve ne olup bittiğinin görünürlüğünün ortadan kalktığı şüphesi taşınmaktadır. Ayrıca yalnızca izlenme sayılarına bakarak eğitim amacıyla oyun kullanma hedefine ulaşılamayacağı çok

açıktır. Bu noktada ilgili oyunun bilinirliğinin ötesinde yazılım geliştirme imkanı sunması aslında daha ön plandadır.

Genel olarak bilgisayar ve mobil oyunlarda oyuncunun kendi oynayacağı oyun haritasını tasarlama imkanı (Make your own game map) veren Brawl Stars Map Maker haritaları da incelenmiş ancak bu özelliğin daha önceden hazırlanmış oyun içi nesnelerin kod satırları yazılmadan oyun haritasına eklenmesi gereğinden dolayı bu çalışmanın dışında tutulmuştur çünkü No Code konsepti ile ders içeriği öğrenciye deney olarak aktarılırken esneklik sağlanamaz ve eğitim olması gerekirken yapı bir oyuna dönüşecek ve ilgiyi fazlasıyla dağıtacaktır endişesi oluşturmaktadır.

Half-Life oyun serileri için kum havuzu (Sandbox) oyun modu özelliği sunan ve 2004 yılında çıkmış Garry's Mod ile Lua programlama dili kullanılarak Microsoft Visual Studio program desteği ile fizik motoru dahil edilerek oyun yazılımı geliştirmeye ve algoritmik programlamayı matematik ve fizik gerçekliğine yakın şekilde programlamaya imkân sunmaktadır. Steam üzerinden güncel sürümün ücretli olarak satılması ve güncel sürümün Steam platformu üzerinden indirilmesi zorunluluğu sebebiyle Lua geliştirmek için oldukça elverişli ve zengin kütüphane desteğinin bulunması gerçeğine rağmen Garry's Mod'un eğitim amacıyla bilgisayar laboratuvarlarında öğrenciye elektronik mühendisliğinin temellerini anlatırken kullanım kolaylığı sunmadığı sebebiyle uygulama eğitimi için uygun bulunmamıştır. [5] [6]

Bu çalışmada aşağıdaki gerekçeler doğrultusunda Roblox Studio'nun eğitim materyali olarak kullanılması tercih sebebi olmuştur.

1. Dünya çapında bilinir olması (Aktif oyuncu sayısı, UGC-User Generated Content'e izin vermesi)
2. Oyun şirketinin "Roblox Corporation" adı ve "RBLX" kısa adıyla "The New York Stock Exchange" olarak bilinen ve merkezi Amerika Birleşik Devletleri'nde bulunan Menkul Kıymetler Borsasına kote olması (Platformun güvenilirliği ve yasalara uygun hareket ediyor olması)
3. Oyun oynanabilirliğin ötesinde oyun geliştirme imkânı sunması
4. İnternet bağlantısıyla her bireye ulaşılabilir ve açık olması
5. Ücretsiz oyun deneyimi ve oyun deneyimi geliştirme imkânı sunması
6. C programlamayı bilen biri için Lua kodu yazmanın nispeten kolay olması, öğrenmenin hızlılığı. Roblox Studio'da Lua dilinde programlama yapabilmek için Lua geliştiricilerinin göstermiş olduğu ilgi, Lua eğitim içeriklerinin oluşturulması, Lua dilinin güncelleme almaya devam etmesiyle aktif kalmaya devam etmesi [7] [8]
7. Roblox platformuna kayıtlı 9.5 milyon geliştiricinin bulunması ve 40 milyon oyun deneyiminin bulunmasının yanı sıra şirket çalışanı sayısının 2021 yılında 1600'e ulaşmasının verdiği uzmanlık, deneyim, kalite yönetimi ve olası hataların giderilmesinde çevik önlem almanın müşteri nezdindeki memnuniyeti [9]
8. developer.roblox.com internet sitesi üzerinden ücretsiz Roblox Studio eğitimlerinin (tutorial) internet üzerinden dünyanın herhangi bir yerinden talep edebilecek kişilere verilmesi ve bunun için ücret talep edilmemesi [10]
9. Roblox Studio ile yapılan tasarımın Roblox Player'da anlık olarak test edilebilmesi ve hemen sonrasında yayına alınarak dünya'nın her yerine internet üzerinden erişime açık hale getirilmesi kolaylığı. Günümüzün popüler kod geliştirme odaklı sosyal medya platformlarından GitHub ve Stack Overflow gibi internet sitelerinden yapılan paylaşımların ve içeriklerin doyurucu ve sorun gidericilik açısından topluluk desteğinin sürdürülebilirliği
10. Temel olarak C programlama diline benzeyen ancak öğrencilere ders saatinde anlatılması kolay, öğrencinin anlayabileceği, hızlı ve pratik çalışma performansı gösteren ve C programlama diline göre biraz daha basitleştirilmiş. (Örneğin, değişken tanımlamaları için Lua dili için local yazmak yeterli olurken C için değişkenin nümerik veya alfanümerik, kelime, boolean değişken gibi durumları ve değişken tanımlamalarındaki alt ve üst eşik sınırları (Overflow ve Underflow) tek bir değişken ile gerçekleştiriyor olması gibi) Roblox Studio'nun geliştiriciler için ücretsiz üyelik sunması, geliştiricilerin ürettiği oyun deneyimi neticesinde Robux adı verilen ve sonrasında paraya çevirebilme imkanı sunması ile başarının platformda desteklenmesi, yıllık geliştirici konferansı düzenlemesi. [11]

Yukarıda belirtilen özellikler başta olmak üzere Roblox Studio ile öğrencinin eğitimi için içerik hazırlamak adına motivasyon kazanılacağı beklentisi oluşmaktadır.

Normalde öğrencinin ekran karşısında oyun oynayarak zamanını boşa harcaması yerine okulda aldığı teknik ve mühendislik bilgisini uygulayarak oyunlaştırma deneyimi geliştirmesi ile vaktin verimli kullanılmasının öğrenilmesi bu çalışmada esas olarak amaçlanmıştır.

Ek olarak STEM Eğitimleri olarak kısaltılan (Science, Technology, Engineering, Math – Bilim, Teknoloji, Mühendislik ve Matematik) [18] çalışmaların içeriğine yazılımın, Lua programlama dili ile eklenmesi sağlanabilir.

Bazı gerçek zamanlı uygulamaların geliştirilmesinde kullanılan zaman modellemesi [16] çalışmaları kapsamında Roblox Studio programı ile gelecekte üç boyutlu zaman bazlı kontrol ve ölçme uygulamaları simülasyon olarak Roblox Studio'da gerçekleştirilebilir.

II. MATERYAL VE METOT

A. Elektrik Bilgisi

Öğrenciye elektriğin temel bilgisini vermek elektrik devresinin tanımı ile başlayabilir. Bir elektrik devresini oluşturan en temel özellik iletken tellerle birbirine bağlanmış gerilim kaynağı ve devreye bağlı bir yük arasındaki ilişkiyi Ohm Kanununa dayandırarak açıklamak olabilir. Lise müfredatı içerisinde ve üniversite tercihini yapmış yeni lise mezunlarının günümüzdeki potansiyellerine bakıldığında özellikle bilgisayar kullanımı, cep telefonu kullanımı ve/veya tablet bilgisayar kullanımı deneyimi sahip oldukları ve 2000'li yıllarda dünyaya gelen bir çocuğun 2022 yılı için 20'li yaşlarda olması ve bu tür elektronik cihazları kullanarak oyun oynamış veya halen oynadığı bir oyunun süre geldiği düşünülmektedir.

Böylesine çeşitli teknolojik cihazların olduğu bir döneme doğan ve elektrik-elektronik bilgisi öğrenmek isteyen bir öğrenci için elektriğin temel prensipleri bilgisayar ortamında nasıl öğretilmelidir diye sorulduğunda özellikle lise öğretmenleri ve üniversitede ders veren akademik personele yönelik olarak Roblox platformunun kullanılmasının daha kolay olacağına dair bir kanaat geliştirilmiştir.

Bu çalışmanın sunduğu yenilik, mühendislik formüllerinin öğrenciye öğretilirken Lua dilini de kullanabileceğini anlatmak, Roblox Studio platformunda ilgili formüllerin

denenerek mühendislik bilgisini bilgisayarda üç boyutlu simüle ederek görselleştirmek şeklindedir. Öğrencinin elde ettiği deneyimi bilgisayar ortamında simülasyon yaparak neticelendiriyor olması öğrencinin şimdiye kadar arkadaşlarıyla oynadığı oyunlardan sonra bu oyunları üniversite düzeyinde mühendislik için ve lise düzeyinde fen bilimleri esaslı eğitim için kullanabileceği bilgisini ortaya çıkartmaktır.

B. Roblox Şirketi

Roblox, bir şirket olarak 2004 yılında şu anki CEO görevine de devam eden David Baszucki tarafından kurulmuştur. New York Stock Exchange (NYSE) borsanına (RBLX kısaltmasıyla) kotedir. Şirket merkezi San Mateo, California eyaleti, Amerika Birleşik Devletleri'dir. Market büyüklüğü 19,065,238,801 USD şeklindedir. [12] [13]

C. Roblox Player

Roblox, dünya çapında yaygın olarak bilenen, internet erişimi olan her yerden erişilebilen, ücretsiz ancak oyun içi satın alma imkânı sunan, çevirim içi bağlantılı bir oyun ve deneyim platformu olarak tanımlanabilir. Oyuncular kendi karakterlerini Avatar Shop adı verilen karakter oluşturma, düzenleme ve karakter aksesuarlarının bulunduğu bir yapı barındırır ve oyuncular kendi istedikleri gibi karakterlerini oluşturabilirler.

Roblox adına, oyun geliştiren yazılımcılar, oyun geliştiricileri, grafik ve animasyon uzmanları, oyun hikayesi ve oyun senaryosu yazarları kendi evrenlerini (metaverse) kendi istedikleri şekilde oluşturabilir ve ücretsiz olarak Roblox platformundan yayınlayabilmektedir. Oyun içi satın alma özelliği veya bazı zamanlarda oyun erişimi için ücret ödenmesi, Roblox platformu için reklam gösterimleri ve Premium içeriklerin oyun deneyimine dahil edilmesi için Robux adı verilen ve yalnızca platform içerisinde geçerli bir ödeme/bakiye sistemi geliştirilmiştir. Başlangıç seviyesinde Roblox platformu ile ilgili basılmış bazı kitaplar bulunmaktadır. David Jagneaux tarafından "The Ultimate Roblox Book" isimli kitap 2018 yılında yayınlanmıştır. [17]

D. Roblox Studio

Bir oyun geliştiricisi Roblox platformunda kendi tasarımını, kendi yazılımını yayına almak, çalışmasını test etmek, oynanabilirliğin kalitesini kontrol etmek (UX) adına Roblox Studio programını kullanabilir. Bu program Roblox Player ile birlikte ücretsiz olarak bilgisayara indirebilir ve kurulum sağlanabilir.

Roblox Studio ile oyun deneyimi için ücretsiz ve hazır nesneler, sesler, animasyonlar ve hedefler (dummy objects) denilen önceden tanımlı oyun içi nesneleri kullanabilir.

E. Lua Programlama

Roblox'ta oyun deneyimi tasarlamak adına Lua (Portekizce dilinde ay anlamındadır.) yazılım geliştirme dili kullanılabilir. Lua dili temelde C programlamaya benziyor olsa da kendi içerisinde kod yazılış stili ve kodların satır sonlarında noktalı virgül (;) karakterinin bulunmasına gerek olmaması bakımından (satır başları kod satırını sonlandırmaktadır.) dikkat çekmektedir. [14]

Lua kodlarının yazılacağı alanlar Roblox Studio içerisinde "Script" dosyası olarak anılmaktadır. Bu dosyalar oyun deneyimi projesi geliştirmesi kapsamında Roblox Studio tarafından program (IDE) içerisinde derlenerek çalışmaya hazır hale getirilir. Çalıştır (RUN) komutundan sonra Script içeriğindeki Lua kodları çalışmış olur.

Lise düzeyinde verilen eğitimde ve üniversitelerde okutulan giriş seviyesindeki dersler için C dilinde program yazmak öğrencinin C kodlarıyla ilk kez karşılaşmasında zorluk oluşturabiliyor. Özellikle daha önce bilgisayarda programlamayı kendi başına deneyen öğrenci başarısız olduğunu hissetmeye başladığı an özgüveni kaybolabiliyor.

C programlamanın yerine Lua dili kullanılarak bu noktada öğrenciye hali hazırda bilgisayarda Roblox Player'da bir oyun deneyimi yaşamak yerine değerli vaktini Roblox Studio'da geçirmesini söyleyerek kendi oyun deneyimini programlamasını ve hayata geçirebileceğinin göstermesini dile getirmek öğrencide tatlı bir heyecan oluşturduğu gözlemlenmiştir.

C programlama dersinde iki boyutlu ve siyah bir konsol ekranı gören öğrenci Lua programlamayı öğrendiğinde tüm renklerin olduğu, karakterin üç boyutlu kontrol edilebildiği, fizik motorunun yerleşik olduğu ve programlama becerisini deneme yanılma ile görsel olarak (Object Oriented – OO) gerçekleştirebileceği bir imkân bulmuş olmaktadır. Öğrenciler Roblox'u daha önceden duymuş ve en az bir kez oyun oynadılarsa bu platformda oyun da geliştirmek için kendilerinde özgüven duyabileceklerdir. Eğitim ve öğretim amaçlı mühendislikte kullanılan matematiksel formüllerin Lua programlama dili ile öğrenci tarafından kodlanması eğitim faaliyetini kolaylaştırabilir. Öğrencinin mühendisliği algılama becerisini arttırmak, algoritma geliştirmeye zihinsel açık olma durumu ve Lua dilinin sunduğu eğitimi kolaylaştırıcı kod geliştirme yapısı, Lua dilinin yalınlığı bu noktada hızlı ve kolay öğrenmeyi öğrenci adına pekiştirebilir şeklinde bir yaklaşım sunmaktadır.

F. Roblox Deneyiminin Tasarlanması

Öncelikle Ohm kanunun en temelde gerilimin direnç değerine bölünerek akım ifadesinin elde edildiği, gerilim seviyesinin, direnç değerinin arayüzden (GUI) girilerek değer atamasının yapıldığı, neticesinde devrede yük olarak bir lamba ve lambaya ait parlaklık değerindeki değişikliğin üç boyutlu grafik alanında canlandırılmasına odaklanılmıştır.

Roblox internet sitesi roblox.com ziyaret edilir. İlgili kullanıcı adı ve şifreden oluşan yeni bir hesap açılır. Profil sayfası oluştuktan sonra Roblox sitesinin üst satırında yer alan Create (oluştur) düğmesine tıklanır. Yeşil renkli tıklanabilir bir buton içerisinde Create New Experience düğmesi tıklanır. Eğer daha önceden bilgisayarınıza Roblox Player ve Roblox Studio programlarını indirmediyseniz bu aşamada açılan pencereden ilerleyebilirsiniz. Roblox Studio programı açıldıktan sonra sol üst köşede (+) simgesinden oluşan "New" seçeneği seçilir. Bir sonraki sayfada hazır tanımlı şablonlardan istediğinizi seçebilirsiniz. Bu aşamada "Baseplate" seçimi ilk uygulama yapanlar için önerilebilir. Roblox Editor programı açılacaktır ve çizim alanı görülecektir. Üst kısımda "Home" sekmesi aktifken o satırda "Game Settings" seçilerek oyun ile ilgili temel bilgi girişi yapılır. Proje adı, oyun deneyimi projesi açıklaması bu sayfadan verilir. Benzer şekilde Roblox internet sitesinde "Create" sekmesi seçilerek de bazı temel özellikler kontrol edilip düzenlenebilmektedir.

Üç boyutlu grafiklerin tasarlanması için Roblox Editor içerisinde "Part" seçenekleri kullanılabilir ve projenin uygunluğuna göre üç boyutlu çizim alanında tasarımlar yapılabilir. Bu aşama her geliştirici için farklı olabileceği için isteğe bağlı olarak yapılabilir.

Bu çalışmada elektrik devresinin oluşması için çizim alanında bir lamba görseli, seri bağlantıda bir ampermetre ile devreye ait ana kol akımının ölçülmesi için bir ampermetre bağlantısı, devreye uygulanacak gerilim düzeyinin kontrolü için bir DC enerji panosu, devrede akım kontrolünü sağlayabilmek ve lambanın parlaklığını değiştirebilmek için direnç görünümlü ayarlı nesne grubu kullanılmıştır. Deneyim alanında Ohm Kanunu hakkında temel bir bilgi ve direnç renk kodları tablosu eklenmiştir. "Ohm's Law Experiment" başlığıyla açıklamalar verilmiştir. Oyuncu karakterin deneye başlayabilmesi ve çizim alanında yer alabilmesi için "Spawn" nesnesi eklenmiştir. Çeşitli yardımcı nesneler ile oyuncu karakterin engel (collider) amaçlı oyun alanının çıkması önlenmek üzere dört adet duvar birleştirilerek kapalı bir deneyim alanı oluşturulmuştur. Lamba'nın parlaklığının gözlemlenebilmesi için Roblox Editor ayarlarından deneyimin gece karanlığı olacak şekilde ortamın karanlık olması özelliği seçilmiştir.

Şekil 1'de Roblox Studio'ya yapılan devre kurulumu görülmektedir. Oyuncuya ait karakter oyun içerisindeyken bu şekilde görülmektedir. Şekil 2'de ise devreye uygulanan 5 volt, 1 ohmluk yük için devreden geçecek olan 5 amper ampermetre göstergesinden okunacak şekilde lambanın parlaklık vermeye başlayacağı gözlemlenmektedir.

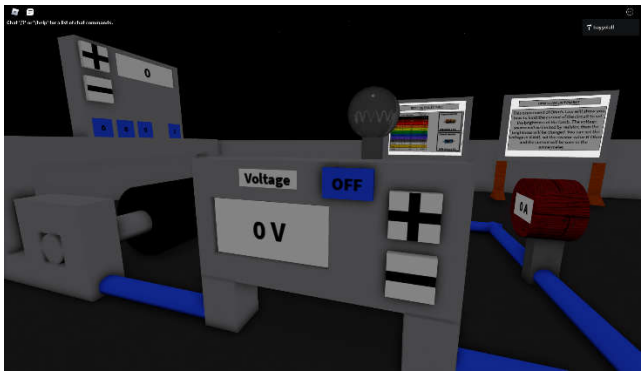

Şekil 1: Devrenin kurulu yapısı

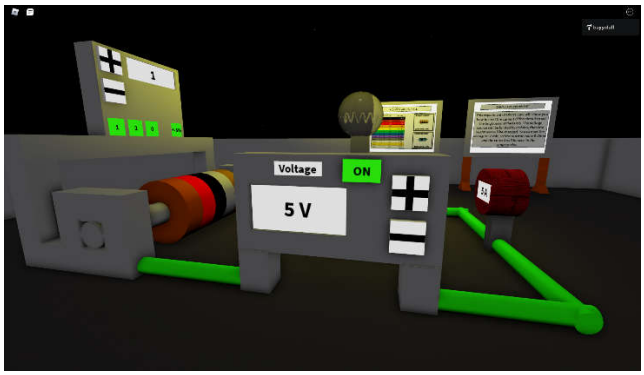

Şekil 2: Devrenin 5V, 1Ω ve 5A için lambanın parıltısı

Roblox Editor ile deneyim alanındaki nesne bazlı tasarım için temel olarak yedi grup içerisinde devrenin çalışması parçalara ayrılarak organize edilmiştir. Bunlar: VoltageControl, ResistorParts, ResistanceControl, Cables, Bulbmodel, AmpMeter ve Values şeklindedir.

VoltageControl grubunun içerisinde VDC, V_Decrease, V_Increase, Voltagebutton, switchbutton yer almaktadır. Birçoğu kendi içerisinde ClickDetector, Script, SurfaceGui ile detaylandırılmıştır.

ResistorParts grubunun içerisinde Res1, Res2, Res3, Res4 ve Res5_tolerance olmak üzere beş şeritli direnç renk kodları tanımına uygun olarak silindir kesit gösterimi üzerinden tanımlama yapılmıştır. Res_4 görsel olarak gri renkli tanımlıdır ve anlam olarak bir birimlik boş şerit olacak şekilde boş bırakılmıştır. Bu şekilde direncin bir ucunda üç şerit, diğer ucunda ise bir şerit olacak şekilde renk kodlarını okumak üzere şerit sırası anlaşılması sağlanmaktadır. İlgili Res öğeleri kendi içerisinde ClickDetector ve Script nesnelerini barındırmaktadır.

ResistanceControl grubunun içerisinde ResistanceValues, Res_Table_View_Bot, Res_Table_View_Top, R_Decrease, R_Increase, ResistanceVal, colorfour, colorthree, colortwo, colorone, BotSurfaceGui, SurfaceGui yer almaktadır. İlgili yapılar içerisinde gerekli olacak şekilde ClickDetector, Script, SurfaceGui eklenmiştir.

Cables grubunun içerisinde Cable1, Cable2, Cable3, Cable4 ve Cable5 olmak üzere görsel olarak silindirik yapıda kablo hattları nesne olarak eklenmiştir ve başka bir içerik eklenmesine gerek yoktur. Varsayılan kablo rengi gri olacak şekilde seçilmiştir.

Bulbmodel grubunun içerisinde Spring, Lamba ve birkaç nesne yer almaktadır. Üç boyutlu lamba yapısı verilirken küre nesnesine şeffaflık özelliği tanımlanmış ve küre içerisine lambaya ait flaman görünümü tasarlanmıştır.

AmpMeter grubunun içerisinde Valuepart, SurfaceGui ve bazı tasarımsal parçalar eklenerek devreye seri bağlantıda ampermetre modelinin özelliğini taşıyan yapı tasarlanmıştır.

Son olarak Values klasörü grubu oluşturularak içerisine Amps, Resistance, Switch, Volts isimli "value" değerli içerikler eklenmiştir. Bir adet Script eklenerek ValueChanges bu alandan kontrol edilecektir.

Bu aşamaya kadar olan tanımlamalar ValueChanges script dosyası içerisinde sırasıyla tanımlanmış ve Ohm formülünün kullanımına dair formülün yazım kısmı burada Lua dilinde kodlanmıştır.

G. Lua Kodları

ValueChanges içerindeki Lua Kodları

```
local amps = script.Parent:WaitForChild("Amps")
local switch = script.Parent:WaitForChild("Switch")
local volts = script.Parent:WaitForChild("Volts")
local Resistance = script.Parent:WaitForChild("Resistance")
local cables = script.Parent.Parent:WaitForChild("Cables")
local lamp = script.Parent.Parent:WaitForChild("Bulbmodel")
local ResControl = script.Parent.Parent:WaitForChild("ResistanceControl")
local limits = {volts ={}, amps = {max = 1000}}
local cablecolors = {off =Color3.fromRGB(66, 107, 255), on = Color3.fromRGB(59, 255, 29), unknown = Color3.fromRGB(255, 255, 255)}
local function switchlights(switchval)
if switchval == 1 then
for i,v in pairs(cables:GetChildren())do
if v:IsA('BasePart') then
v.Color = cablecolors.on
```

```
    end
    end
    ResControl.colorone.Color = cablecolors.on
    ResControl.colorone.SurfaceGui.TextLabel.BackgroundC
olor3 = cablecolors.on
    ResControl.colortwo.Color = cablecolors.on
    ResControl.colortwo.SurfaceGui.TextLabel.BackgroundC
olor3 = cablecolors.on
    ResControl.colorthree.Color = cablecolors.on
    ResControl.colorthree.SurfaceGui.TextLabel.Background
Color3 = cablecolors.on
    ResControl.colorfour.Color = cablecolors.on
    ResControl.colorfour.SurfaceGui.TextLabel.BackgroundC
olor3 = cablecolors.on
    lamp:WaitForChild("Lamba").SurfaceLight.Enabled= true
    elseif switchval == 0 then
    for i,v in pairs(cables:GetChildren())do
    if v:IsA('BasePart') then
    v.Color = cablecolors.off
    end
    end
    lamp:WaitForChild("Lamba").SurfaceLight.Enabled=
false
    ResControl.colorone.Color = cablecolors.off
    ResControl.colorone.SurfaceGui.TextLabel.BackgroundC
olor3 = cablecolors.off
    ResControl.colortwo.Color = cablecolors.off
    ResControl.colortwo.SurfaceGui.TextLabel.BackgroundC
olor3 = cablecolors.off
    ResControl.colorthree.Color = cablecolors.off
    ResControl.colorthree.SurfaceGui.TextLabel.Background
Color3 = cablecolors.off
    ResControl.colorfour.Color = cablecolors.off
    ResControl.colorfour.SurfaceGui.TextLabel.BackgroundC
olor3 = cablecolors.off
    else
    for i,v in pairs(cables:GetChildren())do
    if v:IsA('BasePart') then
    v.Color = cablecolors.unknown
    end
    end
    lamp:WaitForChild("Lamba").SurfaceLight.Enabled=
false
    ResControl.colorone.Color = cablecolors.unknown
    ResControl.colorone.SurfaceGui.TextLabel.BackgroundC
olor3 = cablecolors.unknown
    ResControl.colortwo.Color = cablecolors.unknown
    ResControl.colortwo.SurfaceGui.TextLabel.BackgroundC
olor3 = cablecolors.unknown
    ResControl.colorthree.Color = cablecolors.unknown
    ResControl.colorthree.SurfaceGui.TextLabel.Background
Color3 = cablecolors.unknown
    ResControl.colorfour.Color = cablecolors.unknown
    ResControl.colorfour.SurfaceGui.TextLabel.BackgroundC
olor3 = cablecolors.unknown
    end
    end

    switchlights(switch.Value)
    switch.Changed:Connect(function(newvalue)
    switchlights(newvalue)
    end)
    volts.Changed:Connect(function()
    amps.Value = volts.Value/Resistance.Value
    end)

    Resistance.Changed:Connect(function()
    amps.Value = volts.Value/Resistance.Value
    end)

    amps.Changed:Connect(function(newvalue)
    if newvalue>limits.amps.max then
    lamp:WaitForChild("Lamba").SurfaceLight.Brightness
=limits.amps.max
    else
    lamp:WaitForChild("Lamba").SurfaceLight.Brightness
=newvalue
    end
    end)
```

64. kod satırında gerilim değişimlerinde ana kol akım değeri güncellenirken, 68. kod satırında ise direncin değişimleri sonrasında devredeki anakol akım değeri akım değeri güncellenmektedir.

71. kod satırlarında ise lamba tanımına ait “Brightness” parlaklık değeri kontrol edilmektedir. Akımın değerinde direnç sebepli ve/veya gerilim sebepli meydana gelebilecek değişiklik sonrasında lambanın parlaklığı bu aşamadaki if-else-end kod bloklarıyla değiştirilmektedir.

Şekil 1 ve Şekil 2’de devre simülasyonunun çalışması esnasındaki deneyim alanının canlı görüntüleri karşılaştırmalı olarak sunulmuştur. “Circuit Simulator” ismi verilerek Roblox platformuna Roblox Studio içerisinden “Publish to Roblox” denilerek tasarım yayına 17.06.2018 yılında alınmıştır. 19.05.2022 tarihi itibarı ile 10 oyuncu favorilerine eklemiş ve bu deneyim 152 kez ziyaret edilmiştir. [15]

III. SONUÇLAR

Bilgisayarda programlama dersleri kapsamında ve özellikle C/C++ programlama konusunu içeren dersler için müfredat içerisinde Lua programlamanın da bahsedilerek Roblox oyun deneyimi geliştirmenin anlatılması önerilmektedir. Bu çalışmada aslında bu işlemin zor olmadığı, birkaç Roblox örneğinin öğrenciye gösterildikten sonra öğrencinin kendi oyununu geliştirebileceği konusunda motive edilmesi önerilmektedir.

Doğrudan mantıksal bir dayanağa sahip olacak şekilde “Hocam, neyi neden yapıyoruz?” benzeri sorular karşısında C programlama yaparken öğrencinin soyut düşünmeyi öğrenmesi aşamasında Roblox’ı Lua ile deneyimleyerek hem C programlamadan başka dillerin de olabileceği, farklı dillerle farklı çalışmaların icra edilebileceği hem de üç boyutlu olarak görsele hitap eden programlamacılığın soyuttan somuta doğru temellendirilmesi gösterilebilir.

Roblox Studio ve Lua dilinde yapılan kodlamaların eşliğinde eğitim ve öğretim faaliyetleri kapsamında lise ve üniversite düzeyinde programcılık örnekleri bu çalışma şeklinde gösterilebilir.

Hali hazırda vaktini oyun oynayarak geçiren 20 yaş ve altındaki kişilerin oyun oynayarak geçirecekleri vakitlerini oyun deneyimi programlama ile geçirmelerinin mümkün olabileceği gösterilmektedir. Üniversite düzeyindeki öğrenciler için ise mühendislik eğitimi başta olmak üzere matematiksel olarak formüllerin kullanıldığı herhangi bir alan

için uygulama ve deney çıktılarının Roblox Studio kullanarak simülasyon edilebileceği bu çalışmada gösterilmek istenmiştir.

Uzaktan eğitim gerektiren, evde ödev olarak bilgisayar destekli çalışma gerektiren, laboratuvarda devre kurmanın mümkün olmadığı fakat bilgisayarın bulunduğu şart ve koşullar için bilgisayarda programlamanın çevirim içi ve dünya çapında ücretsiz olarak erişim imkânı sunan Roblox Studio üzerinden imkanlı hale getirilebileceği düşünülmektedir.

C/C++ programlama yapmaktan soğuyan veya sıkılan bireyler için Lua dilinin alternatif olarak ortaya çıkması ve algoritma geliştirmeye yönelik olarak üç boyutlu tasarım imkanının devamlılığının ve sürdürülebilirlik sağlanabilir.

KAYNAKLAR

[1] https://fritzing.org/download/ (Son erişim: 19.05.2022)
[2] https://www.youtube.com/gaming/games (Son erişim: 19.05.2022)
[3] https://www.dexerto.com/roblox/how-many-people-play-roblox-player-count-tracker-2022-1726491/ (Son erişim: 19.05.2022)
[4] https://education.minecraft.net/en-us/blog/download-the-code-builder-update-to-learn-coding-in-minecraft (Son erişim: 19.05.2022)
[5] https://tr.wikipedia.org/wiki/Garry's_Mod (Son erişim: 19.05.2022)
[6] https://store.steampowered.com/app/4000/Garrys_Mod/?l=turkish (Son erişim: 19.05.2022)
[7] https://www.sec.gov/ (Son erişim: 19.05.2022)
[8] https://www.sec.gov/edgar/browse/?CIK=1315098&owner=exclude (Son erişim: 19.05.2022)
[9] https://backlinko.com/roblox-users (Son erişim: 19.05.2022)
[10] https://developer.roblox.com/en-us/ (Son erişim: 19.05.2022)
[11] https://www.baeldung.com/java-overflow-underflow (Son erişim: 19.05.2022)
[12] https://en.wikipedia.org/wiki/Roblox_Corporation (Son erişim: 19.05.2022)
[13] https://www.nasdaq.com/market-activity/stocks/rblx (Son erişim 17.05.2022)
[14] https://www.lua.org/about.html (Son erişim: 19.05.2022)
[15] https://www.roblox.com/games/1944835284/Circuit-Simulator (Son erişim: 19.05.2022)
[16] Yolal, O. & Artuğ, T. (2019). Gerçek Zamanlı Veri Takibinde Zamanın Modellenmesi. Avrupa Bilim ve Teknoloji Dergisi, Özel Sayı 2019, 164-170. DOI: 10.31590/ejosat.637768
[17] David Jagneaux. (2022). Retrieved May 19, 2022, from Amazon.com website: https://www.amazon.com/David-Jagneaux/e/B0758LCXPX/ref=dp_byline_cont_pop_book_1
[18] https://www.oranokullari.com/tr/sayfa/147/yabanci-dil-kazanimi (Son erişim: 19.05.2022)

International Journal of Multidisciplinary Studies and Innovative Technologies

e-ISSN: 2602-4888
dergipark.org.tr/en/pub/ijmsit
Research Article

2022, 6 (1), 58 -60
DOI: DOI: 10.36287/ijmsit.6.1.58
Received: May 20, 2022; Accepted: June 25, 2022

Sentiment Analysis Of Tweets Using Natural Language Processing

Firas Fadhil Shihab[1] and Dursun Ekmekci[2]

1 Karabuk University, College of Engineering,Computer Engineering,Karabük 78000, Turkey (ORCID: 0000-0001-5956-4183)
[2] Karabuk University, College of Engineering,Computer Engineering,Karabük 78000, Turkey (ORCID: 0000-0002-9830-7793)

1928126539@ogrenci.karabuk.edu.tr
dekmekci@karabuk.edu.tr

Abstract – Millions of people use Twitter and other social media sites to share their everyday thoughts in the form of tweets. It is a short and straightforward way of expressing oneself, which is a hallmark of tweeting. As a result, we concentrated on sentiment analysis of Twitter data in our research. Sentiment Analysis is a subset of natural language processing and text data mining. It is feasible to investigate sentiment analysis using Twitter data. performed in a number of different circumstances The technique of finding valuable patterns from textual data is referred to as sentiment analysis. Using particular analysis tools, these valuable patterns include evaluating and categorizing feelings as neutral, positive, or negative.

The study's authors look at a range of information processing approaches, including sentiment analysis, Twitter's network structure, event dispersion across the network, and impact identification. There have been several ways described for exploring semantics for sentiment analysis, which can be classified into contextual semantic and conceptual semantic approaches. One of the most important disciplines of natural language processing is sentiment analysis. The technique of finding valuable patterns from textual data is referred to as sentiment analysis. According to this research, sentiment analysis applications will continue to develop in the future, and sentiment analytical approaches will become more standardized across systems and services. Because of the vast amount of data available, Twitter is one of the best virtual environments for tracking and monitoring information.

Keywords *– Sentiment Analysis, Natural Language Processing, Twitter Data.*

Citation: Shihab, F., Ekmekci, D. (2022). Sentiment Analysis Of Tweets Using Natural Language Processing . International Journal of Multidisciplinary Studies and Innovative Technologies, 6(1): 58-60

I. INTRODUCTION

Twitter is a prominent micro blogging platform that allows users to post status updates (called "tweets"). These tweets contain a lot of human expressions, such as enjoying, disliking, and contributions to many issues. Sentiment Analysis is a technique for identifying and extracting opinions from text. Natural Language Processing The simplest definition of NLP is the processing and analysis of (spoken) natural languages represented by texts; With the aim of achieving optimal interaction between humans and computers. Returning to the main topic of the article, sentiment analysis is one of the most important branches of NLP.by sentiment analysis, we mean the process of extracting useful patterns from textual data. These useful patterns include interpreting and categorizing feelings into: neutral, positive, or negative, from that data using certain analysis techniques. proposed a method that focuses on the distribution or frequency of sentiment classes in the dataset they're looking at.to study and forecast a situation, a based classification algorithm is used. The polarity of a user's feelings. On words, it used positive, comparative, and superlative degrees of comparison. Our study aimed to apply sentiment analysis to evaluate public opinion and detect any rising antagonistic or unfavorable feelings on social media. Despite the fact that we believe censorship is unjust, This recent trend in sentiment research is a good example of one to follow.

Twitter mining can be applied to a wide range of situations. a variety of real-world applications, ranging from business (market research, product and service development)Applications as subcomponent technology (recommender systems; benchmarking and improvement);to applications in (summarization; question-answering)politics. As a result, we came up with a model. Using the Twitter API, obtains tweets on a specific subject. And determines each sentiment's sentiment orientation/score tweet.

II. RELATED WORK

Many articles have talked about sentiment analysis. I will summarize some of them, Boia et al. [1] and Manuel et al. [2] developed two ways that use emoticons to detect tweet polarity and slang terms to provide an emotion score to online writings, respectively. Akcora et al. [3] provided a method for determining public opinion changes over time and identifying the news that led to public opinion breakpoints. Gao and Sebastiani [4] .proposed a method that focuses on

the distribution or frequency of sentiment classes in the dataset they're looking at. Mandal, to study and forecast a situation, a based classification algorithm is used.

The polarity of a user's feelings. On words, it used positive, comparative, and superlative degrees of comparison.[5] companies can respond to their needs, and improve their services and products to suit those needs.[6] For example, a company used sentiment analysis to analyze more than 3,000 opinions about a particular product of its own, and the company discovered that those opinions were satisfied with the price of that product but in return complain about the company's customer service. What this information helps us not only understand the current context of a particular topic, but also enables us to predict the future, in addition to the possibility of using that information contained in the texts to calculate the positive/negative index, which is an important indicator in the decision-making process. Case in point: some governments use sentiment analysis results during their election campaigns.

Despite the fact that sentiment analysis and emotional intelligence are sometimes employed interchangeably, they are not the same thing. While sentiment analysis relies on data to classify sentiments as positive, negative, or neutral, EQ digs deeper into the nuance of the emotions expressed in the remarks. EQ is far more challenging and complex than sentiment analysis.[7]

Sentiment analysis, for example, will determine if a given statement is good, negative, or neutral, but emotional intelligence will determine whether the comment causes grief, discontent, or sarcasm if it is determined to be negative.

III. Material and Method

Sentiment analysis is based on several models (according to the goal), starting with the models that are concerned with polarity only (positive, negative, neutral), and passing through the models capable of determining emotion (anger, love, happiness…), ending with those that are concerned with revealing intentions (interested, not). interested).[8]

2.1 Fine-grained Sentiment Analysis:

In some cases, polarity accuracy is required, and then the classes of polarity are expanded as follows: very positive, positive, neutral, negative, very negative Items in this model can also be viewed as a numerical rating, such as those based on five stars. very positive =very negative.

2.2 Emotion Detection:

In this model, the goal is to identify emotions, such as: happiness, fear, anger, etc., and dictionaries are usually used here (a list of words with their corresponding emotions), and automatic learning algorithms can also be used. Here it is worth noting that when using these dictionaries, the problem of different emotions in words arises, especially that humans can express their emotions in different ways. An example of this is: “Oh, peace!” It can have a meaning of joy or a negative meaning, such as sarcasm.

2.3 Aspect-based Sentiment Analysis:

In this model, the goal is to identify emotions, such as: happiness, fear, anger, etc., and dictionaries are usually used here (a list of words with their corresponding emotions), and automatic learning algorithms can also be used. Here it is worth noting that when using these dictionaries, the problem of different emotions in words arises, especially that humans can express their emotions in different ways. An example of this is: “Oh, peace!” It can have a meaning of joy or a negative meaning, such as sarcasm. Sentiment analysis systems rely on a number of natural language processing algorithms and methods, and we will mention them below:

1- rule-based methodologies: rule-based methodologies. These methodologies rely on manually defining a set of rules to determine the polarity and target entity (eg product name). Some of the techniques used to build these bases: Stemming, tokenization, and parsing.Dictionaries (a group of words and expressions with corresponding feelings).Example: Create two strings of words that directly identify polarity (negative words, such as: bad, failed..., and positive words, such as: good, great...).

Count the words with positive feelings and words with negative feelings, that are in a particular context.[9]rule-based methodologies: rule-based methodologies. These methodologies rely on manually defining a set of rules to determine the polarity and target entity (eg product name). Some of the techniques used to build these bases: Stemming, tokenization, and parsing.

2-Methodologies based on machine learning techniques. Based methodologies. Unlike the previous methodology, these methodologies do not rely on hand-written rules, but rather on machine learning algorithms. The issue of sentiment analysis is a classification problem. The input to this classifier is textual data, and its output is one of the kinds of sentiment (for example: positive, negative, neutral). The following figure shows how the sentiment analysis classifier works:

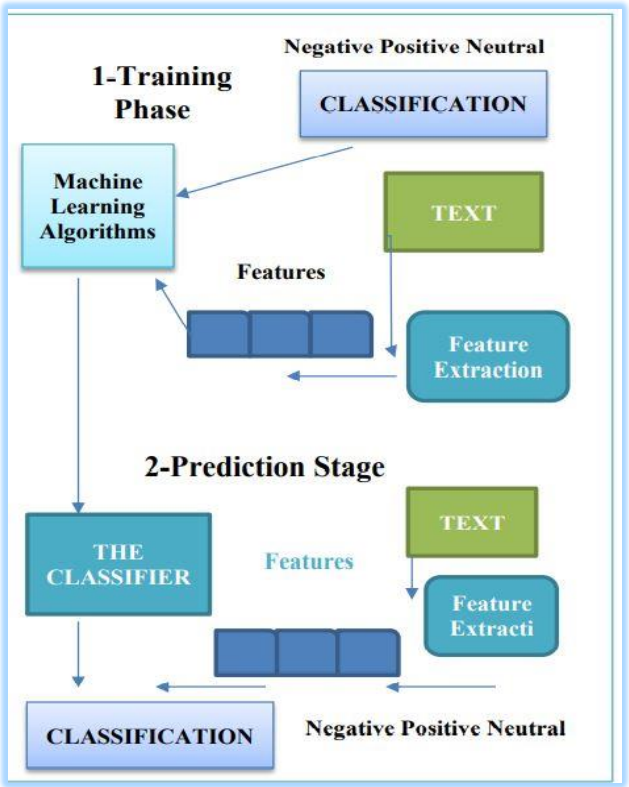

Fig. 1 analysis classifier works

IV. RESULTS AND DISCUSSION

Twitter posts on electronic products were used to create the dataset. Tweets are short statements that are rife with slang and misspellings. As a result, we conduct a sentiment analysis at the sentence level. This is accomplished in three stages. Pre-processing is completed in the first phase. Then, utilizing relevant features, a feature vector is produced. Finally, tweets are divided into positive and negative categories using several classifiers. The final emotion is calculated based on the number of tweets in each class.

HUANG, Lei generated a novel dataset by collecting tweets over a period of time lasting from April 2013 to May 2013 because conventional Twitter datasets are not accessible for the electronic products industry.[10]

The Twitter API is used to automatically collect tweets, which are then manually tagged as good or negative. Using 600 good and 600 negative tweets, a dataset is produced.

Creation of a Dataset

Table 1 shows how the dataset is divided into two sets: training and test.

Table 1. STATISTICS OF THE DATASET USED

Dataset	Positive	Negative	Total
Training	500	500	1000
Test	100	100	200

V. CONCLUSION

In this review, Customers' opinions on the key to success in the marketplace are analysed using Twitter sentiment analysis. Machine-based learning is used in the software. Method for evaluating a feeling that is more accurate; Natural language processing techniques will be used in conjunction with each other. We studied how to collect data from users of the Twitter platform and study the content of their posts and analyse them using machine learning features that benefit companies, advertisements. Twitter sentiment analysis was created to examine customers' perspectives on the critical to market success. The program employs a machine-based learning approach that is more accurate for sentiment analysis; natural language processing techniques will also be employed

REFERENCES

[1] Boia, Marina, et al. "A:) is worth a thousand words: How people attachsentiment to emoticons and words in tweets." Social computing (socialcom),2013

[2] Manuel, K., Kishore Varma Indukuri, and P. Radha Krishna. "Analyzinginternet slang for sentiment mining." 2010 Second VaagdeviInternationalConference on Information Technology for Real World Problems. 2010.

[3] Akcora, Cuneyt Gurcan, et al. "Identifying breakpoints in publicopinion." Proceedings of the first workshop on social media analytics. ACM,2010. B. Hammi, R. Khatoun, S. Zeadally, A. Fayad, and L. Khoukhi, “Iot technologies for smart cities,” IET Networks, vol. 7, no. 1, pp. 1–13, 2017.

[4] Gao, Wei, and Fabrizio Sebastiani. "Tweet sentiment: From classification to quantification." Advances in Social Networks Analysis and Mining (ASONAM), 2015 IEEE/ACM International Conference on. IEEE, 2015.

[5] Mandal, Santanu, and Sumit Gupta. "A Lexicon-based text classificationmodel to analyses and predict sentiments from online reviews." Computer, Electrical & Communication Engineering (ICCECE), 2016 International Conference on. IEEE, 2016.

[6] Wagh, R., & Punde, P. (2018, March). Survey on sentiment analysis using twitter dataset. In 2018 Second International Conference on Electronics, Communication and Aerospace Technology (ICECA) (pp. 208-211). IEEE.

[7] C hakraborty, K., Bhatia, S., Bhattacharyya, S., Platos, J., Bag, R., & Hassanien, A. E. (2020). Sentiment Analysis of COVID-19 tweets by Deep Learning Classifiers—A study to show how popularity is affecting accuracy in social media. Applied Soft Computing, 97, 106754.

[8] S harma, N., Pabreja, R., Yaqub, U., Atluri, V., Chun, S. A., & Vaidya, J. (2018, May). Web-based application for sentiment analysis of live tweets. In Proceedings of the 19th Annual International Conference on Digital government research: Governance in the data Age (pp. 1-2).

[9] MEDHAT, Walaa; HASSAN, Ahmed; KORASHY, Hoda. Sentiment analysis algorithms and applications: A survey. Ain Shams engineering journal, 2014, 5.4: 1093-1113.

[10] GO, Alec; HUANG, Lei; BHAYANI, Richa. Twitter sentiment analysis. Entropy, 2009, 17: 252.

International Journal of Multidisciplinary Studies and Innovative Technologies

e-ISSN: 2602-4888
dergipark.org.tr/en/pub/ijmsit
Research Article

2022, 6 (1), 61-65
DOI: DOI: 10.36287/ijmsit.6.1.61
Received: May 21, 2022; Accepted: June 20, 2022

American Sign Language Recognition using YOLOv4 Method

Ali Mahmood AL-Shaheen[1] *, Mesut Çevik (Adviser)[2], Alzubair Alqaraghuli[3]

[1*]*Electrical and Computer Engineering, Altinbas Uni, Istanbul, Turkey (ali4realx@gamil.com) (ORCID: 0000-0002-9668-9556)*
[2] *Electrical and Computer Engineering, Altinbas Uni, Istanbul, Turkey (Mesut.cevik@altinbas.edu.tr) (ORCID: 0000-0000-0299-9076)*
3 Electrical and Computer Engineering, Altinbas Uni, Istanbul, Turkey Country (zubairsk53@gmail.com) (ORCID: 0000-0002-6117-8051)

Abstract – Sign language is one of the ways of communication that is used by people who are unable to speak or hear (deaf and mute), so not all people are able to understand this language. Therefore, to facilitate communication between normal people and deaf and mute people, many systems have been invented that translate gestures and signs within sign language into words to be understandable. The aim behind this research is to train a model to be able to detect and recognize hand gestures and signs and then translate them into letters, numbers and words using You Only Look One (YOLO) method through pictures or videos, even in real time. YOLO is one of the methods used in detecting and recognizing things that depend in their work on convolutional neural networks (CNN), which are characterized by accuracy and speed in work. In this research, we have created a data set consisting of 8000 images divided into 40 classes, for each class, 200 images were taken with different backgrounds and under lighting conditions, which allows the model to be able to differentiate the signal regardless of the intensity of the lighting or the clarity of the image. And after training the model on the dataset many times, in the experiment using image data we got a very good results in terms of MAP = 98.01% as an accuracy and current average loss=1.3 and recall=0.96 and F1=0.96, and for video results it has the same accuracy and 28.9 frame per second (fps).

Keywords *– American sign language, Real-Time Detection, You Only Look Once, YOLO, CNN, Recognition, Hand Gestures, Computer Vision, Machine Learning, Deep Learning.*

Citation: Al-Shaheen, A. M., Cevik, M., Alqaraghuli, A. (2022). American Sign Language Recognition using YOLOv4 Method. International Journal of Multidisciplinary Studies and Innovative Technologies, 6(1): 61-65.

I. INTRODUCTION

Sign language is one of the forms of visual communication between (deaf, mute people) and normal people through signs, gestures, and hand movements. Because of many normal people don't understand sign language because it's not wanted, they will not be able to communicate with deaf and mute people. With the great development in this technology and artificial intelligence, computer vision technology has got a great development, as it's used in building projects and systems for detecting and classifying objects according to certain specifications, including detection and recognition of hand signs and movements. Previous researches has been conducted in detection and recognition sign language, we can divide it into two parts. The first one is the use of special apparatuses like the accelerometer [1], the sensory glove [2], or the Kinect [3]. All of these types depend in their work on capturing sensory signals from equipment with motion sensors to identify the captured signals. This type of equipment provides high accuracy, but there will be a need to use a variety of equipment that is expensive and unwieldy for daily use. And for the second type, it's based on vision, which isn't expensive and available, and requires only a camera to take pictures or videos and is suitable for daily use, as we can use phone cameras or web cameras. For example, there is a research in which the k-Nearest Neighbors (KNN) classifier was used to classify, discover and identify signs [4]. Convolutional neural networks were once used to detect and identify American Sign Language Signs, and Google Net was used in the CNN architecture, which was trained on the ILSVRC dataset in 2012. This training gained an accuracy of 72%, and this shortage of accuracy is because of the similarity between the signs of some letters such as g, h, m, n, s, t. [5] R-CNN It is a method that combines the proposals of region and convolutional neural networks where you localize the sores in a convolutional neural network and then train a high capacity model with little annotated detection data. This algorithm achieves good accuracy in object detection by using the deep network ConvNet to classify object proposals. Also, it has the ability to detect thousands of objects without the need for approximate techniques. One of its drawbacks is the weakness in detecting small things, and also that it predicts only a sign and not a hash square. [12] [20] [21] [22] Fast R-CNN It's an algorithm written in Python programming language and is a training algorithm for object detection, developed to solve R-CNN problems regarding to accuracy and speed. One of its advantages is that it has a high accuracy than R-CNN in objects detecting and it also trains in one stage and the training can update all layers of the network. But one of its drawbacks is that it's slow when detecting objects, and this is due to the slow establishment of the selective search area. [13] [17] [18] [19] Faster R-CNN It's an object detection method similar to R-CNN that uses a Region Proposal Network (RPN), which is

effectively shares the convolutional features of the image with the detection network. Faster R-CNN is much faster than Fast R-CNN and R-CNN because it's used RPN (Region Proposal Network) for generating anchor boxes (region proposals). And It can be used in real-time object detection. There is one drawback in this method, which is after the RPN is trained, all the anchors are extracted in the mini-batch, because of the great similarity in the features of all the objects in the same image, which causes slow detection and the network may take a long time to reach a point of similarity between the objects. [14] [15] [16] YOLO is a newly recognition methods in deep learning, which has been developed on the basis of CNN, it's more effective and accurate in objects detection [6]. Deep learning models have achieved great success and tremendous developments in the field of object detection, including YOLO, which is a highly efficient model capable of differentiating and detecting objects through images, videos, or in real-time. It's an algorithm that depends in its work on the principle of regression, which means that instead of detecting and specifying the clear and interesting part, it analyzes and predicts the categories and boxes that surround the entire image, and that is done through one run of the algorithm. YOLO used in researches that require the detection of certain objects, or in determining the time, detection of traffic lights, pedestrians, cars plates and parking spaces, people, animals, etc. [10].

II. THEORY

2.1 Object Detection

Object detection It is a computer technology directly relies on computer vision and image processing that deals with recognition the states of objects within certain categories (such as people, cars, animals, hand movements, etc.) through images or videos. This technology is used in several areas, including the discovery of traffic lights and car plates for security reasons, as well as the facial recognition system in the protection systems of phones. It is also used to track certain things such as the movement of pedestrians, cars, etc. [23] [24] [25]

2.2 Convolutional Neural Networks (CNN)

CNN are a type of neural networks used to process data with a network structure such as images. It consists of neurons with weights, biases and activation functions. These neural networks consist of two layers, the feature extraction layer and the fully connected layer. The feature extraction layer consists of two layers, the convolutional layer and the pooling layer. The idea of convolutional neural networks was inspired by the shape of the cortex of the human brain. The artificial neurons in a CNN connect to a local area of the visual field, called the receptive field. This is achieved by performing discrete convolutions on the image using filter values as trainable weights. Multiple filters are applied to each channel, and with neuronal activation functions, they form feature maps. This is followed by the aggregation scheme, where only the interesting information of the feature maps is grouped together. [7] [8]

These techniques are implemented in various layers as shown in the figure (1).

.

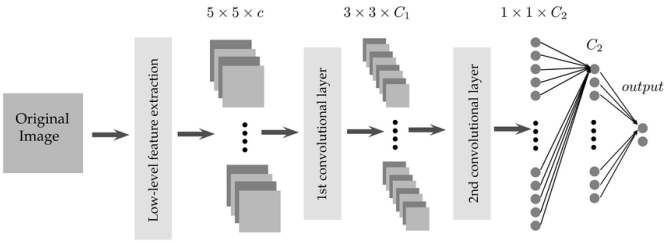

Fig. 1. Deep learning Model Architecture [8]

2.3 You Only Look Once

The YOLO algorithm used in the field of computer vision. It's able to classify the objects inside a particular image (human, fruit, car) in addition to determining the location of these objects inside the image (Object detection). YOLO algorithm is an acronym for "You Only Look Once", meaning that it requires only one pass (forward propagation) through the convolutional neural network to discover multiple objects within an image, so that the image is divided into regions and the bounding box is predicted and the probabilities for each region. [9]

2.4 YOLOv4

YOLOv4 is a real-time object discovery model developed and published in 2020 by three developers, Alexey Bochkovskiy, Chien-Yao Wang, and Hong-Yuan Mark Liao, and it has achieved impressive performance. YOLOv4 depends in its work on convolutional neural network (CNN), this neural network divides the image into a group of regions and predicts the boxes of limits and probability for each region. This version of YOLO has been developed in terms of speed and accuracy, now YOLOv4 has high accuracy and speed compared to the rest of the versions. The average accuracy (AP) and the fps (frames per second) increased by 10% and 12% compared to YOLOv3. The YOLOv4 object recognition model used in this research is mainly divided into three sections:

1) Backbone Model: Extracts features from the input image.

2) Neck Model: Generates a feature pyramid.

The Neck Model helps the object detector to detect the same object at different scales, thus helping with the generalization of the convolution neural network.

3) Head Model: Obtains features from the previous section and predicts the bounding-box area and the associated class, as shown in the figure (2) below. [10] [11]

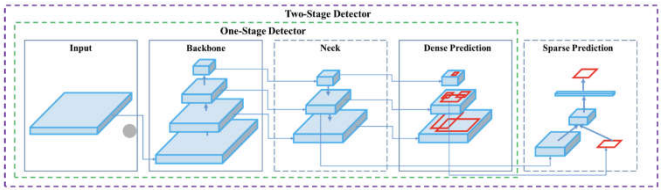

Fig. 2.: YOLOv4 Architecture [10]

III. DESIGN

3.1. Dataset

3.1.1. Image Collecting

The dataset used as input data for the recognition system was taken by the author in the form of a set of 8000 images divided into 40 classes, each class representing a number and a letter

from the alphabet and some words, with a total of 200 images for each class as shown in the table (1) below.

Table 1. Dataset Specification

Specification	Value
Resolution	1920*1080
Extension	.JPG
Number of images	8000
Number of class	40
Number of images per class	200
Image size	900-1000 Kb

The data set was divided into two parts, the first for training and the second for testing, it was divided by 80% for training to 20% for testing under different lighting conditions and divided into four groups as shown in the table (2) below.

Table 2. Dataset Conditions

Conditions	Description
Condition1	Brightness, taken from 20-30 cm away
Condition2	Brightness, taken from 50-60cm away
Condition3	Low Brightness, taken from 20-30 cm away
Condition4	Low Brightness, taken from 50-60cm away

(a) Condition1

(b) condition2

(c) condition3

(d) condition4

Fig. 3. dataset conditions

3.1.2. Image labelling

Each class was given a name using "labelimg" as a Labelling program which is draws a box around the object to be detected and specifies five values for the object, which are a specific value or number for the class, two values represented by X and Y for the object location, and other values for the object size, and Then save these values into a XML file as shown in the figure (4) and figure (5) below. This process is done for each picture in the class for one and also for the rest of the classes.

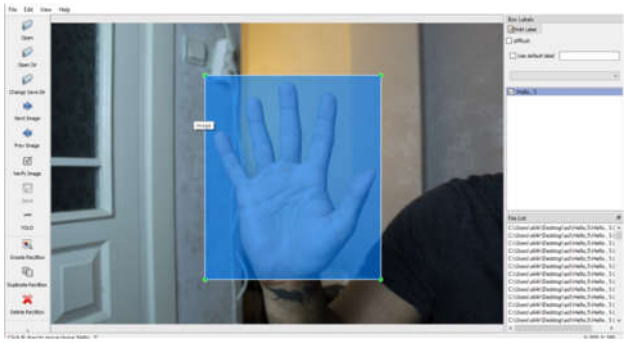

Fig. 4. Image labelling using labelimg

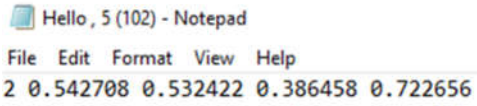

Fig. 5. Object Values

3.2. Model training and results

3.2.1. Platform

In the training we used windows 10 as an operating system with NVIDIA RTX3070 GPU (graphics card) and Ryzen 7 5800H (processer) and python 3.7 as programming language. The YOLOv4 model has been run under the Darknet framework.

3.2.2. Training

The model was trained on a data set collected by the author, but it did not give good results because of the large size of the images, which led to training problems, so we modified the size of the images and retrained the model on the new data set more than once.

In the first training, the model was trained for 3000 iterations, and we got good results as shown in figure (6) below.

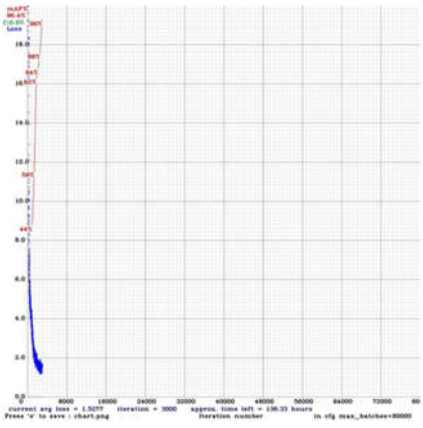

Fig. 6. First training results

As we can see in the figure (6) that the accuracy started to rise, so at iteration 1000 the accuracy was 44%, and rise to 96% at iteration 3000 and the rate of loss started decreasing at iteration 1000 also down to iteration 3000 where it was 1.52 and in this iteration stopped decreasing and the first training ended here.

After that, we re-trained for 4000 iterations, and we got an increase in accuracy and a lower average loss, as shown in figure 7 below.

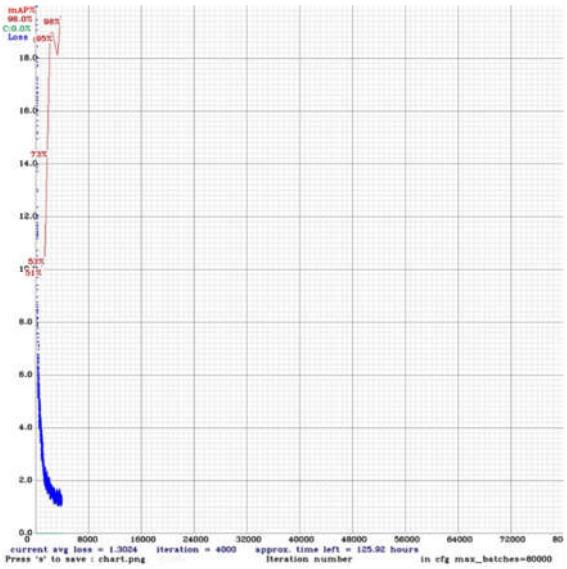

Fig. 7. Second training results

And as we can see in the figure (7) that the accuracy started to rise, so at iteration 1000 the accuracy was 51%, and rise up to 98% at iteration 4000 and the rate of loss started decreasing at iteration 1000 also down to iteration 4000 where it was 1.3 and in this iteration stopped decreasing and the second training ended here.

The increase in iterations does not mean getting better results. The number of iterations has been increased, but we did not get good results and Training has been stopped when the current average loss doesn't decrease anymore.

3.3 Results

The latest results for each class of the data set can be summarized according to the accuracy and the percentage of true and false in precision in the table (3) below.

Table 3. Classes Results

Class name	Average Precision (ap)	True positive (tp)	False positive(fp)
1	100.00%	40	0
2,V	99.10%	39	2
3	100.00%	40	0
4	83.88%	18	4
5,Hello	99.62%	39	3
6,W	97.78%	39	5
7	100.00%	40	0
8	100.00%	40	0
9	100.00%	40	0
Zero ,O	100.00%	40	0
A	99.88%	40	1
B	100.00%	40	0
C	100.00%	40	0
D	100.00%	40	0
E	100.00%	39	1
F	100.00%	40	4
G	100.00%	40	0
H	100.00%	40	0
I	100.00%	40	0
J	100.00%	40	1
K	100.00%	40	0
L	100.00%	40	0
M	86.87%	35	7
N	100.00%	40	0
P	100.00%	40	1
Q	96.00%	39	1
R	100.00%	40	0
S	100.00%	40	0
T	99.40%	40	6
U	100.00%	40	5
X	92.86%	20	1
Y	100.00%	40	4
Z	100.00%	40	0
Yes	100.00%	40	0
No	100.00%	40	2
Please	76.03%	25	8
Thanks	100.00%	40	0
Ok	100.00%	40	0
Sorry	89.10%	40	11
I Love You	100.00%	40	0

3.4 Examples of images testing results:

Hello

9

G

I Love You

V,2

8

And we can summarize the results in both trainings in the table (4) below

Table 4. Last Trainings Results

Results	First Training	Second Training
Precision	0.88	0.96
Recall	0.94	0.96
F1-Score	0.91	0.96
TP	1510	1533
FP	215	67
FN	90	67
Average IoU	69.86%	76.67%
mAp	96.44%	98.01%

Detection Time	41 seconds	42 seconds

And for video testing results in first training we got 28.3 frame per second (fps) and in second training we got 28.9 frame per second (fps).

IV. CONCLUSION

In this research, a recognition system for The American Sign Language (ASL) using YOLOv4 method has been done. Also we introduced a new dataset of American Sign Language. The experiment on images got 98% MAP as an accuracy which is very good and the current average loss is 1.53 and for video testing results we got 28.9 fps. In the future, we will work to increase the dataset by adding new words and signs. We will also improve the accuracy of the images in the data set to get better results.

REFERENCES

[1] Z. Zafrulla, H. Brashear, P. Yin, P. Presti, T. Starner, and H. Hamilton, "American sign language phrase verification in an educational game for deaf children," in 2010 20th International Conference on Pattern Recognition, 2010, pp. 3846–3849.

[2] C. Oz and M. C. Leu, "American sign language word recognition with a sensory glove using artificial neural networks," Eng. Appl. Artif. Intell., vol. 24, no. 7, pp. 1204–1213, 2011.

[3] S. Lang, M. Block, and R. Rojas, "Sign language recognition using kinect," in International Conference on Artificial Intelligence and Soft Computing, 2012, pp. 394–402.

[4] D. Aryanie and Y. Heryadi, "American sign language-based finger-spelling recognition using k-Nearest Neighbors classifier," in 2015 3rd International Conference on Information and Communication Technology (ICoICT), 2015, pp. 533–536.

[5] R. A. Kadhim and M. Khamees, "A real-time american sign language recognition system using convolutional neural network for real datasets," Tem J., vol. 9, no. 3, p. 937, 2020.

[6] J. Redmon, S. Divvala, R. Girshick, and A. Farhadi, "You only look once: Unified, real-time object detection," in Proceedings of the IEEE conference on computer vision and pattern recognition, 2016, pp. 779–788.

[7] J. Du, "Understanding of object detection based on CNN family and YOLO," in Journal of Physics: Conference Series, 2018, vol. 1004, no. 1, p. 12029.

[8] S. Daniels, N. Suciati, and C. Fathichah, "Indonesian Sign Language Recognition using YOLO Method," in IOP Conference Series: Materials Science and Engineering, 2021, vol. 1077, no. 1, p. 12029.

[9] M. J. Shafiee, B. Chywl, F. Li, and A. Wong, "Fast YOLO: A fast you only look once system for real-time embedded object detection in video," arXiv Prepr. arXiv1709.05943, 2017.

[10] A. Bochkovskiy, C.-Y. Wang, and H.-Y. M. Liao, "Yolov4: Optimal speed and accuracy of object detection," arXiv Prepr. arXiv2004.10934, 2020.

[11] J. Yu and W. Zhang, "Face mask wearing detection algorithm based on improved YOLO-v4," Sensors, vol. 21, no. 9, p. 3263, 2021.

[12] R. Girshick, J. Donahue, T. Darrell, and J. Malik, "Rich feature hierarchies for accurate object detection and semantic segmentation," in Proceedings of the IEEE conference on computer vision and pattern recognition, 2014, pp. 580–587.

[13] R. Girshick, "Fast r-cnn," in Proceedings of the IEEE international conference on computer vision, 2015, pp. 1440–1448.

[14] S. Ren, K. He, R. Girshick, and J. Sun, "Faster r-cnn: Towards real-time object detection with region proposal networks," Adv. Neural Inf. Process. Syst., vol. 28, 2015.

[15] Y. Chen, W. Li, C. Sakaridis, D. Dai, and L. Van Gool, "Domain adaptive faster r-cnn for object detection in the wild," in Proceedings of the IEEE conference on computer vision and pattern recognition, 2018, pp. 3339–3348.

[16] Z. He and L. Zhang, "Multi-adversarial faster-rcnn for unrestricted object detection," in Proceedings of the IEEE/CVF International Conference on Computer Vision, 2019, pp. 6668–6677.

[17] J. Li, X. Liang, S. Shen, T. Xu, J. Feng, and S. Yan, "Scale-aware fast R-CNN for pedestrian detection," IEEE Trans. Multimed., vol. 20, no. 4, pp. 985–996, 2017.

[18] X. Wang, H. Ma, and X. Chen, "Salient object detection via fast R-CNN and low-level cues," in 2016 IEEE International Conference on Image Processing (ICIP), 2016, pp. 1042–1046.

[19] X. Wang, A. Shrivastava, and A. Gupta, "A-fast-rcnn: Hard positive generation via adversary for object detection," in Proceedings of the IEEE conference on computer vision and pattern recognition, 2017, pp. 2606–2615.

[20] X. Xie, G. Cheng, J. Wang, X. Yao, and J. Han, "Oriented r-cnn for object detection," in Proceedings of the IEEE/CVF International Conference on Computer Vision, 2021, pp. 3520–3529.

[21] Z. Cai and N. Vasconcelos, "Cascade r-cnn: Delving into high quality object detection," in Proceedings of the IEEE conference on computer vision and pattern recognition, 2018, pp. 6154–6162.

[22] C. Chen, M.-Y. Liu, O. Tuzel, and J. Xiao, "R-CNN for small object detection," in Asian conference on computer vision, 2016, pp. 214–230.

[23] S. Dasiopoulou, V. Mezaris, I. Kompatsiaris, V.-K. Papastathis, and M. G. Strintzis, "Knowledge-assisted semantic video object detection," IEEE Trans. Circuits Syst. Video Technol., vol. 15, no. 10, pp. 1210–1224, 2005.

[24] L. Guan, Multimedia image and video processing. CRC press, 2017.

[25] J. Wu, A. Osuntogun, T. Choudhury, M. Philipose, and J. M. Rehg, "A scalable approach to activity recognition based on object use," in 2007 IEEE 11th international conference on computer vision, 2007, pp. 1–8.

International Journal of Multidisciplinary Studies and Innovative Technologies

e-ISSN: 2602-4888
dergipark.org.tr/en/pub/ijmsit
Research Article

2022, 6 (1), 66-70
DOI: DOI: 10.36287/ijmsit.6.1.66
Received: May 21, 2022; Accepted: June 20, 2022

Increasing Water Efficiency by Using Fuzzy Logic Control in Tomatoes Seedling Cultivation

Selami Kesler[1], Abdil Karakan[2*] and Yüksel Oğuz [3]

[1] *Electrical and Electronics Engineering, Pamukkale Universty, Denizli, Turkey, (skesler@pau.edu.tr) (Orcid ID: 0000 0002 7027 1426)*
[*2] *Electrical Department, Afyon Kocatepe Universty,Afyonkaraisar, Turkey, (akarakan@aku.edu.tr), Orcid ID: 0000 0003 1651 7568)*
[3] *Electrical and Electronics Engineering, Afyon Kocatepe Universty, Afyonkarahisar, Turkey, (yukseloguz@aku.edu.tr), Orcid ID: 0000-0002-5233-151X)*

Abstract – The biggest problem in agriculture is the insufficient amount of water. Sowing cannot be done in the fields due to water scarcity. Some fields become barren land due to excessive irrigation. For these reasons, it is important to use water wisely. In the study, irrigation of tomatoes seed is controlled with fuzzy logic. The use of water is made automatically according to the humidity, temperature and soil moisture of the air. The study was carried out in two stages. First stage; The irrigation system is designed in the MATLAB program. For this, temperature, humidity and soil moisture were used as three inputs. Irrigation time was calculated as output. All inputs and outputs are set to low, medium and high. In the second stage; equal amounts of tomatoes seeds were planted in two separate containers. Normal irrigation was done in the first pot. The control of irrigation in the second bowl was made with fuzzy logic. All data are shown on the screen and recorded for 1 minute. As a result of the study, 22500 milliliters of water were used in normal irrigation, and 10410 milliliters of water were used in a fuzzy logic-controlled circuit. As a result, a water saving of 53.77% was achieved. Arduino microcontroller is used for control. The code was written for the fuzzy logic control circuit simulated in the Arduino microcontroller MATLAB program to work. At the same time, temperature and humidity sensors are connected to the Arduino microcontroller. Incoming data is remotely monitored and controlled by a modem connected to the microcontroller. When the records in the database are examined, 83% energy was saved with lighting algorithm and energy flow control algorithms.

Keywords *– Fuzzy logic, Productivity, Tomato seedling, Remote control*

Citation: Kesler, S., Karakan, A., Oğuz, Y. (2022). Increasing Water Efficiency by Using Fuzzy Logic Control In Tomatoes Seedling Cultivation. International Journal of Multidisciplinary Studies and Innovative Technologies, 6(1): 66-70.

I. INTRODUCTION

The most important food source of people is agricultural products. Some agricultural lands become arid with excessive irrigation and some cannot be irrigated due to water scarcity. Efforts are being made to overcome the problems occurring in agriculture [1]. In the study of Khandere and his friends; They made an irrigation system based on solar energy. Their main purpose is low-cost and time-based irrigation. The control of the selonid valve in the irrigation system was carried out automatically [2]. In the study by Parameswaran et al. Ambient temperature, humidity and soil moisture were measured. Arduino microcontroller is used in this measurement. The irrigation system was carried out manually according to the data from the sensor [3]. Rehman et al. Controlled the irrigation system on a GSM basis in their study. In their systems, temperature, humidity and soil moisture have been measured with sensors. Data from the sensors are shown on GSM. Irrigation control is performed with the data coming from GSM [4]. Venkatapur et al used temperature, humidity and soil moisture sensors. The data from the sensors are connected to the Arduino microcontroller. Raspberry is connected with Arduino via ZigBee. The opening and closing of the irrigation valve were through raspberry [5]. Zhang et al. carried out an application study in a region in the north-west of China. In this study, they aimed to increase irrigation efficiency. They also aimed to reduce salinization accumulations. They used fuzzy logic controller in their work. The study was done in simulation. As a result of the study, suitable solution plans for irrigation planning were presented [6]. Honorato tried to reduce the water consumption used in tulip production in his study. For this, fuzzy logic control, which is the most ideal method, is used. He tried to adjust the irrigation time with temperature control for the consumption of water in tulip production. As a result of the study, it has succeeded in reducing water consumption significantly [7]. Ehsan worked on a surface irrigation system. In this study, it was aimed to increase irrigation efficiency. He also worked on increasing productivity and efficiency with this study. SIRMOD and WinSRFR simulation programs were used in the study. As a result of this study, labor has been reduced by 10%. It also increased practicality by 9% and performance by 13% [8]. Perea et al. have worked on pressurized irrigation systems. In these studies, they aimed to reduce water consumption. His work was based on data used in a site located in the south-west of Spain. As a result of the study, a decrease of 19.5% was achieved in water consumption [9].

In the study, firstly, fuzzy control was designed in MATLAB simulation program. For this, three inputs and one output were created. Inputs are temperature, humidity, and soil moisture. Output is the irrigation time. Each variable is set to low, medium and high. Second, the real application has been made. Two containers were used for this. Equal amount of soil was placed in two containers and tomatoes seeds were planted. Outdoor temperature and humidity AHT10 sensor were measured. Humidity sensor is used to measure soil moisture. Normal irrigation was done in one. In the second bowl, irrigation was done with fuzzy logic. The irrigation result has been compared.

II. Materials and Method

The main purpose of the study is to increase water efficiency in tomatoes seedling cultivation with fuzzy logic control. Thus, less water will be used. The general scheme of the study performed is shown in Figure 1.

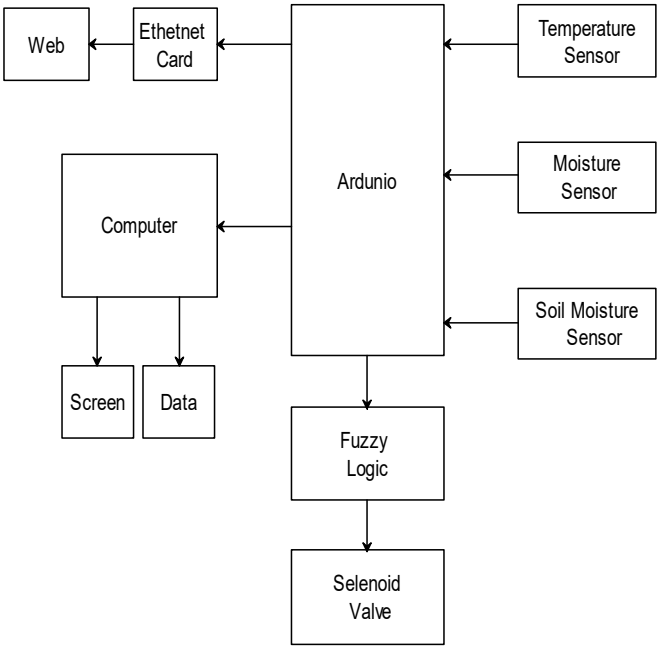

Fig. 1. General Scheme

A. Fuzzy Logic

Three factors necessary for the cultivation of tomatoes seed; temperature, humidity and soil moisture were taken as inputs. The output is the irrigation time. All input and output are named low, medium and high. The fuzzy logic architecture is shown in Figure 2.

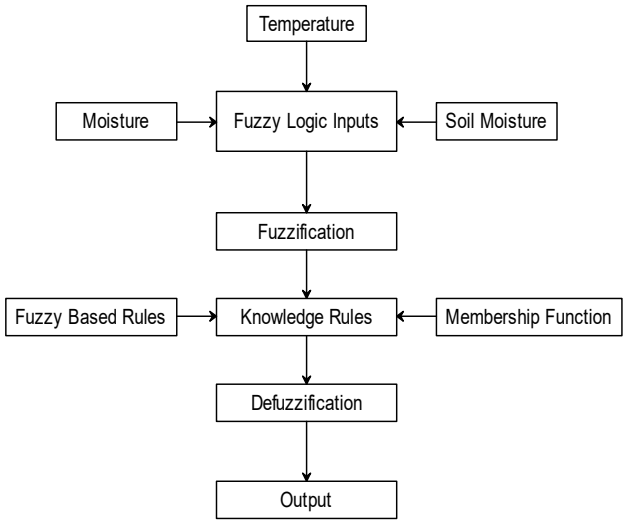

Fig. 2. *Fuzzy logic architectural*

In order for fuzzy logic to take a decision, the rules must be uploaded to the system. Table 1 shows the rules designed for the system. The table shows three inputs and one output.

Table 1. Fuzzy logic rules

Soil Moisture	Moisture	Temperature	Watering
Low	Low	Low	High
Low	Low	Normal	Normal
Low	Low	High	Normal
Low	Normal	Low	High
Low	Normal	Normal	Normal
Low	Normal	High	Low
Low	High	Low	High
Low	High	Normal	High
Low	High	High	Normal
Normal	Low	Low	Normal
Normal	Low	Normal	Normal
Normal	Low	High	Low
Normal	Normal	Low	Normal
Normal	Normal	Normal	Normal
Normal	Normal	High	High
Normal	High	Low	Normal
Normal	High	Normal	Low
Normal	High	High	Low
High	Low	Low	Low
High	Low	Normal	Low
High	Low	High	Low
High	Normal	Low	Low
High	Normal	Normal	Low
High	Normal	High	Low
High	High	Low	Low
High	High	Normal	Low
High	High	High	Low

All inputs and outputs are loaded in the MATLAB simulation program to provide fuzzy logic control. Soil moisture is shown in Figure 3.

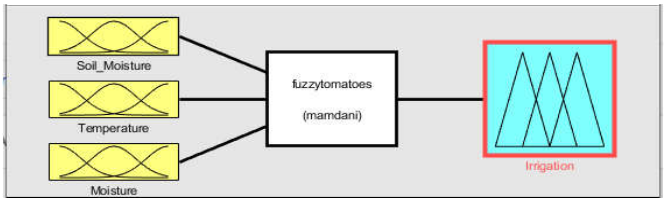

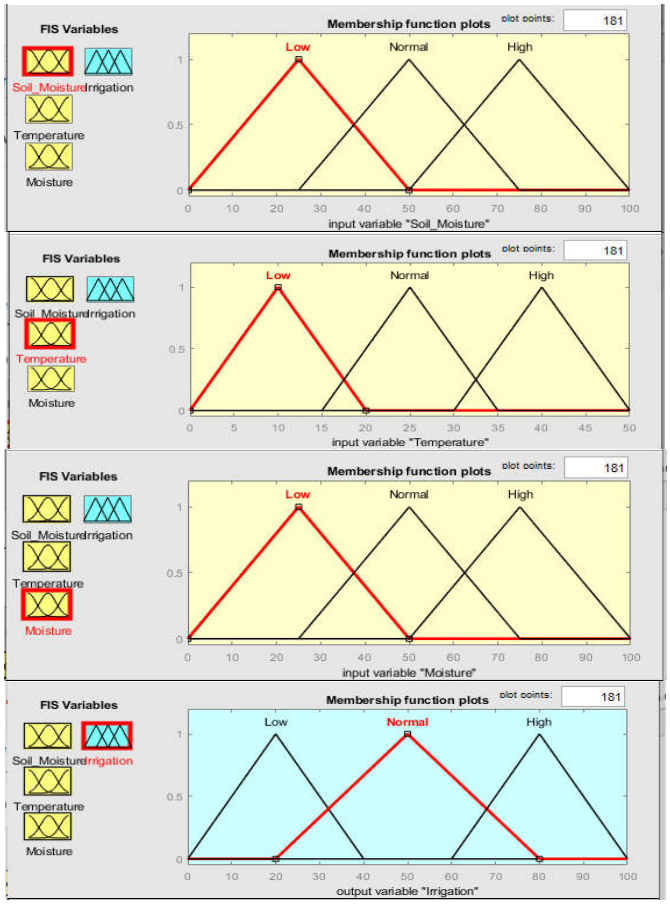

Fig. 3. *Soil moisture, temperature, moisture, irrigation*

Temperature, humidity and soil moisture inputs and irrigation time inputs were made. While making these entries, the time and amount of irrigation were determined with the rules. Irrigation is not done especially in hot weather. Irrigation is effective when temperatures are low. This is in the early morning or evening hours. Figure 4 shows the fuzzy logic control output.

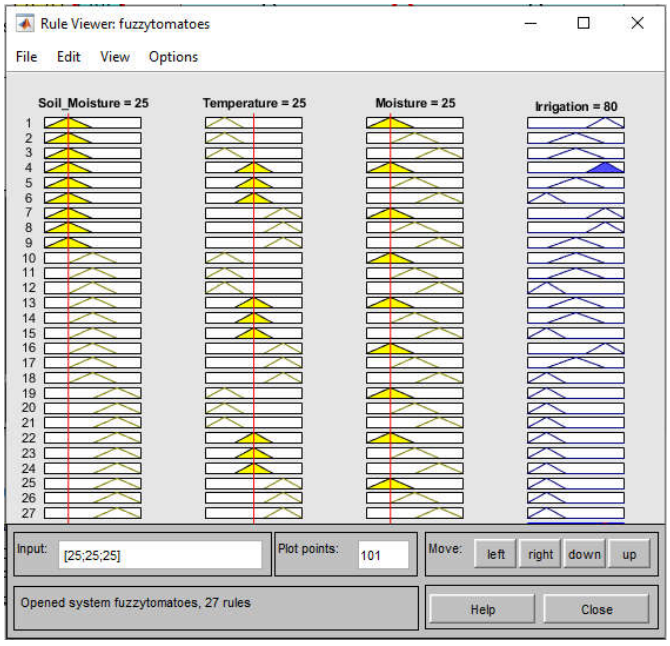

Fig. 4. *Fuzzy logic*

B. Ardunio Microcontroller

The system has two components. One is the MATLAB simulation part and the other is the part where the control system takes place. The control part takes place with the Arduino microcontroller. Temperature, humidity and soil moisture sensors are connected to the Arduino microcontroller. Fuzzy control works with the data from these sensors, and the tomatoes seedlings are irrigated accordingly. The control of the irrigation pump is provided by the relay. During the irrigation period, the relay is working and when the time is over, the relay stops. Thus, the irrigation pump is controlled. Figure 5 shows the control part designed for the system.

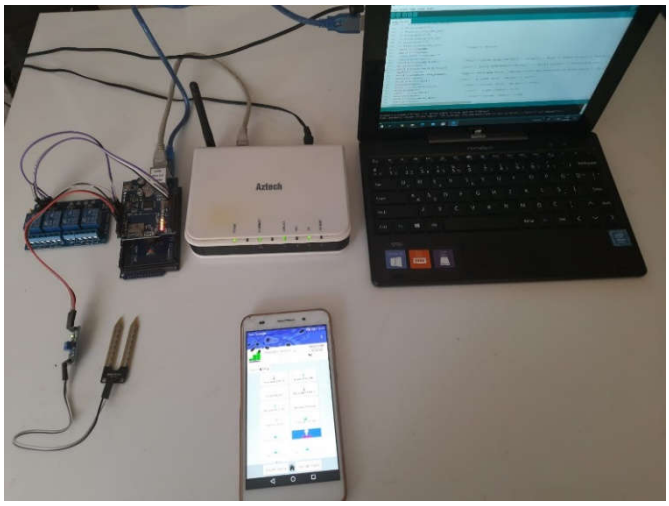

Fig. 5. Designed for system ardunio control

An Ethernet module was added to the Arduino microcontroller and wireless broadcast was made via the modem. Thus, remote access was provided. All data in the system could be monitored with all devices with Wi-Fi broadcast capability.

III. RESULTS

The applied system covers a period of 15 days. At this time, the tomatoes seedling was planted in two half-pots. Figure 7 shows the containers.

Fig. 6. *Daily highest and smallest temperature*

One was normal irrigation. The other container was irrigated with fuzzy control. Figure 7 shows the lowest and highest temperatures that occur during the seedling growing period.

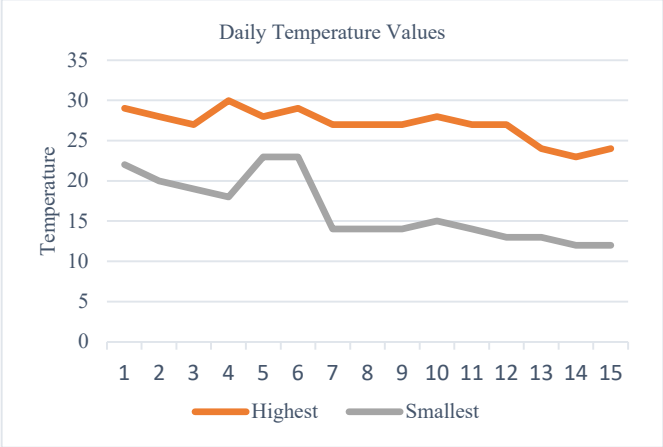

Fig. 7. *Daily highest and smallest temperature*

The temperature changes daily. The humidity level changes depending on the temperature. Temperature and humidity are the two main factors during irrigation. Figure 8 shows the daily moisture level.

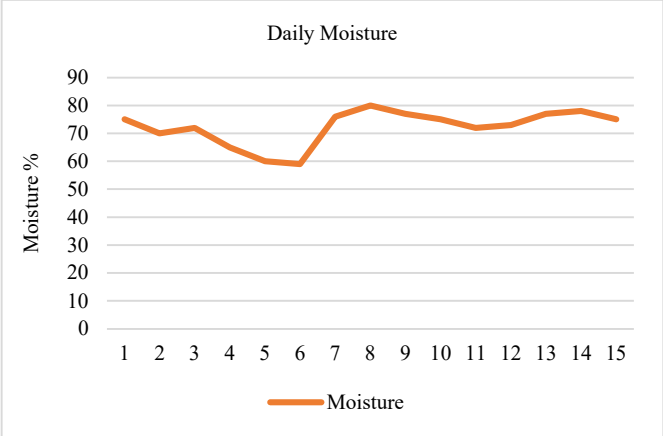

Fig. 8. *Daily moisture*

In my site, irrigation water of each container has been provided from a sized container. Thus, it was determined how much water was used daily. Daily water consumption is shown in Figure 9.

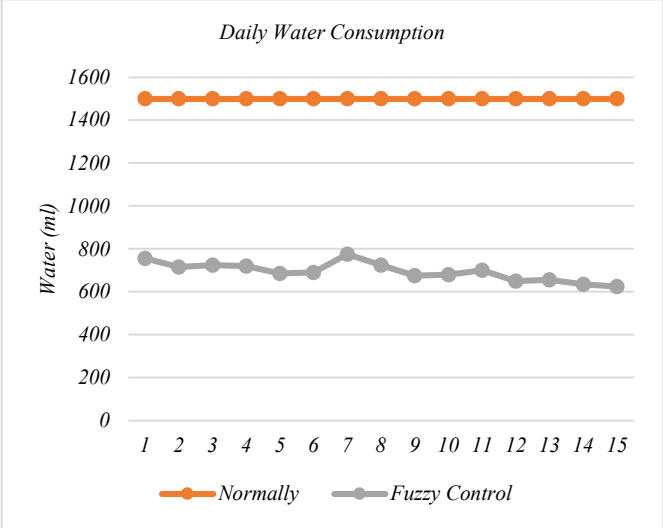

Fig. 9. Daily water consumption

IV. DISCUSSION

The study covers a period of fifteen days. These days, different temperature and humidity values have occurred. The temperature varied between 24 and 31 degrees at the highest. The lowest was 12 degrees. Humidity values vary between 60 and 80. For irrigation, outdoor temperature and humidity are as important as soil moisture. In parallel with the increase in the outdoor temperature, the irrigation water should increase. Decrease in the outdoor temperature will decrease the evaporation and will cause a decrease in the irrigation water. Likewise, an increase in outdoor humidity means a decrease in irrigation water.

In the study, tomato seedlings grown in two different environments were compared. Normal irrigation was done in the first tomato seedling. In the second seedling, the irrigation system was carried out with fuzzy logic control. For fuzzy logic control, simulation was first done in MATLAB. According to the simulation results, code was written with Arduino microcontroller. Irrigation was done with this code. At the same time, remote monitoring is provided.

In the first seedling growing, daily constant irrigation was applied. Watered with 1500ml of water daily. Irrigation value changes daily in the second seedling growing. Some days it is 900 ml, sometimes this value decreases to 600 ml. The main reason why these values vary so much; is the change in outdoor temperature and humidity values. In a second important factor; is soil moisture. As the moisture values in the soil increase, the irrigation water decreases. Since the moisture values in the soil were low in the first days, the irrigation values were high. As the soil is irrigated, the need for irrigation water decreases when the soil moisture values increase.

V. CONCLUSION

With unconscious irrigation, some soils become barren and some cannot be irrigated. With the work carried out, an efficiency of 53.77% has been achieved in irrigation water in seedling cultivation. In addition, the human factor, which is the biggest risk in irrigation, has been minimized. It has been automated with the irrigation system that varies from person to person. Irrigation was carried out with fuzzy logic control with a sensor coming from temperature, humidity and soil moisture. Thus, adaptation to the ambient conditions was achieved quickly. In addition, the data from the sensors could be monitored instantly with remote access.

ACKNOWLEDGMENT

Authors' Contributions

The authors' contributions to the paper are equal.

Statement of Conflicts of Interest

There is no conflict of interest between the authors.

Statement of Research and Publication Ethics

The authors declare that this study complies with Research and Publication Ethics

REFERENCES

[1] Sudharshan N., Kasturi K., Sandeep K., Geetha S. Renewable Energy Based Smart Irrigation System. Procedia Computer Science 165 pp. 615–623, 2019

[2] Khandare S., Alone A., Patil S., Raut P. A Review on Solar Based Plant Irrigation System. International Research Journal of Engineering and Technology (IRJET) 5(2) pp. 1516-1518. 2018.

[3] Parameswaran G., & Sivaprasath K. Arduino based smart drip irrigation system using Internet of Things. International Journal of Engineering Science and Computing 6(5) pp. 5518-5521. 2016.

[4] Rehman A., Asif R., Tariq R., Javed A. GSM based solar automatic irrigation system using moisture, temperature and humidity sensors. International Conference on Engineering Technology and Technopreneurship (ICE2T) pp. 1-4. 2017.

[5] Venkatapur R. & Nikitha S. Review on Closed Loop Automated Irrigation System. The Asian Review of Civil Engineering 6(1): pp. 9-14. 2017.

[6] Zhang C., Li X. , Guo P., Huo Z. , Huang G. Enhancing irrigation water productivity and controlling salinity under uncertainty: a fuzzy dependent linear fractional programming approach. Journal of Hydrology. Vol:606 pp.127428-127439. 2022.

[7] Pacco H. C. Simulation of temperature control and irrigation time in the production of tulips using fuzzy logic. Procedia Computer Science. Vol:200 pp.1-12. 2022

[8] Pazouki E. Practical surface irrigation design based on fuzzy logic and meta-heuristic algorithms. Agriculture Water Management Vol:256 pp:107659-107669.2022.

[9] Perea R. G., & Camacho E. Forecasting of applied irrigation depth at farm level for energy tariff periods using coactive neurogenetics fussy system. Agriculture Water Management Vol:256 pp:107068-107075. 2021.

International Journal of Multidisciplinary Studies and Innovative Technologies

e-ISSN: 2602-4888
dergipark.org.tr/en/pub/ijmsit
Research Article

2022, 6 (1), 71 -76
DOI: DOI: 10.36287/ijmsit.6.1.71
Received: April 20, 2022; Accepted: June 1, 2022

Explication of the Remote Education Through Department Statistics: ESOGU-CENG Case Study

Merve Ceyhan[1*], Yusuf Kartal[2], Sinem Bozkurt Keser[3], Savaş Okyay[4] and Nihat Adar[5]

[1*]*Department of Computer Engineering, Eskişehir Osmangazi University, Eskişehir, Turkey, e-mail: mceyhan@ogu.edu.tr, ORCID: https://orcid.org/0000-0003-0733-3652*
[2]*Department of Computer Engineering, Eskişehir Osmangazi University, Eskişehir, Turkey, e-mail: ykartal@ogu.edu.tr, ORCID: https://orcid.org/0000-0002-0402-1701*
[3]*Department of Computer Engineering, Eskişehir Osmangazi University, Eskişehir, Turkey, e-mail: sbozkurt@ogu.edu.tr, ORCID: https://orcid.org/0000-0002-8013-6922*
[4]*Department of Computer Engineering, Eskişehir Osmangazi University, Eskişehir, Turkey, e-mail: osavas@ogu.edu.tr, ORCID: https://orcid.org/0000-0003-3955-6324*
[5]*Department of Computer Engineering, Eskişehir Osmangazi University, Eskişehir, Turkey, e-mail: nadar@ogu.edu.tr, ORCID: https://orcid.org/0000-0002-0555-0701*

Abstract – Education has been reshaping with the increasing use of the Internet and creation various online models. Lifelong learning has been evolving with each passing day. Nevertheless, Covid-19 has caused necessary changes in the education field and affected all people, from students to instructors. However, students' concerns about remote education have emerged during this forced circumstance. This unintentional situation directly hit the quality of education. In this study, the last ten years of education were interpreted through department statistics. The effect of Covid-19 on students from the ESOGU Computer Engineering Department was investigated by considering the activity status, success rates, and letter grades along with course statistics within remote education. The statistical findings can play a significant role in automation and suggestion systems design. In addition, it has been explicated that compulsory transitions in every field can have great impacts and that it is necessary to be prepared for such conditions in advance, especially in the field of education.

Keywords *– Covid-19, effects of the pandemic, online education, remote education*

Citation: Ceyhan, M., Kartal, Y., B. Keser, S., Okyay, S., Adar, N. (2022). Explication of the Remote Education Through Department Statistics: ESOGU-CENG Case Study. International Journal of Multidisciplinary Studies and Innovative Technologies, 6(1): 71-76

I. INTRODUCTION

Innovative changes have been occurring in many areas with the widespread use of the Internet. Changes have primarily been experienced in social, economic areas, and especially the education field, which is one of the first areas to keep up with today's innovative approaches and changes. With the use of the Internet in education, new models were created [1]. It is aimed to catch up with technology and provide quality education. The concept of remote or distance education is an innovative model that emerged with computer-internet technologies. This model is the digital version of traditional face-to-face education. Many institutions recognize that online programs are strategically crucial to the institution. It is observed that the number of students taking online courses continues to increase at a rate far above the increase in enrollment in general higher education [2]. With the transition to remote education, people of all ages and levels have the opportunity to learn regardless of physical classrooms. This education style provides efficiency by combining virtual and remote laboratory conditions and easily visualizing objects beyond perception [3]. Accessibility to education is also provided for disabled users. Users can come together in the remote education environment and communicate with people from different fields of expertise living in different places. Students prefer remote education because of its independence from the environment, the flexibility of online courses, unlimited replayability, and easy accessibility with a smartphone [4]. The spread of the Internet as a potential remote education environment and the creation of remote education programs with the awareness of lifelong learning is becoming more common day by day [5]. Although this spread is voluntary, it can also be due to health issues surrounding the whole world, such as the Covid-19 pandemic. Covid-19 caused a change in many branches of activity and even made it necessary. As of March 10, 2020, schools and universities worldwide were closed due to Covid-19, and as of April 2020, many countries experienced full closure [6-8].

Face-to-face education has been moved to online education platforms during the pandemic. This situation directly touched the quality of education. The compulsory change that came with Covid-19 also affected the subjects of universities, such as working, research, activity, and education style. Educational institutions using online education systems have easily adapted. While this transition was an innovative approach, suitable for technology and the era, not everyone

was equally ready for it [9]. Students' concerns about online education platforms, such as access speed, reliability, timely delivery of video information technology, course management, communication and interaction, and technical support, have emerged [10]. In the institutions that do not use distance education, problems such as infrastructure inadequacies, internet problems, insufficient knowledge of the personnel about distance education were encountered. It also has other technical requirements such as the design and preparation of e-learning environments, internet bandwidth, and device incompatibilities [11]. These adverse situations have caused the expected efficiency from education, dissatisfaction with students, and prejudice against online platforms. Institutions and students have preferred remote education according to its advantages and disadvantages. However, during the Covid-19 period, choices turned into obligations. With the spread of the pandemic, distance education has become a necessity.

Preparing data for analysis and processing is essential in an automation or recommender system. Interpretation of student data is equally important in the design of course recommendation systems, especially during the transition period to the pandemic. In this study, the effect of the pandemic period on student success was examined through a semester perspective. The pandemic effects on student grades were examined from term to term. The face-to-face and remote education were analyzed comparatively. It has been seen that the obtained results and comments can play a significant role in course/student automation and suggestion systems design.

II. Materials and Method

In this study, the statistics of the Eskişehir Osmangazi University Computer Engineering Department (ESOGU-CENG) were utilized. The data of the last ten years regarding the semesters between 2010/11-Fall and 2020/21-Spring were analyzed. Nevertheless, summer terms were not included. The dataset involves anonymized student and course information for both face-to-face and remote education semesters [12]. There was a transition to remote education in the 2019/20 education period with the onset of the Covid-19 pandemic. Fig. 1 illustrates the forced transition and the remote education period due to Covid-19 through the dataset in practice.

The grading system for letter grades DD, DC, CC, CB, BB, BA, and AA ranges from 1 to 4, and increases by 0.5 for each letter grade, respectively. FF is not a valid passing grade, and its numerical value is zero. Moreover, for non-credit courses, there are two grades, YT and YZ, respectively, pass and fail.

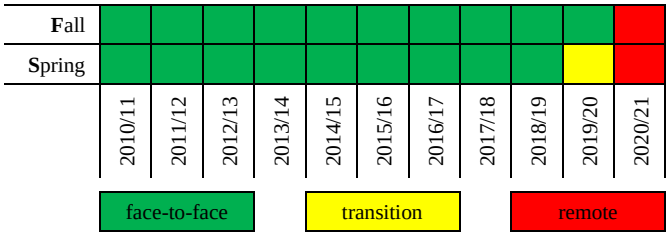

Fig. 1. The Covid-19 period in education through the dataset

III. Results and Discussion

While interpreting the data according to the research questions, it was handled in three main perspectives. Details of these approaches are presented in Figures 2-4 as student, course, and performance statistics, respectively. Within the framework of the curriculum, the courses offered in the fall and spring semesters are fixed. For this reason, a semester-based analysis was carried out while conducting the course and performance analysis, nearly for all subplots.

A. Student Perspective

With the first effect of the pandemic, an increase in the number of new enrollments for students of both genders is seen in Fig. 2 (a). The number of new students shows a general increase until the 2015/16 academic year. Between the 2015/16 and 2018/19 academic years, there has been a decrease in the number of female students in particular. With the first effect of the pandemic, an increase in the number of new enrollments for both male and female students is seen. This shows that distance education does not have a negative effect on the number of students.

According to Fig. 2 (b), the number of active students has increased continuously every year. Considering the fall and spring semesters separately, the high number of graduations in the fall semester causes a decrease in the number of active students in the spring semester. The number of active students increases with the course taken in the fall semester. Especially after the transition to distance education, there is a higher increase in the first fall semester compared to previous years. It may result from students thinking that they can attend classes more comfortably and flexibly with distance education. Besides, students who could not continue their education due to financial difficulties and were in the position of passive students due to accommodation problems were able to switch to active student status with the distance lessons.

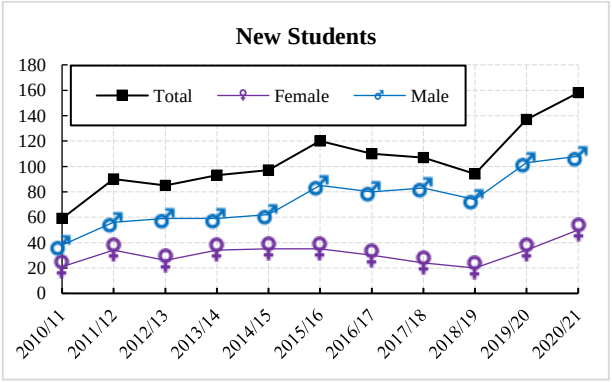

(a) Total number of new students

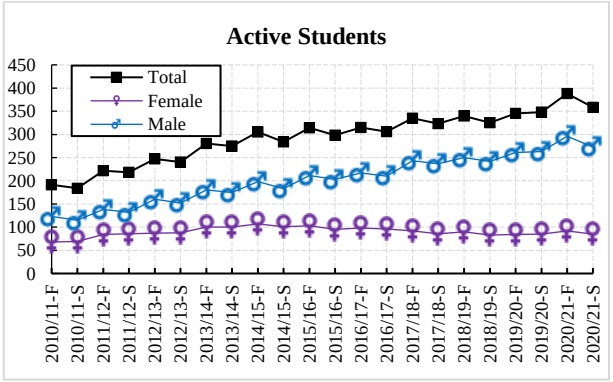

(b) Total number of active students

Fig. 2. Student statistics

B. Course Perspective

Considering the number of courses during the pandemic, it can be deduced that there is a noticeable decrease. Figure 3 (a) shows that with Covid-19 (starting with the 2019/20-F), the number of courses opened has decreased with the opportunity to conduct courses remotely. Before distance education, there were courses that students demanded intensely but could not take due to physical classroom capacity and laboratory facilities. With distance education, students' preference for these courses may have caused fewer or no-preferred courses to be not opened. In addition, reducing the courses to a single online class may also be effective in this decrease.

When the effect of the number of courses opened is reduced to the types of courses, there has been a serious decrease in the number of compulsory courses, as can be seen in Fig. 3 (b). This can be explained by the elimination of physical classroom capacity constraints with online education and the reduction of compulsory courses to a single class. Besides, it is seen that there is a decrease in the number of technical courses and an increase in the number of non-technical courses. This may be due to the fact that students want to reduce the number of responsible courses by taking courses that are not directly related to the department they are studying in and do not contain technical knowledge but have an impact on graduation. In addition, they want to take technical elective courses that will contribute greatly to their professional development, with face-to-face training in case the pandemic disappears.

As seen in Fig. 3 (c), the highest decrease is observed in the number of courses offered in English when analyzing the courses based on the language. Apart from the non-technical elective German course itself, there is no other course whose language is German. Therefore, one increase in the number of courses taught in German can be ignored. However, students may have decided to take Turkish lessons as easier to understand. The decrease in the total number of courses in Figure 3 (a) with the transition to distance education may explain the decrease in the number of Turkish courses offered in Figure 3 (c).

According to Fig. 3 (d), before the transition to distance education, it was not possible to draw a definite conclusion about the increase or decrease in the number of courses offered on a class basis. However, with the decrease in the total number of courses offered through distance education, it is seen that there is also a decrease in the number of courses offered on a class basis.

C. Grade and Performance Perspective

Considering the students' success, letter grades can be seen properly improved; however, the GPAs cannot be clearly classified. Total grade counts in different semesters are shown in Fig. 4 (a). In this subplot, although there is a periodic increase in the number of courses taken by students for the first time in both the Fall and Spring semesters, it is seen that the increase is higher in percentage with the pandemic (starting with 2019/20-F). Moreover, the number of courses students re-take in the 2020/21-F semester is higher than in the 2020/21-S semester. This situation can be explained by the increase in the number of courses students re-take at the beginning of the pandemic.

Fig. 4 (b) shows the counts for Mandatory, Technical Elective, and non-Technical Elective courses. This graph shows that there has been an increase in the number of courses taken for the first time as of the 2018/19-F term. The Covid-19 period did not greatly affect a student's taking a course for the first time. However, considering the number of courses taken again, there has been an increase in the number of courses taken again from the 2019/20-F Covid-19 transition period to the 2020/21-F term. With the 2020/21-S term, the number of courses students take again has decreased.

Grade percentage values are given in Figure 4 (c). In this graph, an increase was observed in the number of students with especially high letter grade values in the fall semester. In the spring semester, an increasing-decreasing variable situation was observed for all letter grades. In particular, the percentage increases that started with the 2019/20-F period doubled during the Covid-19 period, and the percentages of students taking AA increased significantly. Although the similar situation is not as high as the change in the percentages of students taking AA, it was also observed in the percentages of BA letter grades during the Covid-19 period. Due to these increases, there has been a decrease in the percentage of students who received DC+DD letter grades, which can be considered below the average. Despite this success, an increase was detected in the number of students who received FF for the same semester. Although the percentage of students who failed the course by taking FF started to decrease, the biggest decreases coincided with the Covid-19 period. This shows that there has been an increase in student success percentages and a decrease in school dropout rates during the Covid-19 period. This situation can be explained by the fact that students focus on their success in education together with the restrictions on going out due to the pandemic.

The letter grade percentages of the courses that the students take as non-credit and evaluate as pass (YT) or fail (YZ) are given in Fig. 4 (d). Although the number of courses opened in the semester varies, the percentages show that the YT grade percentages decreased at low rates until the 2018/19-S period. As of 2019/20-F, there has been an increase in YT letter grade rates until the 2020/21-S period. While there was an increase in YT course grade rates, students' YZ grade rates decreased. This shows that the success rates of students in non-credit courses have increased during the Covid-19 period or that students pass the courses more easily.

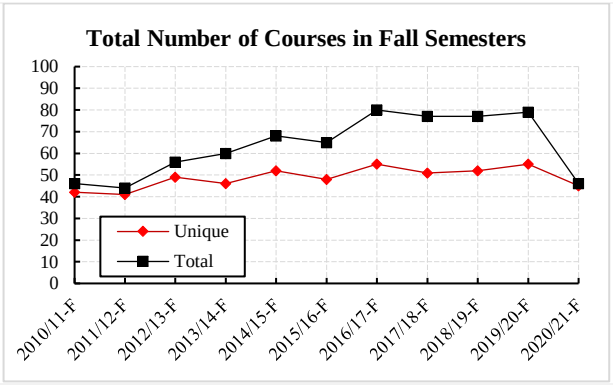

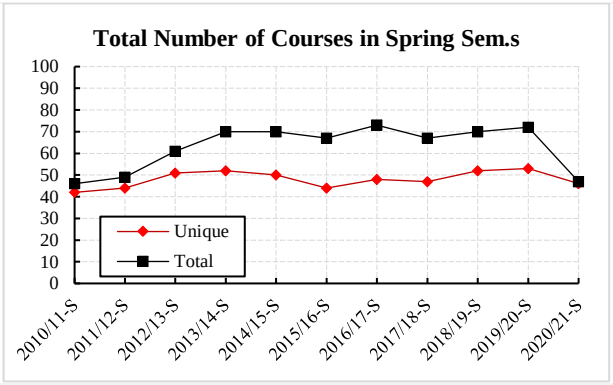

(a) Total number of courses in different semesters

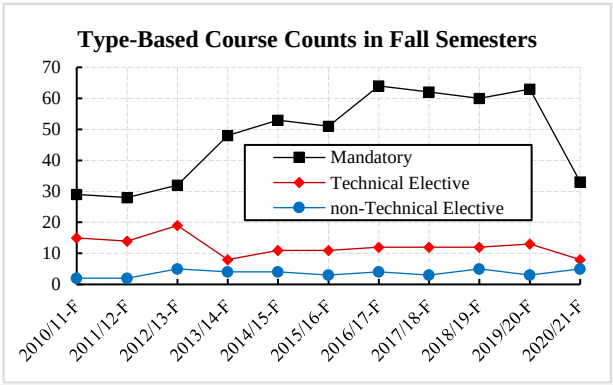

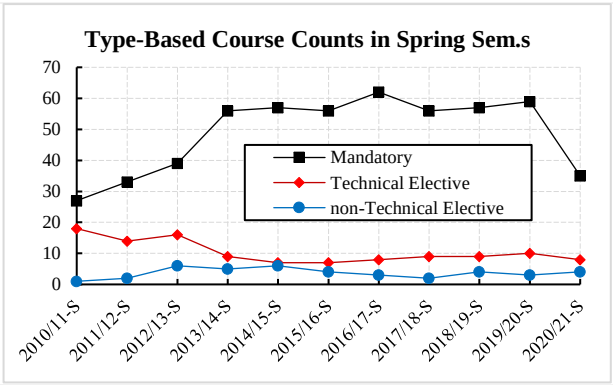

(b) Course type counts in different semesters

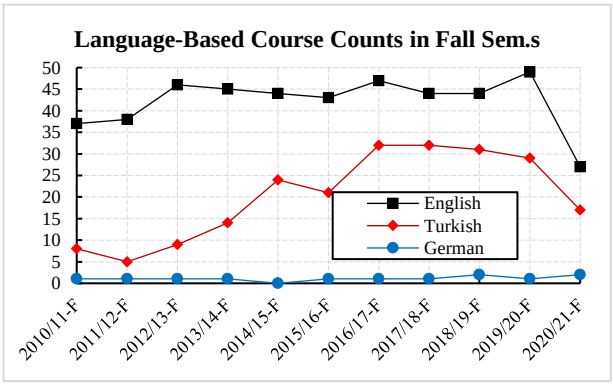

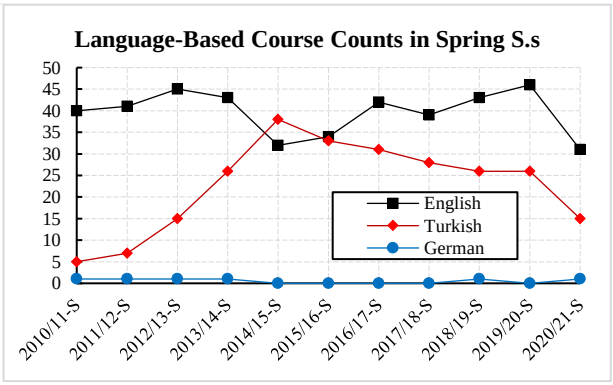

(c) Course language counts in different semesters

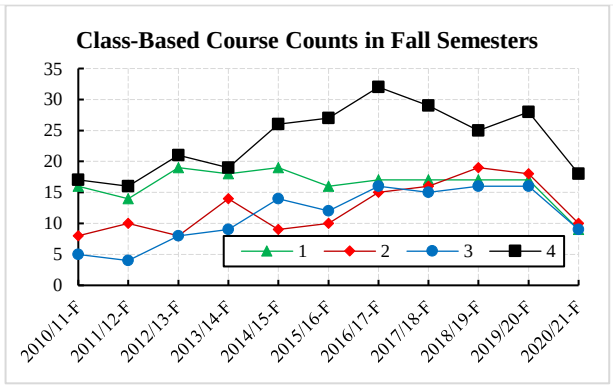

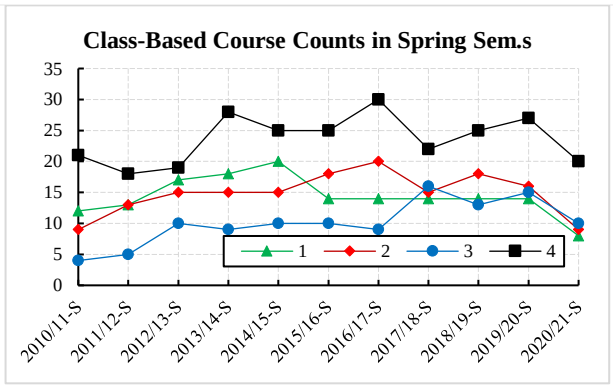

(d) Course class counts in different semesters

Fig. 3. Course statistics

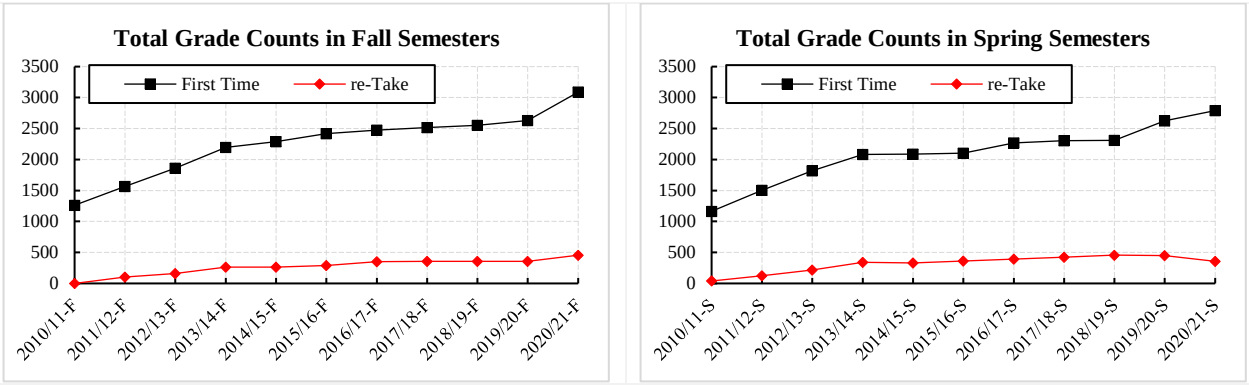

(a) Total grade counts in different semesters

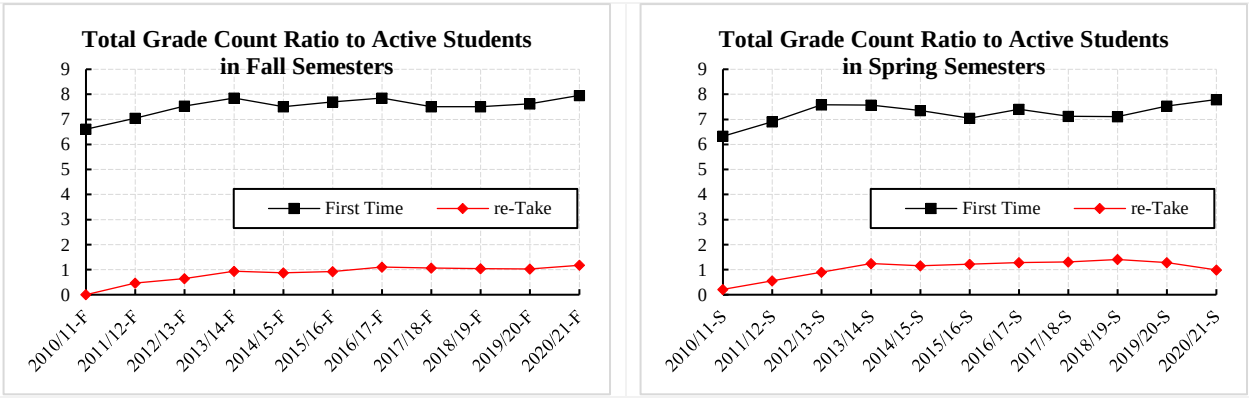

(b) The grade count ratio to active students in different semesters

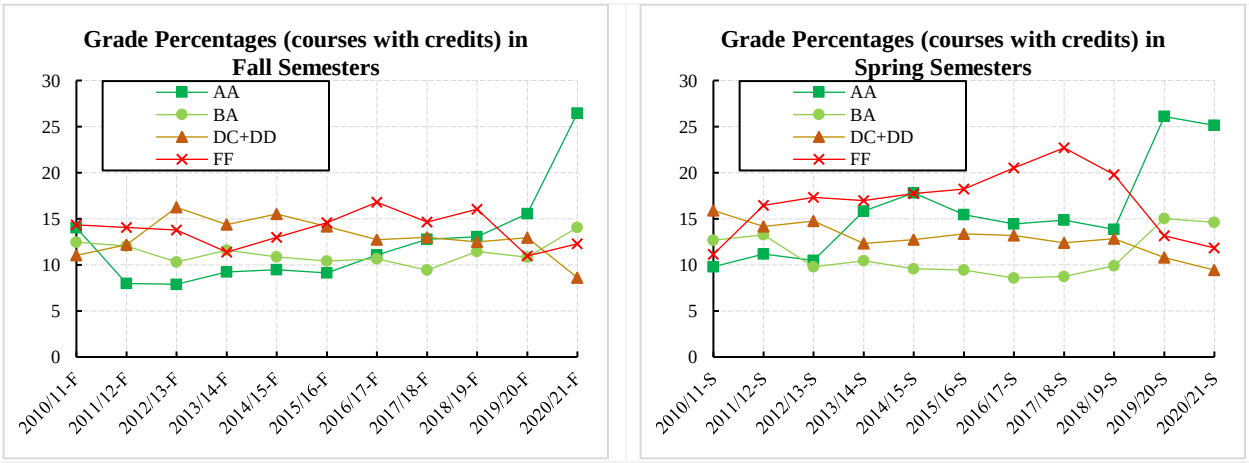

(c) Letter grade percentages in different semesters (with credits)

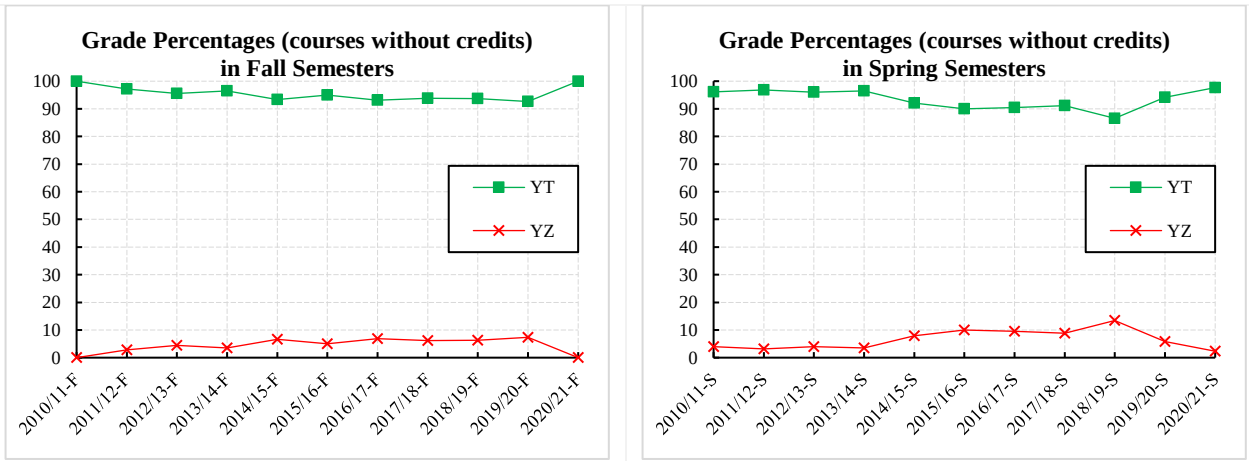

(d) Letter grade percentages in different semesters (without credits)

Fig. 4. Grade and performance statistics

IV. CONCLUSION

The Covid-19 pandemic, which has affected the world since 2020, negatively affected the whole world in many areas. Countries decided on full shutdowns and tried to keep health measures at the maximum level. Unexpected events due to Covid-19 and uncertainties about the course of the pandemic affected many organizations, especially educational institutions. Considering the complete closure, the one alternative way applied in education has been distance applications. While some universities were prepared for this compulsory transition, some were caught otherwise. In this study, the effect of Covid-19 on students from the ESOGU Computer Engineering Department was investigated by considering student activity status, success rates, and letter grades within distance education. With statistical analysis during Covid-19, an increase was observed in the number of students, while an obvious decrease was observed in the number of offered courses. This is explained by the reduction of the multiple classes (which have to be divided due to the number of students) of the same course to a single, especially for compulsory courses, with the elimination of physical class condition constraints and the increase in students' orientation to certain technical courses. Especially in the 2020/21-F period, when the pandemic started, a remarkable improvement was observed in the academic success of the students, while this situation preserved itself in the spring period as well.

All in all, these kinds of statistical findings can affect the automation and suggestion systems design powerfully. Moreover, it has been clarified that it is necessary to be prepared for compulsory transitions in advance, especially in the field of education.

Authors' Contributions

The authors' contributions to the paper are equal.

Statement of Conflicts of Interest

There is no conflict of interest between the authors.

Statement of Research and Publication Ethics

The authors declare that this study complies with Research and Publication Ethics.

REFERENCES

[1] L. Harasim, "Shift Happens: Online Education as a New Paradigm in Learning," The Internet and Higher Education, vol. 3, no. 1-2, pp. 41-61, 2000.

[2] I. E. Allen and J. Seaman, Going the Distance: Online Education in The United States, 2011. ERIC, 2011.

[3] R. Heradio, L. De La Torre, D. Galan, F. J. Cabrerizo, E. Herrera-Viedma, and S. Dormido, "Virtual and Remote Labs in Education: A Bibliometric Analysis," Computers & Education, vol. 98, pp. 14-38, 2016.

[4] C. N. Pittman and A. K. Heiselt, "Increasing accessibility: Using Universal Design principles to address disability impairments in the online learning environment," Online Journal of Distance Learning Administration, vol. 17, no. 3, 2014.

[5] T. Volery and D. Lord, "Critical Success Factors in Online Education," International Journal of Educational Management, 2000.

[6] ReliefWeb. (2021, September 8, 2021). One Year into COVID-19 Education Disruption: Where Do We Stand? Available: https://reliefweb.int/report/world/one-year-covid-19-education-disruption-where-do-we-stand

[7] B. University. (2021, September 16, 2021). Baylor's COVID-19 Resources - Online Program Status. Available: https://onlinegrad.baylor.edu/covid-19/

[8] U.S. Department of Education. (2021, September 15, 2021). Education in a Pandemic: The Disparate Impacts of COVID-19 on America's Students. Available: https://www2.ed.gov/about/offices/list/ocr/docs/20210608-impacts-of-covid19.pdf

[9] A. V. Pesha and T. A. Kamarova, "Online Education: Challenges and Opportunities for Developing Key Competencies of the 21st Century During the COVID-19 Pandemic," in Research Technologies of Pandemic Coronavirus Impact (RTCOV 2020), 2020, pp. 155-160: Atlantis Press.

[10] T. Chen, L. Peng, B. Jing, C. Wu, J. Yang, and G. Cong, "The Impact of the COVID-19 Pandemic on User Experience with Online Education Platforms in China," Sustainability, vol. 12, no. 18, p. 7329, 2020.

[11] T. Muthuprasad, S. Aiswarya, K. S. Aditya, and G. K. Jha, "Students' Perception and Preference for Online Education in India During COVID -19 Pandemic," Social Sciences & Humanities Open, vol. 3, no. 1, p. 100101, 2021.

[12] A. Arik, S. Okyay, and N. Adar, "Hybrid Course Recommendation System Design for a Real-Time Student Automation Application," European Journal of Science and Technology, no. 26, pp. 85-90, July 2021.

International Journal of Multidisciplinary Studies and Innovative Technologies

e-ISSN: 2602-4888
dergipark.org.tr/en/pub/ijmsit
Research Article

2022, 6 (1), 77 -85
DOI: 10.36287/ijmsit.6.1.77
Received: May 21, 2022; Accepted: June 27, 2022

ANTENNA TRACKER DESIGN WITH A DISCRETE LYAPUNOV STABILITY BASED CONTROLLER FOR MINI UNMANNED AERIAL VEHICLES

Mehmet Iscan*, Ali Ihsan Tas [2] Berkem Vural [3] Ali Burak Ozden [4] and Cuneyt Yilmaz[8]

[1*] *Mechatronics Engineering Department, Yildiz Technical University, Istanbul, Turkey, miscan@yildiz.edu.tr, (ORCID*: 0000-0003-2261-8218*)*

[2] *Mechatronics Engineering Department, Yildiz Technical University, Istanbul, Turkey, ihsan.tas@yildiz.edu.tr, (ORCID*: 0000-0002-4918-3587*)*

[3] Control and Automation Engineering Department, *Yildiz Technical University, Istanbul, Turkey, berkem.vural@yildiz.edu.tr, (ORCID*: 0000-0002-3891-6642)

[4] Control and Automation Engineering Department, *Yildiz Technical University, Istanbul, Turkey, burak.ozden@yildiz.edu.tr, (ORCID*: 0000-0003-4685-9825)

[5] *Mechatronics Engineering Department, Yildiz Technical University, Istanbul, Turkey, cuneyt@yildiz.edu.tr, (ORCID*: 0000-0002-4263-8411*)*

Abstract – Communication systems have recently been very important in mini unmanned aerial vehicles (UAV), which include many research subjects. Directional antennas are generally used in communication systems, and they should continuously and efficiently follow the UAVs with minimal errors. For this purpose, an "Antenna Tracker" system, which is capable of real-time autonomous orientation based on GPS data from the UAV, was designed. In the beginning, the system's 3-dimensional solid model was obtained in SOLIDWORKS™ and its dynamical model was made in MATLAB / Simulink™ environment. For controlling the system, a discrete-time model-based computed torque proportional controller, which is the state-of-the-art innovation in this study, was designed in two axes, and then its simulation studies were conducted on the STM32 board. The simulation studies showed that controlling the pan and tilt axes is sufficient for effective tracking, and the presented antenna tracker system is suitable for use in mobile ground control stations (GCS). By using a short sampling time for the controller, stable and precise antenna tracking is accomplished for a given reference path. When a 0.5 Hz sinusoidal reference signal input which is the maximum speed for any antenna tracker was used as a sample reference track, ±0.3- and ±0.6-degrees position error of pan and tilt angles were obtained, respectively. The controller can easily satisfy a smooth tracking operation with high accuracy.

Keywords *– Mini UAVs, Antenna trackers, Lyapunov stability, discrete control, UAV tracking*

Citation: Iscan M., Tas A., Vural B., Ozden A., and Yilmaz C., (2022). Antenna Tracker Design with A Discrete Lyapunov Stability Based Controller for Mini Unmanned Aerial Vehicles. International Journal of Multidisciplinary Studies and Innovative Technologies, 6(1): 77-85

I. INTRODUCTION

Unmanned Aerial Vehicles (UAV) are utilized in a vast of application goals and it continues its developing day by day. As one of these aims, namely observation, is operated for several different purposes in the civilian field, in fact, it is more frequently and importantly in the military [1] [2]. As the main factor of such systems, the directional antennas are generally used for live video streaming and telemetry transmission in Mini UAVs [3][4]. In order to avoid any interruption in the telemetry data or images which are obtained by the UAV, they are providing communication between antennas that must always be located as facing each other at a certain angle. Especially, in such systems where the Ground Control Station (GCS) is mobile, obtaining the right directions of the antennas is a serious problem [5][6]. Actually, the autonomous antenna tracking systems which are called Antenna Trackers, are working for used on military or civil UAVs that communicate with directional antennas. According to the GPS or barometer data were taken by the UAV, Antenna Trackers are positioning the antennas in the communication process to the UAV throughout the flight. It is sufficient to control the pan and tilt axes for tracking; the system rotates 360 degrees on the pan axis and 90 degrees on the tilt axis for optimum tracking [4]. Indeed, for this optimum tracking, one of the most important prerequisites is sensitive positioning with respect to the controller of the system. The most frequently used antenna tracker system in civil UAVs is ARDUPILOT that is an open-source controller [12][13]. One of the biggest advantages of this kind of controller is its compatibility with an open-source Ground Control Station interface and its wide range of documentation. However, it has some drawbacks in terms of practical and academic perspectives.

For practical considerations, it is limited by their cost. Although, its control software is free of charge, the system is designed to be conducted with an expensive controller card such as Pixhawk™ [14]. Besides, the controller of ARDUPILOT's antenna tracker has been developed specifically for servo motors which are costly comparing to common DC motors. The presently designed antenna tracker can be customized through applying open-source systems such

as Mission Planner freely, it is an obvious advantage when compared with the other expensive commercial software [15][16].

In academic perspectives, open-source software, and codes do not give a way to accomplish complicated controller design attaining high performance to track the reference UAV signal path due to the complexity of the source codes and lack of capability of the whole functions required for Lyapunov controller [17]. Apart from that the controller which is designed in this open-source libraries, the performance of the controller rules depends directly on the electronic capabilities such as analog/digital readings speed/resolutions and coding techniques such as sampling time and one cycle at processors. The continuous-time control theory does not meet these criteria for the control system in terms of the sampling period and resolution values at measurements in real-life applications [18].

When the current studies are criticized, it could be apparently seen that there is inadequacy on discrete-time modeling and controller design to sensitive position control [7][8][9][10][11].

Astari et al [7] has developed a PID controller in continuous time for such systems. However, these kinds of continuous-time models could not be realized in the real applications adequately. In real systems, the sampling rate is one of the crucial elements which has to be considered due to the process members. Besides, Riyandi et al [8] have designed a PID controller with fuzzy logic for a GPS-based antenna tracker system to increase the system quality compared to the conventional PID controllers. Although this controller achieved high accuracy and a better response than the previous ones, the fuzzy logic usage in such systems has a low implementation quality. Actually, the fuzzy logic algorithm must be developed for each unique case therefore it may not be an optimum solution. Uthman et al [9] has mentioned that a discrete control system using a PID controller is better in terms of achieved a better control on satellite angle deviation while they designed a PID controller in continuous time. Accordingly, the various research studies on the antenna tracker control systems show that general approaches constituted in continuous time, which yields less realizable systems.

Due to the whole reasons given above, the discrete-time modeling and controller design is the best approach to implement the Antenna tracker device. Otherwise, the implementation of any code with the basis of continuous one cannot be easily performed in practice.

In this study, the antenna tracker system with a Lyapunov-based proportional controller in discrete time to track the mini-UAVs has been designed. First, the mathematical model of the mechanical system is obtained. Then, a torque computed controller in discrete time based on the Lyapunov Stability Theorem is applied. Moreover, the model is reformed within the capability of the usage for any antenna tracker system, since can be modified by changing the moment of inertia and damping ratio coefficients. This makes an innovative improvement in academic manners. The system consists of a GPS-based, two-axis antenna tracker with a discrete proportional controller. The controller is embedded on an STM32 board. The deficiencies of the previous research projects were tried to be eliminated by the developed antenna tracker.

II. METHOD

A. System in General

The designed antenna tracker system has a structure that can move 360 degrees in the pan axis and 90 degrees in the tilt axis. Tracking will be carried out according to the GPS data received from the UAV. GPS will be used to measure the position of the Antenna tracker and the Inertial Measurement Unit (IMU) to measure its angle. Basically, the coordinate points of the UAV are determined by GPS and transmitted to the GCS, the antenna receives the coordinates of the UAV and transmits them to the GCS antenna position and the position of the plane. After specifying the orientation by using the angle calculation algorithm, the data is sent to the controller which triggers the drive system and the IMU gives feedback to the controller to identify the error.

B. Figures and Tables

Three major factors were taken into consideration during the design phase; the antenna should be capable to rotate in two axes freely; the cost should be competitive compared to the other trackers in the market, the system should be compact, accessible, and easy to carry by one person. To meet these requirements firstly it was decided to use 3D printed ABS part due to its effective cost, practical design, and fast production ability; it can be printed in complex parts within hours, which is much faster than the molding process or machined parts [19]. In figure 1, the view of the 3D design is given. To be simply accessible, the system will be mounted over a tripod that can be quickly detachable to ensure proper transportability to the fly zone. Also, to distribute the weight of the antenna, two bearings will be used. The system consists basically of a scaffold, two brushed DC motors, an antenna, an inertia measurement unit, a tripod, and several fasteners. SOLIDWORKS™ was used to design the two axes Antenna Tracker. The part over the tripod can rotate in the pan axis, the upper part can rotate on the tilt axis. The antenna and the tripod can be easily detached during transportation. During the realization of the system, a major challenge that had been encountered was wrapped cables around the device.

Fig. 1. 3D Design of Tracker System

C. System Modelling

As a design restriction, it is assumed that the tilt and pan axis move independently since the model is operated under low angular velocity conditions. Dynamic equations for the biaxial antenna tracker have been obtained by using Lagrangian mechanics [20]. All the related equations have

been applied to the system which was based on the earth fixed frame.

In the antenna trackers, the main mechanical concern is calculating the net moment of inertia during tracking to find the central gravity of the system. Then, the net torque which is fitted by the design requirements has been determined that were calculated as τ_{tilt} , τ_{pan} on tilt and pan axis, respectively. Basically, l distance from the center of gravity to torque applied point, J_{eq}^{tilt},J_{eq}^{pan} are the equivalent moment of inertia of the antenna tracker system, C_{eq}^{tilt},C_{eq}^{pan} are equivalent damping coefficient of antenna tracker. θ is the tilt axis and γ is the pan axis angle, and m refers to the mass of rotating part of the system. The model of pan and tilt axes are as follows:

$$\tau_{tilt} = J_{eq}^{tilt}\ddot{\theta} + C_{eq}^{tilt}\dot{\theta} + mglcos(\theta) \quad (1)$$

$$\tau_{pan} = J_{eq}^{pan}\ddot{\gamma} + C_{eq}^{pan}\dot{\gamma} \quad (2)$$

The state-space model of the system for tilt axis is as follows:

$$\dot{z}_{tilt} = \begin{bmatrix}\dot{\theta}\\ \ddot{\theta}\end{bmatrix} = \begin{bmatrix}0 & 1\\ 0 & -\frac{C_{eq}^{tilt}}{J_{eq}^{tilt}}\end{bmatrix}\begin{bmatrix}\theta\\ \dot{\theta}\end{bmatrix} + \begin{bmatrix}0\\ \frac{1}{J_{eq}^{tilt}}\end{bmatrix}(\tau_{tilt} - mgl\cos(\theta)) \quad (3)$$

Besides, the pan axis as follows:

$$\dot{z}_{pan} = \begin{bmatrix}\dot{\gamma}\\ \ddot{\gamma}\end{bmatrix} = \begin{bmatrix}0 & 1\\ 0 & -\frac{C_{eq}^{pan}}{J_{eq}^{pan}}\end{bmatrix}\begin{bmatrix}\gamma\\ \dot{\gamma}\end{bmatrix} + \begin{bmatrix}0\\ \frac{1}{J_{eq}^{pan}}\end{bmatrix}(\tau_{pan}) \quad (4)$$

To achieve a precise amount of moment of inertia as a requirement of the operation; all required variables were found by computer-aided simulations, besides the damping ratio which was defined by experimental data. Indeed, all the design parameters were shown in *the Experiment* chapter.

D. Controller Design

The key factor of the system as a decision parameter is the net torque due to the main part of the system is rotatable. Therefore, for the controller design, the computed torque control method centric model is used. Moreover, position control is used with respect to the Lyapunov-based proportional discrete controller. To attain flexibility on the sampling time during the tracking, the discrete controlling approach would be more beneficial than the other. Furthermore, using one controller parameter comes with an advantage for sake of simplicity. Thus, by changing only one parameter, the system can be modified easily [20][21][22]. In theory, there are many different controller design approaches that have a wide range such as PID, PD, PI, Fuzzy Logic, etc. In this study, the main core is the energy-based controller. So, through constituting a Lyapunov stability theorem-based proportional controller, it is obtained. Here, the main purpose is achieving the convergence to zero in the error over energy equations which gives stability condition of the system. The controller diagram is given in figure 2.

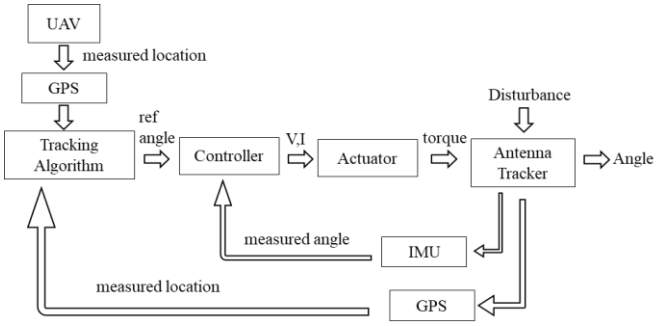

Fig. 2. The controller diagram

Basically, the coordinate of the UAV is determined by its GPS and transmitted to the ground control station. The antenna receives the coordinates of the UAV and transmits its position and the position of the plane to the ground station. After determined the orientation by using the tracking algorithm, the data is sent to the controller which triggers the actuator. The IMU gives feedback to the controller to determine the error. Finally, the system location is attained successfully by the position. This algorithm is repeated for both axes, namely the tilt and pan.

To accomplish the robust control the novel approach has been developed which is based on discrete-time controller design. Firstly, the system has been modeled mathematically, then discretization is done. Finally, an energy-based proportional controller through the Lyapunov Stability Theorem has been designed [17]. Thus, position control of the system was better than the ones whose previous studies.

The results of discretization of (1) and (2) in time are shown in equations (5) and (6), respectively:

$$\begin{aligned}\theta[k+1]\left[\frac{J_{eq}^{tilt}}{d_t^2} + \frac{C_{eq}^{tilt}}{2d_t}\right] + \theta[k]\left[\frac{-2J}{d_t^2}\right] \\ + \theta[k-1]\left[\frac{J_{eq}^{tilt}}{d_t^2} - \frac{C_{eq}^{tilt}}{2d_t}\right] \\ + mg(r+l)\cos(\theta[k-1]) \\ = \tau_{tilt}[k-1]\end{aligned} \quad (5)$$

$$\begin{aligned}\gamma[k+1]\left[\frac{J_{eq}^{pan}}{d_t^2} + \frac{C_{eq}^{pan}}{2d_t}\right] + \gamma[t]\left[\frac{-2J}{d_t^2}\right] \\ + \gamma[k-1]\left[\frac{J_{eq}^{pan}}{d_t^2}\ \frac{C_{eq}^{pan}}{2d_t}\right] \\ = \tau_{pan}[k-1]\end{aligned} \quad (6)$$

In the Lyapunov controller, the selected energy function must always be positive and its change over time must be a negative value to achieve system stability.

Selected the energy function of the system whose e[t] refers to the error of the system as follows:

$$L[e[k]] = e[k]^2 \quad (7)$$

and

$$L[e[k+1]] - L[e[k]] = e[k+1]^2 - e[k]^2 \quad (8)$$

If,

$$e[k+1] = A_e e[k] \tag{9}$$

and substitute for the equation (8):

$$L[e[k+1]] - L[e[k]] = e[k]^2(A_e^2 - 1) \tag{10}$$

It can be expressed as. So, the equality that the system must provide stability which is shown:

$$e[k]^2(A_e^2 - 1) < 0 \; so \; -1 < A_e < 1 \tag{11}$$

The error in the system is as follows:

$$e[k] = \theta_{ref}[k] - \theta[k] \tag{12}$$

and

$$e[k+1] = \theta_{ref}[k+1] - \theta[k+1] \tag{13}$$

To reach the correct results of equation (9), the controller input must be equal to one in equation 14 and equation 15 as for the tilt and pan axis, respectively, by using feedback linearization. Then, according to equation 11, the stabilization of the system can be achieved over controller parameter Ae.

$$\tau_{tilt}[k-1] = (\theta_{ref}[k+1] - A_e^{tilt}(\theta_{ref}[k] - \theta[k]) - (-\frac{\theta[k]\frac{-2J_{eq}^{tilt}}{d_t^2}}{\frac{J_{eq}^{tilt}}{d_t^2}+\frac{c_{eq}^{tilt}}{2d_t}} - \frac{\theta[k-1]\left(\frac{J_{eq}^{tilt}}{d_t^2}-\frac{c_{eq}^{tilt}}{2d_t}\right)}{\frac{J_{eq}^{tilt}}{d_t^2}+\frac{c_{eq}^{tilt}}{2d_t}} - \frac{(mg(r+l)\cos(\theta[k]))}{\frac{J_{eq}^{tilt}}{d_t^2}+\frac{c_{eq}^{tilt}}{2d_t}}))/\frac{1}{\frac{J_{eq}^{tilt}}{d_t^2}+\frac{c_{eq}^{tilt}}{2d_t}} \tag{14}$$

and

$$\tau_{pan}[k-1] = (\gamma_{ref}[k+1] - A_e^{pan}(\gamma_{ref}[k] - \gamma[k]) - (-\frac{\gamma[k]\frac{-2J_{eq.pan}}{d_t^2}}{\frac{J_{eq.pan}}{d_t^2}+\frac{C_{eq.pan}}{2d_t}} \ldots \ldots - \frac{\gamma[k-1]\left(\frac{J_{eq.pan}}{d_t^2}-\frac{C_{eq.pan}}{2d_t}\right)}{\frac{J_{eq.pan}}{d_t^2}+\frac{C_{eq.pan}}{2d_t}}))/\frac{1}{\frac{J_{eq.pan}}{d_t^2}+\frac{C_{eq.pan}}{2d_t}} \tag{15}$$

If it ranges between

$$-1 < A_e < 1 \tag{16}$$

the stable system can be obtained. As it is shown in the eq. (11), the energy of the error always converges to zero. Therefore, the system could be stable. However, the negative values of A_e can make the system stable but oscillated. Thus, in practice, A_e is taken as between 0 and 1.

E. Tracking Algorithm

To process the calculations to determine the tilt angle, knowledge of the distance between the UAV and the GCS are required. The distance as seen in figure 3, "d" can be calculated using the Spherical Law of Cosines Equations as follows:

$$\Delta\emptyset = \emptyset_2 - \emptyset_1 \tag{17}$$

$$d = cos^{-1}(sin\emptyset_1 \text{ x } sin\emptyset_2 + cos\emptyset_1 \text{ x } cos\emptyset_2 \text{ x } cos\Delta\varphi) \text{ x } R \tag{18}$$

where φ_1 is longitude of the GCS, φ_2 is longitude of the UAV, $\emptyset_1$ is latitude of the GCS, $\emptyset_2$ is altitude of the UAV and R is average radius of earth (6.371×10^6 m).

$$\Delta h = h_2 - h_1 \tag{19}$$

$$\theta = tan^{-1}\left(\frac{\Delta h}{d}\right) \tag{20}$$

h_2 is altitude of UAV, h_1 is altitude of GCS. θ is the tilt angle for antenna tracker. Thus, the required reference angles are calculated [23].

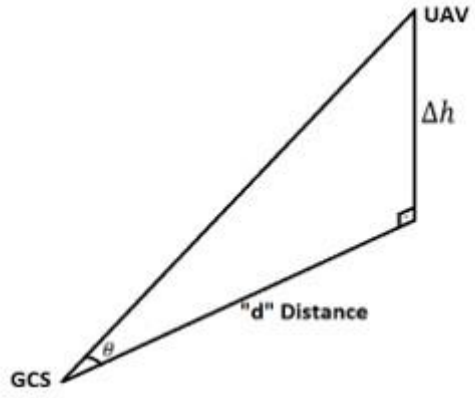

Fig. 3. Tracking angle

Table I. Design Parameters for Simulation

-	PAN AXIS	TILT AXIS
Solver Type	Centered difference approximation	Centered difference approximation
Refence Signal	$(\pi/4)\sin(2\pi ft)$ (f = 0.5)	$(\pi/3)\sin(2\pi ft)$ (f=0.5)
Torque Limit	2.5 [Nm]	2.5 [Nm]
J_{eq}	$2502.11x10^{-6}[Kgm^2]$	$3459.55\ x\ 10^{-6}\ [Kgm^2]$
C_{eq}	0.2 $[Nm/(\frac{rad}{s})]$	0.2 $[Nm/(\frac{rad}{s})]]$
m	1.17 Kg	
l	0.13 m	

III. EXPERIMENTS

The design made in SOLIDWORKSTM was transferred to MATLAB / Simulink™ environment and controlled by Lyapunov based proportional discreate controller. Relevant parameter values are given in Table 1.

Various simulations were performed at different sampling times and with different controller coefficients. The simulations conditions under which the test was performed are the coefficients with 0.1, 0.5, 0.9 for pan and tilt axis.

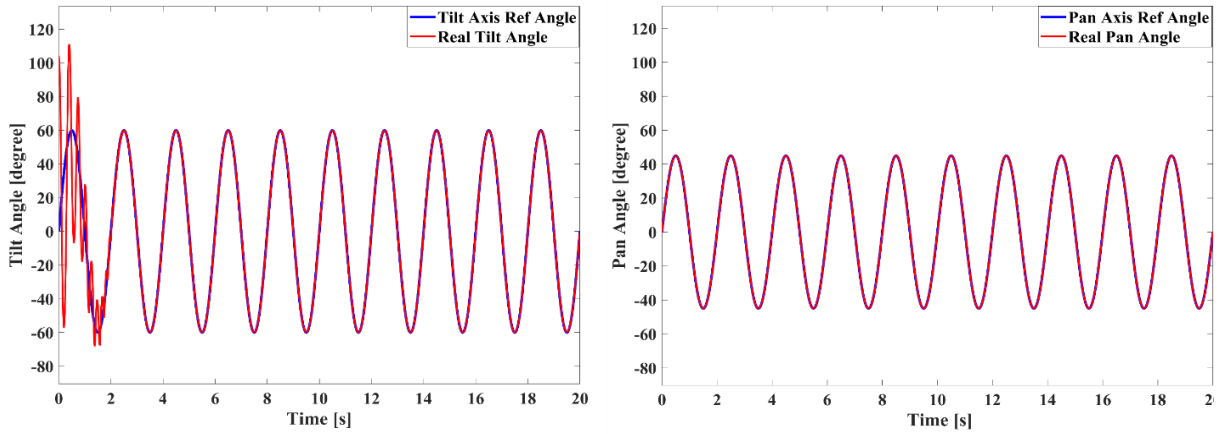

Fig.4. Pan and Tilt Axis References Tracking with 1 ms and 0.1 Controller Coefficient

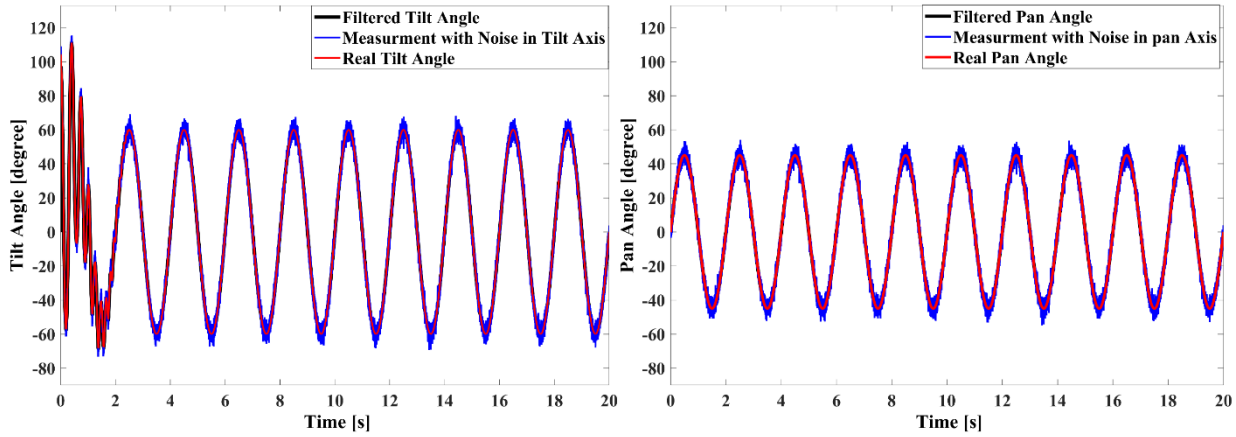

Fig. 5. Pan and Tilt Axis Kalman Filter Results with 1 ms and 0.1 Controller Coefficient

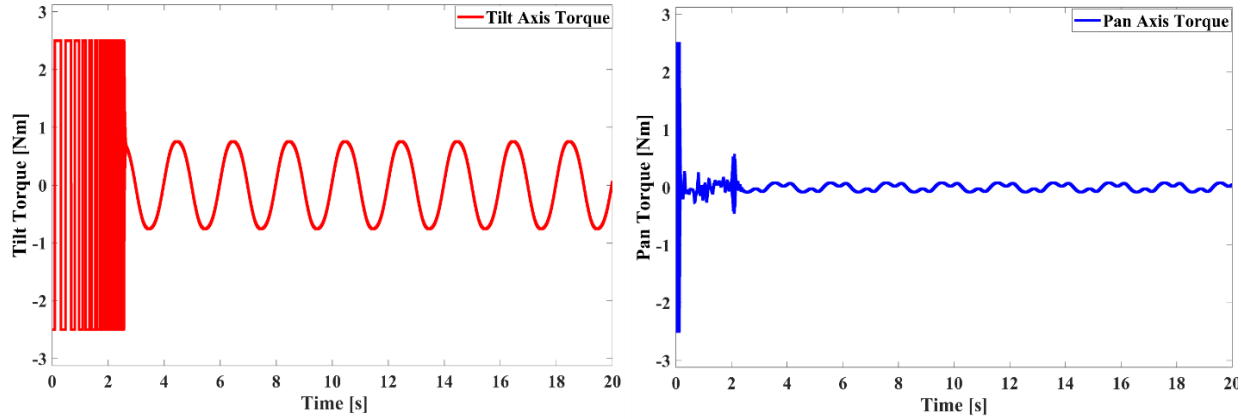

Fig. 6. Pan and Tilt Axis Controller Input with 1 ms and 0.1 Controller Coefficient

As a result of the simulations, the best result for 1 ms sampling time was obtained with a controller coefficient of 0.1 for both pan and tilt axes. Reference tracking controller input and Kalman filter performance are given with these parameters in figures 4, 5 and 6, respectively.

For the tilt axis, a 60-degree 0.5 Hz sine signal can be referenced with an error of 0.02 degrees in 1 [ms] sampling time. For the pan axis, reference tracking can be made with an error of 0.001 degrees for a 0.5 Hz sine signal of 45 degrees. As it can be seen in figure 4, in the tilt axes, the "jitter" is occurred in the beginning of the application due to limiting the torque 2.5 [Nm] as it can be shown table 1. In figure 6 the torque output of the system can be seen clearly. The similar phenomenon is observed for the other simulations of this study. In the same conditions, in a noisy measurement with a standard deviation of 5.7 degrees, the standard deviation of the measurement error for the pan axis was reduced to 0.03 degree for the pan axis and 0.25 degree for the tilt axis. To make the system follow the reference, 0.75 Nm torque is required for the tilt axis and 0.1 Nm torque is required for the pan axis.

IV. EXPERIMENTAL STUDIES AND RESULTS

The system was set up and tested as in figure 7. The system consists of an STM32F4, two 12V Geared DC motors with encoder, two motor drivers, a power supply, a tripod, an antenna, and connection elements. The feedback for the position of motors for the controller was received by the encoder.

The values in the simulation were used for the system model, except for the damping coefficient. The tests were performed for different sampling times and different controller coefficients. The tests were repeated for different damping coefficients to arrive at the actual damping coefficient of the system.

To make real tests compatible with the simulation, the system was first tested with the same values in the simulation at sampling times of 1 ms. The results are given in figure 8.

For the same test, the error graph in the pan and tilt axes is as shown in figure 8.

Fig. 7. Test System for Antenna Tracker

V. DISCUSSION

Antenna trackers are the included subsystems that are important for operational appliances. The main requirement of such systems is reaching the tracking with a proper desired path on the tilt and pan axis. However, the generic problem of such systems is possible deviations during communication of directional antennas among the other attendant ones in practice. In this case, the suggested solution in this paper has achieved success to obtain proper tracking of the reference inputs.

As the experimental results showed, the reference path has been tracked with 180 degrees/sec angular velocity within the position error ranges in 0.3 degrees and 0.6 degrees in pan and tilt axes, respectively in 1 ms sampling time. Among the previous research, it can be mostly seen that the error values have been indicated as zero degrees with respect to pan and tilt axes, since they were operated as only simulations and in continuous time cases [9][24][25][26]. However, there is also a narrow range of real-time case studies which have higher error values than this study. Nugroho & Dectaviansyah [23] showed small errors such as 5.62 degrees in the pan axis and 1.51 degrees in the tilt axis in their study. Actually, these error values are even higher than the output of our test in real-time. Also, Hancioglu et al [27] have given their test data results through several test attempts. Their output was higher than our results. Therefore, when comparing to the previous studies the controller of the system shows huge development in terms of positioning.

The performed angular velocity value is above the average for the standard applications and controlled successfully [28][29]. This made huge advantage for tracking especially during take-off and landing phases of flight. Hence the commercial problem for the UAV antenna trackers is reduced.

The controller of the system has been tested for sampling times as 1 ms. As mentioned above under the given sampling time conditions, the system showed good quality tracking with the small error values given in Results section. This benefit came with a flexibility in choosing components of the system. By the way, for the longer sampling time the position error variables are expanded. Therefore, the more sampling time is tested for the controller, the more position error is observed. In any case, the system stays in the stable ranges.

Overall, the design system archives robust control for the tasks whose high angular velocity with high sensitivity. Comparing to commercial antenna tracker systems and academic research, better stability, and less deviation in terms of positioning even if high angular velocities have been

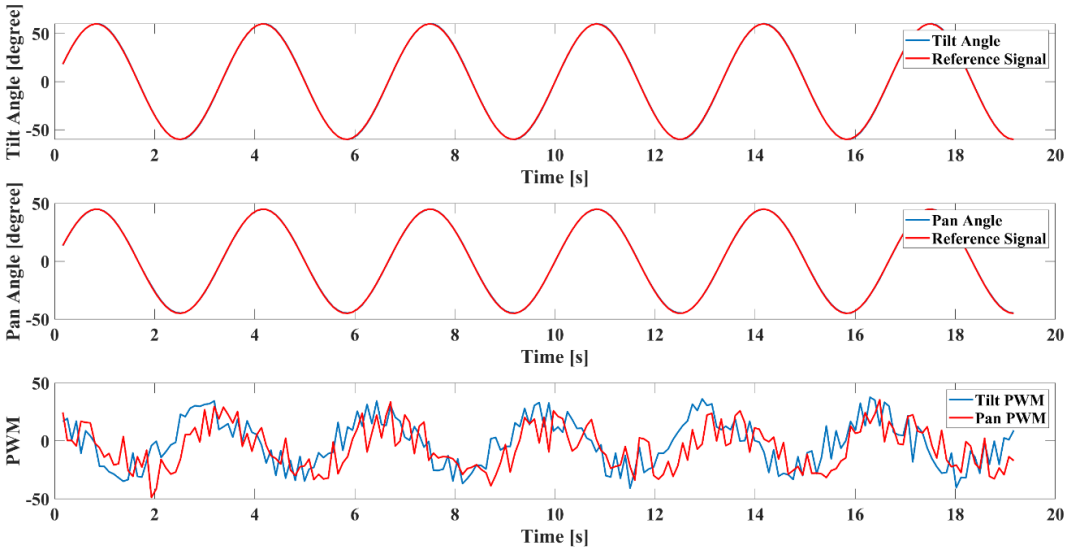

Fig.8 Pan and Tilt Axis Reference Tracking and Controller PWM Input with 1ms, 0.1 Controller Coefficient

obtained as the system superiority. Nevertheless, the vast majority of research in this field has a lack of capability of realizing with continuous-time modality; this study could show higher realizable results in terms of discrete-time controller design. This phenomenon has been proven in Xiong & Zhang's [30] study as well. As an improvement to this study, our work has accomplished the operation task well in practice.

VI. CONCLUSION

In this study, a discrete-time, the energy-based proportional controller has been presented using the Lyapunov Stability Theorem for antenna tracker systems that is suitable for mini-UAVs. From the results of the study, it can be clearly concluded that the designed controller shows high performance in terms of stability. The UAVs can be tracked within a very low range of error compared to the previous studies in the literature, specifically less than 1 rad range of position error as it mentioned before. By using a 0.5 Hz sinusoidal reference signal input that is actually very high speed for such systems, within the sample reference track; less fluctuated and more stable tracking was obtained in terms of the position of the system in comparison to the other commercial antenna trackers and related previous research. Most importantly, this study involved a brand-new design and achieved a successful discrete-time controller task in this field. By doing so, this approach fills the huge gap in antenna tracker research applications.

List of Symbols

τ	Torque [Nm]
θ	Tilt Angle [rad]
γ	Pan Angle [rad]
d	Distance [m]
d_t	Sampling time [s]
m	Mass [Kg]
J	Inertia [kgm^2]
l	Distance [m]
C	Damping Coeff. [Nm/(rad/s)]
R	Average Radius of Earth [m]
$\emptyset$	Latitude [rad]
φ	Longitude [rad]
h	Altitude [m]
e	Error [rad]
A_e	Controller Coeff. [-]
z	State Matrix
L	Energy function

References

1. Udeanu, G., Dobrescu, A. and Oltean, M., 2016, May. Unmanned aerial vehicle in military operations. In *The 18th International Conference "Scientific Research and Education in the Air Force–AFASES", Brasov, Romania* (pp. 199-205). DOI: 10.19062/2247-3173.2016.18.1.26

2. Orfanus, D., de Freitas, E.P. and Eliassen, F., 2016. Self-organization as a supporting paradigm for military UAV relay networks. IEEE Communications letters, 20(4), pp.804-807. DOI: 10.1109/LCOMM.2016.2524405

3. Dimc, F. and Magister, T., 2006, December. Mini UAV communication link systems. In Proc. ICTS (pp. 95-118).

4. Xiao, Z., Xia, P. and Xia, X.G., 2016. Enabling UAV cellular with millimeter-wave communication: Potentials and approaches. IEEE Communications Magazine, 54(5), pp.66-73. DOI: 10.1109/MCOM.2016.7470937

5. Zhao, N., Yang, X., Ren, A., Zhang, Z., Zhao, W., Hu, F., Rehman, M.U., Abbas, H. and Abolhasan, M., 2018. Antenna and propagation considerations for amateur uav monitoring. *IEEE Access*, *6*, pp.28001-28007. DOI: 10.1109/ACCESS.2018.2838062

6. Kumari, N., Kumar, R. and Bajaj, R., 2018. Energy efficient communication using reconfigurable directional antenna in MANET. *Procedia Computer Science*, *125*, pp.194-200.

7. Astari M, Rusimamto P, Rancang Bangun Sistem Pengendalian Posisi Azimut Antenna Tracker Berbasis Global Positioning System (Gps) Dengan Kendali PID, 2018, Jurnal Teknik Elektro, 7(03).

8. Sumardi, S., 2018. PlD Parameters Auto-Tuning on. *Jurnal Teknologi dan Sistem Komputer*, *6*(3), pp.122-128. DOI: https://doi.org/10.14710/jtsiskom.6.3.2018.122-128.

9. Uthman, A. and Sudin, S., 2018. Antenna azimuth position control system using PID controller & state-feedback controller approach. *International Journal of Electrical and Computer Engineering (IJECE)*, *8*(3), pp.1539-1550. DOI: 10.11591/ijece.v8i3.pp1539-1550

10. Hui, J., Xudong, Z. and Haiyu, J., 2018. Research on ship-borne UXB antenna servo system based on LQG

controller.

11. Lin, J.M., Lin, C.H. and Hu, J.N., 2017, July. Mobile robot-based antenna tracking system on RPV using intelligent neural controller. In *2017 International Conference on Machine Learning and Cybernetics (ICMLC)* (Vol. 2, pp. 633-639). IEEE. DOI: 10.1109/ICMLC.2017.8108980

12.https://ardupilot.org/

13. Ganti, Sai R, Yoohwan K. Design of low-cost onboard auto-tracking antenna for small UAS. 2015 12th International Conference on Information Technology-New Generations. IEEE, 2015. DOI: 10.1109/ITNG.2015.50

14. Changoluisa, I., Barzallo, J., Pantoja, J., Cayo, S., Navarro-Méndez, D.V. and Cruz, P.J., 2019, October. A Portable UAV Tracking System for Communications and Video Transmission. In 2019 IEEE 4th Colombian Conference on Automatic Control (CCAC) (pp. 1-6). IEEE. DOI: 10.1109/CCAC.2019.8921053

15. Peterson, A., 2019. Benthic biodiversity in the north-eastern Baltic Sea: mapping methods, spatial patterns, and relations to environmental gradients.

16. Firmansyah, R., Mustofa, M.B.A., Prasetya, M.E. and Saputra, P.P.S., 2020, November. Weather Monitoring Telemetry System Based on Arduino Pro Mini With Antenna Tracker Using Transceiver Module SV651 and SV611. In International Joint Conference on Science and Engineering (IJCSE 2020) (pp. 322-330). Atlantis Press.

17. LEWIS, F.L., 2004. NEIL MUNRO, PH. D., D. SC.

18. Podržaj, P., 2018, February. Contionuous VS discrete PID controller. In 2018 IEEE 9th International Conference on Mechanical and Intelligent Manufacturing Technologies (ICMIMT) (pp. 177-181). IEEE.

19. Morón C et al. New prototype of photovoltaic solar tracker based on arduino. *Energies* 10.9 (2017): 1298. DOI https://doi.org/10.3390/en10091298

20. Lewis, F.L., Dawson, D.M. and Abdallah, C.T., 2003. *Robot manipulator control: theory and practice*. CRC Press.

21. Ogata, K., 1995. *Discrete-time control systems*. Prentice-Hall, Inc..

22. Kuo, B.C. and Golnaraghi, M.F., 1995. *Automatic control systems* (Vol. 9). Englewood Cliffs, NJ: Prentice-Hall.

23. Nugroho, G. and Dectaviansyah, D., 2018. Design, manufacture and performance analysis of an automatic antenna tracker for an unmanned aerial vehicle (UAV). Journal of Mechatronics, Electrical Power, and Vehicular Technology, 9(1), pp.32-40. DOI 10.14203/j.mev.2018.v9.32-40

24. Ajiboye, A.T., Ajayi, A.R. and Ayinla, S.L., 2019. Effects of PID Controller on Performance of Dish Antenna Position Control for Distributed Mobile Telemedicine Nodes. Arid Zone Journal of Engineering, Technology and Environment, 15(2), pp.304-313.

25. Temelkovskia, B. and Achkoskia, J., 2014. Modeling and simulation of antenna azimuth position control system. International Journal of Multidisciplinary and Current Research, 4.

26. Romsai, W., Nawikavatan, A., Lurang, K. and Puangdownreong, D., 2021, May. Optimal PID Controller Design for Antenna Azimuth Position Control System by Lévy-Flight Intensified Current Search Algorithm. In 2021 18th International Conference on Electrical Engineering/Electronics, Computer, Telecommunications and Information Technology (ECTI-CON) (pp. 858-861). IEEE. DOI: 10.1109/ECTI-CON51831.2021.9454731

27. Hancioglu, O.K., Celik, M. and Tumerdem, U., 2018, May. Kinematics and tracking control of a four axis antenna for Satcom on the Move. In *2018 International Power Electronics Conference (IPEC-Niigata 2018-ECCE Asia)* (pp. 1680-1686). IEEE. DOI: 10.23919/IPEC.2018.8507963

28. Díaz, D.F.M., Montilla, M.E.R. and Suddarth, S., 2011, October. Active tracking position antenna base: A low cost approximation with servo gimbals. In IX Latin American Robotics Symposium and IEEE Colombian Conference on Automatic Control,

2011 IEEE (pp. 1-6). IEEE. DOI: 10.1109/LARC.2011.6086855

29. Chen, Z., Yin, D., Chen, D., Pan, M. and Lai, J., 2017, December. WiFi-based UAV Communication and Monitoring System in Regional Inspection. In 2017 International Conference on Computer Technology, Electronics and Communication (ICCTEC) (pp. 1395-1401). IEEE. DOI: 10.1109/ICCTEC.2017.00305

30. Xiong, J.J. and Zhang, G., 2016. Discrete-time sliding mode control for a quadrotor UAV. *Optik*, *127*(8), pp.3718-3722. DOI https://doi.org/10.1016/j.ijleo.2016.01.010

International Journal of Multidisciplinary Studies and Innovative Technologies

e-ISSN: 2602-4888
dergipark.org.tr/en/pub/ijmsit
Research Article

2022, 6 (1), 86-90
DOI: DOI: 10.36287/ijmsit.6.1.86
Received: May 23, 2022; Accepted: June 28, 2022

Machine Learning for E-triage

Şebnem Bora[1], Aylin Kantarcı[2], Arife Erdoğan[3], Burak Beynek[4*], Bita Kheibari[5], Vedat Evren[6], Mümin Alper Erdoğan[7], Fulya Kavak[8], Fatmanur Afyoncu[9], Cansu Eryaz[10], Hayriye Gönüllü[11]

[1]*Computer Engineering, Ege University, Izmir, Turkey, (sebnem.bora@ege.edu.tr) (ORCID: 0000-0003-0111-4635)*
[2]*Computer Engineering, Ege University, Izmir, Turkey, (aylin.kantarci@ege.edu.tr) (ORCID: 0000-0001-7019-1613)*
[3]*Faculty of Medicine, Bakırçay University, Izmir, Turkey, (arife.erdogan@yahoo.com) (ORCID: 0000-0003-2488-2012)*
[4*]*Software Engineering, Kirklareli University, Kirklareli, Turkey, (burakbeynek@klu.edu.tr) (ORCID: 0000-0003-3395-0451)*
[5]*Computer Engineering, Ege University, Izmir, Turkey, (bita.kheibari@gmail.com) (ORCID: 0000-0002-1930-2311)*
[6]*Faculty of Medicine, Ege University, Izmir, Turkey, (vedat.evren@ege.edu.tr) (ORCID: 0000-0003-0274-0427)*
[7]*Faculty of Medicine, Izmir Katip Celebi University, Izmir, Turkey, (muminalper.erdogan@ikcu.edu.tr) (ORCID: 0000-0003-0048-444X)*
[8]*Computer Engineering, Ege University, Izmir, Turkey, (fulya-kavak@outlook.com) (ORCID: 0000-0002-1938-9293)*
[9]*Computer Engineering, Ege University, Izmir, Turkey, (fatmanur.afyoncu@gmail.com) (ORCID: 0000-0002-6580-8735)*
[10]*Faculty of Medicine, Bakırçay University, Izmir, Turkey, (cansu.eryaz@bakircay.edu.tr) (ORCID: 0000-0002-7246-8847)*
[11]*Faculty of Medicine, Bakırçay University, Izmir, Turkey, (hayriye.gonullu@bakircay.edu.tr) (ORCID: 0000-0002-9587-6261)*

Abstract – Due to the rising number of visits to emergency departments all around the world and the importance of emergency departments in hospitals, the accurate and timely evaluation of a patient in the emergency section is of great importance. In this regard, the correct triage of the emergency department also requires a high level of priority and sensitivity. Correct and timely triage of patients is vital to effective performance in the emergency department, and if the inappropriate level of triage is chosen, errors in patients' triage will have serious consequences. It can be difficult for medical staff to assess patients' priorities at times, therefore offering an intelligent method will be pivotal for both increasing the accuracy of patients' priorities and decreasing the waiting time for emergency patients. In this study, we evaluate the machine learning algorithms in triage procedure. Our experiments show that Random Forest approach outperforms the others in e-triage.

Keywords *– Triage, Machine Learning, Emergency Department, Random Forest, Support Vector Machine, Decision Trees, Kth Nearest Neighbor*

Citation: Bora et.al., (2022). Machine Learning for E-triage. International Journal of Multidisciplinary Studies and Innovative Technologies, 6(1): 86-90.

I. INTRODUCTION

The number of people who visits an emergency service in our country and in the world is constantly increasing. Increasing patient volume may lead to the inability to treat in a timely manner for patients who need emergency health care. Therefore, it is important to distinguish between emergency patients and non-emergency patients and determine the treatment priority of the patients. The method that is used for this purpose is called triage [1].

Each country has its own triage system and a triage decision is made by the authorized health personnel at the time of application. In our country, the color-coding determined by the Ministry of Health is applied for the triage [2].

- "*Category 1 (red): Among the patients examined in the main red code, the ones who are unconscious or with no airway safety, respiration and circulation risks will be taken to the resuscitation room immediately.*
- *Category 2 (yellow): Patients examined in this category should be taken directly to the relevant diagnosis/treatment area, with the knowledge of the physician responsible for triage.*
- *Category 3 (green): Patients in this category should be examined in the green area in the emergency department."*

Triage enables the segregation of critically ill patients and thus determines what needs to be done for emergency care. In the patient care area, patient sequence and timing issues are regulated and the decision maker is guided on resource use. Therefore, in crowded emergency rooms, it is important to perform the right triage to quickly distinguish and prioritize those with critical conditions from those with lesser emergencies [3].

Although it seems simple, triage is complex in practice as it relies on limited patient knowledge, time pressure, various medical conditions, and a high degree of intuition and staff experience. Consequently, the predicted clinical course (i.e., triage) is unclear for the majority of emergency room patients. It can differ greatly depending on the assessment of the person performing the triage and poorly distinguishes the various patient groups despite the aim of the triage. The inability of the personnel without adequate training to distinguish this situation creates safety risks for critically ill patients, and the unnecessary use of emergency resources due to over triage of patients, whose risk levels are not clear,

causes a decrease in efficiency. Patient safety problems in crowded emergency departments, limitations in applying emergency triage standards, and assessing the need for accurate risk necessitated the development of an electronic triage system using machine learning algorithms. Machine learning acquires patterns in data with a series of computational methods [4].

There are several studies on triage and machine learning in the literature. In the literature studies, triage systems based on machine learning have been implemented on data groups obtained according to different standards in the emergency services of different countries. In [5], Levin et.al. classified emergency department applications with random forest trees and the results were compared with the ESI (Emergency Severity Index). Choi et al. performed a classification using logistic regression, random forest, and XGBOOST with the help of the KTAS system valid in Korea [6]. Bong et al. differentiated high-risk patients from others with the help of deep learning [7]. Kwon et al. used a deep learning method, a multilayer perception, for a retrospective observational study using data from the Korea National Emergency Service Information System (NEDIS), which collects data on all emergency department admissions in real-time [8]. In another study focusing on SVM and KNN, which are machine learning methods, it was aimed at helping doctors identify and treat diabetic diseases. It was concluded that improvements in classification accuracy help machine learning models achieve better results. In addition, it was concluded that the accuracy of the current system is less than 70%, and therefore it was recommended to use a combination of classifiers known as the hybrid approach. The hybrid approach combines the benefits of two or more techniques. It was found that SVM and KNN provide 75.75% accuracy vs. 80% accuracy when using ADA Boost. Therefore, it was concluded that Adaboost was the best option among all classifiers [9].

In this study, with the help of the triage standards of the Ministry of Health of the Republic of Turkey, the methods of machine learning-based triage has been examined. Thanks to the e-triage software developed for this, it is aimed to correctly guide the patients by making correct predictions and right decisions in a short time. In literature studies, triage data were collected according to different standards and classified by different methods; however, there is no e-triage software for the triage process applied in our country.

The Materials and Methods that we used in our study are introduced in the next session. In Chapter 3, the findings of our study are shared. In the last section, the results are discussed.

II. MATERIALS AND METHOD

A. Data set

The data set used in our study was prepared by retrospective sampling from the records of patients who applied to the Izmir Cigli Training and Research Hospital, emergency service. Complaints, vital signs, and basic demographic information of each patient at the time of admission to the emergency department were recorded in the table. When the patients' admission complaints are handled separately, many categories would be formed which could complicate the analysis. For this reason, patients were grouped according to their complaints as much as possible. For example, all extremity traumas that did not affect vital organs and did not involve blood loss were included in the same category.

B. Machine Learning methods used in this study:

Support Vector Machine (SVM): SVM is a classification algorithm that is easy to manage and use. It can be used for purposes of classification and regression. In this algorithm, each point that is a data item is plotted in a dimensional space, also known as the n-dimensional plane, where 'N' represents the number of features of the data. Classification is based on differentiation in classes, where these classes are dataset points located on different planes.

SVM is a very popular research area in machine learning, validated in experiments and successfully put to use across a range of fields. However, traditional SVM is mainly used to solve supervised learning problems, i.e. it handles large amounts of unlabeled data that is too time-consuming to label in real life when it needs to label sample data to train classifiers. This has contributed to taking machine learning to a new level. A study investigated the properties of SVM and searched for a new way to improve the performance of classifiers, a practical approach to classify a small number of labeled samples and a large number of unlabeled samples, and consequently an algorithm was developed [10].

SVM is a kind of method in which the nonlinear problem in low-dimensional space is mapped to a high-dimensional space so that a simple linear classification technique can be considered. SVM is suitable for small sample learning [11].

Kth Nearest Neighbor (KNN): KNN algorithm is an algorithm by which the proximity of the new individual to be classified to k times of the previous individuals is checked [12]. During classification, test samples are compared with each other using training samples. Euclidean distance is used for neighborhood distance. Estimates are based on a majority vote of neighboring samples. Care should be taken as it tends to overfit high k values [13].

Decision Trees: Decision trees not only show decisions, but they also contain explanations of decisions. The training process that creates the decision tree is inductive. The procedure for constructing a decision tree from a set of training objects is called tree induction. The tree induction method is one of the most common methods for self-knowledge discovery. It serves to discover tree-like patterns that can be used for purposes of classification or prediction.

Decision trees try to find the best order to predict the target by performing a variety of tests during knowledge discovery. Each test creates branches in the decision tree, and these branches cause other tests to occur. This continues until the test process ends on a leaf node. The path from the root to the target leaf is called the “rule” that classifies the target. The rules reflect the “if-then” pattern [14].

Random Forest: Random forest algorithm, which is a supervised learning algorithm, is used with classification and regression tasks. The random forest algorithm creates multiple decision trees and combines them to obtain a more accurate and stable prediction. The approach, which combines several random decision trees and averages their predictions, performs better in environments where the number of variables is much larger than the number of observations [15].

Random forest is used in many fields such as banking, commerce, health. In the healthcare field, it is used to identify the right combination of ingredients in medicine as well as to identify diseases and analyze the patient's medical history using a patient's medical records [16].

The random forest classifier consists of a combination of tree classifiers in which each classifier is generated using a random vector that is sampled independently of the input vector with each tree putting in their one unit vote for the most popular class to classify an input vector. The design of a decision tree requires the selection of an attribute selection measure and a pruning method. There are many approaches to the selection of attributes used for decision tree extraction, and most approaches directly assign a quality measure to the attribute. The most frequently used attribute selection measures in decision tree induction are the Information Gain Ratio [17] and the Gini Index [18]. The random forest classifier uses the Gini Index as an attribute selection standard, measuring the purity of an attribute relative to classes.

These overgrown trees are not pruned when a tree expands into maximum depth on new training data using a combination of features. This is one of the major advantages of the random forest classifier over other decision tree methods such as that proposed by Quinlan [17]. Studies suggest that the selection of pruning methods, not attribute selection measures, affects the performance of tree-based classifiers [19-20]. In [18] Breiman argues that as the number of trees increases, the generalization error always converges even without pruning the tree, and overfitting is not a problem due to the Strong Law of Large Numbers. The number of attributes used at each node to build a tree and the number of trees to grow is two user-defined parameters required to generate a random forest classifier. In each node, only the selected attributes are searched for the best split. Thus, the random forest classifier consists of N trees; where N is the number of trees to grow and this can be any user defined value. To classify a new dataset, each state of the datasets is transferred to each of the N trees. In this case, the forest chooses a class with the highest number of N votes [20].

III. RESULTS

The data set is classified into three triage emergency categories. For classification SVM, KNN, Decision Tree and Random Forest classification algorithms were used. All algorithms tested for accuracy with tenfold cross validation. Cross validation is a method applied to a model and a dataset to estimate out-of-sample error. When a model is fitted to a data set, the aim is to minimize the loss function. This most often produces overfitting training or overly optimistic results. In k-fold cross validation, the data set split in to k equal parts. In each iteration, a single part is used as test data while k-1 parts used as training data. This procedure generates k different trained model that tested with different testing data. K=10 is the most widely used cross validation. This is known as tenfold cross validation. The results are shown in Table 1.

Table 1. Tenfold Cross Validation Accuracy Score

Alg.	SVM	KNN	DT	RF
F1	0.7	0.79	0.76	0.74
F2	0.74	0.84	0.86	0.76
F3	0.89	0.86	0.76	0.79
F4	0.81	0.7	0.84	0.84
F5	0.76	0.84	0.79	0.92
F6	0.82	0.87	0.66	0.84
F7	0.68	0.71	0.84	0.95
F8	0.87	0.79	0.86	0.89
F9	0.92	0.76	0.78	0.73
F10	0.82	0.84	0.68	0.78
Avg.	0.80	0.80	0.78	0.82

As we can see in the results, all of the four algorithms scores are close but Random Forest Algorithm yields the best rates. In Figures 1, 2, 3 & 4, results of confusion matrixes of each algorithms for a single fold are given. After the analysis of these tables, data of triage emergency level 1 has the most false-positive and false-negative results.

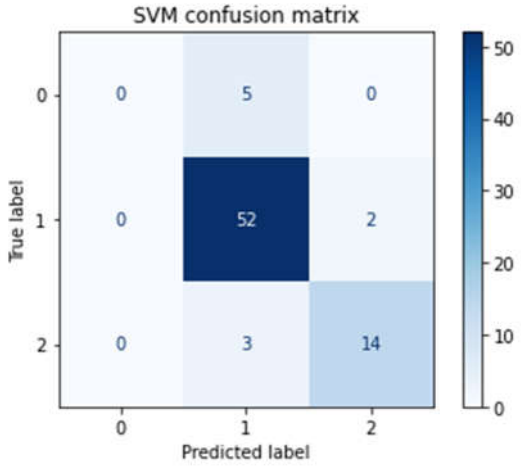

Fig. 1. SVM Confusion Matrix

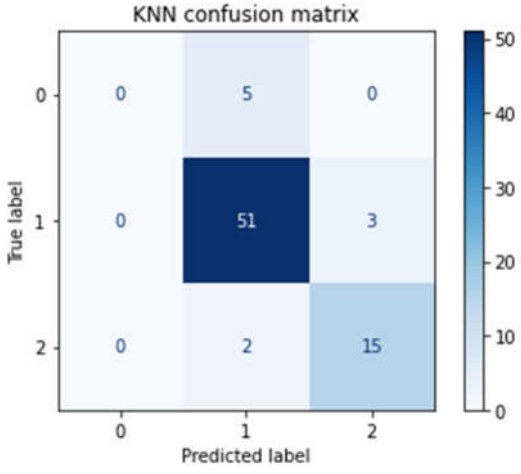

Fig. 2. KNN Confusion Matrix

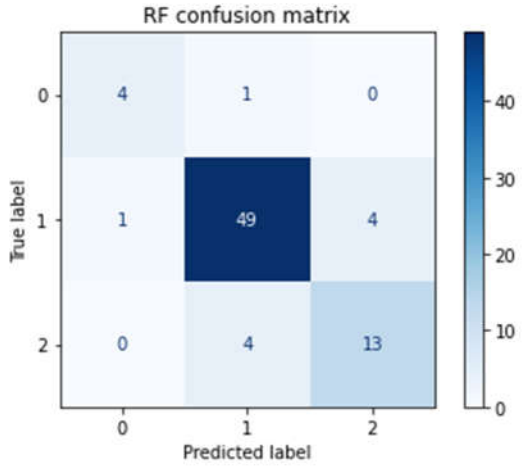

Fig. 3. Random Forest Confusion Matrix

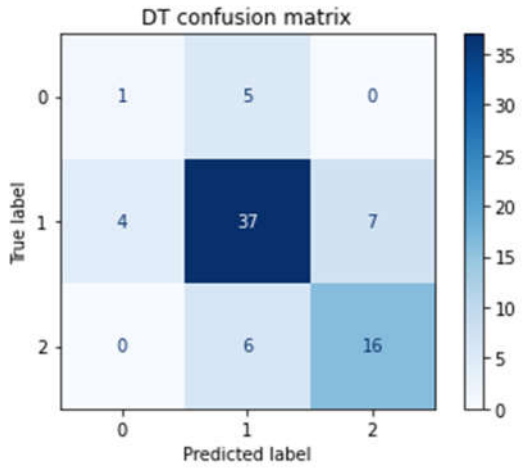

Fig. 4. Decision Tree Confusion Matrix

IV. DISCUSSION

With help of the confusion matrixes, the triage data seems to have a lot of overlapping data. This means that some of the complaints are in a gray area that can be both level 0 and 1 or both level 1 and 2. This can also indicate that some of the targets in this data set might be wrongly labeled. Both of these arguments have its own validating points. Thinking about the emergency service of hospitals, that can have around 1000 patients per day, there have to be mistakes and misinformation.

V. CONCLUSION

The triage, which is the initial evaluation of a patient at the time of admission to the emergency room, determines the urgency of the situation and the priority of treatment, which could draw the line between life and death. In this important decision process, many factors, such as proficiency of the healthcare provider, motivation, and the number of patients at a given time can affect the success. This particular topic is especially important since erroneous decisions during triage could result in increased morbidity or even death. Absolute consistency in triage is not possible because of the human factor. It is predicted that artificial intelligence will increase this consistency when sufficient data is provided; therefore, it will be increasingly used in emergency triage. The results we obtained in this preliminary study have played a decisive role in determining the methodologies we will use both for the acquisition of patient data and for learning algorithms.

Our study shows that Random Forest Algorithm has better results in classifying the triage data. The results are promising for better results. With the collection of more local data, a more detailed analysis will be provided and it will be possible to use methods that require a large amount of data such as deep learning. In future studies, in addition to the triage area, the probability of patients being hospitalized, discharged or sent to intensive care after the emergency department can be estimated.

Authors' Contributions

The authors' contributions to the paper are equal.

Statement of Conflicts of Interest

There is no conflict of interest between the authors.

Statement of Research and Publication Ethics

The authors declare that this study complies with Research and Publication Ethics

REFERENCES

[1] M. Oberlin, E. Andr`es, M. Behr, S Kepka, L. Borgne, P., Bilbault, , "Emergency overcrowding and hospital organization: Causes and solutions", *La Revue de Médecine Interne*, vol. 41(10),pp. 693-699, 2020.

[2] Ministry of Health of the Republic of Turkey. "Yataklı Sağlık Tesislerinde Acil Servis Hizmetlerinin Uygulama Usul Ve Esasları Hakkında Teblig". https://www.saglik.gov.tr/TR,11321/yatakli-saglik-tesislerinde-acil-servis-hizmetlerinin-uygulama-usul-ve-esaslari-hakkinda-teblig.html, Access date: 22 April 2022

[3] H. M. Buschorn, T. D. Strout, J. M. Sholl, M. R. Baumann and G. Junction, "Emergency Medical Services Triage Using the Emergency Severity Index: Is it Reliable and Valid?", *Journal of Emergency Nursing, vol. 39(5), pp. 55-63, 2013.*

[4] M. Christ, F. Grossmann, D. Winter,, R. Bingisser and E. Platz "Modern triage in the emergency department", *Deutsches Ärzteblatt International*, vol. 107(50), pp. 892, 2010.

[5] S. Levin, M. Toerper, E. Hamrock, J. S. Hinson, S. Barnes, A. Dugas, B. Linton, T. Kirscj and G. Kelen "Machine Learning based electronic triage more accurately differentiates patients with respect to clinicaloutcomes compared with the emergency severity index", 71(5*), Annals of Emergency Medicine*, pp. 565-574, 2018.

[6] A. W. Choi, T. Ko K.J. Hong and K. H. Kim,."Machine learning-based prediction of the Korean triage and acuity scale level in emergency department patients", *Healthcare Informatics Research*, vol. 25(4), pp. 305-312, 2019.

[7] S. Bong, L. H. Kim, H. Kim, C. Kang, S.H. Lee, J. H. Jeong, S. C. Kim, Y. J Park. and D. Lim, "Emergency department triageearly warning score (TWERS) predicts in-hospital mortality in the emergency department", *The American Journal of Emergency Medicine*, vol. 38(2) , pp. 203-210,2020.

[8] J. M. Kwon, Y. Lee, S. Lee, H. Park, J. Park, "Validation of deep learning based triage and acquity score using a large national dataset", *PLoS One*,vol. 13(10), 2018.

[9] M. K. Patil, , S. D. Sawarkar and, M. S. Narwane, "Designing a model to detect diabetes using machine learning", *Int. J. Eng. Res. Technol*, 8(11), 333-340,2019.

[10] L. Cunhe and W. Chenggang,"A new semi-supervised support vector machine learning algorithm based on active learning", 2nd International Conference on Future Computer and Communication, pp. 638-641, 2010.

[11] V. Vapnik, The Nature of Statistical Learning Theory. New York:Springer-verlag, 2000.
[12] T. Cover and P. Hart, "Nearest neighbor pattern classification", *IEEE transactions on information theory*, vol. 13(1),pp. 21-27, 1967
[13] T. Hastie, R. Tibshirani and J. H. Friedman, The elements of statistical learning: data mining, inference, and prediction, New York Springer, 2009.
[14] Bounsaythip, C., Rinta-Runsala, E. 2001. "Overview of data mining for customer behavior modeling", VTT Information Tech. Rep., vol 1, pp.1-53, 2001.
[15] G. Biau and E. Scornet, "A random forest guided tour" , *Test*, vol 25(2), pp. 197-227, 2016.
[16] S. Raschka, Python Machine Learning.UK: Pack Publishing, 2015.
[17] J. R. Quinlan , *C4.5 Programs for Machine Learning,* USA, Morgan Kauffman, 1993
[18] L. Breiman, "Random Forests", *Machine Learning*, vol. 45, pp. 5-32,Springer,2001.
[19] J. Mingers, "An empirical comparison of pruning methods for decision tree induction", Machine Learning, vol. 4, pp. 227-243, 1989.
[20] M. Pal, "Random forest classifier for remote sensing classification*", International journal of remote sensing*, *26*(1), 217-222, 2005.

International Journal of Multidisciplinary Studies and Innovative Technologies

e-ISSN: 2602-4888
dergipark.org.tr/en/pub/ijmsit
Research Article

2022, 6 (1), 91-96
DOI: 10.36287/ijmsit.6.1.91
Received: June 1, 2022; Accepted: July 2, 2022

2-(2- İyodofenil)isoindolin-1,3-dion) Molekülünün Hesaplamalı Kimya Yöntemiyle Yapısal Analizi

Gonca Özdemir Tarı[1*] ve Güneş Demirtaş [2]

[1*]*Vezirköprü Meslek Yüksekokulu, Ondokuz Mayıs Üniversitesi, Samsun, Türkiye, (gozdemir@omu.edu.tr)(ORCİD:0000-0001-5919-1778)*
[2]*Fen Edebiyat Fakültesi Fizik Bölümü, Ondokuz Mayıs Üniversitesi, Samsun, Türkiye (gunesd@ou.edu.tr)(ORCİD:0000-0001-9953-4026)*

Özet– Bu çalışmanın amacı daha önce yapı çözümü x-ışını kırınımı ile gerçekleştirilmiş olan 2-(2-iyodofenil)isoindolin-1,3-dion, $C_{14}H_8INO_2$ [1], molekülünün hesaplamalı kimya yöntemiyle yeniden incelenmesini kapsamaktadır. Molekülün teorik hesaplamaları Yoğunluk Fonksiyoneli Kuramı (YFK) ve Lee-Yang-Par, korelasyon enerjili 3 parametreli Becke karma modeli olan B3LYP yöntemi ve 6-311++G(d,p) temel baz seti kullanılarak yapılmıştır. Molekülün sınır orbitalleri ve bunlardan türetilmiş parametreler, Mulliken ve doğal yük analizleri (NPA), Moleküler Elektrostatik Potansiyel (MEP) haritaları belirlenmiştir. İlave olarak moleküle ait Hirsfeld Yüzey analizi yapılarak molekülün elektrofilik ve nükleofilik bölgeleri belirlenmiştir.

Keywords – Hirsfeld Yüzey Analizi, Hesaplamalı Kimya, Yoğunluk Fonksiyonel Kuramı,

Atıf: Özdemir Tarı, Gonca, Demirtaş, Güneş. (2022). 2-(2- İyodofenil)isoindolin-1,3-dion) Molekülünün Hesaplamalı Kimya Yöntemiyle Yapısal Analizi. International Journal of Multidisciplinary Studies and Innovative Technologies, 6(1): 91-96.

Structural Analysis Computational Chemistry Method of 2-(2-Iodophenyl)isoindoline-1,3-dione

ABSTRACT: The aim of this study includes the re-examination of the molecule of 2-(2-iodophenyl)isoindolin-1,3-dione, $C_{14}H_8INO_2$ [1], whose structure solution was carried out by x-ray diffraction, by computational chemistry method. Theoretical calculations of the molecule were made using Density Functional Theory (DFT) and Lee-Yang-Par, the B3LYP method, which is a 3-parameter Becke mixed model with correlation energy, and the 6-311++G(d,p) fundamental basis set. The boundary orbitals of the molecule and their derived parameters, Mulliken and Natural Charge Analysis (NPA), Molecular Electrostatic Potential (MEP) maps were determined. In addition, the electrophilic and nucleophilic regions of the molecule were determined by performing Hirsfeld Surface analysis of the molecule.

Keywords: Hirsfeld Surface Analysis, Computational Chemistry, Density Functional Theory.

I. GIRIŞ

Ftalimid türevi moleküller özellikle biyolojik aktivitelerinden dolayı, antikolvülsan, antiinflamatuvar, antimikrobiyal, antitümör gibi geniş bir medikal uygulama ağına sahip olduğu için araştırmalarda öncelikli ve önemli bir role sahiptir [2-7]. Yapısal analizi x-ışınları tarafından aydınlatılmış olan 2-(2-iyodofenil)isoindolin-1,3-dion, $C_{14}H_8INO_2$ [1], molekülünün teorik hesaplamaları için Yoğunluk Fonksiyoneli Kuramı (YFK)/B3LYP yöntemi ve 6-311++(d,p) temel baz seti olarak kullanılmıştır. Hesaplama sürecinde kullanılan yöntemler belirlenirken benzer moleküllere uygulanan seviyelere bakılarak bir literatür araştırması yapılmıştır. Bu molekül gruplarında çok yaygın şekilde kullanılan YFK/B3LYP/6-311++G(d,p) yönteminden elde edilen verilerin deneysel verilerle [1] oldukça uyumlu olduğu gözlenmiştir. Hesaplamalı kimya yöntemi bu şekildeki organik bileşiklerin yapısal ve elektronik özelliklerinin belirlenmesinde son yıllarda yaygın şekilde kullanılmaktadır.

Böylelikle hem deneysel verileri desteklemek hem de deneysel yöntemlerle elde edilemeyen ilave bilgilere ulaşmak için araştırmacıların tercih ettiği yöntemler arasında yerini almaktadır. Bu yöntemler sayesinde moleküllerin geometrik parametreleri, sınır orbitalleri ve sahip oldukları enerji düzeyleri ve bunlardan türetilen kimyasal parametreler hesaplanabilmektedir.

II. MATERYAL VE METOT

Çok elektronlu sistemlerin dalga fonksiyonlarının matematiksel olarak çözülebilmesi ve bunun yorumlanabilmesi ilkesine dayalı olarak çalışan hesaplamalı kimya sayesinde deneysel olarak ulaşılması mümkün olmayan kimyasal özelliklere ulaşılabilmektedir.

Daha önce sentezi gerçekleşmiş ve yapısı x-ışınları kırınımı yöntemiyle aydınlatılan [1] molekülün teorik hesaplamaları için işlemcisi yüksek yeni nesil kişisel bilgisayarlar kullanılmıştır. Tüm hesaplamalar Gaussian 03W [8] programı kullanılarak YFK'nın Lee-Yang-Par korelasyon enerjili 3 parametreli Becke karma modeli olan B3LYP yöntemi ile 6-311++G(d,p) temel baz seti kullanılarak yapılmıştır. Elde edilen geometrik parametrelerin deneysel değerlerle uyumlu olduğu görüldükten sonra diğer hesaplamalar tamamlanmıştır.

III. BULGULAR VE TARTIŞMA

A. Optimize Yapı

YFK yöntemiyle elde edilen geometrik parametrelerle, x-ışını kırınımından elde edilen geometrik parametrelerin [1] birbirleri ile oldukça uyumlu ve yakın değerler verdiği tespit edilmiştir ve sonuçlar Tablo 1'de karşılaştırmalı olarak verilmiştir. Şekil 1.(a)'da deneysel verilerden elde edilen Ortep şekli [1] ve (b)'de ise teorik hesaplamalardan elde edilen optimize şekil verilmektedir. Teorik yöntemlerden elde edilen geometrik parametrelerle deneysel parametrelerin uyumunu göstermek için optimize yapı ve deneysel yapı üst üste örtüştürülerek hata değerleri belirlenmektedir. Bağ uzunlukları ile bağ açılarına ait bu örtüşmelere ait hata değeri 0.075 olup molekülün örtüşme şekli ise Şekil 2'de verilmiştir.

Geometrik parametrelerin teorik ve deneysel sonuçları arasındaki kabul edilebilir farklılıklar ise teorik hesaplamaların gaz fazdaki izole molekül üzerinden yürütülmüş olması ile, deneysel verilerin ise katı fazdaki moleküle ait olması ile açıklanabilmektedir. Kabul edilebilir deneysel hatalarla birlikte molekülün düzlemsel bir yapıya sahip olmadığı gözlenmiş olup iki moleküler halka arasındaki dihedral açı $84.78^0(0.10)$'dir. Halkalar arasındaki hata değerleri ise C1-N1 için 0.0088 ve C9-C14 için ise 0.0020'dir.

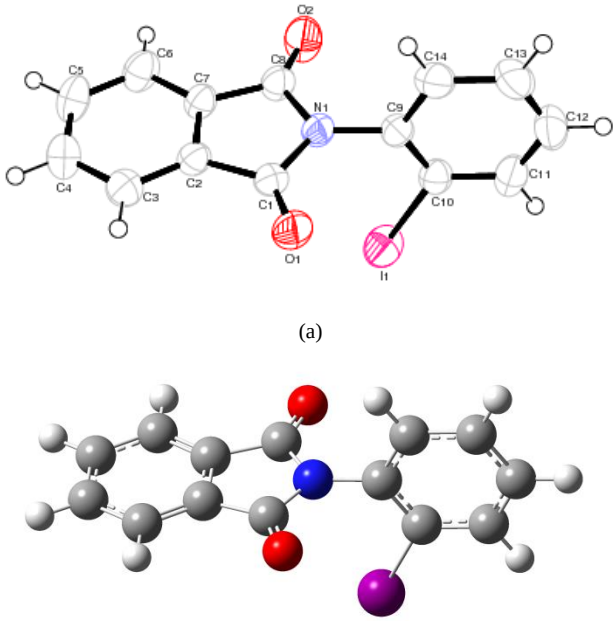

(a)

Şekil 1. a) 2-(2-iyodofenil)isoindolin-1,3-dion, $C_{14}H_8INO_2$ molekülüne ait x-ışını kırınımından [1] ve **b)** Optimize yapıdan elde edilen molekül şekilleri.

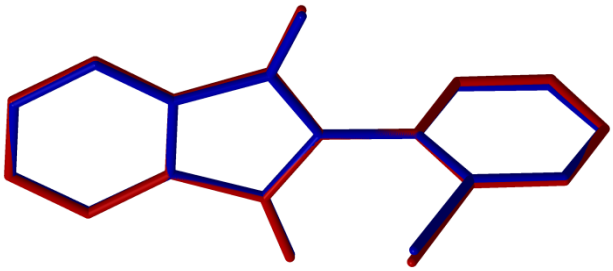

Şekil 2. Moleküle ait x-ışını kırınımından elde edilen optimize geometrisi (mavi) ve YFK yöntemlerinden elde edilen optimize geometrilerin (kırmızı) üst üste örtüşmesi.

Tablo 1. Bileşiğine ait bazı deneysel ve kuantum mekaniksel hesaplamalara ait geometrik parametreler.

Bağ uzunluğu	***X-ışını [1]***	***B3LYP 6-311++G(d,p)***
C1-O1	1.204(3)	1.20518
C1-N1	1.399(4)	1.41477
C1-C2	1.485(4)	1.49138
C2-C3	1.374(4)	1.38586
C7-C8	1.481(4)	1.49138
C8-O2	1.196(4)	1.20518
C9-C14	1.382(4)	1.39381
C9-N1	1.432(4)	1.42571
C12-C13	1.369(6)	1.39238
C10-I1	2.094(3)	2.10278

Maks. Fark		***0.02338***
KOK		***0.0119***
Bağ açısı		
O1-C1-N1	124.8(3)	125.53999
O1-C1-C2	129.2(3)	129.15350
N1-C1-C2	106.0(2)	105.30208
C3-C2-C1	130.5(3)	129.81815
N1-C8-C7	105.8(2)	105.30218
C14-C9-N1	118.2(3)	119.01836
C10-C9-N1	121.4(3)	121.12721
C9-C10-I1	121.2(2)	120.67457
C9-C14-C13	119.2(3)	120.53874
C1-N1-C9	124.7(2)	123.95799
Maks. Fark		***1.33874***
KOK		***0.715***
Burulma açısı		
O1-C1-C2-C3	1.0(6)	0.7190500
N1-C1-C2-C3	-178.1(3)	179.97648
O1-C1-C2-C7	180.0(3)	-178.67995
N1-C1-C2-C7	0.9(3)	0.57748
C14-C9-C10-I1	179.0(2)	179.99800
C1-C2-C3-C4	-179.7(3)	-179.48784
C2-C7-C8-O2	-179.4(4)	178.67868
C14-C9-N1-C8	85.6(4)	-89.61406
C6-C7-C8-N1	178.0(3)	-178.97801
C7-C8-N1-C9	179.4(3)	-179.6986
C10-C9-N1-C1	84.2(4)	-90.37463

B. Moleküler Elektrostatik Potansiyel

Moleküler Elektrostatik Potansiyel (MEP) haritaları bir moleküler sistemdeki elektron yoğunluklarını hayali bir birim pozitif yük yardımıyla yüzey taraması yaparak bulmayı hedeflemektedir. Tarama sonucu kırmızıdan maviye doğru, görece en zengin elektron yoğunluğunun olduğu bölgelerden en zayıf elektron yoğunluğunun bulunduğu bölgelere doğru renk kodları ile verilmektedir. MEP haritalarında ortaya çıkan bu yüzey, molekülün büyüklüğünü, şeklini, dipol momentini, yük dağılımını ve elektrostatik potansiyel değeri V(r)'yi göstermektedir. MEP haritaları moleküldeki elektrofilik ve nükleofilik tepkimelerin olabileceği muhtemel bölgelerin belirlenmesinde çok önemli bilgileri barındırmaktadır ki böylelikle yeni sentezi yapılacak moleküller içinde araştırmacılar için rehber niteliği taşımaktadır. Bu çalışmada MEP haritası ve molekülün elektrofilik ve nükleofilik reaktif bölgeleri YFK/B3LYP/6-311++G(d,p) yöntemi ile hesaplanılmış olup 3-boyutlu yüzey haritası Şekil 3'de verilmiştir. Haritaya bakıldığında en neagtif bölgelerin O1 ve O2 atomları üzerinde konumlandığı (V(r) değerleri sırasıyla -0.0484503 ve -0.0490046) en pozitif bölgelerin ise hidrojen atomları üzerinde konumlandığı görülmektedir.

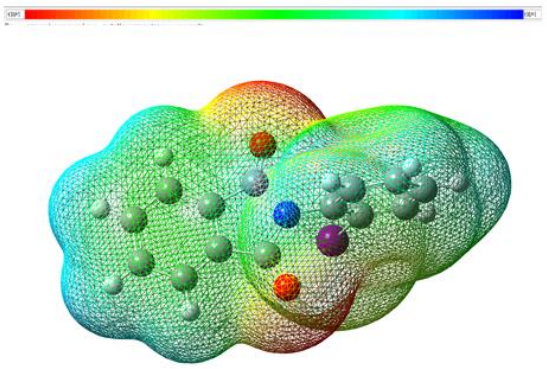

Şekil 3. Moleküle ait MEP haritası.

C. Mulliken ve Doğal Yük Analizi (NPA)

Mulliken yüklerinin [8] hesaplanması, molekülün reaktif bölgelerinin öngörülmesini sağlamaktadır ki böylelikle elde edilen verilerin MEP haritalarından elde edilen verileri destekler olması beklenilmektedir. Yük analiz metotları moleküle ait elektron yoğunluğunu moleküldeki atomlar üzerine dağıtan ve atomların sahip oldukları yük miktarlarını belirlemeye çalışan yöntemlerdir. Moleküle ait net yükler Mulliken ve NPA analizi ile YFK/B3LYP/6-311++G(d,p) yöntemleriyle hesaplanmış ve sonuçlar hem Tablo 2'de yük miktarları paylaşılmıştır. Bu sonuçlara göre, negatif yükler molekülün elektronegativitesi en yüksek olan O ve C atomları üzerinde, pozitif yükler ise elektronegativitesi daha düşük olan hidrojenler üzerinde yoğunlaşmış şekildedir.

Tablo 2. Atomlar üzerindeki Doğal ve Mulliken yük miktarları.

NPA	*6-311++(d,p)*	*Mulliken*	*6-311++(d,p)*
C1	0.70379	C1	-0.380000
C2	-0.11103	C2	0.890314
C3	-0.16060	C3	-0.609031
C4	-0.18155	C4	-0.231074
C5	-0.18155	C5	-0.231065
C6	-0.16060	C6	-0.609110
C7	-0.11103	C7	0.890285
C8	0.70379	C8	-0.380056
C9	0.11520	C9	-2.664776
C10	-0.20387	C10	-0.006911
C11	-0.21870	C11	0.478542
C12	-0.17956	C12	0.475304
C13	-0.19517	C13	-0.455105
C14	-0.16617	C14	1.294956
O1	-0.54102	O1	-0.208211
O2	-0.54103	O2	-0.208200
N1	-0.55015	N1	0.643330
I1	0.22386	S1	0.188687

D. HOMO-LUMO Enerjileri ve Bunlardan türetilen Kuantum Kimyasal Nicelikler

Moleküler sistemlerin tanımlanmasında ve moleküllerin diğer moleküllerle etkileşimini açıklamak için sınır molekül orbitalleri (FMOs) oldukça sık şekilde kullanılmaktadır. HOMO terimi 'en yüksek işgal edilmiş moleküler orbital' anlamına gelirken, LUMO terimi 'en düşük boş moleküler orbital' anlamına gelir. HOMO orbitalleri nükleofilik moleküller için, LUMO orbitalleri ise elektrofilik moleküller için karakteristiktir. HOMO-LUMO sınır orbital enerjilerinden faydalanılarak iyonlaşma enerjisi (I), elektron ilgisi (A), elektronegatiflik (χ), kimyasal sertlik (η) ve yumuşaklık (S), elektrofilisiti indeksi (ω) gibi kuantum kimyasal nicelikler hesaplanıp, yorumlanabilmektedir. Şekil 4'te YFK/B3LYP/6-311++G(d,p) baz seti ile hesaplanmış sınır orbitalleri ve Tablo 3'de ise bu orbitallerin sahip olduğu enerjiler ve bunlardan türetilmiş kuantum kimyasal nicelikler verilmektedir.

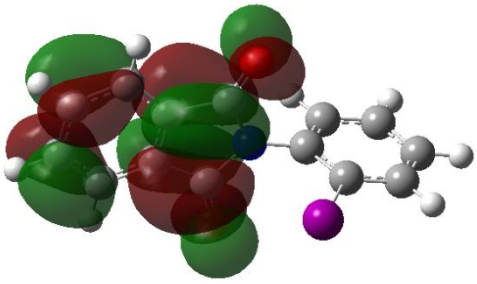

LUMO (-2.5837 eV)

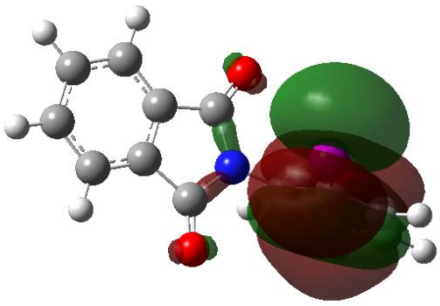

HOMO (-6.7003 eV)

Şekil 4. Moleküle ait HOMO ve LUMO şekillenimleri.

Tablo 3. Moleküle ait hesaplanmış kuantum kimyasal parametreler.

B3LYP/6-311G++(d,p)	
İyonizasyon enerjisi,I	6.7003
Elektron ilgisi, A	2.5837
Enerji aralığı, ΔE	4.1166
Elektronegatiflik, χ	4.6420
Kimyasal sertlik, η	2.0583
Kimyasal yumuşaklık, S	0.2429
Elektrofilisiti indeksi, ω	-5.2344

E. Doğrusal Olmayan Optik Özellikler (NLO)

Son yıllarda doğrusal olmayan optik özellikler taşıyan materyaller bilgi teknolojilerinde, optik sinyal işleme ve veri kaydetme, optik bağlantı materyallerinin tasarımında, lazer ve hologramlarda, endüstriyel uygulamalarda ve moleküler sistemlerin özellikleri belirlenirken oldukça sık şekilde kullanılmaktadır [19-21]. Moleküle ait dipol moment (μ), doğrusal kutuplanabilirlik (α), yönelime bağlı kutuplanabilirlik (β) değerleri hesaplanmış ve Tablo 4'de verilmiştir.

Tablo 4. Moleküle ait optik özellik hesaplamaları ve bileşenleri.

	Dipol Moment (Debye)		**Doğrusal kutuplanabilirlik, Yönelime bağlı kutuplanabilirlik (esu)**		**1. mertebeden kutuplanabilirlik (esu)**	
B3LYP						
	μ_x	0.7723762	α_{xx}	260.9057544	β_{xxx}	-202.2595433
	μ_y	0.1267074	α_{xy}	-29.4025142	β_{xxy}	66.6878137
	μ_z	0.0000283	α_{xz}	180.8100248	β_{xyy}	-52.0517076
	μ	**0.7827**	α_{yy}	-0.0028552	β_{yyy}	280.2180035
gaz			α_{yz}	-0.0037941	β_{xxz}	-0.0944106
			α_{zz}	168.1501446	β_{xyz}	-0.0531844
			α	**30.0940**	β_{yyz}	-0.0096249
			Δα	**109.4145**	β_{xzz}	125.5242199
					β_{yzz}	5.6188463
					β_{zzz}	-0.0505083
					β	**$3.24244x10^{-30}$**
	μ_x	1.1219591	α_{xx}	346.1672794	β_{xxx}	-711.7886438
	μ_y	0.180912	α_{xy}	-40.5313849	β_{xxy}	211.6823461
	μ_z	-0.000002	α_{xz}	259.5879915	β_{xyy}	-122.1153091
	μ	**1.1364**	α_{yy}	0.0011398	β_{yyy}	707.1357378
			α_{yz}	-0.0126374	β_{xxz}	-0.1487687
Etanol			α_{zz}	253.8046509	β_{xyz}	-0.0245621
			α	**42.4152**	β_{yyz}	-0.0150011
			Δα	**110.9606**	β_{xzz}	311.7702144
					β_{yzz}	10.337739
					β_{zzz}	0.1994119
					β	**$9.20787x10^{-30}$**
	μ_x	1.1393109	α_{xx}	349.1851352	β_{xxx}	-742.7445914
	μ_y	0.182711	α_{xy}	-40.8954129	β_{xxy}	219.7299807
	μ_z	-0.0005068	α_{xz}	263.079875	β_{xyy}	-122.6770221
dmso	**μ**	**1.1538**	α_{yy}	-0.0007798	β_{yyy}	729.3653373
			α_{yz}	-0.0087439	β_{xxz}	0.0867978
			α_{zz}	258.106652	β_{xyz}	-0.0403237
			α	**42.9487**	β_{yyz}	0.1038941

		Δα	**109.6680**	β_{xzz}	320.4004892
				β_{yzz}	9.5016726
				β_{zzz}	0.7361613
				β	**$9.52659x10^{-30}$**
μ_x	1.1420238	α_{xx}	351.3397932	β_{xxx}	-758.3387975
μ_y	0.1808352	α_{xy}	-40.9525889	β_{xxy}	219.766505
μ_z	0.0011768	α_{xz}	266.0257721	β_{xyy}	-128.6958367
μ	**1.1562**	α_{yy}	0.0017889	β_{yyy}	757.6804467
		α_{yz}	-0.0327237	β_{xxz}	-0.6383873
		α_{zz}	262.9710128	β_{xyz}	-0.0440086
		α	**43.4404**	β_{yyz}	-0.1122887
		Δα	**107.040**	β_{xzz}	331.8692689
				β_{yzz}	11.3476561
				β_{zzz}	-0.6396047
				β	**$9.79685x10^{-30}$**

su

F. Termodinamik Özellikler

Termodinamik fonksiyonlar entalpi, entropi ve ısı kapasitesi gibi değişkenler olup termodinamiğin çoğu uygulamasında bir ya da daha çok değişken sabit tutulurken diğer değişkenlerin bunlara göre nasıl değiştiği incelenir. Bir moleküler sistemin toplam enerjisi öteleme, elektronik, dönme ve titreşim enerjilerinin toplamıdır. Molekülün toplam enerjisini elde etmek için; ısı sığası, entropi, sıfır nokta enerjisi, elektronik ve termal serbest enerjiler toplamı, sıfır nokta titreşim enerjisi ve düzeltmesi, enerjide, entalpide ve Gibbs serbest enerjisi için termal düzeltme, dönme sabitleri ve dönme sıcaklıkları gibi enerji değerlerinin katkısı termodinamik fonksiyonlardan elde edilmiştir. Moleküle ait bu fonksiyonlar 298.15 K sıcaklıkta, 1 atm basınç ve gaz fazında belirlenerek Tablo 5'de tüm bileşenleri ile birlikte verilmiştir.

Tablo 5. Moleküle ait hesaplanan termodinamik değişkenler ve bileşenleri.

B3LYP	***6-311G(d,p)***
Termal, E (cal/mol K)	
Elektronik	0.000
Öteleme	0.889
Dönme	0.889
Titreşim	123.584
Toplam	125.361
Isı kapasitesi, Cv (cal/mol K)	
Elektronik	0.000
Öteleme	2.981
Dönme	2.981
Titreşim	47.984
Toplam	53.946
Entropi, S (cal/mol K)	
Elektronik	0.000
Öteleme	43.443
Dönme	34.013
Titreşim	47.053
Toplam	124.509
Dönme Sıcaklıkları (Kelvin)	
A	0.02369
B	0.01071
C	0.00896
Dönme sabitleri (GHz)	
A	0.49358
B	0.22324
C	0.18666
Sıfır-nokta tireşim enerjisi (kcal/mol)	116.46665
Sıfır-nokta düzeltmesi*	0.185601
Enerjide termal düzeltme*	0.1999776
Entalpide termal düzeltme*	0.200720
Gibbs serbest enerjisine termal düzeltme*	0.141562
Elektronik ve sıfır nokta enerjisinin toplamı *	-7633.694607
Elektronik ve termal enerjilerin toplamı *	-7633.680432
Elektronik ve termal entalpi toplamı *	-7633.679488
Elektronik ve termal serbest enerjilerin toplamı *	-7633.738646
Toplam enerji (Hartree)	-7633.8802082

G. Hirshfeld Yüzey Analizi

Molekülün Hirshfeld Yüzey Analizi ve iki boyutlu parmak izi haritası Crystal Explorer 3.0 programı ile gerçekleştirildi [22]. Hirshfeld yüzey analizi moleküller arası etkileşmeleri araştırmak için sık şekilde kullanılmaktadır [23,24] ve bunu Van der Waals mesafelerini görselleştirerek yapar. Diğer taraftan molekülde bulunan atomların birbirleri ile olan etkileşimlerini de 2D parmak izi analizi ile belirlemektedir. Hirshfeld yüzey analizi mavi ve kırmızı alanlar içermektedir ve bu alanların mavi ile gösterilenleri van der Waals yarıçapından daha büyük, kırmızı ile gösterilenleri ise van der Waals yarıçapına yakın olan kısımları ifade etmektedir. Molekül için d_{norm} -0.257 ile 1.258 aralığındadır. Hirshfeld yüzey analizinde molekülün O2 atomunun çevresinin moleküller arası hidrojen bağı için aktif bir bölge olduğu görülebilmektedir. X-ışını kırınımı verilerinden bu bölgede moleküller arası I1···O2 bağı olduğu rapor edilmiştir [1]. Molekülün Hirshfeld Yüzey analizi ve molekülün komşu moleküller ile moleküller arası I1···O2 etkileşimleri ile Şekil 5'de verilmiştir.

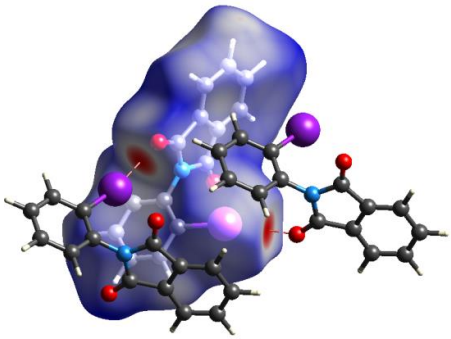

Şekil 5. Molekülün Hirshfeld Yüzeyi

Hirhfeld yüzeyine en fazla katkıyı sunan bazı etkileşimlere ait 2D parmak izi haritaları Şekil 6'da görülmektedir. O···H /H···O etkilerimleri iki sivri uç şeklinde kendini göstermektedir. Bu etkileşim Hirshfeld yüzeyine % 23.7 katkı sunarken, kristalin sahip olduğu moleküller arası I···O etkileşiminin Hirshfeld yüzeyine katkısı % 5.1 dir. 2D parmak izi haritasının sol üst kısmında ve sağ alt kısmında bulunan karakteristik kanatlar C—H···π etkileşimlerini temsil eder [25,26]. C···H / H···C etkileşimlerinin Hirshfeld Yüzeyine katkısı % 25.2 dir. Ayrıca molekülde Hirshfeld yüzeyine katkı sunan tüm etkileşimler ve oranları Tablo 6'da listelenmiştir.

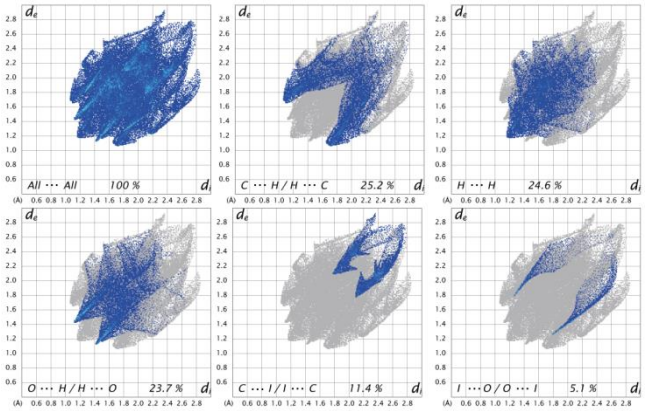

Şekil 6. Molekülün bazı moleküller arası etkileşimlerine ait iki boyutlu parmak izi haritaları.

Tablo 6. Hirshfeld yüzeyine katkısı olan etkileşimler

C···C	C···H / H···C	C···I / I···C	C···O / O···C	H···H	I···H / H···I	N···H / H···N	O···H / H···O	I···I	I···O / O···I
2.0	25.2	11.4	1.1	26.4	6.4	0.2	23.7	0.2	5.1

IV. SONUÇ VE YORUM

Bu çalışmada 2-(2-iyodofenil)isoindolin-1,3-dion, $C_{14}H_8INO_2$ bileşiğinin kuantum kimyasal hesaplamalar ile YFK yöntemiyle hesaplanmış ve elde edilen sonuçlar karşılaştırılmıştır. Optimize moleküle ait elde edilen geometrik parametrelerin x-ışını verilerinden [1] elde edilen verileri desteklediği gözlenmiştir. Elektron yoğunluğunun HOMO'da fenil halkası üzerinde dağıldığı gözlenirken, LUMO'da ise diğer ikili halka üzerine dağıldığı gözlenmektedir. Ek olarak sınır orbitallerinden HOMO ve LUMO enerjileri ve bunlardan türetilen diğer kimyasal nicelikler belirlenerek sonuçlar rapor edilmiştir. Elde edilen α ve β değerleri molekülün iyi bir optik materyal adayı olduğunu göstermektedir.

Böylelikle moleküle ait yapısal ve elektronik yeni bilgilere ulaşılmış ve gelecekte kullanım alanlarının artırılmasına yönelik olan hedeflerin gerçekleşmesine katkıda bulunulmuştur.

REFERENCES

[1] G. Demirtaş, N. Dege, A.Alaman Ağar and Orhan Büyükgüngör, 2-(2-Iodophenyl)isoindoline-1,3-dione, Acta Cryst. (2011), E67,o857.

[2] H. Jelali, L. Monsour, E. Deniau, M. Sauthier and N. Hamdi, An Efficient Synthesis o of Phthalimides and Their Biological Activities, Polycyclic Aromatic Compounds, 2020, 1-8.

[3] 3. Y. Nozawa, M. Ito, K. Sugawara, K. Hanada, and K. Mizoue, "Stachybotrin C and Parvisporin, Novel Neuritogenic Compounds. II. Structure Determination," The Journal of Antibiotics 50, no. 8 (1997): 641–5.

[4] L. A. Sorbera, P. A. Leeson, J. Silvestre, and J. Castaner, "Drugs Future," Journals on the Web 26 (2001): 651.

[5] C. Maugeri, M. A. Alisi, C. Apicella, L. Cellai, P. Dragone, E. Fioravanzo, S. Florio, G. Furlotti, G. Mangano, R. Ombrato, et al. "New anti-Viral Drugs for the Treatment of the Common Cold,"Bioorganic & Medicinal Chemistry 16, no. 6 (2008): 3091–107.

[6] X. Z. Zhao, K. Maddali, C. Marchand, Y. Pommier, and T. R. Burke, "Diketoacid-Genre HIV-1 Integrase Inhibitors Containing Enantiomeric Arylamide Functionality," Bioorganic & Medicinal Chemistry 17no. 14 (2009): 5318–24.

[7] Guertin K. R. (2002) US Patent 6482951 (B2)

[8] Frisch M. J. et al., Gaussian 03, Revision E.01, Gaussian, Inc., Wallingford CT, 2004.

[9] Mulliken, R. S., Electronic Population Analysis on LCAO-MO Molecular Wave Functions. I. *J.* Chem. Phys., 23, 1833-1840, 1955.

[10] Laudise R. A., Ueda R. and Millin J.B. 1975. *Crystal Growth and Characterization*, North-Holland Publishing Co.

[11] Brice J. C., *Crystal Growth Processes*, Halsted Press, John Wiley and Sons, New York, 1986.

[12] Nalwa H. S. and Miyata S. 1996. *Nonlinear Optics of Organic Molecules and Polymers*, CRC Press Inc., New York.

[13] Leite, R. C. C., Porto, S. P. S., and Damen, P. C., 1967. The thermal lens effect as a power-limiting device. *Appl. Phys. Lett.*, 10-100.

[14] Gambino, R. J., 1990. *Bull. Mater. Res. Soc*. 15-20.

[15] Belt, R. F., Gashurov, G. and Liu, Y.S., 1985. *Laser Focus* 10-110.

[16] Clark, R. S., 1988. *Photonics Spectra* 22.

[17] Zyss, J., 1994. *Molecular Non-linear Optics*, Academic Press, Boston.

[18] D. Dajan, J. Huert, VS. Jayakumar, J. Zaleski, J. Mol. Struct. 785:43, 2006.

[19] S.Uzun, Z. Demircioğlu, Karadeniz Fen Bilimleri Dergisi, 9(2), 275-288, 2019.

[20] F. Tekin, Ö. Kalfa, B. Koşar, C. Cüneyt Ersanlı, Dumlupınar Üniversitesi Fen Bilimleri Enst. Dergisi, Özel Sayı, 1302-3055.

[21] G. Özdemir Tarı, G. Demirtaş, European Journal of Science and Technology Special Issue 32, pp. 761-769, December 2021.

[22] D. S. K. Wolff, D. J. Grimwood, J. J. McKinnon, M. J. Turner, J. and M.A. Spackman, CrystalExplorer (Version 3.1), Univ. West. Aust. (2012). https://doi.org/10.1039/b704980c.

[23] Z. Gültekin, Z. Demircioğlu, W. Frey, O. Büyükgüngör, XRD, Spectroscopic characterization (FT-IR, UV–Vis), Hirshfeld surface analysis and chemical activity of (E)-benzyl 2-((2S,3S,4R)-2,3,4-tris(benzyloxy)hex-5-enylidene) hydrazinecarboxylate, J. Mol. Struct. (2018). https://doi.org/10.1016/j.molstruc.2018.05.076.

[24] S. Wu, L. Qi, Y. Ren, H. Ma, 1,2,4-triazole-3-thione Schiff bases compounds: Crystal structure, hirshfeld surface analysis, DFT studies and biological evaluation, J. Mol. Struct. 1219 (2020) 128591. https://doi.org/10.1016/j.molstruc.2020.128591.

[25] S.K. Seth, G.C. Maity, T. Kar, Structural elucidation, Hirshfeld surface analysis and quantum mechanical study of para-nitro benzylidene methyl arjunolate, J. Mol. Struct. (2011). https://doi.org/10.1016/j.molstruc.2011.06.003.

[26] Y.-H. Luo, B.-W. Sun, Pharmaceutical Co-Crystals of Pyrazinecarboxamide (PZA) with Various Carboxylic Acids: Crystallography, Hirshfeld Surfaces, and Dissolution Study, Cryst. Growth Des. 13 (2013) 2098–2106. https://doi.org/10.1021/cg400167w.

International Journal of Multidisciplinary Studies and Innovative Technologies

e-ISSN: 2602-4888
dergipark.org.tr/en/pub/ijmsit
Research Article

2022, 6 (1), 97-103
DOI: 10.36287/ijmsit.6.1.97
Received: June 2, 2022; Accepted: July 2, 2022

Makine Öğrenimi ile Uzun Kuyruk Ürünler için İyileştirilmiş Sonraki Öğe Önerisi

Ahmet Zencirli[1*], Harun Çetin[2], Nedim Tuğ[3], Engin Seven[4], and Tolga Ensari[5]

[1*] *Ar-Ge Departmanı, MNM Teknoloji, İstanbul, Türkiye (ahmet@mnm.com.tr) (ORCID: 0000-0002-9456-395X)*
[2] *Ar-Ge Departmanı, MNM Teknoloji, İstanbul, Türkiye (harun@mnm.com.tr) (ORCID: 0000-0001-8681-8919)*
[3] *Ar-Ge Departmanı, MNM Teknoloji, İstanbul, Türkiye (nedim@mnm.com.tr) (ORCID: 0000-0001-8449-2230)*
[4] *İstanbul Üniversitesi-Cerrahpaşa, Bilgisayar Mühendisliği, İstanbul, Türkiye (engin.seven@ogr.iuc.edu.tr) (ORCID: 0000-0002-7994-2679)*
[5] *Arkansas Tech University, Computer and Information Science, Russellville, USA (tensari@atu.edu) (ORCID: 0000-0003-0896-3058)*

Türkçe Özet – Elektronik ticaret platformlarında birçok farklı ürün türü müşterilerin nerede olduklarından bağımsız olarak satılabilmektedir. Bu platformlarda bulunan öneri sistemi kullanıcılar için ilgi çekici ürünlerin seçilmesi ve görüntülenmesinde kritik rol oynamaktadır. Yapılan bu çalışmada elektronik ticaret platformlarında bulunan müşterilere bir sonraki alacakları ürünlerin en doğru şekilde tavsiye edilmesi için makine öğrenmesi algoritmaları kullanılmış sonuçlar karşılaştırılmıştır. Tekil değer ayrışımı (Singular value decomposition-SVD) yönteminin daha başarılı sonuçlar elde ettiği gösterilmiştir.

Anahtar Kelimeler *– Uzun kuyruk ürünler, tekil değer ayrışımı, en yakın komşuluk, matris ayrıştırma, sonraki öğe önerisi.*

Atıf: Zencirli, A., Çetin, H., Tuğ N., Seven E., Ensari T. (2022). Makine Öğrenimi ile Uzun Kuyruk Ürünler için İyileştirilmiş Sonraki Öğe Önerisi. International Journal of Multidisciplinary Studies and Innovative Technologies, 6(1): 97-103.

Improved Next Item Recommendation for Long Tail Products with Machine Learning

Extended Abstract – Many different types of products can be sold on electronic commerce platforms. Products can be sold regardless of where customers are. The recommendation system on these platforms plays a critical role in selecting and displaying interesting products for users. In the study, the products to be purchased next to the customers were recommended in the most accurate way. For this, machine learning algorithms were used and the results were compared. The singular value decomposition (SVD) method has achieved more successful results.

Research Problem/Questions – *To make the most appropriate match between an infinite number of products and many customers in the most accurate way.*

Short Literature Review – *Many algorithms have been developed for the best solution in recommendation systems that try to persuade their customers to sell niche products, and it is currently a subject open to research.*

Methodology – *Singular value decomposition (SVD) and k nearest neighbor (kNN) algorithms are used. Products in the long queue in electronic commerce have been improved by developing the next item recommendation system.*

Results and Conclusions – *Machine learning algorithms can be used to solve problems in product recommendation systems. The SVD method suggested less erroneous recommendations for large datasets.*

Keywords *–Long tail products, singular value decomposition, k-nearest neighbor, matrix factorization, next item recommendation*

Citation: Zencirli, A., Çetin, H., Tuğ N., Seven E., Ensari T. (2022). Improved Next Item Recommendation for Long Tail Products with Machine Learning. International Journal of Multidisciplinary Studies and Innovative Technologies, 6(1): 97-103.

I. GIRIŞ

[1] numaralı referansta yapılan çalışmada, elektronik pazarlarda satılan ürünler için e-ticaret talebinin uzun kuyruğu gösterilmiştir. Toplanan veriler amazon.com sitesinden alınmış olup 200 den fazla kitap kategorisinde ve 250.000 den fazla kitap ile çalışma yapılmıştır. Talep ve gelir arasındaki ilişki incelenmiştir. PageRank algoritmasının bir türevi kullanılarak bir ürünün tavsiye sistemi ile olan ilişkisi gözlemlenmiştir. Ayrıca Gini katsayısı kullanılarak gelir ve talep dağılımındaki anormallik ortaya konulmuştur [1].

Öneri sistemlerinde sadece doğruluk oranlarına odaklanmak tavsiye kalitesinin ölçülmesinde eksikliklere yol açmaktadır. Bu nedenle doğruluğun tek ölçüt olarak alınması değil doğruluk ölçütüne ek olarak çeşitlilik, benzerlik ve uzun kuyruk teorisi gibi ölçütlerde eklenmiştir. Yapılan çalışmada bu ek ölçütleri de dikkate alarak Markovian grafiğine dayalı bir öneri sistemi geliştirilmiştir. Minnesota Üniversitesi'ndeki GroupLens Araştırma Projesi tarafından toplanan Movielens100K veri kümesi ile Last.fm çevrimiçi müzik sisteminden toplanan Last.fm veri kümesi kullanılmıştır [2].

İşbirlikçi filtre tabanlı öneri sistemlerinde popüler ürünlerin daha fazla önerildiği ancak ürünlerin daha az önerildiği belirtilmiştir. Bu sorunun üstesinden gelmek için grafik tabanlı öneri sistemi geliştirilmiştir. Vuruş süresi, emme süresi ve emme maliyeti algoritmaları kullanılarak sistemin performansı arttırılmaya çalışılmıştır. Ayrıca, farklı kullanıcı kalemi derecelendirme çiftlerindeki varyasyonu ayırt etmek için entropi-maliyet modeli önerilmiştir. İki veri kümesi üzerinde testler gerçekleştirilmiştir. Bu veri kümeleri sırasıyla bir Çin Web 2.0 web sitesi, en büyük çevrimiçi Çince kitap, film ve müzik veritabanı ve 50 milyondan fazla kullanıcısı olan Çin'deki en büyük çevrimiçi toplulukdan alınan Douban Veri Kümesi, ikinci olarak MovieLens'ten gerçek bir film veri kümesidir [3].

[4] numaralı referansta yapılan çalışmada, pazara geleneksel olarak en çok satan birkaç ürün hakimdir. Ancak internet pazarları, ürünlerin yarattığı satışların payını artırma potansiyeline sahiptir. Ürün mevcudiyetindeki varyasyonları kontrol edip ve talep yönlü faktörlerin İnternet üzerinden niş ürünlerin artan satışlarıyla ilişkili olup olmadığı araştırılmıştır. Yapılan çalışmada internet kanalı ve katolog kanalı ürün satışları üzerine çalışılmıştır [4].

[5] numaralı referansta yapılan çalışmada, çok seviyeli benzerlik özellikleri ve kullanıcı geçmişi kullanılarak içerik tabanlı filtrelemeye dayanan yeni bir anahtarlama yöntemi önerilmiştir. Önerilen hibrit yöntem benzer kullanıcılara dayalı olarak tahmin edilen derecelendirmeyi hesaplayan ortak bir filtreleme bileşeni ve kullanıcının geçmişte derecelendirdiği diğer benzer öğeleri kullanarak tahmin edilen derecelendirmeyi hesaplayan içerik tabanlı filtreleme bileşeninden oluşmaktadır. İki gerçek veri kümesi üzerinde deneyler gerçekleştirilmiş başarılı sonuçlar elde edildiği ifade edilmiştir. Bu veri kümeleri sırasıyla MovieLens 100K ve MovieLens Im'dir.

Doğruluk ve uzun kuyruk tavsiye sistemleri için iki önemli hedef olmakla birlikte aynı zamanda bunlar çelişkilidir ve aynı anda maksimize edilemezler. Doğruluk ve yeniliği dikkate alan uzun kuyruk önerisi çok amaçlı bir optimizasyon problemi olarak formüle edilmiştir. İkili olarak formüle edilen bu problem için çok amaçlı evrimsel algoritma kullanılmıştır. Evrimsel algoritma aday çözümler üreterek en iyi çözümü kullanıcıya iletmektedir. Üç veri kumesi MovieLens, Jester veri kümesi ve Netflix veri kümesi, önerilen algoritmanın performansını değerlendirilmiştir [6].

[7] numaralı referansta yapılan çalışmada, bir uzun kuyruk değerlendirme kriterleri önerilmiştir ve farklı modeller arasında uzun kuyruk tavsiyesindeki performansı karşılaştırılmıştır. Davranış özellikleri, ürün özellikleri ve zaman özellikleri olarak tasnif edilmiştir. Ayrıntılı uzun kuyruk kriterleri belirlenmiştir. Böylece uzun kuyruk probleminin daha iyi ölçülmesi sağlanmıştır. Veri kümesi, bir e-ticaret platformu olan Tmall'ın 200 günlük kullanıcı ve öğelerin temel bilgilerini ve ayrıca kullanıcı davranışlarını içeren kayıtlardan oluşmaktadır.

Öte yandan, ürünlerin nasıl ele alındığı ve ürünlerin uzun süre neden durgun kaldığı tartışılmaktadır. Denetimli öğrenme algoritmalarında Random Forest algoritması ile soğuk ürün ve uzun kuyruk problemine çözüm aranmıştır [8].

[9] numaralı referansta yapılan çalışmada, popülerliklerinin neden olduğu önyargıyı dengelemek için uzun kuyruklu ürünlere daha yüksek ve popüler ürünlere daha az ağırlık veren bir ağırlıklandırma şeması kullanılmıştır. Uzun kuyruklu katalog kapsamı ile doğruluk arasındaki dengeyi, herhangi bir kullanıcı ve öğe çifti için ağırlıklı bir karma puan hesaplaması olarak modellenmiştir. Movielens1M ve Epinions isimli iki veri kümesi üzerinde deneyler gerçekleştirilmiştir.

Kullanıcı davranışını temel alan işbirlikçi filtreleme algoritmaları grup açısından yola çıktığı için bireysel yetenekler göz ardı edilmektedir. [10] numaralı referansta yapılan çalışmada, önerilen model iki ana bölüme ayrılmış olup sırasıyla kişisel deneyim gelişimine dayalı puanlama tahmini ve deneyim düzeyine dayalı en iyi öneridir. Bireysel seviyeden kullanıcı beğenilerinin evrimi modellenip daha sonra kullanıcı deneyimi düzeyine ve öğelerin ilgili popülaritesine göre öneri puanlama modelini oluşturulmuştur. Veri kümesi olarak inceleme sitesi RateBeer'in inceleme verileri kullanılmıştır.

[11] numaralı referansta yapılan çalışmada, talep tarafı faktörünün (çevrimiçi kullanıcı incelemeleri) ve arz tarafı faktörünün (ürün çeşitliliği) çevrimiçi yazılım indirme bağlamında uzun kuyruk ve süper yıldız fenomeni üzerindeki etkisini incelemektedir. Ürün çeşitliliğinin tüketicilerin çevrimiçi karar verme sürecinde oynadığı rolün daha kapsamlı bir şekilde anlaşılmasını sağlamayı amaç edinilmiştir. Çevrimiçi kullanıcı incelemelerinin ve ürün çeşitliliğinin, farklı popülerliğe sahip yazılım programlarının kullanıcı seçimlerini etkilemek için nasıl etkileşime girdiğini araştırmak için nicel regresyon metodolojisi kullanılmıştır. Bu makalenin amacı, çevrimiçi alışveriş ortamındaki hem talep hem de arz yan faktörlerinin kullanıcı seçimlerini nasıl etkilediğini ve böylece toplu olarak çevrimiçi tüketim kalıplarındaki değişikliklere nasıl katkıda bulunduğunu göstermektir. Veri kümesi 30.000'den fazla ücretsiz veya denemesi ücretsiz

yazılım programının bir koleksiyonu olan CNET Download.com'dan (CNETD) alınmıştır.

[12] numaralı referansta yapılan çalışmada, üçlü grafik öneri sistemi geliştirilmiştir. Geliştirilen model kullanıcı öğesi, kullanıcı türü ve tür öğesi olmak üzere üç katmanı birbirine bağlamaktadır. Verileri daha iyi kullanmak için kullanıcı-tür ilişkisini ve grafikte daha fazla yol oluşturmak için tür-öğe ilişkisi kullanılmıştır. Üçlü grafikte daha fazla yol oluşturmak için "temel türler" kavramını kullanılır ve daha düşük dereceli türlere çok fazla ağırlık vermekten kaçınmak için basit bir ortalamayı kullanmaktan Bayes ortalamasını tercih edilmiştir. Ayrıca, uzun kuyruklu öneri problemini çözmek için Gizli Semantik İndekslemede kullanılan Tekil Değer Ayrıştırması benimsenmiştir. Veri kümesi olarak MovieLens üzerinde testler gerçekleştirilmiştir.

[13] numaralı referansta yapılan çalışmada, işbirliğine dayalı filtre ile yapılan tavsiye sistemlerini iyileştirmek için Hybrid Reranking Framework in Collaborative Filtering (HyReCF) isimli yeni bir cerveve önermişlerdir. Önerilen yaklaşım iki aşamada gerçekleştirilir. İlk kısımda (tahmin aşaması olarak anılır), bir tahmin listesi geleneksel bir işbirlikçi filtreleme tekniği uygulayan her kullanıcı için oluşturulur. Bu yaklaşımın ana fikri, kullanıcılara daha çeşitli ve uzun kuyruklu öğeler sunmak için bu çerçeveyi mevcut işbirlikçi öneri sistemiyle birlikte dağıtmaktır. Tahmin listesi için kullanıcı tabanlı CF, madde tabanlı CF, matris faktoring gibi bilenen yöntemler kullanılmıştır. İkincı kısımda, öğenin popülerliği, kullanıcıların geçmiş derecelendirmelerine benzemeyen öğelerin bulunması ve iyi tahmin edilen öğeler gibi önemli faktörlerin gözlemlenmesi gerekir. Öngörülen öğeler, maksimum çeşitliliği elde etmek ve uzun kuyruk öğe önerilerini iyileştirmek için farklı sınıflara ayrılmıştır. MovieLens ve Netflix olmak üzere iki gerçek dünya film derecelendirme veri seti ile test edilmiştir.

[14] numaralı referansta yapılan çalışmada, Hitting Tıme Clustered Algorithm (HTCL) isimli bir model önerilmiştir. Önerilen model temel olarak vuruş süresi (Hitting Time) ve kümeleme (clustering) yaklaşımlarını temel almaktadır. Vuruş süresi ile öğeler ve kullanıcılar arasındaki yakınlığı hesaplamak amaçlanmıştır. Kümeleme yaklaşımı ile önerileri daha uzun kuyruklu maddelere odaklayacaktır. Veri kümesi olarak Movielens100k kullanılmıştır.

[15] numaralı referansta yapılan çalışmada, Co-occurrence based Enhanced Representation model (CER) isimli bir model önerilmiştir. Önerilen model hedef öğelerin anlamlarını tamamlamak için geliştirilmiş bir temsil etmeye çalışılmıştır. Burada, hedef öğenin birlikte meydana gelen öğelerine dayalı olarak geliştirilmiş temsilini öğrenme önerilmiştir. Gürültü azaltma ve hesaplama karmaşıklığı önlemek için birlikte meydana gelen öğe setinden sabit sayıda öğeyi örneklemiştir. Bu örnekleme stratejilerinde iki kriter göz önünde bulundurulur. Birincisi, hedef öğeye yüksek anlamsal benzerliğe sahip öğeleri örneklemektir. Bir diğeri, yerleştirmeleri düşük anlamsal belirsizliğe sahip öğeleri örneklemektir. Birlikte meydana gelen öğelerin farklı önemini ayırt etmek için dikkat mekanizması kullanılmıştır. AmazonBeauty and Amazon-Books veri kümelerinde deneyler yapılmıştır.

Matris çarpanlara ayırma, öğe tabanlı, kullanıcı tabanlı, çeşitli alanlarda yaygın olarak kullanılan teknik olan işbirlikçi filtreleme adı verilen bir öneri sistemi sınıfına aittir. Bu sistemlerin genelde pöpüler ürünleri önermede ön yargılı olduğu ifade edilmiştir. Önerilen model, yaygın olarak kullanılan ortak filtreleme tekniğini yeni bir grafik tabanlı teknikle birleştirilmiştir. Önerilen yaklaşımdaki öneriler üç aşamada gerçekleştirilir. İlk aşamada, uzun kuyruklu kalemlere odaklanmak için grafik tabanlı yaklaşım kullanılır. Daha sonra öğe-öğe etkileşim matrisinden yararlanarak her aktif kullanıcı için ağırlıklı bir graf oluşturulur, son olarak, oluşturulan grafın her düğümü (öğesi) için entropi ve ters popülerlik hesaplanır ve ardından, bunlara dayalı öneriler için öğeleri seçilmiştir. MovieLens 100K and MovieLens 1M datasets veri setlerinde deneyler gerçekleştirilmiştir [16].

Yapılan çalışmada güç yasası dağılımı ile birleşen bir işbirlikçi filtreleme öneri algoritması önermektedir. Ayrıca, güç yasası dağılımını yerelliğe duyarlı karma (locality sensitive hashing-LSH) ile birleştirilmiştir. bu yazıda, yaklaşık en yakın komşu araması için verimli bir indeks yapısı olan seyahat verileri ve yerelliğe duyarlı karma (LSH) özelliklerini kullanarak (tourism recommendation systems) TRS'lerin öneri çeşitliliğini ve hesaplama verimliliğini iyileştirmeye çalışılmıştır. Lokasyona duyarlı hash fonksiyonlarını kullanarak, kullanıcıları yüksek boyutlu vektörlerden düşük boyutlu ikili tamsayılara hash eder ve benzer seyahat tercihlerine sahip kullanıcıları aynı paketlere ayrılır. Sadece aynı paketteki kullanıcılar arasındaki benzerlikleri hesaplınır ve aynı paketteki kullanıcıların seyahat tercihlerine göre önerilerde bulunulur, bu da yüksek boyutlu seyahat verilerinin hızlı en yakın komşu araması ve aşırı seyreklik sorununa uygulanabilir bir çözüm üretir. Kullanılan veri seti Sina Weibo check-in verileridir [17].

[18] numaralı referansta yapılan çalışmada, içerik tabanlı filtreleme baz alınarak otonom olarak kendisini güncelleyen öneri tavsiye sistemi oluşturulmuştur. Oluşturulan modelde RBM ve ContentKNN, RBM ve SVD++, AutoEncoder ve ContentKNN, AutoEncoder ve SVD++ gibi algoritmalar bir arada kullanılmış ve hibrit bir model tasarlanmıştır. Sonuçlar karşılaştırmalı olarak analiz edilmiştir. Çalışmada, gerçek online ticari satış ortamından elde edilen kullanıcı-ürün veri kümesi kullanılmıştır.

[19] numaralı referansta yapılan çalışmada, önerilen model, ürün popülerlik bilgilerinin kullanılmasına dayanmaktadır. "Uzun kuyruk" önerisinin, her kümenin dengeli öğe popülaritesi ile kesin olarak çıkarılabileceği gösterilmiştir. Veri seyrekliği sorununu ele almak için, modellemeyi ve güçlü etkili temsilleri anlamak için SDAE (Yığın Gürültü Giderici Otomatik Kodlayıcı) kullanan derin öğrenme modeli önerilmiştir. Web hizmeti önerisi için veri seyrekliğini ele almak ve performansı artırmak için evrişimli sinir ağları önerilmiştir. Gerçek dünya veri kümesi üzerindeki deneysel sonuçlar, bu tür ortak otomatik kodlayıcı tabanlı temsil ve içerik kullanımı öğrenme çerçevesi ile önerilen algoritmanın en son teknoloji temel çizgilerinden önemli ölçüde daha iyi performans gösterdiğini göstermektedir.

Literatürde, genellikle kullanıcıları ve öğeleri düşük boyutlu uzayda vektörler olarak temsil eden matris ayrıştırmaya (matrix factorization-MF) dayalı yerleşik bir metodoloji kullanılmaktadır. Bu çalışmada, MF tabanlı kişiselleştirilmiş

öneriler için hızlı ve doğru erişim sağlayan literatürdeki son gelişmeleri ve son teknoloji yaklaşımları araştırılmıştır. Ayrıca farklı boyutlardaki yaklaşımların analitik tartışmalarda incelenmiştir. Bu anket, tavsiye alma aşamasına odaklanır ve matris çarpanlara ayırma önerisinin verimli bir şekilde alınması için son gelişmelere genel bir bakış sunmuştur. Her adım için, yüksek öneri doğruluğunu korurken, alma verimliliğini artırmak için ilgili yöntemleri ilgili stratejilerine göre kategorize edilmiştir [20].

Geleneksel öneri algoritmasının doğruluğuna dayalı yaklaşımı yeterli görülmemektedir. Bundan dolayı yenilik, çeşitlilik, doğruluk ve hatırlamadan oluşan dört öneri hedefini aynı anda optimize etmek ve çok amaçlı optimizasyon önerisi için geliştirilmiş bir matris çarpanlara ayırma tabanlı model önerilmiştir. Çift katmanlı öneri modeli tasarlanmıştır. Alt katman, geliştirilmiş bir MF algoritmasını benimser. Alt katmanın (improved matrix factorization-IMF) rolü, bilinmeyen öğelerin derecesini tahmin eden geleneksel öneri yöntemlerine benzer. Önerilen IMF algoritmasının avantajı , elde edilen tahmin derecelendirmesinin çeşitlilik, yenilik ve doğruluk olmak üzere üç hedefi bütünleştirmesi için ek düzenleme öğelerine sahip olmasıdır. Önerilen algoritmayı optimize etmek ve parametre matrisini elde etmek için stokastik gradyan inişi (SGD) kullanılır. En üst katmanda, çok amaçlı evrimsel algoritmaya dayanan temsili algoritmalardan biri olan ve Pareto'nun egemenliğine dayanan NSGA-III (klasik bir model for many-objective optimization recommendation), önerilen öneri modelimize uyacak şekilde uygun şekilde düzenlemişlerdir [21].

İşbirliğine dayalı öneri sistemlerinin çoğu, kullanıcıları ve öğeleri ortaklaşa temsil etmek için yerleştirmeleri (embeding) öğrenerek çalışmaktadır. Yapılan çalışmada Matrix Factorization (MF) tarafından öğrenilen yerleştirmelerin güvenilirliğini ne derece doğru olduğu tartışılmıştır. Gizli faktörlere verilen ilk değerleri değiştirmek suretiyle aynı MF yönteminin çok farklı öğeler ve kullanıcılarda oluşturduğu etkiyi ölçmeye çalışılmıştır. Bu etkinin daha az popüler olan öğeler için ne derecede etkili olduğu incelenmiştir. Bu problemi çözebilmek için öğeler ve kullanıcılar hakkındaki bilgileri komşularına yayan En Yakın Komşular Matrisi Çarpanlarına ayırma (NNMF) adı verilen bir MF genellemesi tasarlanmıştır. Tavsiyeleri ve temsilleri destekleyen bilgi miktarını genişletmek için yaygın MF yaklaşımının NNMF varyantlarını tanımlanmıştır. Beş farklı veri kümesi üzerinde kapsamlı deneyler gerçekleştirilmiştir [22].

[23] numaralı referansta yapılan çalışmada, öneri sistemlerinde uzun kuyruk problemlerinin sebeplerinden birinin birçok öğenin sadece birkaç derecelendirilmesi ile temsil edilmesinden kaynaklandığı belirtilmiştir. Bu problemin üstesinden gelmek için tüm öğe kümesini baş ve kuyruk parçalarına bölerek sadece kuyruk öğelerini kümelemektedir. Kuyruk da kümelenmiş öğeler için öneriler aynı kümedeki derecelendirmelere dayanmaktadır. Bölümleme ve kümeleme en uygun şekilde yapılırsa iyi bir hesaplama performansını korur, kuyruk öğeleri için öneri hata oranlarını azalttığı ifade edilmiştir.

[24] numaralı referansta yapılan çalışmada, tavsiye sistemleri için genel bir çerçeve oluşturulmuştur. Etkileşimin yaratıcı öneriler için bir dizi fırsat sunduğu bir örnek olarak eBay'i kullanılmıştır. Bir pazar platformu için tavsiye sistemleri oluşturmadaki zorlukları, fırsatları ve yaklaşımları tanımlanmaya çalışılmıştır. Tavsiye sistemlerindeki sorunların, sıklıkla görüldüğü gibi, sadece çapraz satışın ötesinde olduğu ve bu ruhla, Kim, Ne, Neden, Nerede, Ne Zaman ve Nasıl tavsiyelerini içeren tavsiye sisteminin 5 W ve H'sini tartışılmıştır. Ayrıca, öneriler yalnızca ürünler ve öğeler için değil, öğe kategorileri, ilgili sorgu önerileri ve markalar için de geçerli olduğu belirtilmiştir [24].

[25] numaralı referansta yapılan çalışmada, daha önceki hiçbir araştırmanın, çeşitli satış stratejileri bağlamında tavsiyenin sağlandığı perspektife ve stratejilerin müşteriler, ürünler ve USP ile nasıl bağlantı kurduğuna dikkat etmemiş olması bakımından önemli olduğu vurgulanmıştır. Daha doğru önerilerde bulunmak için kontrollü değişkenleri ve satış stratejilerini içermektedir. Bu çalışmada üç hipotez (H1, H2 ve H3) önerilmektedir. H1 ve H2 hipotezleri birincil verilerle test edilir ve doğrulanır. Hipotez H3 , mevcut literatüre karşı test edilmiş ve doğrulanmıştır. H1, İşletme kişiselleştirilmiş dijital pazarlamayı ne kadar çok gerçekleştirirse, gelir artış oranı o kadar yüksek olur. Kişiselleştirilmiş dijital pazarlama ve gelir yönetimi arasındaki potansiyel sinerji, pazarlama hunisinin iki farklı bileşeninin kontrolünü sağlar. Daha yüksek bir değer, şirketin sürdürülebilir büyümesi anlamına gelir. H2, işletme kişiselleştirilmiş dijital pazarlamayı ne kadar çok gerçekleştirirse, AOV (Average Order Value-kullanıcı tarafından bir siparişi tamamlamanın potansiyel değerine ilişkin bir tahmin sağlar ve yüksek bir değerin performansı ve satışları artırması muhtemeldir.) oranı o kadar yüksek olduğu ifade edilmiştir. Daha yüksek bir değer, müşterinin satın alma alışkanlıklarında bir artış anlamına gelmektedir. H3, İşletme kişiselleştirilmiş dijital pazarlamayı ne kadar çok gerçekleştirirse, halka arz oranı o kadar yüksek olur. Daha yüksek bir değer, toplam gelirde daha fazla kazanılan, yani daha fazla yeni müşteri çekmek anlamına gelmektedir. Önerilen model e-pazarın tasarımı, kişiselleştirilmiş tavsiye modeli ve tavsiye süreci olmak üzere üç katmanlıdır. Modelin gücü, öğeleri e-pazaryeri tasarımına uygun olarak önermek ve önerilen kişiselleştirilmiş öneri modelinin benimsenmesiyle önerilen öneri sürecini takip etmek olarak belirtilmiştir [25].

[26] numaralı referansta yapılan çalışmada, ilk olarak geri bildirim puanı olarak kullanıcının satın alma sayısına dayalı bir kullanıcı-öğe matrisi oluşturarak bu sorunu ele almaktadır. İkinci olarak genelde kullanılan İşbirlikçi Filtreleme yaklaşımını belirli algoritmalar altında incelemektir. Hedef müşteri tarafından verilen derecelendirmeyi tahmin etmek için Bellek tabanlı ve Model tabanlı İşbirlikçi Filtreleme kullanarak daha iyi bir yaklaşım bulmak için testler gerçekleştirilmiştir. Sonuç olarak, k-NN'li Bellek tabanlı CF'nin SVD aracılığıyla Model tabanlı CF'den daha iyi performans gösterdiği vurgulanmıştır [26].

[27] numaralı referansta yapılan çalışmada, derecelendirme sayısına, derecelendirmelerin ortalama değerine veya tavsiye sıklığına dayalı olarak bir öneri veri setinden uzun kuyruk öğelerini tahmin etmek için belirli stratejiler önerilmiştir. Her uzun kuyruk öğesi için bir uygunluk modeli oluşturan olasılıksal bir işbirlikçi filtreleme algoritması olan (item-based Relevance Model) IRM2'yi tasarlanmıştır. Alaka Tabanlı Dil Modelleri (Relevance-based Language Models) kullanılmıştır (Sıklıkla Uygunluk Modelleri veya RM olarak kısaltılır). Bu yöntem, sözde alaka düzeyi geri bildirimi yoluyla otomatik sorgu genişletme gerçekleştirmek

için en gelişmiş tekniktir. İlgi Modellerini de kullanarak işbirlikçi filtrelemeye farklı bir yaklaşım tasarlanmıştır. Her uzun kuyruklu ürün için bir Uygunluk Modeli oluşturulmasını önerilmiştir. Benzer öğelerden gelen bilgileri kullanarak öğe profillerini ilgili kullanıcılarla genişleterek modelin performansı iyileştirilmiştir.

[28] numaralı referansta yapılan çalışmada, işbirlikçi filtreleme için sağlam bir negatif olmayan matris çarpanlara ayırma modeli oluşturulmuştur. Ek olarak modelin kararlılığının bir analizini yapılmıştır. Tahmin edilen derecelendirmelerin doğru ve negatif olmadığını garanti eden, negatif olmayan matris çarpanlarına ayırmanın yinelemeli güncelleme algoritmasına dayanan özellik matrislerinin yinelemeli bir optimizasyon yöntemi önerilmiştir. Önerilen yöntemde matris çarpanlarına ayırma sürecinde, öznitelik vektörlerinin girişlerindeki negatif olmayan kısıtlama çok önemlidir çünkü öğrenilen özniteliklerin CF sistemlerinde kullanıcı ilgileri veya tercihleri gibi gerçek dünya anlamlarını temsil etmesini sağlayabilmektedir. NMF yöntemleri, CF sistemlerinde kullanıcı derecelendirmelerinin doğal olarak negatif olmamasını garanti eden gizli özellikler üzerinde negatif olmayan kısıtlamalar getirebilmektedir. NMF modeli, kullanıcı öğesi derecelendirme matrisi **R'yi** iki düşük dereceli negatif olmayan faktör matrisi **W** ve **H'ye** ayırır ve belirli bir öğe için belirli kullanıcının tercihlerini tahmin etmek için bunların doğrusal kombinasyonunu kullanmaktadır. Model Movielens 10M ve Netflix veri kümesi üzerinde test edilmiştir.

Tüketiciler, çevrimiçi incelemeler yazarak bir ürünle ilgili deneyimlerini paylaşmaya giderek daha fazla katılmaktadır. Web içinde kullanıcı tarafından oluşturulan içeriğin ortaya çıkması ve etkisi, klasik WOM'u İnternet ve çevrimiçi iletişim tarafından etkinleştirilen (Electronic word of mouth) eWOM'a doğru hareket ettirmiştir. Güç yasası ile ürün kategorilerinin dağılımının modellenmesi tasarlanmıştır. Güç yasası dağılımına uyması için içerik değil, inceleme sayısı kullanılmıştır. Bu nedenle, kısa başlıkta yüksek frekanslı olaylar mı yoksa kuyrukta düşük fakat daha büyük olaylar mı olduğunu ayırt etmek için ürün kategorilerinin dağılımını güç yasası ile modellemek uygun olacaktır. Araştırmalar, çevrimiçi incelemelerin mesaj içeriğinin, kullanıcılar bir satın alma kararı vermek üzereyken çok sayıda incelemeye baktıklarında daha az etkiye sahip olduğunu göstermiştir. Veri toplama ve analiz için seçilen eWOM topluluğu, 7 milyondan fazla yorum yazan 1,3 milyondan fazla kullanıcının yaklaşık 1,4 milyon ürün hakkında yazdığı popüler bir web sitesi olan Ciao UK kullanılmıştır [29].

II. MALZEME VE YÖNTEMLER

Bu çalışmada, makine öğrenmesi yöntemlerinden tekil değer ayrışımı (Singular value decomposition-SVD), SVD++ ve en yakın komşuluk (k nearest neighbor-kNN) algoritmaları kullanılarak, uzun kuyruklu ürünler kullanılarak, özellikle elektronik ticarette sonraki öğe öneri sistemi geliştirilerek iyileştirilmiştir.

Tekil değer ayrışımı algorıtması (Singular value decomposition-SVD), ortonormal bir matris, köşegen bir matris ve ortonormal bir matris olmak üzere üçlü bir çarpıma ayrıştıran bir algoritmadır [30]. K en yakın komşuluk algorıtması ise (k-nearest neighbour-kNN) çeşitli metrik tanımlarını kullanarak en yakın eleman değerine göre veri noktasının sınıflandırma tahmininin yapıldığı eğiticili öğrenme algortımalarından biridir.

Bu bölümde, deneysel çalışmalar için veri toplama, model oluşturma ve deneysel çalışmalar gerçekleşitirilmiştir. Veri kümesini toplamak için JS ve Java programlama diliyle bir veri toplayıcı modül yazılmıştır. Kullanıcıların, ürün görüntüleme, tıklama, sepete atma ve satın alma verilerini kaydedilmiştir. Kullanıcı-ürün etkileşimleri (view, click, basket, order) dış değerlere (rating) çevrilmiştir (0-5 arası). Ön işleme işlemleri gerçekleştirilmiş ve anonimleştirleşitrilmiştir. Bu bağlamda, kullanıcı (user), ürün (item), değerleme (rating) bazında bir veri kümesi oluşturduk. Veri kümesinin büyüklüğü 1.1 milyon (1.1M) adettir. Ayrıca, bu veri kümesinden yola çıkarak 100.000 (100K) adetlik daha küçük boyutlu bir alt veri kümesi daha oluşturulmuştur.

Tekil değer ayrıştırma, tekil değer ayrıştırma++ ve en yakın komşuluk algoritması yöntemleriyle kök ortalama karesel hata (root mean square error-RMSE) ve hatanın mutlak ortalaması (mean absolute error-MAE) hata değerleri ölçülmüştür. Aşağıdaki tabloda (Tablo I) 100K adet veri kümesi için SVD, SVD++ ve kNN algoritmalarının sınıflandırma sonuçları verilmiştir. Bu sınıflandırmada kök ortalama karesel hata (root mean square error-RMSE) ve ortalama mutlaka hata (mean absolute error-MAE) hata değerleri ölçülerek sonuçlar Tablo I'de paylaşılmıştır. En az hata değerine sahip (en başarılı) yöntemler, köyü renkli olarak gösterilmiştir. Buna göre en başarılı yöntemin SVD olduğu gözlenmiştir.

Tablo I: 100K boyutundaki veri kümesi için sınıflandırma sonuçları (Hata değerleri)

Yöntem (Algoritma)	RMSE	MAE
SVD	**0,30**	**0,14**
SVD++	0,34	0,20
kNN Kullanıcı-bazlı (User-based)	0,71	0,47
kNN Ürün-bazlı (Item-based)	0,39	0,16

Öte yandan, 1.1M boyutlu veri kümesi için de aynı makine öğrenmesi yöntemleri kullanılmış ve sonuçlar Tablo II'de paylaşılmıştır. Buna göre, RMSE olarak en iyi yöntemin SVD, MAE olarak ise en iyi yönteminin, kNN Ürün-bazlı (Item-based) yönteminin olduğu belirlenmiştir.

Tablo II. 1.1M boyutundaki veri kümesi için sınıflandırma sonuçları (Hata değerleri)

Yöntem (Algoritma)	RMSE	MAE
SVD	**0,20**	0,10
SVD++	0,30	0,22
kNN Kullanıcı-bazlı (User-based)	0,35	0,13
kNN Ürün-bazlı (Item-based)	0,26	**0,09**

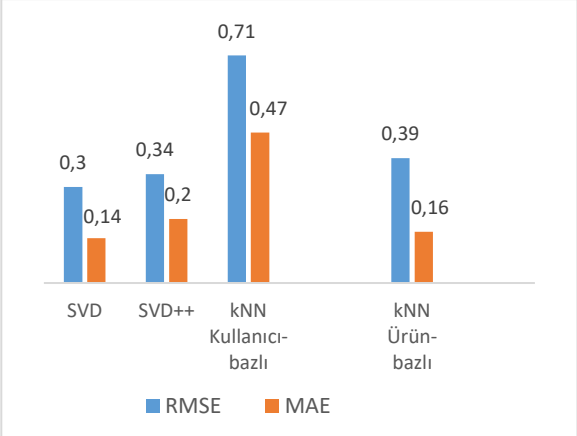

Şekil 1. 100K veri kümesi sınıflandırma sonuçlarının görsel hali

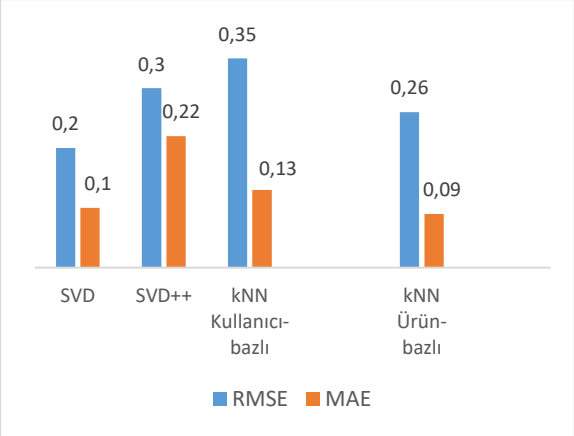

Şekil 2. 1.1M veri kümesi sınıflandırma sonuçlarının görsel hali

III. SONUÇLAR

Ürün tavsiye sistemleri elektronik ticaret sitelerinin kalitesini gösteren ve müşterilere en iyi hizmeti sunmak için oluşturulmuş algoritmalardır. Bir tavsiye sistemi müşterilere en iyi önerileri yapabilmek için onları iyi tanımalıdır. Ayrıca ürünler hakkında bilgileri toplayarak en uygun tavsiyeyi vermeli böylece kullanıcıları ürünleri satın almaya ikna etmelidir. 1.1M veri seti üzerinde tekil değer ayrıştırma, tekil değer ayrıştırma++ ve en yakın komşuluk algoritması yöntemleri test edilmiştir. Kök ortalama karesel hata (root mean square error-RMSE) ve hatanın mutlak ortalaması (mean absolute error-MAE) hata değerleri ölçülmüş sonuçlar karşılaştırılmıştır. Ürün tavsiyesinde SVD yönteminin daha başarılı sonuçlar elde ettiği gözlenmiştir.

BILGILENDIRME

Bu çalışma, 7190894 proje numarasıyla Tübitak tarafından desteklenmiştir. Tübitak'a vermiş olduğu destekten dolayı teşekkürlerimizi sunarız.

Authors' Contributions

The authors' contributions to the paper are equal.

Statement of Conflicts of Interest

There is no conflict of interest between the authors.

Statement of Research and Publication Ethics

The authors declare that this study complies with Research and Publication Ethics.

REFERANSLAR

[1] Oestreicher-Singer, G., and Sundararajan, A. (2012). Recommendation networks and the long tail of electronic commerce. Mis quarterly, pp. 65-83.
[2] Shi, L. (2013). Trading-off among accuracy, similarity, diversity, and long-tail: a graph-based recommendation approach. In Proceedings of the ACM Conference on Recommender Systems (pp. 57-64).
[3] Yin, H., Cui, B., Li, J., Yao, J., and Chen, C. (2012). Challenging the long tail commendation. arXiv preprint arXiv:1205.6700.
[4] Brynjolfsson, E., Hu, Y., and Simester, D. (2011). Goodbye pareto principle, hello long tail: The effect of search costs on the concentration of product sales. Management Science, 57(8), 1373- 1386.
[5] Alshammari, G., Jorro-Aragoneses, J. L., Polatidis, N., Kapetanakis, S., Pimenidis, E., and Petridis, M. (2019). A switching multi-level method for the long tail recommendation problem. Journal of Intelligent and Fuzzy Systems, 37(6), pp. 7189-7198.
[6] Wang, S., Gong, M., Li, H., and Yang, J. (2016). Multi-objective optimization for long tail recommendation. Knowledge-Based Systems, 104, pp. 145-155.
[7] Hu, X., Zhang, C., Wu, M., and Zeng, Y. (2017). Research on long tail recommendation algorithm. In IOP Conference Series: Materials Science and Engineering, vol. 261, no. 1.
[8] Pandey, A. K., and Ankayarkanni, B. (2020). Recommending e-commerce products on cold start and long tail using transaction data. International Conference on Trends in Electronics and Informatics, pp. 661-663.
[9] Abdollahpouri, H., Burke, R., & Mobasher, B. (2018). Popularity-aware item weighting for long-tail recommendation. arXiv preprint :1802.05382.
[10] Wang, Y., Wang, J., & Li, L. (2018). Enhancing Long Tail Recommendation Based on User's Experience Evolution. Int. Conference on Computer Supported Cooperative Work in Design, pp. 25-30.
[11] Zhou, W., and Duan, W. (2012). Online user reviews, product variety, and the long tail: An empirical investigation on online software downloads. Electronic Commerce Research and Applications, 11 (3), pp. 275-289.
[12] Luke, A., Johnson, J., and Ng, Y. K. (2018, November). Recommending long-tail items using extended tripartite graphs. International Conference on Big Knowledge, pp. 123-130.
[13] Agarwal, P., Sreepada, R. S., and Patra, B. K. (2019). A hybrid framework for improving diversity and long tail items in recommendations. International Conference on Pattern Recognition and Machine Intelligence, pp. 285-293.
[14] De Sousa Silva, D. V., De Oliveira, A. C., Almeida, F., and Durão, F. A. (2020). Exploiting Graph Similarities with Clustering to Improve Long Tail Itens Recommendations. Brazilian Symposium on Multimedia and the Web, pp. 193-200.
[15] Cai, Y., Cui, Z., Wu, S., Lei, Z., and Ma, X. (2021). Represent Items by Items: An Enhanced Representation of the Target Item for Recommendation. ArXiv preprint arXiv:2104.12483.
[16] Achary, N. S., and Patra, B. K. (2021). Graph Based Hybrid Approach for Long-Tail Item Recommendation in Collaborative Filtering. ACM IKDD CODS and COMAD (pp. 426-426).
[17] Chen, X., Pan, Y., and Luo, B. (2020). Research on power-law distribution of long-tail data and its application to tourism recommendation. Industrial Management and Data Systems.
[18] Zencirli, A., Çetin, H., Tuğ, N., and Ensari, T. (2021). Deep Learning Classification of Location Oriented Recommendation System for Low-Sale Products. International Congress on Human-Computer Interaction, Optimization and Robotic Applications, pp. 1-4.
[19] Meenakshi, M. (2019). A Novel Approach Web Services Based Long Tail Web Services Using Deep Neural Network. Inte. Conference on Issues and Challenges in Intelligent Computing Techniques, v1, pp 1-9.
[20] Le, D. D., and Lauw, H. (2021). Efficient Retrieval of Matrix Factorization-Based Top-k Recommendations: A Survey of Recent Approaches. Journal of Artificial Intelligence Research, 70, pp. 1441-1479.
[21] Cui, Z., Zhao, P., Hu, Z., Cai, X., Zhang, W., and Chen, J. (2021). An

improved matrix factorization based model for many-objective optimization recommendation. Information Sciences, 579, pp. 1-14.
[22] Gabbolini, G., D'Amico, E., Bernardis, C., and Cremonesi, P. (2021). On the instability of embeddings for recommender systems: the case of Matrix Factorization. In Proceedings of the 36th Annual ACM Symposium on Applied Computing (pp. 1363-1370).
[23] Park, Y. J., and Tuzhilin, A. (2008). The long tail of recommender systems and how to leverage it. ACM conference on Recommender systems, pp. 11-18.
[24] Sundaresan, N. (2011). Recommender systems at the long tail. ACM conference on Recommender systems, pp. 1-6.
[25] Behera, R. K., Gunasekaran, A., Gupta, S., Kamboj, S., and Bala, P. K. (2020). Personalized digital marketing recommender engine. Journal of Retailing and Consumer Services, 53.
[26] Pratama, B. Y., Budi, I., and Yuliawati, A. (2020). Product Recommendation in Offline Retail Industry by using Collaborative Filtering. International Journal of Advanced Computer Science and Applications, 11(9), pp. 635-643.
[27] Valcarce, D., Parapar, J., and Barreiro, A. (2016). Item-based relevance modelling of recommendations for getting rid of long tail products. Knowledge-Based Systems, 103, pp. 41-51.
[28] Zhang, F., Lu, Y., Chen, J., Liu, S., and Ling, Z. (2017). Robust collaborative filtering based on non-negative matrix factorization and R1-norm. *Knowledge-based systems*, *118*, pp. 177-190.
[29] Olmedilla, M., Martínez-Torres, M. R., and Toral, S. L. (2019). The superhit effect and long tail phenomenon in the context of electronic word of mouth. *Decision Support Systems*, *125*, pp. 113-120.
[30] L. Zhaoyang, Matris Ayrışımı, Yüksek Lisans tezi, 2006.

International Journal of Multidisciplinary Studies and Innovative Technologies

e-ISSN: 2602-4888
dergipark.org.tr/en/pub/ijmsit
Research Article

2022, 6 (1), 104-112
DOI: DOI: 10.36287/ijmsit.6.1.104
Received: June 20, 2022; Accepted: July 12, 2022

Hybrid Estimation Model (CNN-GRU) Based on Deep Learning for Wind Speed Estimation

Cem Emeksiz[1*] and Muhammed Musa Fındık[2]

[1*]*Department of Electrical and Electronics Engineering, Tokat Gaziosmanpasa University, Tokat, Turkey (cem.emeksiz@gop.edu.tr) (ORCID: 0000-0002-4817-9607)*
[2]*Department of Electrical and Electronics Engineering, Tokat Gaziosmanpasa University, Tokat, Turkey (fmuhammedmusa@gmail.com) (ORCID: 0000-0003-3786-6089)*

Abstract – Nowadays, the need for energy is increasing day by day. In order to meet this demand, renewable energy sources that have a more environmentally friendly structure than fossil-based sources come to the fore. In recent years, researchers have been paying great attention to wind energy. Because it has the many economic and environmental advantages. In particular, wind speed is very important parameter for electric energy production form wind energy. Therefore, estimation of wind speed is very important for both investors and manufacturers. A hybrid model for wind speed estimation with deep learning methods is proposed in this study. The proposed model consists two main deep learning methods (Convolutional Neural Networks (CNN) and Gated Recurrent Unit (GRU)). The proposed model was applied in two case studies (weekly and monthly wind speed estimation). The reliability and accuracy of the proposed model were tested by performance criteria (MAPE, R^2, RMSE). In order to measure the success of the model, a comparison was made with 5 different deep learning methods (CNN-LSTM, CNN-RNN, LSTM-GRU, LSTM, GRU). It has been observed that the CNN-GRU hybrid model, which was used for the first time in the field of wind speed forecasting, achieved a high percentage of success as a result of comparisons made.

Keywords *– Renewable energy, Wind energy, Wind speed estimation, Deep learning methods, Hybrid estimation model*

Citation: Emeksiz, C., Musa Fındık, M. (2022). Hybrid Estimation Model (CNN-GRU) Based on Deep Learning for Wind Speed Estimation. International Journal of Multidisciplinary Studies and Innovative Technologies, 6(1): 104-112.

I. INTRODUCTION

Energy resources have an extremely important place in the lives of societies in terms of social and economic sustainability. Energy demands are increasing rapidly with the increasing population in the world. However, one of the most important indicators of the social and economic development of countries is energy production and usage [1]. The interest and demand of developed and developing societies for energy has increased with the industrial revolution. This increase continues rapidly in the current century. Meeting the energy needs is important for the survival of societies and individuals [2].

Many of the developing countries still prefer fossil-derived traditional energy sources such as oil, coal and natural gas in order to meet their energy needs and increase their industrialization and production capacities [3]. Despite this, the fact that fossil fuels cannot be supplied in terms of raw materials in the coming centuries, their harmful effects on the environment and their economic disadvantages are very important issues to be considered.

In recent years, renewable energy sources have started to play an active role in meeting the energy needs and demands of societies. Renewable energy sources have low investment costs and are environmentally friendly sources. For this reason, renewable energy sources are of vital importance in order to follow a more sustainable energy policy both environmentally and economically. Renewable energy sources are classified as biomass, solar, wind, geothermal, tidal, hydrogen and hydraulic energy. Among the renewable energy sources, wind energy stands out more than other sources in terms of its advantages [4]. In last decade, the installed capacity of wind energy has been growing increasingly around the world. In 2020, the installed power in the world was reached from 650 GW to 743 GW [5].

Environmental and meteorological conditions should be taken into account in determining the regions planned for the establishment of wind farms. These conditions are wind speed, wind direction, pressure, temperature, etc. consists of parameters. The most important of these parameters is wind speed, because the chaotic behavior of the wind and its discontinuity both increase the production cost and reduce the reliability of the power system [6], [7]. In addition, fluctuations in the wind make it difficult to balance the input and output power in the grid.

Therefore, an accurate wind speed estimation is vital for wind power generation systems. Thus, both the stability of the power systems are ensured and the concerns about the investments to be made in the wind energy industry are eliminated [8], [9]. In recent years, many researchers Many researchers used different estimation models. According to properties of models, these models are divided into basic groups as statistical, physical artificial intelligence and hybrid models, respectively. [10].

Cadenas and Rivera compared autoregressive integrated moving average (ARIMA) and artificial neural networks (ANN) methods. 7 years of wind speed data were used for their study. Data used in the study collected from La Venta, Oaxaca, Mexico [11]. A fractional f-ARIMA model was studied in another study. Researchers of study aimed to estimate wind power generation and wind speed 24 and 48 hours in advance with this model. They compared their results with the persistence model (PM). It was emphasized that the proposed method was more successful [12]. Erdem and Shi estimated wind speed. They used autoregressive moving average (ARMA) models and the accuracy and consistency of these approaches were compared [13]. Ding et al. applied the secondary decomposition method to the wind speed time series in the preprocessing process. They adapted the ARIMA model to the overall structure to make predictions with the decomposed series [14]. Torres et al. estimated the hourly average wind speed by comparing the ARMA and PM model. It was observed that the performance of the ARMA model was better. In particular, it was emphasized that the error rates in the ARMA model were lower [15].

Kalogirou made a feasibility study. He used the ANN in different renewable energy systems. In particular, he focused on solar steam facilities, wind speed estimation, solar radiation photovoltaic systems and solar water heating systems [16]. A new ANN model was proposed in study of Yayla and Harmancı. In the model, two stations were used and estimation process was made by using hourly wind speed data [17]. Wavelet recurrent neural networks (WRNN) were used in another study. Results obtained show that performance of the proposed model is within a defined and acceptable error range [18]. Li estimated wind power generation in his study. Recurrent multilayer perceptron neural networks (RMLP) were used in the study. The Kalman-based back propagation algorithm was tried while the network was being trained. When the estimation results were compared, it was determined that the proposed method for long-term estimation was more beneficial [19].

Nowadays, popular deep learning methods have been commanly prefered in many literature studies for wind speed estimation [20]. Convolutional neural networks (CNN) [21], long-short term memory (LSTM) [22], neural network structural learning [23], recurrent neural network (RNN) [24] Transfer learning [25], etc. These deep learning methods are the most popular ones and used widespread.

LSTM was used to estimate electrical energy demand in other study. Authors created a multi-input and multi-output structure by using the seasonal data in long-term forecasting [26]. A 2D CNN structure was prefered for estimating short- and long-term wind energy in another study. Also data used in study were preprocessed bu using wavelet transform. A particle swarm optimization algorithm was preferred to determine the CNN weights [27]. An attention-based gated repetitive unit (AGRU) method was used for estimating short-term wind energy in the study of Niu et al. [28]. In another study, time series data were decomposed. Classification and complexity were calculated using decomposed data. LSTM and fuzzy entropy were used to perform these operations [29].

In presented study, a hybrid model based on deep learning was proposed as an alternative to the classical methods used in wind speed estimation. The proposed hybrid model consists of Gated Recurrent Unit (GRU) neural network and Convolutional Neural Network (CNN). Similarly, although there are literature studies using independent deep learning methods, the hybrid structure created was tried for the first time in the field of wind speed estimation. This situation constitutes the original and innovative aspect of the study. In addition, the hybrid estimation model obtained by using deep learning methods showed better performance in wind speed estimation. The proposed model has been compared with 5 different deep learning methods. It has been observed that the proposed model gives more accurate and reliable results in all comparisons. Mean Absolute Percentage Error (MAPE), Coefficient of Determination (R^2), Root Mean Square Error (RMSE), which are widely used in the literature, as performance metrics, were preferred.

II. Materials and Method

The combination of Convolutional Neural Network and Gated Repetitive Unit (CNN-GRU) was preferred in the creation of the proposed hybrid model for wind speed estimation. As mentioned earlier, this combination is used for the first time in wind speed estimation. Similarly, it was tested with combinations in other literature studies in which deep learning methods were used together. The structures commonly used in the literature and tested in comparison with the proposed model are CNN-LSTM, CNN-RNN and LSTM-GRU was selected. Moreover, these methods were also used independently in estimation, and the estimation performance was compared. The structures that make up the proposed hybrid model, the acquisition of data and the preprocessing steps applied to the data are explained in detail in the following sections. In addition, experimental studies were carried out using MATLAB software on a computer with an Intel i7 processor, a 1650ti graphics card, and a 16 gigabyte RAM capacity.

A. Data collection and preprocessing

The measurement station established in Tokat Gaziosmanpasa University Taslıciftlik Campus. All wind speed data used in study were collected this station. The measurement mast of the measurement station from which the wind speeds are obtained is given in Figure 1. The measuring mast is 12m and has 1 wind direction measurement sensor and 2 wind speed measurement sensors on it. Pressure and temperature sensors are located inside the power box located at the bottom of the measuring mast. The energy needed for the sensors is met by a solar panel with a power of 10 W. In addition, a marina type AIRX-400W wind turbine was placed on the wind turbine measurement mast to be used in the wind power analysis studies planned later.

The wind speed data used in the study were collected at 1-hour intervals, and a 3-year data (2018-2020) set was used. The collected data were divided into groups on average weekly, and monthly. Normalization process was applied between 0-1 in order to eliminate noise-containing values from the separated data and to obtain a clearer result. The normalization process is extremely important in order to determine the data ranges for more accurate analysis and also to increase the success of the regression process. Normalization process is applied in order to transform the data into a more regular format. The operations given in Equation 1 are applied to linearly normalize the data [30].

$$x' = \frac{x_i - x_{min}}{x_{max} - x_{min}} \quad (1)$$

x' represents the normalized data. x_i represents the data to be normalized. x_{min} and x_{max} represent the lowest value and the highest value in the data, respectively.

Fig. 1. Measurement station

Average weekly and monthly histogram graphs of wind speed data obtained by grouping and normalization process were created. Figure 2 and 3 show the histogram distribution graph and the variation of the average weekly wind speeds.

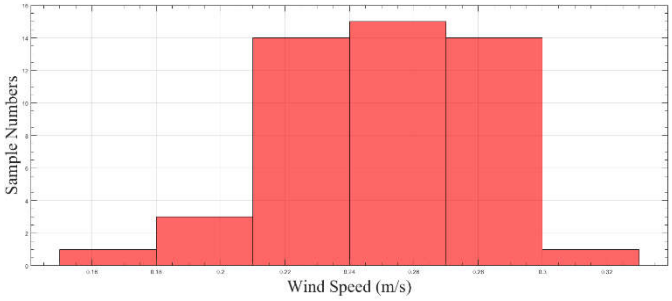

Fig. 2. Histogram distribution of average weekly wind speeds

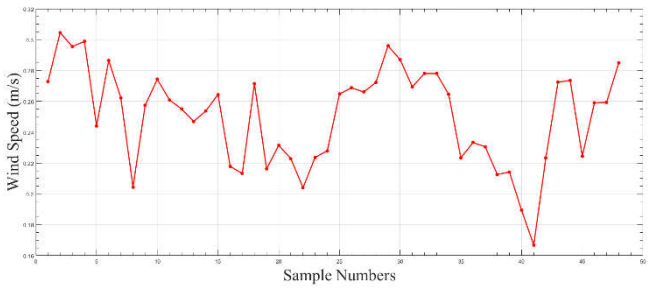

Fig. 3. Average weekly wind speeds

While creating the weekly data, grouping was made in the first 4 weeks of each month in order to provide a standard in the analyzes and to be compatible with the literature studies. Thus, an average of 48 weekly data sets were created. The main purpose of estimating on average weekly data is to observe the effect of low number of data sets on network performance. In this data set, 36 (75%) wind speed data were used for training and 12 (25%) wind speed data were used for testing.

Figures 4 and 5 show the histogram distribution graph and variation of monthly average wind speeds. While creating this data set, a total of 8760 wind speed data were used by taking the averages of each month of the 3 years. Of these data, 6570 (75%) data belonging to the first 9 months were separated as training data, and the average monthly data for the last 3 months of 2190 (25%) as test data.

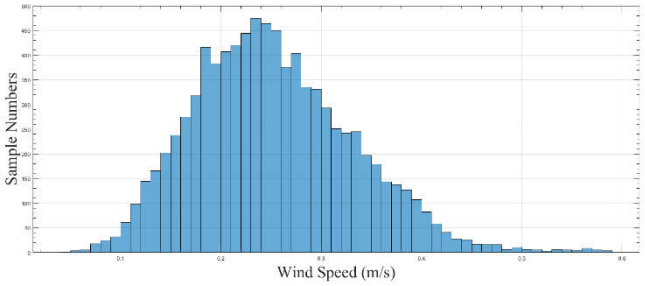

Fig. 4. Histogram distribution of average monthly wind speeds

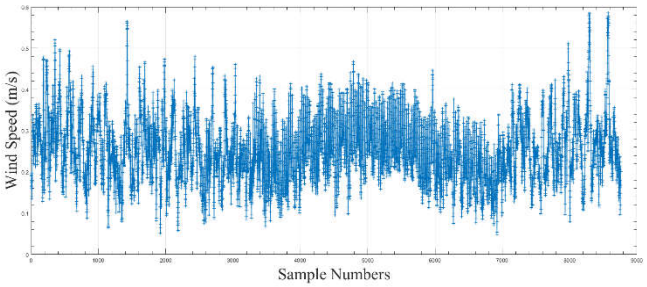

Fig. 5. Average monthly wind speeds

B. *Convolutional Neural Networks (CNN)*

Convolutional Neural Networks (CNN) is a deep neural network structure that can operate in many areas such as classification, identification, prediction [31] and many other deep learning methods [32]. These used methods draw attention with their high classification accuracy [33], [34]. CNN is an architecture inspired by artificial neural networks and can learn end-to-end information collected. CNN can also handle large-scale data thanks to its sufficient capacity and smart model structure. The advantages of convolutional neural networks can be listed as separating objects from the background without applying preprocessing, providing higher performance compared to image identification processes with traditional methods, and predicting with high accuracy in time-series-based operations. The disadvantages of CNN are the long training period, the need for powerful Graphics Processing Unit (GPU) cards and high memory capacities.

Convolutional neural networks consist of more than one parameter and layer. Its layered structure enables it to achieve very successful results in attribute determination [35]. Convolutional neural network architecture is given in Figure 6. There are two basic layers in CNN. One is the

convolution layer and the other is the pooling layer. CNNs aim to extract the important features of the image with some basic operations in these two layers [34].

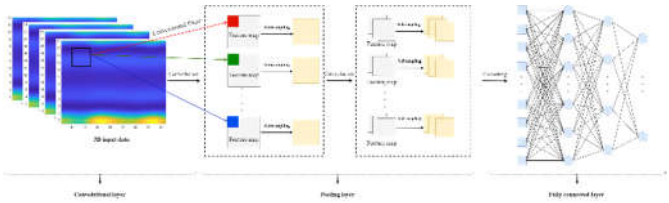

Fig. 6. CNN architectural structure [36]

The convolution operation is the process of convoluting the image filter with initially random values with the input image. The convolution layer is the basic building block of CNN, which is not found in traditional ANN. Instead of connecting the cells in all layers and renewing the connection weights, the convolution process is used in small regions. The output is a powerful algorithm presented to solve the over-learning problem, which reduces the overall error of the large neural network. In a dropout algorithm, a single neuron does not rely on the formation of other neurons, thus reducing the neuron's adaptation complexity. Thus, CNN was developed to learn more robust features and stable structure [37-41]. The term of dropout means that not including some of the units in a neural network in the next layer. The proposed hybrid model was obtained by combining two-dimensional CNN and GRU networks and the parameters of the hybrid model were summarized in Table 1.

Table 1. Model parameters

Convulation Layer 1	Filter size: 32 Mini Batch size: 64
Convulation Layer 2	Filter size: 32 Mini Batch size: 64
Convulation Layer 3	Filter size: 32 Mini Batch size: 64
Convulation Layer 4	Filter size: 32 Mini Batch size: 64
Convulation Layer 5+ Pooling	Filter size: 32 Mini Batch size: 64 Pooling method: Average pooling
GRU Layer	Filter size: 128 Mini Batch size: 64 Dropout: 0.25

C. Gated Repeating Unit (GRU)

Nowadays, there are many different variations of the LSTM architecture. One of these variations, and generally the most preferred, is the Gated Repetitive Unit (GRU). It aims to solve the disappearing gradient problem that comes with the classical recurrent neural network. GRU and LSTM are designed similarly, so they can produce very successful results [42].

In the structure of the GRU architecture, the forget gate and the entrance gate are combined. Basically, these are two vectors that decide what information should be passed to the output. What's special about gates is that they can be trained to hide information long before it washes out information over time or deletes non-predictive information.

The gated repetitive unit, for example in speech recognition, is part of a particular recurrent neural network model that aims to use connections through a series of nodes to perform machine learning tasks associated with memory and clustering. The gated recurrent unit helps to adjust the neural network input weights to solve the vanishing gradient problem, which is frequently encountered in recurrent neural networks [43]. The GRU architecture is presented in Figure 7.

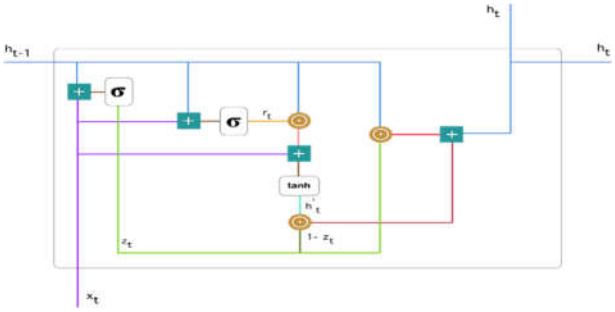

Fig. 7. Gated repetitive unit architecture [44]

The port update process takes first place in GRUs. The z_t update gate is calculated with the formula given below.

$$z_t = \sigma(W^{(z)}x_t + U^{(z)}h_{t-1}) \quad (1)$$

When x_t is added to the mesh unit, its own weight is multiplied by $W^{(z)}$. The update gate helps the model determine how much of the historical information from previous time steps should be forwarded [45]. The model provides great advantages such as copying all the information from the past and eliminating the lost gradient problem [44]. In Figure 8, the gate update process in the GRU architecture is modeled.

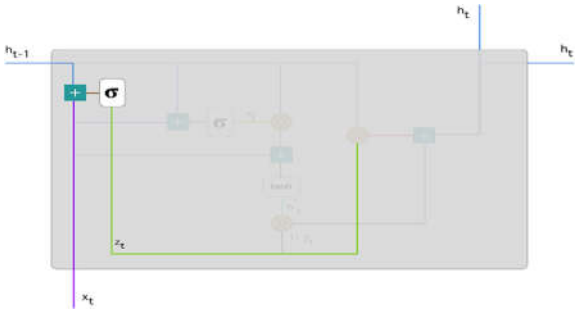

Fig. 8. GRU gate update [44]

The reset gate is used to decide how much of the past information on the model will be forgotten. This process is performed with Equation 2 [42].

$$r_t = \sigma(W^{(r)}x_t + U^{(r)}h_{t-1}) \quad (2)$$

The formula used is the same as the update gate. The difference between the formulas is in the weight and usage of the stage. Figure 9 shows where the reset gate is located.

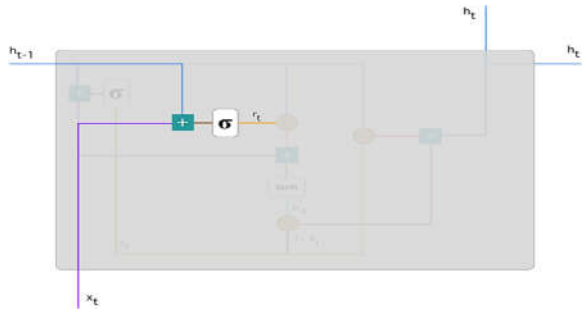

Fig. 9. Reset gate [44]

As in the previous operations, the weights corresponding to h_{t-1} and x_t values are multiplied and the results are summed, and then the sigmoid function is applied. If it is taken a look at exactly how the gates will affect the final output in the current memory context; firstly, it is started with the usage of the reset gate. A new memory context is introduced that will use the reset port to store relevant information from the past.

The operations given in Equation 3 are applied sequentially. The current memory operation is shown in Figure 10.

$$h'_t = \tanh(Wx_t + r_t \cdot Uh_{t-1}) \quad (3)$$

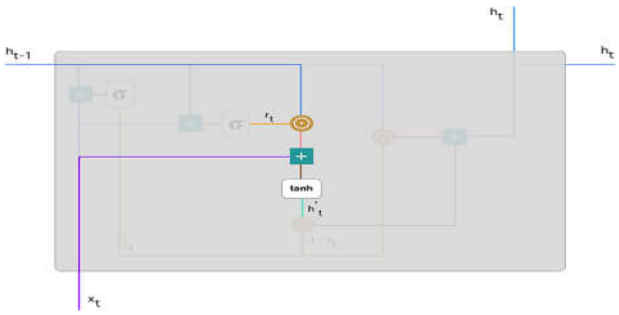

Fig. 10. Current memory operation [44]

r_t and h_{t-1} are multiplied. After that the result obtained is summed with input x_t. h'_t is produced by using tanh function.

As a final step, the network has to calculate the h_t vector, which holds the information for its current unit and transmits it to the network by using Equation 4. In order to do this, the update port is needed. Determines what to collect from the current memory content.

$$h_t = z_t \cdot h_{t-1} + (1 - z_t) \cdot h'_t \quad (4)$$

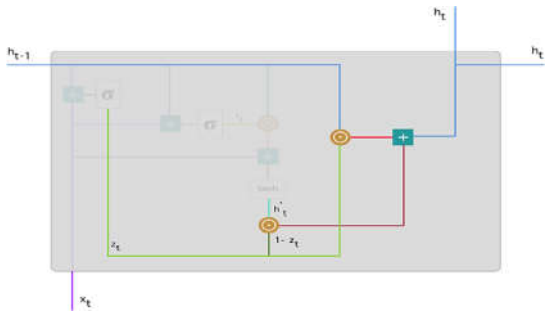

Fig. 11. Calculation of the function that holds and transmits information for the current unit [44]

$1 - z_t$ is calculated by using z_t according to Figure 11. It produces a result in the dark red line combined with h'_t. z_t is also multiplied with h_{t-1} blue line in item-by-item multiplication. Finally, the h_t blue line is obtained as a result of the sum of the outputs corresponding to the red lines in Figure 11.

III. Results

The hybrid CNN-GRU model proposed in the study was used independently for weekly and monthly wind speed estimations. The results obtained were interpreted and evaluated according to performance metrics. In addition, the performance of the hybrid model used in 2 separate case studies was compared with GRU, LSTM, LSTM-GRU, CNN-LSTM and CNN-RNN network structures. The results of the case studies are presented in detail in the following sections.

A. First Case Study

The hybrid estimation model proposed for weekly estimation, which constitutes the first stage of the study, performed the estimation process with a higher accuracy rate than the other models as a result of the analyzes made. The performance of both the proposed hybrid model and other models is presented in Table 2. The RMSE value in the proposed hybrid model is 0.0306, and the closest value to this error value was obtained with the LSTM model. The highest error rate occurred in the standalone GRU model. The variation of the error metrics of the models and the regression rates are clearly seen in Figure 12.

Table 2. Performance comparison of weekly estimation

Metrics	**CNN-GRU**	**LSTM**	**LSTM-GRU**
RMSE	**0.0306**	0.0309	0.0397
R^2	**0.9841**	0.983	0.9732
MAPE	**0.1106**	0.1165	0.1395
Metrics	**GRU**	**CNN-LSTM**	**CNN-RNN**
RMSE	0.0695	0.0387	0.0483
R^2	0.9142	0.9769	0.9681
MAPE	0.227	0.1254	0.1746

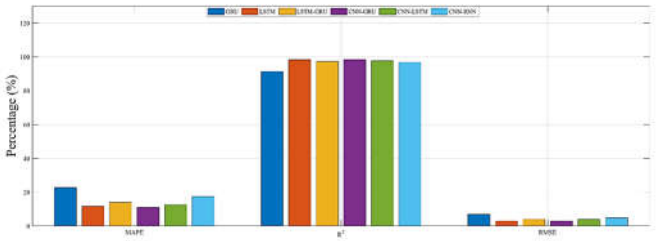

Fig. 11. Performance graph of weekly estimation

It is showed that the comparison of the estimated wind speed changes and the actual wind speed changes in Figure 12 – 17 for all models. When the estimation graphics of the models are examined; The change in the 12-week data group, which was estimated from the 48-week data set, is seen.

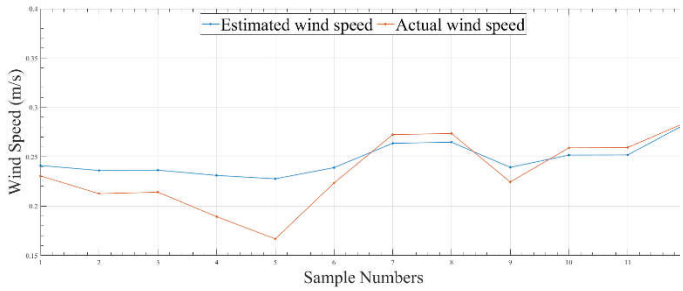

Fig. 12. Estimation graph of CNN-GRU

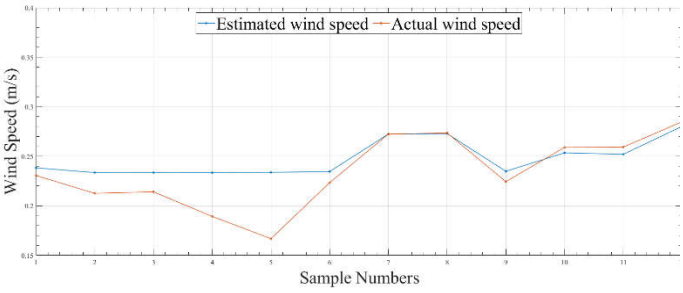

Fig. 13. Estimation graph of CNN-LSTM

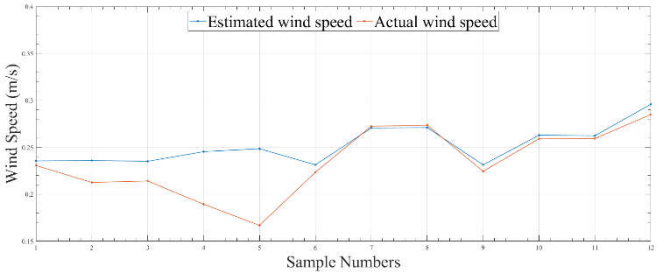

Fig. 14. Estimation graph of CNN-RNN

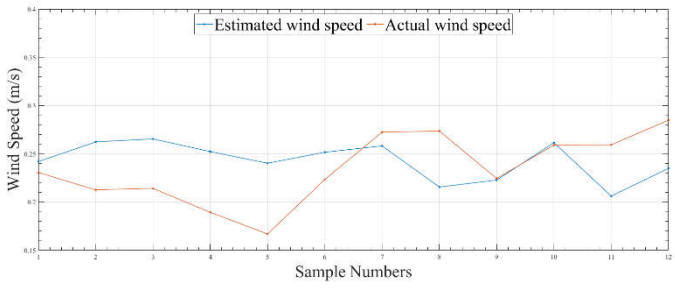

Fig. 15. Estimation graph of LSTM-GRU

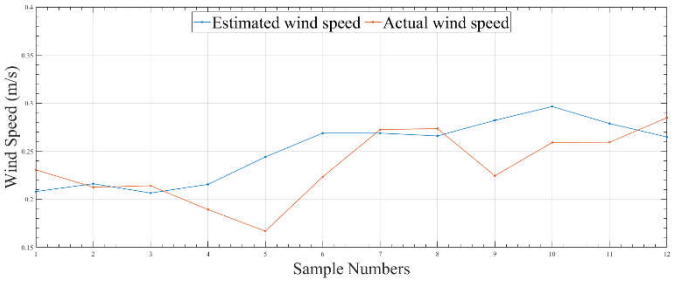

Fig. 16. Estimation graph of GRU

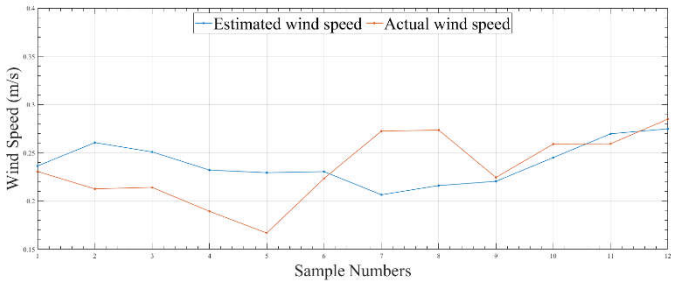

Fig. 17. Estimation graph of LSTM

Also, the aggregate variation of both the actual and the estimated wind speed data is shown in Figure 18. When Figure 18 is examined, it is seen that the proposed model exhibits a trend closer to the actual wind speed data change.

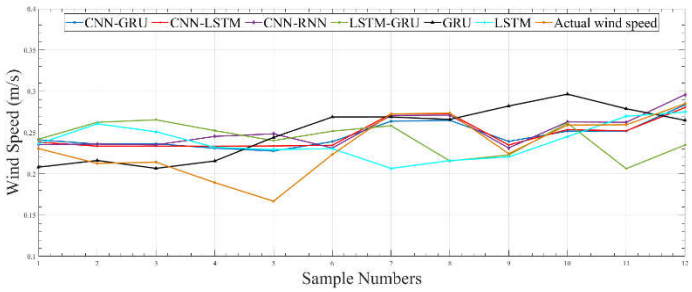

Fig. 18. Variation of actual wind speed and predicted wind speed for all models

B. Second Case Study

The performance of both the proposed hybrid model and other models is presented in Table 3. The RMSE value obtained with the proposed hybrid model is 0.0127, and the closest value to this error value was obtained with the CNN-LSTM model. The highest error rate occurred in the LSTM-GRU model. The variation of the error metrics of the models and the regression rates are clearly seen in Figure 19.

Table 3. Performance comparison of monthly estimation

Metrics	**CNN-GRU**	**LSTM**	**LSTM-GRU**
RMSE	**0.0127**	0.097	0.1194
R^2	**0.9977**	0.8658	0.7966
MAPE	**0.0409**	0.3492	0.3544
Metrics	**GRU**	**CNN-LSTM**	**CNN-RNN**
RMSE	0.1087	0.0189	0.0206
R^2	0.8316	0.9923	0.9893
MAPE	0.3797	0.0498	0.0526

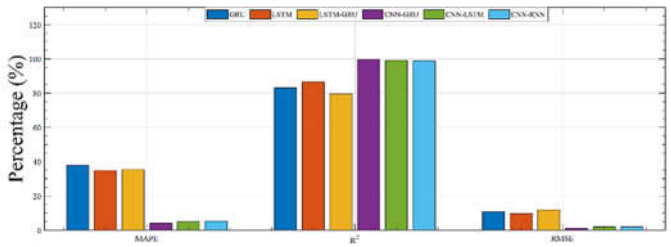

Fig. 19. Performance graph of weekly estimation

It is showed that the comparison of the estimated wind speed changes and the actual wind speed changes in Figure 20 – 25 for all models. In addition, the estimation results in the proposed hybrid model show a behavior closer to the change of actual wind speed data. It was determined that the model memorizes and oscillates continuously in a certain range in the estimations made in these models as a result of the examination of the LSTM-GRU, GRU and LSTM (Figure 23-25) graphs.

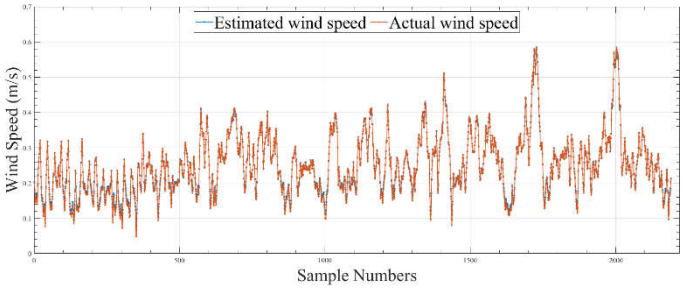

Fig. 20. Estimation graph of CNN-GRU

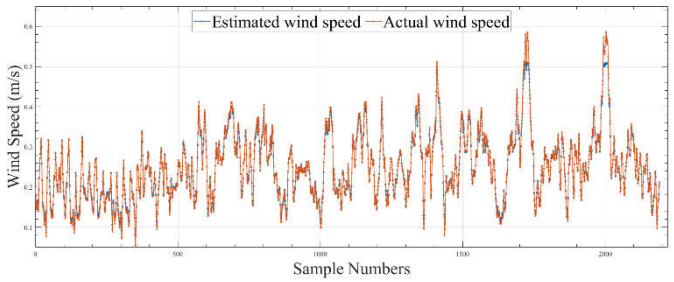

Fig. 21. Estimation graph of CNN-LSTM

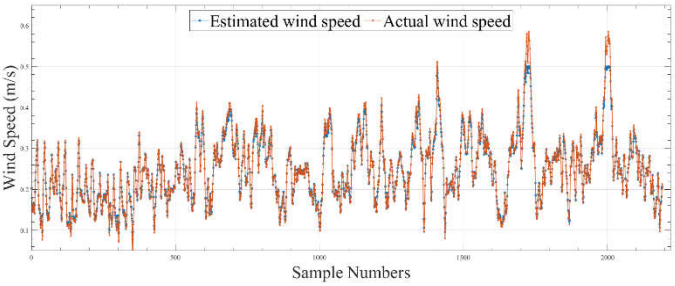

Fig. 22. Estimation graph of CNN-RNN

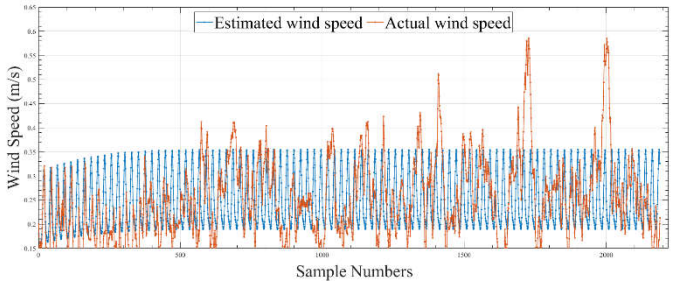

Fig. 23. Estimation graph of LSTM-GRU

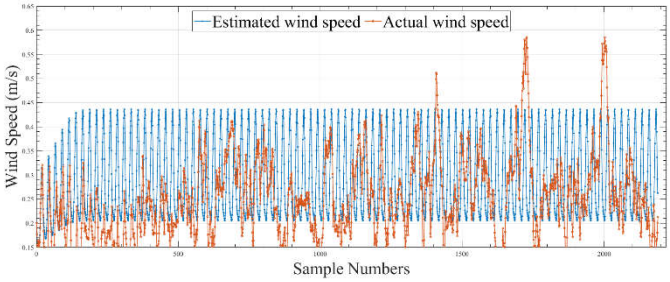

Fig. 24. Estimation graph of GRU

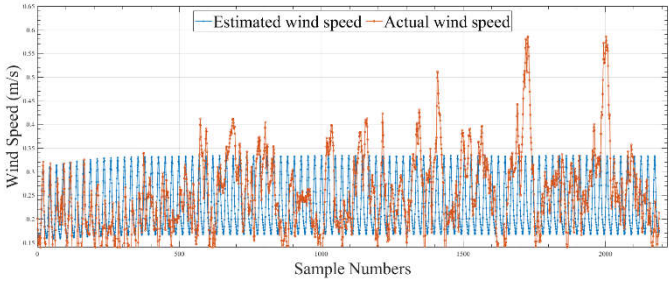

Fig. 25. Estimation graph of LSTM

IV. DISCUSSION

Nowadays, energy has an extremely important place in consumer societies. Energy is needed for the development of societies and a sustainable life. Many successful models in which economic and environmentally friendly approaches are used to meet the increasing energy demands have come to a very important point today. Especially in the field of renewable energy, very important studies and progress have been made in recent years. Considering the advantages of wind energy, which is among these sources, it is seen that it is preferred more than other sources. Wind speed is very important parameter for electric energy production form wind energy. This allows researchers to develop different and useful models in the field of wind speed estimation so that wind energy can be used more efficiently. Therefore, in this study, a hybrid estimation model, which is used for the first time for wind speed estimation, is proposed by using deep learning methods. The proposed hybrid model was used in the estimation process separately in 2 case studies and its performance in these case studies was evaluated according to the determined performance criteria (MAPE, R^2, RMSE). In addition, the performance of the proposed model was compared with 5 different deep learning models in the literature (CNN-LSTM, CNN-RNN, LSTM-GRU, GRU, LSTM) in order to make the interpretation of the performance more meaningful.

In the results obtained in the weekly wind speed estimation process, which constitutes the first case study, it was observed that the hybrid model showed more accurate and reliable results (MAPE: 0.1106, RMSE: 0.0306, R2: 0.9841).

In the monthly wind speed estimation that constitutes the second case study, it is clearly seen that the proposed hybrid model outperforms the other models according to the obtained performance criteria (MAPE: 0.0409, RMSE: 0.0127, R^2: 0.9977). It was observed that in some models (LSTM-GRU, LSTM, GRU) used for comparison purposes in monthly wind speed estimation, the structure goes to memorization rather than estimation.

In this study, it was seen that the hybrid model proposed for the first time for wind speed estimation showed more

successful results. In particular, the obtained results were compared with other models used in the literature and validation was performed. One of the important inferences obtained in the study is that the independent use of the models to be preferred especially in the field of wind speed estimation results in higher error results. The other is emphasized that hybrid forecasting models should be preferred more. Another inference is that the more preferred deep learning methods, especially used in the field of image processing, also show successful results in numerical estimation processes. For this reason, it is planned to evaluate the performance with different data pre-processing methods to be applied to the data in addition to the estimation model proposed in the planned studies for the future.

Authors' Contributions

The authors' contributions to the paper are equal.

Statement of Conflicts of Interest

There is no conflict of interest between the authors.

Statement of Research and Publication Ethics

The authors declare that this study complies with Research and Publication Ethics

REFERENCES

[1] M. Tan, "Multi-step wind speed estimation based on artificial neural network using secondary separation technique", Master's Thesis, Tokat Gaziosmanpasa University, 2020.

[2] C. Emeksiz and M. M. Fındık, "Evaluation of Renewable Energy Resources for Sustainable Development in Turkey", *European Journal of Science and Technology*, (26), 155-164, 2021.

[3] A. Yüksel, "A suitable site selection for sustainable bioenergy production facility by using novelty hybrid multi criteria decision making approach", Master's Thesis, Tokat Gaziosmanpasa University, 2020.

[4] Albostan, A., Çekiç, Y., and Levent, E., "Effect of Wind Energy on Turkey`s Energy Supply Security", J. Fac. Eng. Arch. Gazi Univ., Vol 24, No 4, 641-649, 2009.

[5] REN21, Renewable Energy Global Status Report 2021. https://www.ren21.net/reports/global-status-report/ (accessed May. 03, 2022).

[6] X. He, L. Chu, R. C. Qiu, Q. Ai, Z. Ling, and J. Zhang, J. "Invisible units detection and estimation based on random matrix theory", *IEEE Transactions on Power Systems*, 35(3), 1846-1855, 2019.

[7] B. Yang, T. Yu, H. Shu, J. Dong, and L. Jiang, "Robust sliding-mode control of wind energy conversion systems for optimal power extraction via nonlinear perturbation observers", *Applied Energy*, 210, 711-723, 2018.

[8] B. Yang, X. Zhang, T. Yu, H. Shu, and Z. Fang, "Grouped grey wolf optimizer for maximum power point tracking of doubly-fed induction generator based wind turbine", *Energy Conversion and Management*, 133, 427-443, 2017.

[9] M. W. Zafar, M. Shahbaz, A. Sinha, T. Sengupta, and Q. Qin, "How renewable energy consumption contribute to environmental quality? The role of education in OECD countries", *Journal of Cleaner Production*, 268, 122149, 2020.

[10] S. K. Aggarwal and M. Gupta, "Wind power forecasting: a review of statistical models", *Int J Energy Sci.*, 3(1):1-10, 2013.

[11] E. Cadenas, and W. Rivera, "Wind speed forecasting in the south coast of Oaxaca, Mexico", *Renewable Energy*, 32(12), 2116-2128, 2007.

[12] R. G. Kavasseri, and K. Seetharaman, "Day-ahead wind speed forecasting using f-ARIMA models", *Renewable Energy*, 34(5), 1388-1393, 2009.

[13] E. Erdem, and J. Shi, "ARMA based approaches for forecasting the tuple of wind speed and direction", *Applied Energy*, 88(4), 1405-1414, 2011.

[14] M. Ding, H. Zhou, H. Xie, M. Wu, K. Z. Liu, Y. Nakanishi, Y. and R. Yokoyama, "A time series model based on hybrid-kernel least-squares support vector machine for short-term wind power forecasting", *ISA Transactions*, 108(2021), 58-68, 2021.

[15] J. L. Torres, A. Garcia, M. De Blas, and A. De Francisco, "Forecast of hourly average wind speed with ARMA models in Navarre (Spain)", *Solar Energy*, 79(1), 65-77, 2005.

[16] S. A. Kalogirou, "Artificial neural networks in renewable energy systems applications: a review", *Renewable and Sustainable Energy Reviews*, 5(4), 373-401, 2001.

[17] S. Yayla, E. Harmanci, "Estimation of target station data using satellite data and deep learning algorithms", *International Journal of Energy Research*, 45(1), 961-974, 2021.

[18] G. Capizzi, C. Napoli, and F. Bonanno, "Innovative second-generation wavelets construction with recurrent neural networks for solar radiation forecasting", *IEEE Transactions on neural networks and learning systems*, 23(11), 1805-1815, 2012.

[19] S. Li, "Wind power prediction using recurrent multilayer perceptron neural networks", *In 2003 IEEE Power Engineering Society General Meeting*, Toronto, 2003.

[20] B. Yang, L. Zhong, J. Wang, H. Shu, X. Zhang, T. Yu, and L. Sun, "State-of-the-art one-stop handbook on wind forecasting technologies: An overview of classifications, methodologies, and analysis", *Journal of Cleaner Production*, 283(2021), 124628, 2021.

[21] X. Zhao, N. Jiang, J. Liu, D. Yu, and J. Chang, "Short-term average wind speed and turbulent standard deviation forecasts based on one-dimensional convolutional neural network and the integrate method for probabilistic framework", *Energy Conversion and Management*, 203(2020), 112239, 2020.

[22] H. Li, J. Wang, H. Lu, and Z. Guo, "Research and application of a combined model based on variable weight for short term wind speed forecasting", *Renewable Energy*, 116(2018), 669-684, 2018.

[23] X. Mi, and S. Zhao, "Wind speed prediction based on singular spectrum analysis and neural network structural learning", *Energy Conversion and Management*, 216(2020), 112956, 2020.

[24] L. Cheng, H. Zang, T. Ding, R. Sun, M. Wang, Z. Wei, and G. Sun, "Ensemble recurrent neural network based probabilistic wind speed forecasting approach", *Energies*, 11(8), 1958, 2018.

[25] Q. Hu, R. Zhang, and Y. Zhou, "Transfer learning for short-term wind speed prediction with deep neural networks", *Renewable Energy*, 85(2016), 83-95, 2016.

[26] J. Bedi, and D. Toshniwal, "Deep learning framework to forecast electricity demand", *Applied Energy*, 238(2019), 1312-1326, 2019.

[27] O. Abedinia, M. Bagheri, M. S. Naderi, and N. Ghadimi, "A new combinatory approach for wind power forecasting", *IEEE Systems Journal*, 14(3), 4614-4625, 2020.

[28] Z. Niu, Z. Yu, W. Tang, Q. Wu, and M. Reformat, "Wind power forecasting using attention-based gated recurrent unit network", *Energy*, 196(2020), 117081, 2020.

[29] A. Mardani, A. Jusoh, E. K. Zavadskas, F. Cavallaro, and Z. Khalifah, "Sustainable and renewable energy: An overview of the application of multiple criteria decision making techniques and approaches", *Sustainability*, 7(10), 13947-13984, 2015.

[30] İ. Demir, "Wind speed estimation by effective parameters using different regression models", Master's Thesis, Tokat Gaziosmanpasa University, 2019.

[31] P. Carcagni, A. Cuna, and C. Distante, C., "A Dense CNN approach for skin lesion classification" arXiv preprint arXiv:1807.06416, 2018.

[32] O. Sevli, "Evrişimsel Sinir Ağları ile Bal Arısı Irklarının Tahminlenmesi", *In Proceedings on 2nd International Conference on Technology and Science*, Vienna, 2019.

[33] X. W. Gao, R. Hui, and Z. Tian, "Classification of CT brain images based on deep learning networks", *Computer Methods and Programs in Biomedicine*, 138, 49–56, 2017.

[34] B. Ari, A. Sengur, A. Ari, and D. Hanbay, "Apricot Plant Classification Based On Leaf Recognition by Using Convolutional Neural Networks", *International Conference on Natural Science and Engineering (ICNASE'16)*, Kilis, Turkey, 19-20 March, 2016.

[35] E. Somuncu and N. A. Atasoy, "Evrişimli tekrarlayan sinir ağı ile metin görüntüleri üzerinde karakter tanıma uygulaması gerçekleştirilmesi", *Journal of the Faculty of Engineering & Architecture of Gazi University*, 37(1), 17-27, 2022.

[36] C. Emeksiz and M. Tan, "Wind speed estimation using novelty hybrid adaptive estimation model based on decomposition and deep learning methods (ICEEMDAN-CNN)", *Energy* 249, 123785, 2022, https://doi.org/10.1016/j.energy.2022.123785.

[37] Ü. Budak, "Detection of airport in satellite images", Master's Thesis, Fırat University, 2017.

[38] G. Hinton, S. Osindero, and Y. Teh, "A Fast Learning Algorithm for Deep Belief Nets, Neural Computation," 18(7), 1527-1554, 2006.

[39] A. Ulu, "Deep Convolutıonal Neural Network Based Representatıons For Person Re-Identıfıcatıon", Master's Thesis, Istanbul Technıcal Unıversıty, 2016.

[40] M. Havaei, A. Davy, D. Warde-Farley, A. Biard, A. Courville, Y. Bengio, C. Pal, P. M. Jodoin, and H. Larochelle, "Brain tumor segmentation with deep neural networks," *Medical Image Analysis*, 35, 18– 31, 2017.

[41] N. Alpaslan, A. i . Kara, B. Zencir, and D. Hanbay, "Classification of breast masses in mammogram images using KNN," *Signal Processing and Communications Applications Conference (SIU)*, 1469-1472, Malatya, Türkiye,16-19 Mayıs 2015.

[42] P. Görgel and E. Kavlak, "Uzun kısa süreli hafıza ve evrişimsel sinir ağları ile rüzgar enerjisi üretim tahmini", *Dicle Üniversitesi Mühendislik Fakültesi Mühendislik Dergisi*, 11(1), 69-80, 2020.

[43] H. Ahmetoğlu and D. Resul, "Türkçe Otel Yorumlarıyla Eğitilen Kelime Vektörü Modellerinin Duygu Analizi ile İncelenmesi", *Süleyman Demirel Üniversitesi Fen Bilimleri Enstitüsü Dergisi*, 24(2), 455-463, 2020.

[44] S. Kostadinov, "Understanding GRU Networks", 2017. https://towardsdatascience.com/understanding-grunetworks 2ef37df6c9be. (accessed April. 22, 2022).

[45] R. Dey and F. M. Salem, "Gate-variants of gated recurrent unit (GRU) neural networks", *In 2017 IEEE 60th international midwest symposium on circuits and systems (MWSCAS)*, Boston, 2017.

International Journal of Multidisciplinary Studies and Innovative Technologies

e-ISSN: 2602-4888
dergipark.org.tr/en/pub/ijmsit
Research Article

2022, 6 (1), 113-116
DOI: DOI: 10.36287/ijmsit.6.1.113
Received: June 5, 2022; Accepted: July 17, 2022

FLOOD FORECASTING USING NEURAL NETWORK: APPLYING THE LSTM NETWORK IN THE MOSUL REGION. IRAQ

ABDULLAHI ABDU IBRAHIM[1*], AYAD KHALAF JIRRI HALBOOSH [2]

[1]*Computer Engineering Department, Institute of Graduate Studies, ALTINBAS UNIVERSITY, Istanbul, Turkey*
[2]*Information Technology Department, Institute of Graduate Studies, ALTINBAS UNIVERSITY, Istanbul, Turkey*
[*]*Corresponding author: Abdullahi.ibrahim@altinbas.edu.tr*

Abstract – Flooding is one of the most dangerous natural causes that inflict harm to both life and property on a yearly basis. Therefore, building a flood model for predicting the immersion zone in a watershed is critical for decision-makers. Floods are a perilous tragedy that annually threatens Iraq and the Middle East region, impacting millions of people. In this context, having suitable flood forecasting algorithms may help people by reducing property damage and saving lives by warning communities of potentially severe flooding events ahead of time. Data mining techniques such as artificial neural network (ANN) approaches have recently been applied to model floods. The purpose of this study is to develop a model that extrapolates the past into the future using existing statistical models and recurrent neural networks and is powered by rainfall forecasting data. We investigate a number of time series forecasting approaches, including Long Short-Term Memory (LSTM) Networks. The forecasting methods investigated are tested and implemented using rainfall data from the Mosul region of Iraq. In addition, in flood occurrences and conducting experiments to study the relationship between rainfall and floods.

Keywords *– Artificial-Neural-Network, Long Short-Term Memory, Rainfall, Forecasting, Floods*

Citation: Ibrahim, A.A., Halboosh, A.K.J. (2022). Flood Forecasting Using Neural Network: Applying the LSTM Network in the Mosul Region. Iraq. International Journal of Multidisciplinary Studies and Innovative Technologies, 6(1): 113-116.

I. INTRODUCTION

The study's background is that the geography of Mosul, Iraq, features specific patterns of flood vulnerability that have contributed to intensifying and different patterns of flooding. This study is applied to one place, Mosul, as a proof of concept, although the results might be more beneficial for flood predictions in general.

A flood estimate exhibit will be critical in displaying essential facts about the possibility of unavoidable flooding in populous areas. By constructing such models, disruption in ranges like Mosul may be reduced by reducing the financial and environmental costs of floods. More precisely, the prediction approach designed for South Asia, particularly the Mosul region, will reduce the likelihood of suffering and tragedy in life. If applying LSTM's artificial neural network (ANN) models can provide realistic nitty-gritty expectations, the lead time for flood caution may be increased by one day, and the subsequent flood emergency procedures can be encouraged and boosted.

The primary objective of this research is to investigate and develop bogus neural systems using LSTM Arrange that can be used as a demonstration in an environment such as the city of Mosul as shown in figure (1) to estimate the commencement of floods. Several types of constructed neural network models are examined in order to determine the neural organization characteristics that will have the best estimate for unavoidable floods, including their designs and modifications of associated learning laws.

Fig. 1 Map of Iraq

number of sub-goals were established in order to reach this conclusion. The sub-goal is to show how artificial neural networks (LSTM Arrange) can be used to estimate floods using meteorological data in a reliable and lucrative manner. To define the neural organization architecture that will deliver the greatest anticipated precipitation consequences.

II. Materials and Method

The proposed LSTM flood assessment (LSTM-FF) system is composed of multivariate single-step LSTM systems that acknowledge spatial and common component data from real and anticipated precipitation and early release as inputs. The Mosul case considered, it appears that the proposed models can expect streak surges, especially enormous surge events, with high precision (the degree of the number of qualified occasions to the common number of surge occasions).

Small floods can assist the LSTM-FF consummate in investigating a better rainfall-runoff link for large flood simulations. According to the load impact study in LSTM network topologies, the discharge input has a bigger influence on the 1-hour LSTM network and this influence diminishes with lead-time. Meanwhile, the LSTM networks investigated a similar association in the prior lead-time.

The LSTM surge determining (LSTM-FF) show, which is made up of T multivariate single-step LSTM systems, is outlined for figure release with a 1 hr. lead-time. Each release is anticipated employing a particular LSTM arrangement, as seen in Figure (1). Observations: a. show and past (1 hour, 2-hour, H hour lag) precipitation at each rain station; b. prior discharge at the outlet; and (2) gauge short-term expected precipitation with a T-hour lead-time.

The observed inputs are represented by $X_{t-H}, \ldots, X_{t-1}, X_t$, while the forecasting inputs are represented by X, X, ..., X. The outputs include t+1 t+2 t+T forecast discharge q^{sim}, qsim ...,q^{sim} rectified Linear Unit (ReLU) with values in the range (0, +∞) is used to output non-negative values.

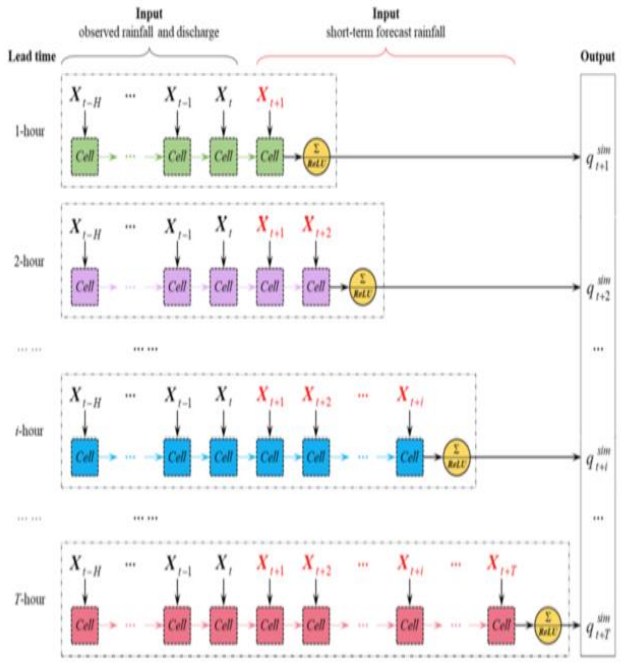

Fig. 2 Structure of the LSTM flood forecasting model

The following are the steps for model training.

Stage 1: Define the release lead-time (T) based on the realistic need for streak spike early warning within the designated watershed. **Stage 2:** Create and standardize a data set. Because precipitation and release have obvious physical consequences and quantities, the data is balanced by using these conditions.

$$\hat{x} = \frac{x - x_{min}}{x_{max} - x_{min}}$$

where $x^{\exists}$ is the normalized value, x denotes the observed value, x_{max} and x_{min} denote the maximum and minimum observed values.

Stage 3: Divide the information set into three sections: preparation, approval, and testing. **Stage 4:** In that sequence, set the hyperparameters (units, bunch estimate, and age) and prepare the 1-hour, 2-hour, and T-hour LSTM systems. C t and h t measurements are presented in units. Batch size determines the number of tests that will be broadcast through the arrangement. The number of passes the machine learning computation has performed across the entire prepared dataset is represented by an age. When the clump estimate is the whole prepared dataset, the clump measure and age are the same. To determine the initialization of weights, an are **Stage 5:** Repeat step 4 using trial and error to compute the ultimate esteem of hyperparameters for 1-hour, 2-hour, and T-hour LSTM systems independently. The learning curve is used to keep a strategic gap between being over- or under-fitting.

Stage 6: Repeat stage 4 using trial and error to compute the ultimate esteem of hyperparameters independently for 1-hour, 2-hour, and T-hour LSTM systems. The learning curve is used to keep a strategic gap between being over-or under-fitting.

Stage 7: Save the best demonstration based on your trial-and-error discoveries from step 6. Apply the previously saved LSTM-FF demonstration to the input test set and normalize the yield to the reenacted releases. **Stage 8:** Examine the LSTM-FF model's reenacted results.

For exploratory preparation reenactments, the day-by-day crude precipitation estimations from an assortment of meteorological stations in and around Fort Worth were utilized. Thirteen years of data (from 2007 to 2109) on daily precipitation records obtained from www.meteoblue.com, where we conducted our research. As the beginning set of exploratory information, the area known as Al-Faisaliyah was chosen. This area was chosen since it's in a locale that's generally close to the Tigris Waterway.

The panda's data frame is a structure that stores two-dimensional data and the labels that go with it. Data-Frames are widely used in data science, machine learning, scientific computing, and a variety of other data-intensive disciplines. Data-Frames are comparable to SQL tables or spreadsheets used in Excel or Calc. Because they are an essential part of the

Python and NumPy ecosystems, Data-Frames are often quicker, easier to use, and more powerful than tables or spreadsheets. The dataframe.sum () method in Pandas returns the sum of the values for the specified axis. If the input is an index axis, it adds all the values in a column and then continues the process for all columns, returning a series with the total of all the values in each column. It also allows you to bypass missing values in the data-frame when computing the total. The data type of the date column was one of the key challenges that arose. The approach was to convert it to a timestamp and then back to Date-Time format.

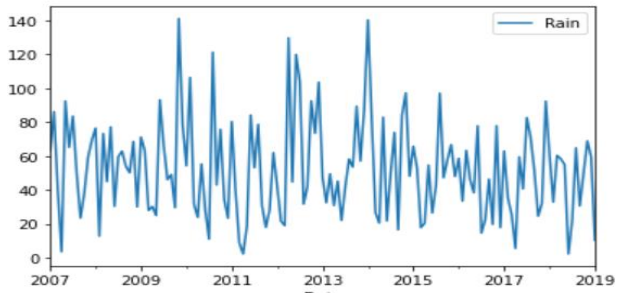

Fig. 3 presenting the data in a plot figure

III. RESULTS

Observe that raising the model's layers marginally improves performance; LSTM layers following the top layer are started with the hidden states and cell states of the preceding LSTM layer. In general, the internal states of each LSTM layer are randomly initialized.

The following period in deciding the execution of the LSTM demonstrate is to match precipitation information from a few long time periods as well as the expected and measured values within the test dataset. Precise surge estimating will serve as a foundation for flood risk administration, planning, and management.

The expected surge crests rise at the same time as the real maxima in this situation. On the occasion of estimating the most extreme flowrate one day and two days ahead, a satisfactory resilience esteem of almost 5% and 14%, respectively, is utilized within the hydrological forecast. This is often due to the trouble of precisely anticipating the greatest discharge value during the surge season, especially in places with complicated landscapes and soaking slopes like the ponder zone. Moreover, the figures (3) suggest that the LSTM could be a data-driven show established on factual associations among input and yield information in all forecast occurrences. As a result, one of the basic criteria impacting the model's exactness is the relationship between the information arrangement at the target-forecast location and further situations.

IV. DISCUSSION

The inquire about given over illustrates the LSTM model's fabulous advantage in its capacity to effectively learn brief conditions, and this demonstration can totally be It is used to forecast the flow two or three days ahead of time with an accuracy of more than 86 percent. Of their effortlessness, data-based procedures are a practical approach with high precision to modeling the hydrological readiness, particularly in developing countries such as Vietnam, where the application of blocked off identifying development inside the improvement of a real-time surge caution system is compelled.

The figure (4) shows that the actual percent rainfall increased, while our model projected that it would increase as well. This clearly demonstrates how effective LSTMs are in analyzing time series and sequential data.

As we can see in figure (4) As we can see, the blue continuous line represents the real data of the rainfall in all the periods of time across the area that it has been represented. It manifests itself in various ways and at various times. Then comes the orange line, which shows the predation of the flood. We are all aware that more rainfall means more flooding. The case of the flood is higher in this graph, where it is more than 2.0. And the graph demonstrates that it is continuous; every time the amount of rainfall goes up in a small area, the orange line appears, showing that the possibility of a flood may be realistic or it will happen. The graphic shows that the actual percent of rainfall increased, while our model projected that it would increase as well. The expected flood line rises at the same time as the real maxima in this situation. On the occasion of estimating the most extreme flowrate one day and two days ahead, a satisfactory resilience index of almost 5% and 14% was achieved, respectively.

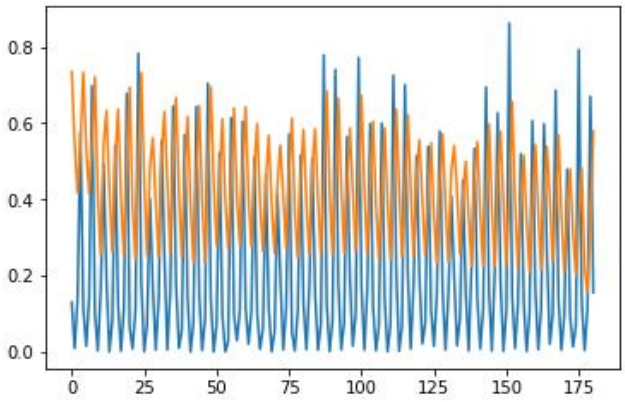

Fig. 4 The Result of LSTM

V. CONCLUSION

Based on the data-driven procedure, this is how they advertised a successful arrangement for surge estimating. To illustrate, the LSTM neural organization show was created and extensively tested. The LSTM show has learnt long-term associations between successive information arrangements and has been demonstrated to be solid in surge estimating.

In spite of the fact that the LSTM show effectively addresses successive information issues, there are different confinements that must be considered. LSTM models, in common, are data-driven models that, like physical-based models, result in destitute modeling of hydrological forms. LSTM (or ANN)-based models in particular, because they provide extremely

precise estimates at specified locations within the investigated area. As a result, these models ought to be coordinated with meteorological models such as precipitation estimating models to make strides in long-term expectation execution.

ACKNOWLEDGMENT

For the ancestors who paved the path for us upon whose shoulders we stand. This is also dedicated to my family and friends who supported me on this journey. Thank you I would like to express my deepest gratitude to my supervisor Dr. ABDULLAHI ABDU IBRAHIM for his unwavering support,collegiality and mentorship throughout this research**.**

.

REFERENCES

[1] S. Mei, A. Montanari, and P.-M. Nguyen, "A mean field view of the landscape of two-layer neural networks," *Proc. Natl. Acad. Sci. U. S. A.*, vol. 115, no. 33, pp. E7665–E7671, 2018.

[2] V. Gulshan *et al.*, "Development and validation of a deep learning algorithm for detection of diabetic retinopathy in retinal fundus photographs," *JAMA*, vol. 316, no. 22, p. 2402, 2016.

[3] Y. Liu, S. Liu, Y. Wang, F. Lombardi, and J. Han, "A survey of stochastic computing neural networks for machine learning applications," *IEEE Trans. Neural Netw. Learn. Syst.*, vol. 32, no. 7, pp. 2809–2824, 2021.

[4] J. Bayer, D. Wierstra, J. Togelius, and J. Schmidhuber, "Evolving memory cell structures for sequence learning," in *Artificial Neural Networks – ICANN 2009*, Berlin, Heidelberg: Springer Berlin Heidelberg, 2009, pp. 755–764.

[5] G. Bellec, D. Salaj, A. Subramoney, R. Legenstein, and W. Maass, : "Long short- term memory and learning-to-learn in networks of spiking neurons," 2018, pp. 787–797.

[6] H. Gao, J. Mao, J. Zhou, Z. Huang, L. Wang, and W. Xu, : "Are you talking to a machine? dataset and methods for multilingual image question," 2015, pp. 2296–2304.

[7] J. Gong, X. Chen, T. Gui, and X. Qiu, : "Switch-lstms for multi-criteria chinese word segmentation," 2019, vol. 33, pp. 6457–6464.

[8] K. Greff, R. K. Srivastava, J. Koutnik, B. R. Steunebrink, and J. Schmidhuber, "LSTM: A search space odyssey," *IEEE Trans. Neural Netw. Learn. Syst.*, vol. 28, no. 10, pp. 2222–2232, 2017.

[9] C. R., K. K. R., and D. E. Newton, "Drthis: Deep ransomware threat hunting and intelligence system at the fog layer," *Future Generation Computer Sys- tems*, vol. 90, pp. 94 – 104, 2019.

[10] T. Horsmann and T. Zesch: "Do lstms really work so well for pos tagging? – a replication study," 2017, pp. 727–736.

[11] Cho, K.; van Merrienboer, B.; Gülçehre, Ç.; Bougares, F.; Schwenk, H.; Bengio, Y. Learning phrase representations using RNN encoder-decoder for statistical machine translation. arXiv 2014, arXiv:1406.1078.

International Journal of Multidisciplinary Studies and Innovative Technologies

e-ISSN: 2602-4888
dergipark.org.tr/en/pub/ijmsit
Research Article

2022, 6 (1), 117-133
DOI: DOI: 10.36287/ijmsit.6.1.133
Received: May 27, 2022; Accepted: July 18, 2022

Geology, Petrographic Characteristics and Tectonic Structure of Paleoproterozoic basement of Kabul Block (North Eastern Afghanistan), Initial Findings

Gürsel Kansun[1*], Ahmad Omid Afzali[2]

[1] Konya Technical University, Faculty of Engineering and Natural Sciences, Department of Geology Engineering, Konya, Turkey (gkansun@ktun.edu.tr) (ORCID: 0000-0002-4581-6076)*
[2] Afghanistan Academy of Sciences, Department of Geosciences, Kabul, Afghanistan (omidaf53@gmail.com) (ORCID:0000-0002-4423-7777)

Abstract – The Paleoproterozoic basement of Kabul Block is a cratonic basement in north eastern Afghanistan. Precambrian Kabul Block including metamorphic rocks only takes place at the base of the study area. The Neo-Proterozoic Welayati formation overlies the Paleo-Proterozoic Sherdarwaza formation with a tectonic contact, and they both overlay Khair Khana formation. In the region, Alghoi meta granitoid intruded into both Khair Khana and Sherdarwaza formations.
The Khair Khana formation contains of granulites, granitic gneisses ve amphibolites. The mineral assemblages of granulites are *plagioclase + quartz + K-feldspar + orthopyroxene + clinopyroxene (diopside/augite).* Granitic gneisses are observed as hornblende gneiss, garnet-biotite gneiss and pyroxene-gneiss. Hornblende-gneisses include *hornblende + quartz + K-feldspar* mineral assemblage, garnet-biotite gneisses are evident with *plagioclase + quartz + K-feldspar + biotite (red) + garnet* mineral assemblage, and pyroxene gneisses include *quartz + plagioclase + biotite + clinopyroxene* mineral assemblage. Amphibolites consist of *hornblende + plagioclase + quartz ± zoisite ± sphene ± ilmenite ± apatite* mineral assemblage. The Sherdarwaza formation contains marbles, amphibolites, biotite gneisses, micaschists and migmatites. Marbles consist of *calcites ± quartz ± apatite*. In amphibolites, *harnblende + plagioclase + quartz ± epidote ± zoisite ± garnet* mineral assemblage are observed. Biotite gneisses include *plagioclase + quartz + microcline + biotite ± sphene ± apatite ± zircon* mineral assemblage. Micachists consist of *quartz + plagioclase + microcline + biotite ± sphene ± apatite* mineral assemblage. Migmatites include *plagioclase + quartz + microcline +biotite ± sphene ± apatite* mineral assemblage. Alghoi meta granitoid is generally observed as stocks and small masses, and sometimes it shows foliation. It consists mainly of meta granites. The meta granites that show granular texture include *plagioclase + quartz + K-feldspar + biotite + hornblende*. The Welayeti formation contains quartzite, kyanite-garnet-staurolite schist, garnet-mica schist, kyanite-garnet-mica schist and garnet-muscovite schist. Quartzite include *quartz ±* muscovite ± biotite. They are observed *hornblende + quartz + plagioclase ± garnet ± epidote ± zoisite ± rutile ±* magnetite in amphibolites. Kyanite-garnet-staurolite schists are evident with *staurolite + kyanite + garnet + mica + biotite + quartz + plagioclase ± apatite ± epidote ± ilmenite ± monazite* mineral assemblage. Garnet-mica schists and kyanite-garnet-mica schists include *quartz + plagioclase + biotite + muscovite + kyanite + garnet ± chlorite ± apatite ± tourmaline ± sphene ± rutile*. In garnet-muscovite schists, *muscovite + quartz + plagioclase + garnet ± tourmaline ± apatite ± zircon* are observed.
The granulites in Kabul Block are together with granite gneisses, and they can be separated under one formation. Granulites show different mineral compositions, Usually, they are without garnet, in some cases they include garnet. The amount of plagioclase is higher in them according to other rocks. In some cases, the composition of granulites is very similar to that of quartz mangarites that indicates high temperature and pressure of the metamorphism process and shows that this block is related to a segment of Columbia and Rodinia supercontinents during Paleoproterozoic collisional events.

Keywords *– Kabul Block, Metamorphites, Afghanistan*

Citation: Kansun, G., Afzali, A.O. (2022). Geology, Petrographic Characteristics and Tectonic Structure of Paleoproterozoic basement of Kabul Block, Initial Findings, North Eastern Afghanistan. International Journal of Multidisciplinary Studies and Innovative Technologies, 6(1): 117-133.

I. INTRODUCTION

The Kabul Block is a tectonic block located in the northeast of Afghanistan (Fig. 1). There is little information about the basement rocks and their geologic characteristics in the Kabul Block. Also, there are some old information based on large-scale and non-detailed geological maps such as 1:100000, 1: 500 000 and 1: 1 000 000 [1], [2]. The studies carried out so far in the region and its immediate vicinity can be summarized in chronological order as follows. Ref.[3] introduced the Kabul Stratigraphic Chart. In this diagram, the Kabul Series is

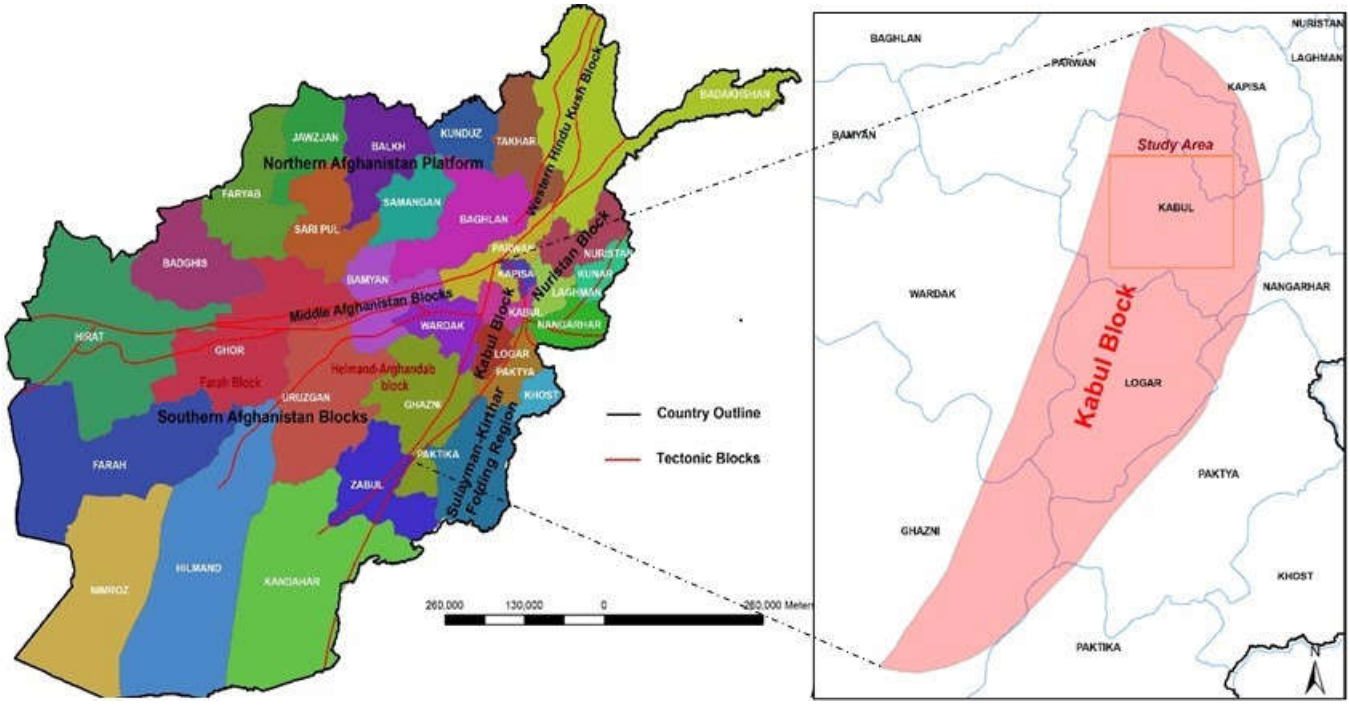

Fig. 1. The study area which is located in the Kabul block in the north-eastern part of Afghanistan

observed above the Khingel Series, which is a carbonate complex.

Ref.[4] in his work titled "Basic Features of Afghan Tectonics" said that the Kabul Block and the Western Hindu-Kush are the two main tectonic blocks in Afghanistan and defined these blocks. Ref. [5] between 1958 and 1961, mapped the area around Kabul. Ref. [6] made partly 1:100000 scale geological maps of Kabul block. Ref. [7] compiled maps of the central and southern parts of Afghanistan at a scale of 1:1000000 and 1: 500000.

Ref. [8] investigated the geological structure and general petrographic features of the Kabul region. Ref. [5] made a detailed study on the biostratigraphy of sedimentary rocks in the Kabul region and developed the study of Manisa. Ref. [9] studied the geological structure and mineral resources of the northern part of the Kabul Block.

Ref. [10] conducted a study on the stratigraphic and tectonic features of the Kabul region. In this study, the interior parts of the Kabul tectonic region were investigated.

Ref. [11], in his study, states that the region gathered around Afghanistan is a collision area consisting of continental blocks derived from Gondwanaland.

Ref. [12] stated that the Kabul Block is composed of the lower Welayati formation and the overlying Sherdarwaza formation, and the Sherdarwaza formation with thickness of about 5.5 km is predominantly composed of marble, amphibolite, quartzitic gneiss and migmatite.

Ref. [13] stated that the Kabul Block collided with the Eurasian Plate during the Late Cretaceous - Early Paleogene.

Ref. [14] suggests that the Indian Plate and the Afghan Block collision during the Pliocene.

Ref. [15] assessed non-fuel mineral resources of Afghanistan.

Ref.[16] defined the gneisses of the Paghman Mountains in the Kabul region as a new series under the Paghman Series.

Ref. [17] stated the Kabul Block is prolonged crustal part that cuts over the Afghan Central Blocks, connecting the Indian and Eurasian continents. After the granulite facies metamorphism, amphibolite facies metamorphism develops. The granulite facies metamorphism took place at a temperature of 850 ºC and a pressure of 7 kbar.

Ref. [18] stated that the Welayeti formation consists of micaschist and quartzite with amphibolite lenses. It unconformably overlies the Neo Archaean Sherdarwaza formation. This formation has undergone a metamorphism progressing from a temperature of 525 ºC and a pressure of 6.2 kbar to a temperature of 650 ºC and a pressure of 9 kbar.

Ref. [19] worked in the Kabul Block, which consists of Sherdarwaza and Welayati formations. According to these researchers, The Sherdarwaza formation consists of migmatites and gneisses.

II. Materials and Method

Within the scope of the field studies, 1/25000 scaled geological maps of an area of 155 km^2 and 1/10000 scaled maps of an area of 120 km^2 were created. Tarauni brand type compass was used during the studies. During the fieldwork performed at all locations, GPS was used to ensure that the points were accurately mapped. The lithologies outcropping in the study area were identified and 300 rock samples were taken for petrographic studies. Considering the top-bottom relationships of the lithologies in the study area, the stratigraphic colon section of the region was revealed. In order to fully understand the geological development of the units, the structural and tectonic elements reflecting the formation mechanisms of the rocks, and their planar and linear structures were measured and recorded on the map.

Among them, 50 samples were selected for petrographic and mineralogical studies. Thin sections were made and assessed using the Nikon and Leica type microscopes at Konya Technical University and Kabul Polytechnic University.

III. Tectonic Evolution and Structural Features of The Region

Afghanistan is located in the tectonically active Alpine-Himalayan orogenic belt in Central Asia, which was formed by the collision between the Indian and Arabian plates and the Eurasian plate in the Late Paleogene [20], (Fig. 2). As the Eurasian continent emerged 65 million years ago, multiple periods of deformation shattered the crust in and around Afghanistan.

Afghanistan consists of a complex assemblage of areas (regions), mostly originating from Gondwana, that was added to the southern margin of Eurasia before and during the collision of the Indo-Eurasian plates [21], [22]. These areas are divided into three separate tectonic zones (Fig. 3). **Afghan-Tajik Platform** in the north consists of fixed blocks, and since the Paleozoic, these blocks have been part of the Eurasian continent [23]. **The Katawaz Basin** which is a major bending basin in the southeast represents the northwestern continental margin of the Indian plate [14]. Among them are the **Afghan Center Blocks** that is NE-SW extension tectonic blocks. The blocks collided with Eurasia during the Mesozoic and Early Cenozoic.

The Afghan Center Blocks contain three separate blocks: the Kabul Block, the Helmand Block, and the Farah Block (Fig. 3). However, the status of the Kabul Block is controversial. Ref. [13] and [14] stated that the Kabul Block represents a detached crustal piece of the Indian subcontinent added to the Afghan Center Blocks in the Paleocene. Against this, accoding to [24] and [25], the Kabul Block belong to Afghan Center Blocks.

The collision of the Indian and Eurasian Plates is caused by the separation of small blocks from India, and the formation of magmatic arcs before the continental collision [13], [14] [21], [26]. Afghanistan's tectonic evolution is related to the closing of the Paleozoic and Mesozoic Tethys. In Fig. 4, the tectonic map of Afghanistan and the western Himalaya-Karakoram-Hindu Kush region is shown.

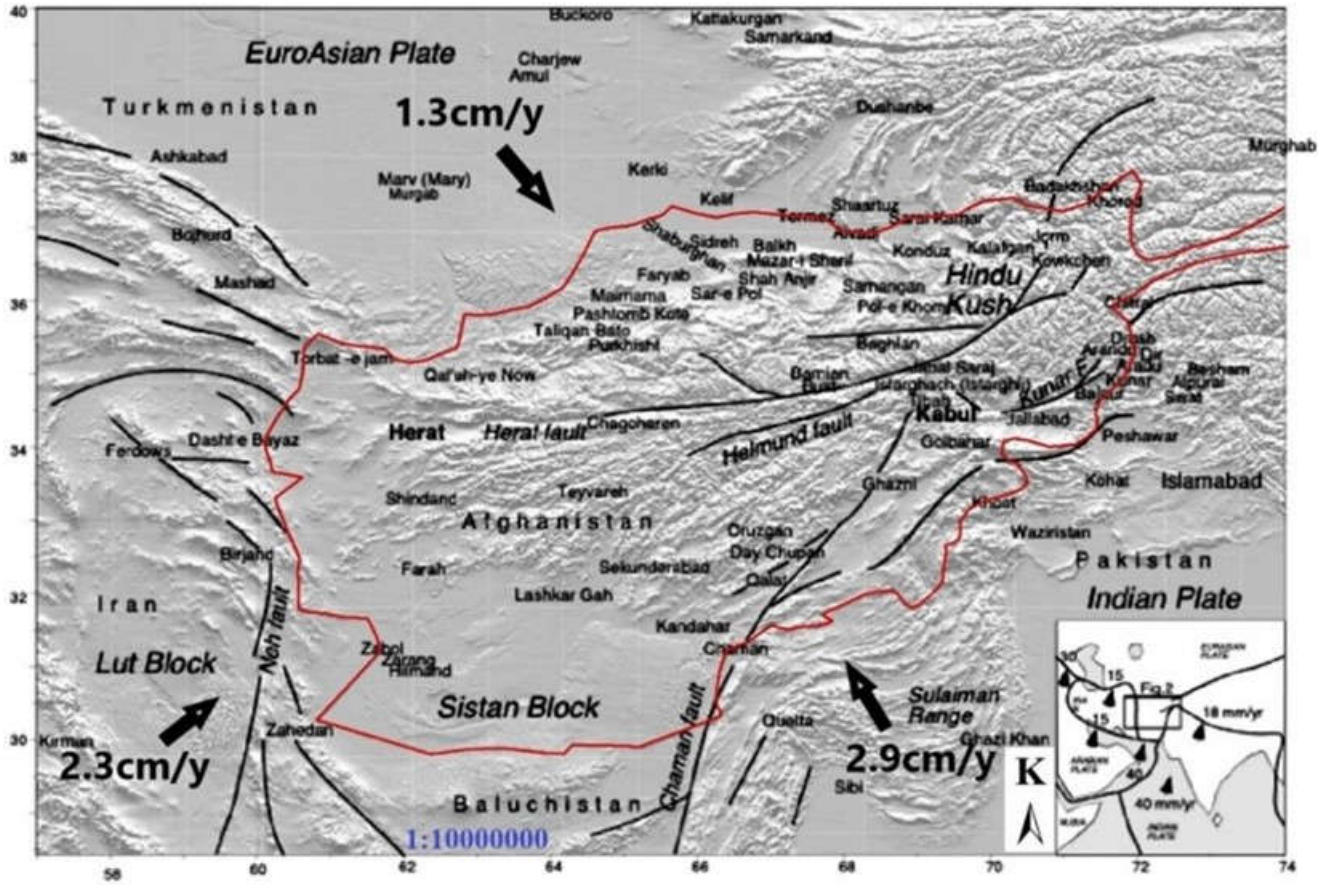

Fig.2. Afghanistan's location and tectonic activities in the Alpine-Himalayan orogenic belt [27]. Vectors show relative plate movements and velocities between Indian, Eurasian, and Arabian plates [28]

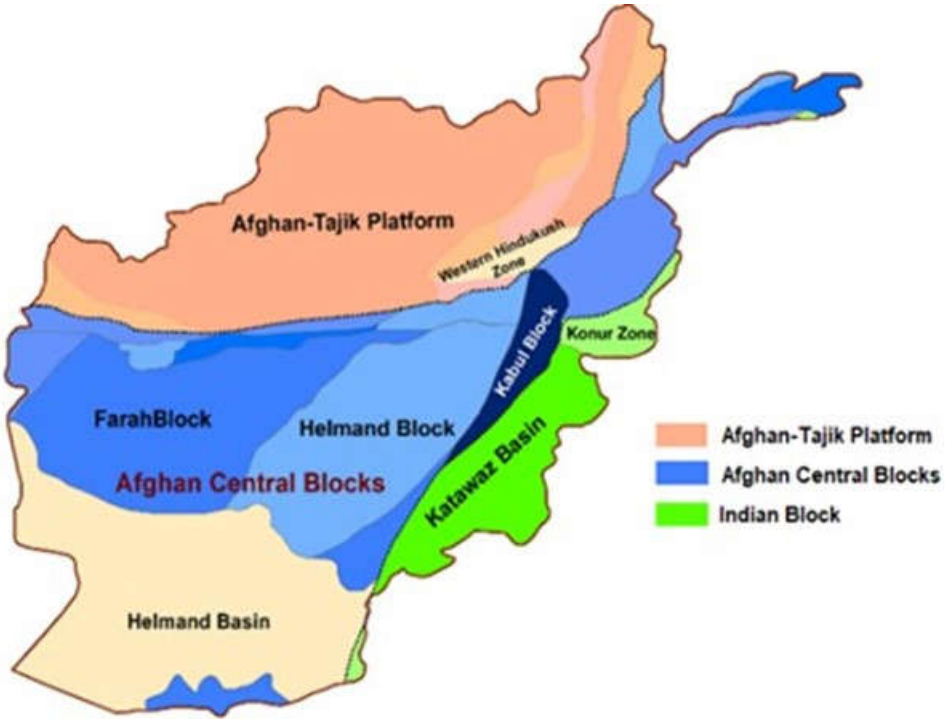

Fig. 3. Tectonic outlines of Afghanistan according to [16], [22]

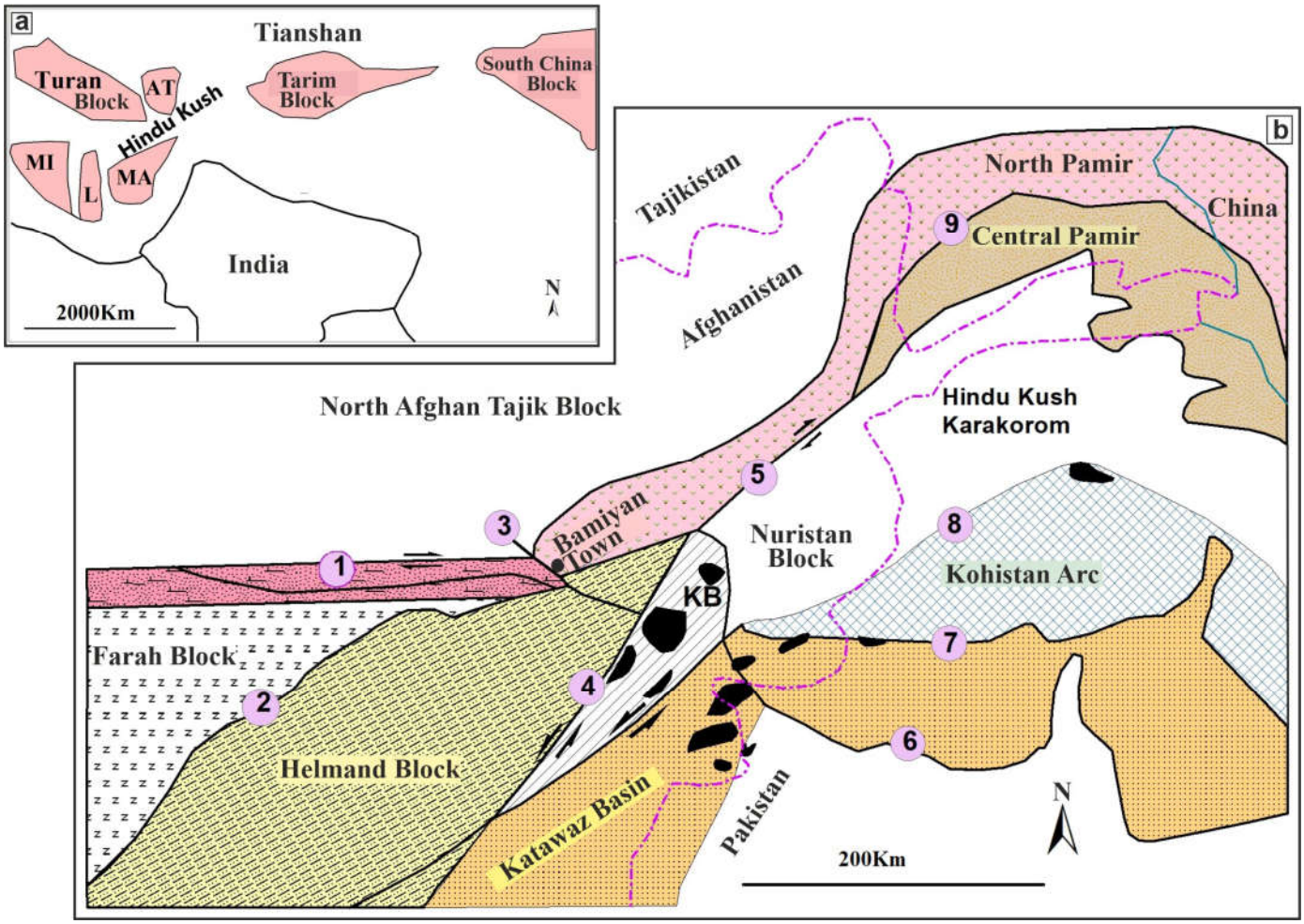

Fig. 4. (a) Current location of Precambrian blocks in South Asia (AT- Afghan-Tajik block, MA-Central Afghan Blocks, MI- Central Iranian Block, L-Lut Block, South China Block, Turan Block, [29]. (b) Tectonic map of Afghanistan - Western Himalaya - Hindu Kush region [11], [13], [26], [30], [31]. The black areas in the Kabul Block (NW) are ophiolite formations. 1-Harirod Fault (Paleozoic Suture), 2-Helmand Fault (Mesozoic Suture), 3-Bamiyan-Shibar Fault, 4-Chaman Fault, 5-Panjshir Fault, 6-Main Boundary Thrust, 7-Foundation Central Thrust (Indus-Tsangpo Suture), 8-Shyok Suture, 9-Mesozoic Suture

The tectonic zones in Afghanistan include **the North Afghan Tajik Block, the Afghan Central Blocks (Farah and Helmand Blocks)** and **Katawaz Basin** (Fig. 3 and 4). The North Afghan Tajik Block is located north of the Harirod-Panjshir fault system (Fig. 4b). The Afghan Center Blocks are located west of the Chaman Fault (Fig. 4b). They were previously part of Gondwanaland. However, they separated from Gondwanaland before the Indian subcontinent was annexed to the southern margin of Eurasia [11], [14], [21], [22]. The Kabul Block was formed at the triple junction of these three regions. According to [24], The Kabul Block is the easternmost part of the Afghan Center Blocks [24]. Against this, according to [13], [14], The Kabul Block is the separate region added to the Afghan Center Blocks before the collision of Eurasia and India. The Kabul Block is a tectonic block between the Indian and Eurasian continents (Fig. 5a). Kabul, Farah and Helmand Blocks forms the Afghan Central Blocks.

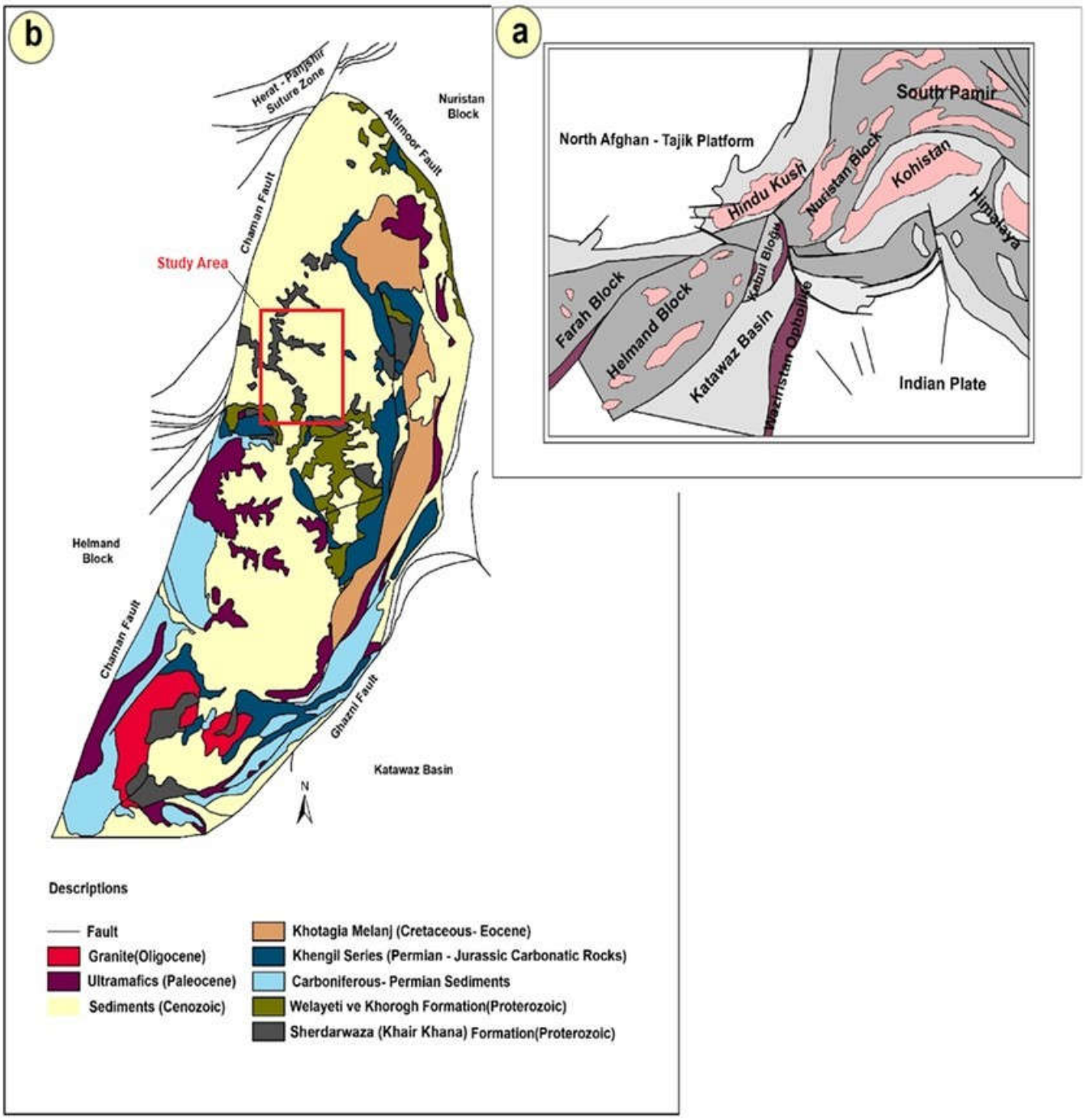

Fig. 5. (a) Tectonic map of the Afghanistan region [32], (b) The geological map of the Kabul Block according to [1], [2]

The Kabul Block is approximately 200 km long and up to 50 km wide (Fig 5a and b). The Kabul block is bounded to the east by the Chaman fault and to the northeast by the Altimoor fault. The Ghazni fault is observed in the southeast of the Kabul block (Fig. 5b). The Herat-Panjshir Suture Zone is observed in the north of the Kabul block.

IV. RESULTS

A. Geological Properties of Kabul Block

In the basement of the Kabul Block, base rocks are shown (Fig. 5b), and Kabul block has an east-west oriented dome structure [12], [24]. Late Paleozoic (Carboniferous-Permian) low-grade metamorphites and Cenozoic volcano-sedimentary succession are observed on the Kabul block [5], [24], [25]. Late Paleozoic aged metamorphites consist of phyllites, metashales, marbles and metaconglomerates. Upper Permian-Triassic aged the Khengil Series consists of conglomerates, limestones and tuffs [5]. The Kotagai melange consisting of peridotites overlies the Jurassic volcano-sedimentary units (Fig. 5b), and Kotagai melange thrusts the eastern and western edges of the Kabul block [6], [25]. The eastern ultramafic thrust layer is reported to belong to the Khost ophiolite complex [13]. The ultramafic rocks in the south and west of the block emerged in the form of clips by thrusting on the unmetamorphized sedimentary cover [13]. Ref. [13] named these ultramafic rocks as the Kabul ophiolite complex. Kabul Block is cut by Eocene-Oligocene aged granitic rocks. These granitic rocks were formed as a result of the collision of the Indian and Eurasian plates [33]. The Kabul block is mostly covered by Cenozoic aged sedimentary rocks [25].

It is assumed that the basement rocks that emerged on the hills around the city of Kabul are the result of a dome-like structure [12], [24]. The basement rocks of the Kabul Block are composed of Proterozoic metamorphites [25]. From bottom to top and in decreasing degree of metamorphism, these are, Khair Khana, Sherdarwaza, Kharog and Welayati formations (Fig. 5b).

According to [17], granulite facies rocks are observed in She Darwaza formation in Khair Khana. These rocks are surrounded by quartz-feldspathic rocks, schists and migmatites [17]. Ref. [10] described granulites from Khair Khana for the first time as Proterozoic orthogneisses. Ref. [12] say that these are xenoliths of a probably Archaean aged formation.

The Sherdarwaza formation is mostly represented by quartzite, amphibolite and marble interbedded migmatites, schists and gneisses. Syenitic and dioritic metamagmatites are observed in the Shedarwaza formation [17].

It is thought that the 0.93 - 0.64 Ga Neoproterozoic ages obtained by K-Ar and Ar-Ar dating [24], [19] of biotite from migmatite and schists correspond to the metamorphism of the Sherdarwaza and Khair Khana formations. In addition, Paleoproterozoic U-Pb zircon ages in the range of 1.8-2.3 Ga were obtained from gneiss and migmatites [16], [19], [34]. According to [19], granulite and amphibolite facies metamorphisms are of Paleoproterozoic and Neo-proterozoic ages.

The Kharog formation consists of meta-quartzite, crystalline schists, gneisses, amphibolites and marbles [25]. The extent and distribution of the Kharog formation have not been fully understood in the studies carried out so far. This formation was defined according to stratigraphic relationships in the Kharog Mountains south of Kabul. The Kharog formation overlies the Sherdarwaza formation with a distinct non-angular unconformity [17].

According [18], the lower boundary of the Welayati formation is in tectonic contact with the Sherdarwaza (Kharog?) formation. The Welayati formation consists of garnet amphibolites and various crystalline schists including biotite schists, staurolite-garnet-biotite schists, muscovite-kyanite-garnet schists and quartzites [25]. According to [18], this formation consists of schist at the base, amphibolite in the middle, and amphibolite-schist alternation at the top.

The identification of the Rodinia and Colombia supercontinents has helped to interpret geodynamic processes on Earth throughout geological time [35], [36], [37], [38], [39], [40], [41], [42], [43], [44]. From the cratonic remains of these supercontinents we can understand sedimentary, magmatic and tectonic processes.

The Kabul block and the Afghan Central Blocks are small continental parts. The block of Cain was separated from Gondwana during the opening of Neotethys. Later collided with Eurasia in the Late Cretaceous - Early Paleogene [13], [14], [45].

We studied in Archean and Proterozoic aged four basement units of the Kabul Block. These are Khair Khana, Sherdarwaza, Welayati formations and Alghoi meta granitoid (Fig. 6, 7, 8).

A.1. Khair Khana formation

It was first named by [12]. Some researchers have defined the Khair Khana formation and the Sherdarwaza formation as a single formation. However, these formations differ from each other in terms of age and lithological features. The Khair Khana formation is older than the Sherdarwaza formation and no quartzite is observed in the Khair Khana formation and meta-carbonates are also very common. The age of the Khair Khana formation was stated by [12] as Archean. The thickness of the formation is 2700 m. Spreading areas of this formations: Khawja Rawash mountains, Paymunar mountains, Kasaba mountains, Khair Khana mountains and Alghoi mountain. The Khair Khana mountains lie in an E-W direction while the Alghoi mountains lie in a N-S direction. This formation consists of granulite, granite-gneisses, marble, calc-silicate rocks, amphibole gneisses and amphibolite. Granite masses have been identified in this region.

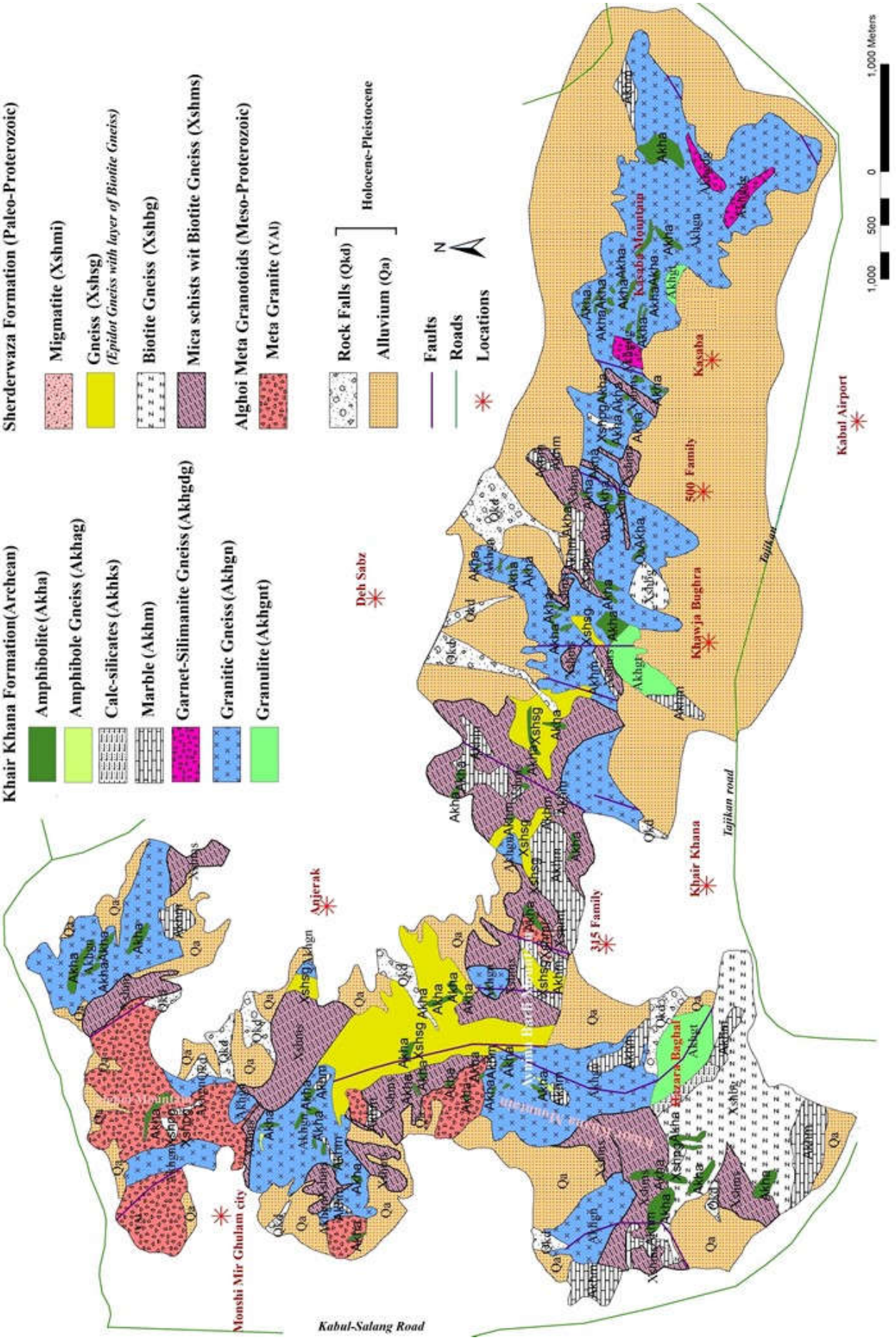

Fig.6. Geological map of the northern part of the study area (north of Kabul)

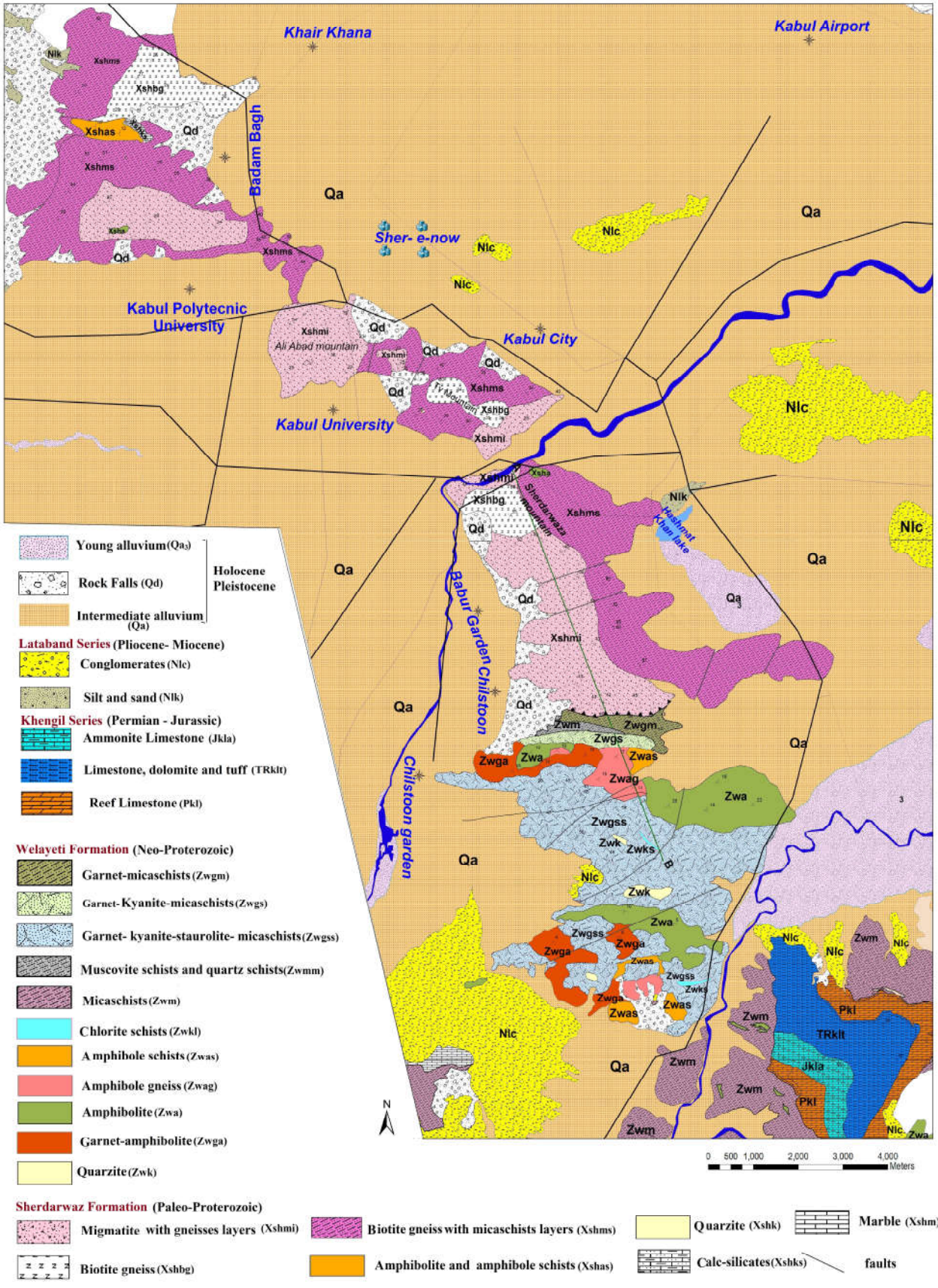

Fig. 7. Geological map of the southern part of the study area (south of Kabul)

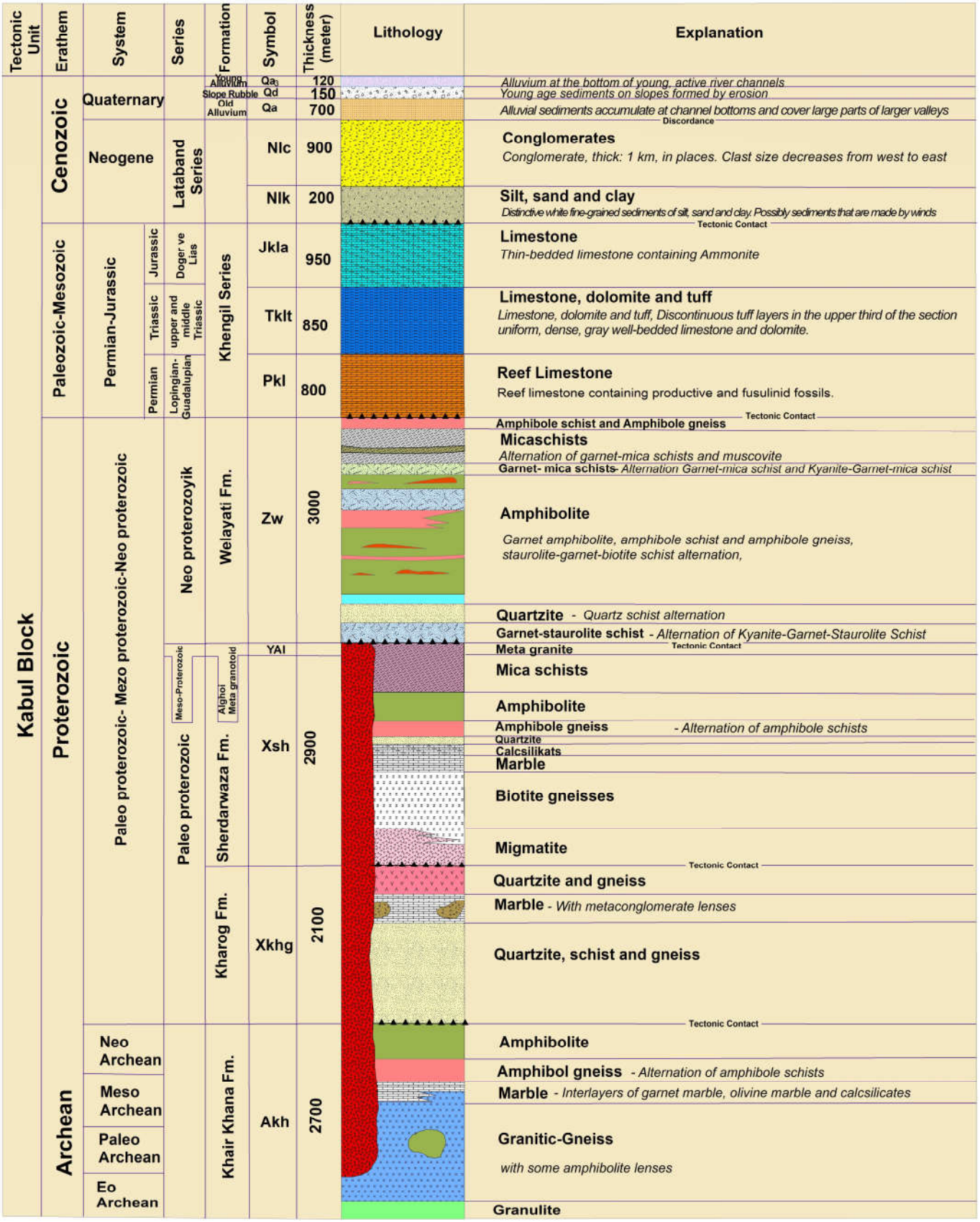

Fig. 8. General stratigraphic column of Kabul Block

Granulite

They are medium-grained, brownish-altered and rather hard rocks. Pyroxenes (clinopyroxene and orthopyroxene) are prominent in the granulite observed in the Khair Khana mountains. In addition, some feldspar minerals are in the form of prophyroblasts (Fig. 9 a, and b). Other granulites were observed in the 500-Family mountains (Kotal-e-Dekapak). Orthopyroxene and clinopyroxenes are observed in these rocks, and are mostly prismatic. Under the microscope, its colour ranges from pale orange to pale green. The amount of clinopyroxene is higher than orthopyroxene and they form small-sized minerals. Minor minerals observed here are magnetite, apatite and sphene. Granulites have a granonematoblastic texture and their structure is foliated (Fig 9 c, d, e and f). Granulites are medium to coarse-grained. As a mineralogical composition, it contains plagioclase (30-40%), quartz (25-30%) and K-feldspar (10-15%), orthopyroxene (<10%) and clinopyroxene (<10%). Orthopyroxenes occur as sub-idioblastic to xenoblastic prismatic grains of approximately 0.8 – 1.9 mm in diameter (Fig 9a and b). Plagioclases have hypo-idomorphic forms that usually have a thin polysynthetic, in which antiperthitic and myrmekitic texture are observed. Potassium feldspars are mostly xenomorphic forms, with a perthitic structure. Orthopyroxenes consist of hypo-idomorphic granules that have an elongated prismatic shape. Monoclinic pyroxenes are augite. In some granulites, amphiboles have developed which have a greenish-brown colour.

Granitic -Gneiss

Granite gneisses in the Khair khana Formation have a very wide distribution and can be called the basement rocks of the Khair khana Formation. Paragneisses are observed in contact with marbles and schists in all sections from the Alghoi Mountains to the Khawjeh Rawash Mountains (Fig. 10 and 11).

Hornblend Gneiss

The composition of these granitic gneisses includes hornblende (10-20%), quartz (15-20%), and feldspar (25-40%). Feldspar is widely observed in it, and in some places, pyroxene relicts are also present among the plagioclases. These rocks have granoblastic texture and massive and rarely foliation structure (Fig.10 c, d and Fig. 11 a, b).

Garnet – Biotite Gneiss

Small garnet porphyroblasts are seen in this type of granitic gneisses. The amount of garnet reaches approximately 5%. These gneisses are commonly found in the Kasaba mountains. The amount of plagioclase is 48%, quartz is 25%, potassium feldspar is 11% and biotite is 11% (Fig. 10 a, b and Fig. 11c). These rocks are massive in structure and lepidogranoblastic in texture.

Pyroxene Gneiss

These gneisses contain both clinopyroxene and orthopyroxene, and these pyroxenes have sometimes been converted to chlorite. In addition, microcline, plagioclase and quartz are observed in these rocks. The structure of these rocks is foliated and, in some cases, a massive structure is seen. The structure is granolepidoblastic. These gneisses contain: quartz (10-20%), plagioclase (20-40%), biotite (10-20%) and pyroxene (5-10%) (Fig. 11 d, e and f)

Marble

Marbles consisting of calcite are very common in the area related to the Khair Khana formation. In appearance, Khair khana marbles are in two different colors, white and light green. Other minerals observed in it are muscovite, garnet, phlogopite and olivine. Marbles are coarse-grained.

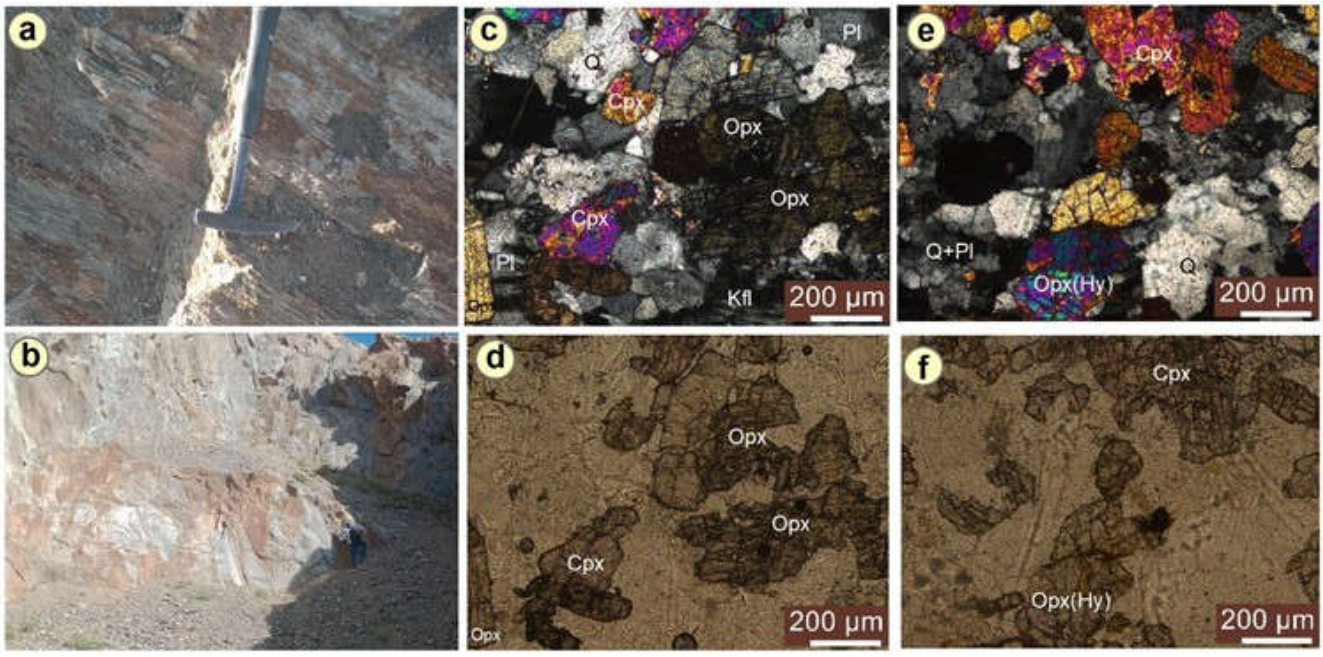

Fig. 9. Granulites of the Khair khana formation, **a**) Granulites with light brown alternating color and foliated structure in places. **b**) Brown altered colored and massive granulites belonging to the Khair khana formation. Location: Khair Khana mountains. c, d, e, f) the microscopic view of granulites, Q: Quartz, Pl: Plagioclase, Kfl. Potassium feldspar Cpx: Clinopyroxene, Opx: Orthoproxene. c, e) // nicol, d, f) / nicol

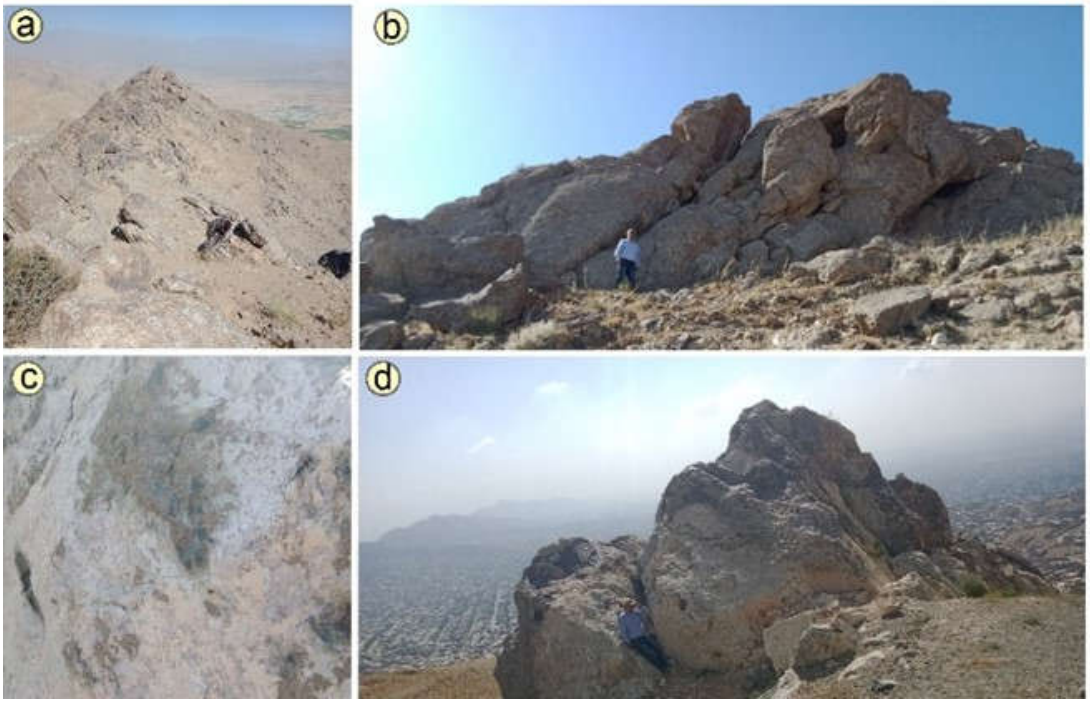

Fig.10. Granite gneisses. Location:kasaba and khair khana Mountains a: Longitudinal view, b: Transverse view c, d) Light gray granite gneisses. These gneisses contain abundant plagioclase contains hornblende and is seen in dark green color. Location: Khair Khana mountains

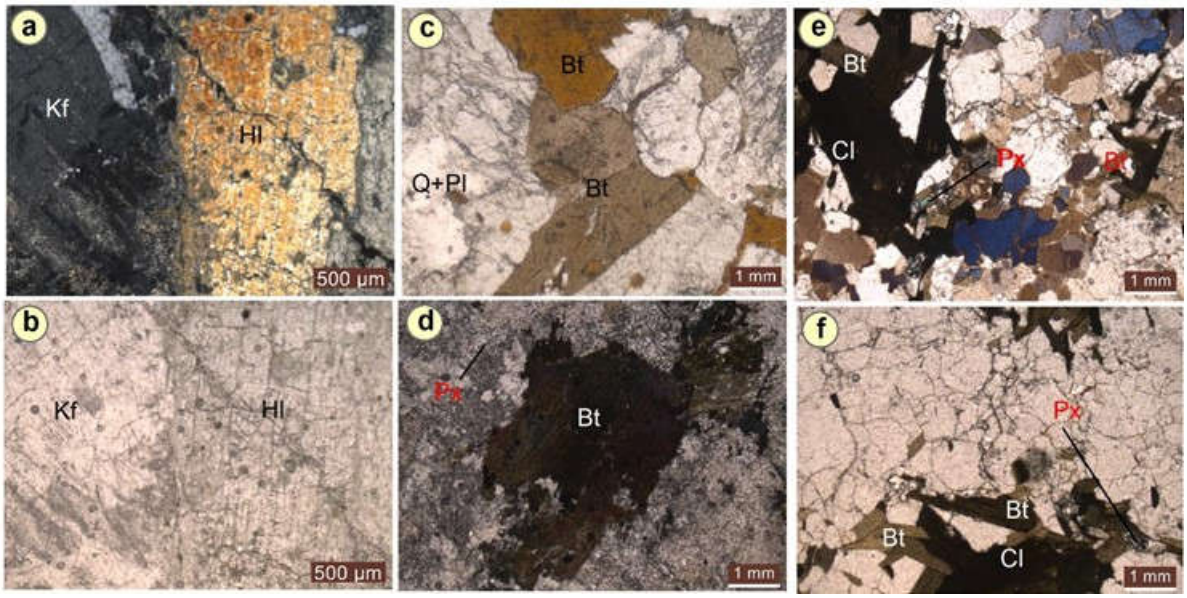

Fig.11. Microscopic view granitic gneiss in study area, a, b) hornblende gneiss, c) garnet biotite gneiss, d, e, f) pyroxene gneiss, a, f) /nicol, a, c, e, d) // nicol. Q: Quartz, Pl: Plagioclase, Cpx: Clinopyroxene, Bt: Biotite, Hl: Hornblende, Px: pyroxene, Cl: Chlorite, Kf: potassium feldspar

Amphibolites and Amphibole Gneiss

The distribution of amphibole-gneisses within the Khair Khana formation is quite low while amphibolites are quite common (Fig. 12a, b and c). Amphibolites are generally found in the form of lenses between granitic gneisses. Especially amphibolites and epidote-amphibolites are quite common. Amphibolite contains small amounts of quartz, but also commonly hornblende and plagioclase. Quartz is 1 - 5%. More than 10% quartz was observed in some samples. Amphibolites are dark green - black in color and fine - medium grained (Fig. 12a, b and c). The main component of amphibolites is hornblende (65-90%), varying from dark green to light green to yellowish green. It contains sphene, ilmenite and apatite as secondary minerals. Especially in amphibolites, sphene is quite common. It is mostly massive and has a granonematoblastic texture (Fig. 12a and d).

Amphibole gneisses have a distinct folate structure and are granonematoblastic in texture. They contain more than 85% hornblende in their composition. They also contain quartz minerals. These are mostly in the form of xenoblasts. Plagioclases are generally subhedral and have abundant inclusions (Fig. 12d, e and f).

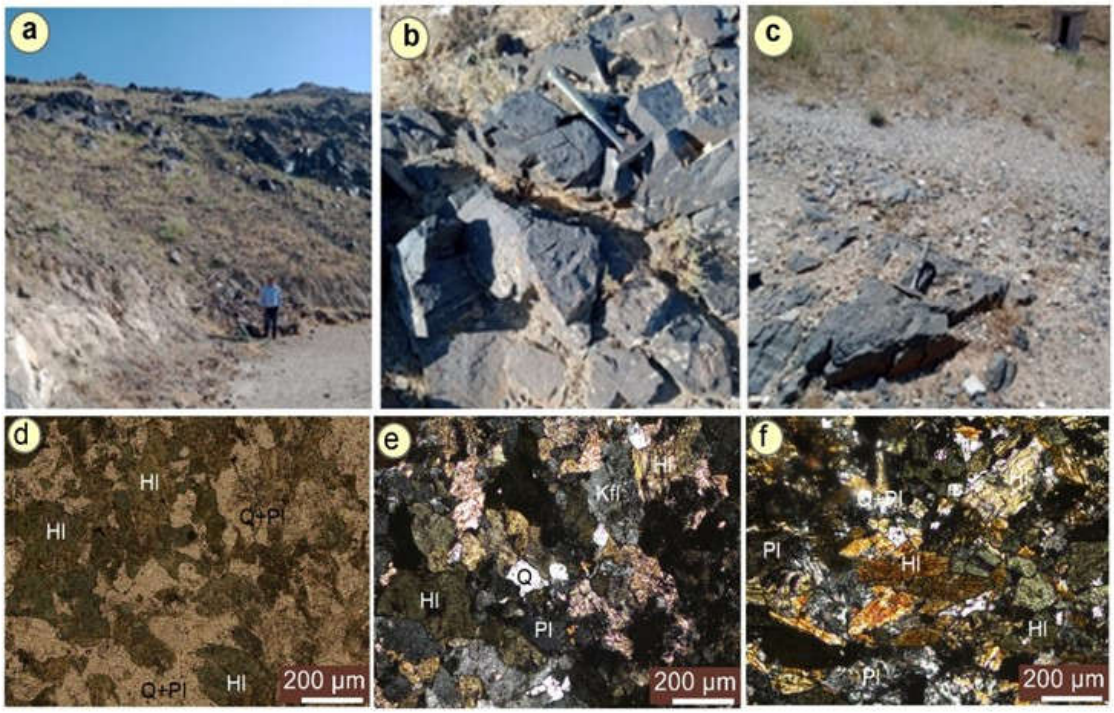

Fig.12. Amphibolite and amphibole gneisses observed in the Khair Khane formation. a, b) Amphibolites observed in the kasaba mountains, c) Amphibole gneisses observed in the Shakar Dara mountains. d, e, f) Microscopic view amphibolite and amphibole gneisses in study area. Q: Quartz, Pl: Plagioclase, Hl: Hornblende

A.2. Sherdarwaza formation

The Sherdarwaza formation is observed in the western part of the Khair Khana mountains, behind the Polytechnic University, Aliabad Mountain, Asmayee mountain Sherdarwaza mountain, Zanburkshah mountain, east of the Kasaba mountains, and north of the Kabul block. It was first named by [12]. The age of this formation was stated as Paleo-Proterozoic by [12]. The thickness of this formation is 2900 meters. Granite, granodiorite, and meta-granites were observed in the formation. According to field observations, the dispersion of marbles in this formation is considerably less than in the Khair Khana formation. The main lithologies in this formation are as a below

Quartzites

In the lower levels of the Sherdarwaza formation, they are in thin layers varying from 0.5 meters to 5 meters in thickness. Their thickness reaches up to 20 meters.

Amphibolites

They are observed at all levels of the Sherdarwaza formation. It is in levels of several meters, sometimes from 10-20 meters to 150 meters, and more in thickness. Garnet porphyroblasts are observed in it. It is observed as massive and foliated. Amphibolites are found in the forms of amphibolites, amphibole gneiss and garnet amphibolites. Amphibolites are composed of up to 90% of hornblende, plagioclase up to 25% of quartz to 15%, and epidote and zoisite are also found in them. Garnets in amphibolites are generally in the form of porphyroblasts (Fig. 13).

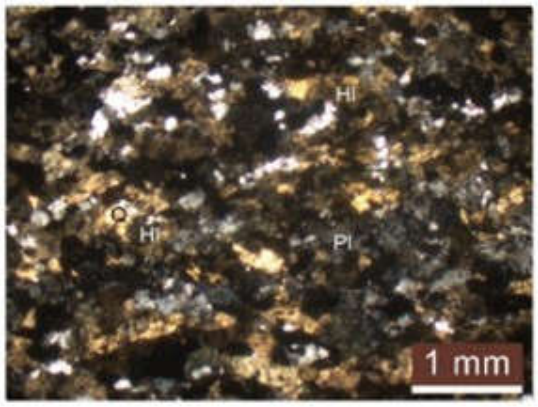

Fig. 13. Amphibole gneisses observed in the Sherdarwaza formation. // Nicol, Q: Quartz, Pl: Plagioclase, Hl: Hornblende

Marbles

They are white-yellow, cream, green-colored, and thick-bedded in the lower levels of the Sherdarwaza formation. Their thickness varies from a few meters to 50 meters. Their texture is granoblastic and their structure is massive, their composition is 75 to 99 percent of calcites and also in their composition serpentine (chrysotile) is observed at 3 to 4 percent and in some cases, apatite is also observed.

Biotite Gneisses

Biotite gneiss is widely observed within the Sherdarwaza formation. It is observed in the north of the Kabul Technical Institute, on Television Mountain, and Khair Khana. These biotite gneisses often contain more than 30% mica with a grain size large enough to be seen with the naked eye. The most common minerals of these gneisses are quartz and mica.

These gneisses are widely distributed within the Sherdarwaza formation, with thicknesses generally varying between 3 meters and 20-40 meters, and reaching up to 100 meters in some places.

Biotite gneiss usually contains biotite, but in some parts, garnet and muscovite are also found in their composition. Quartz (10-20), plagioclase (20-30), microcline (<10%), and also biotite (<10%) are observed in the composition of theses gneisses. These rocks have granoblastic and granolepidoblastic textures and show foliated structures. The secondary minerals in these gneisses are sphene, apatite, and zircon (Fig 14).

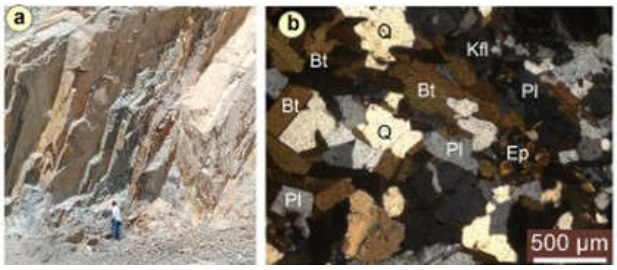

Fig. 14. Biotite gneisses observed in the Sherdarwaza formation. a: field photo, b: microscopic view, Q: Quartz, Bt: Biotite, Pl: Plagioclase, Ep: Epidot, Kfl: Potassium feldspar

Micachists

Schists related to Sherdarwaza formation are usually observed intermittently with biotite gneisses. These rocks have granolepidoblastic texture and show foliated structure. Mica schists usually contain biotite, and also in the composition of these schists: Quartz (20-30), plagioclase (5-10), microcline (<5%) and also biotite (10-20%) are observed (Fig. 15).

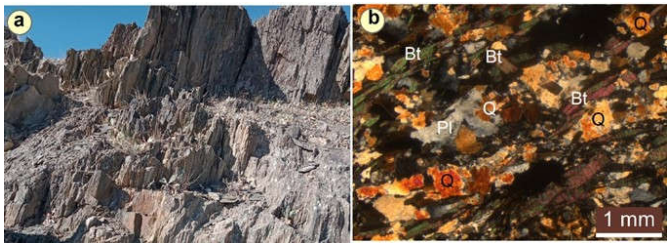

Fig. 15. Mica schists observed in the Sherdarwaza formation. a: field photo, b: microscopic view

Migmatite

Migmatites are observed in the Sakhi Pass valley, north of Kabul Polytechnic University, on Sherdarwaza Mountain near Takhnikam Institute. It was formed by the partial anatexis of gneisses. In migmatites, flebitic structure and folded structure are commonly observed (Fig. 16).

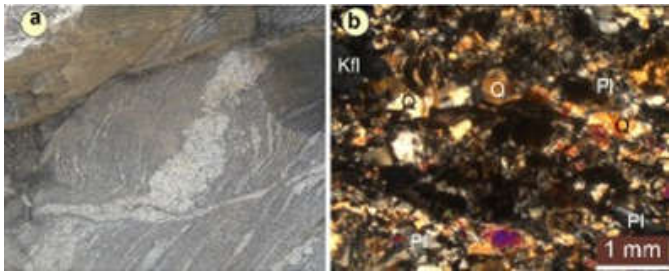

Fig. 16. Migmatite observed in the Sherdarwaza formation. a: field photo, b: microscopic view, Q: Quartz, Bt: Biotite , Pl: Plagioclase, Ep: Epidot, Kfl: Potassium feldspar

A.3. Alghoi Granitoids

Granitoids and granite formations were encountered in the study area, the largest of which was observed in the northern part of the region. These granitoids are observed in the Alghoi mountains and the Khair khana mountains It is also seen in Sherdarwaza and Afshar mountains. Some granite masses are also found in the Sherdarwaza formation and their dimensions vary, usually, from 10 to 100 square meter masses. These granites, which are surrounded by metamorphic in contact, contain coarse quartz, k-feldspar, plagioclase, biotite, and hornblende. Their contacts with the host rocks are conformable (Fig. 17).

These granites are dated as Archean by [12] but, based on field studies and their location among neighbouring rocks, their age can be determined as Mesoproterozoic (Fig. 17).

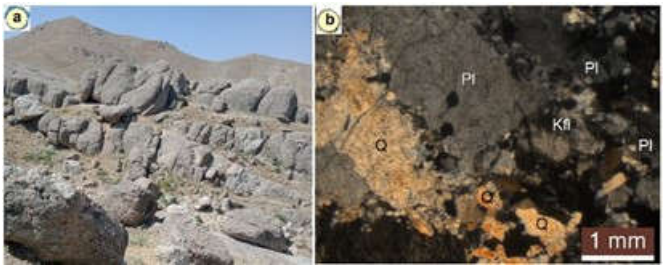

Fig. 17. Granite observed in the Sherdarwaza formation. a, field photo. b, microscopic view, Q: Quartz, Pl: Plagioclase, Kfl: potassium feldspar

A.4. Welayati formation

This formation is observed in the southern part of the study area. It was first named by [12]. This formation is widely observed in the mountains between the Kabul and Logar rivers. It is mostly seen in the Chehelston mountains, the Taraki mountains and the Siahbini mountains. In addition, the Welayati formation is observed in the Shakh-e-berentai mountains, where carbonate rocks belonging to the Khingel formation are observed. The age of this formation was stated as Neo-Proterozoic by [17]. The thickness of the formation is 3000 meters.

The Welayati formation consists of the lower part, which is generally composed of quartzites and their intercalation with schists and amphibolites (micaschist, garnet schist, quartzite, chlorite schist, amphibolite, amphibole schist, amphibole gneiss) and the upper part, which is commonly composed of schists (granite-staurolite schist, micaschist) be divided two sections. The Welayati formation, seen in the south and northeast of Kabul, overlies the Sherdarwaza formation harmoniously. The Welayati formation consists of garnet amphibolites and various crystalline schists including biotite schists, staurolite-garnet-biotite schists, muscovite-kyanite-garnet schists, and muscovite quartzites [25]. According to [17], this formation consists of schist at the base, amphibolite in the middle, and amphibolite-schist alternation at the top. Thus, the Welayati formation is divided into two parts: the lower part, which is generally composed of quartzites and alternating with schists and amphibolites, and the upper part, which consists of schists (Fig. 18 a, b and c).

The following lithologies are observed in the Welayati formation: Quartzite, amphibolites (amphibolite, garnet amphibolite) and amphibole gneisses, schists (garnet-staurolite schist, garnet-kyanite schist, mica schist, garnet-muscovite schist).

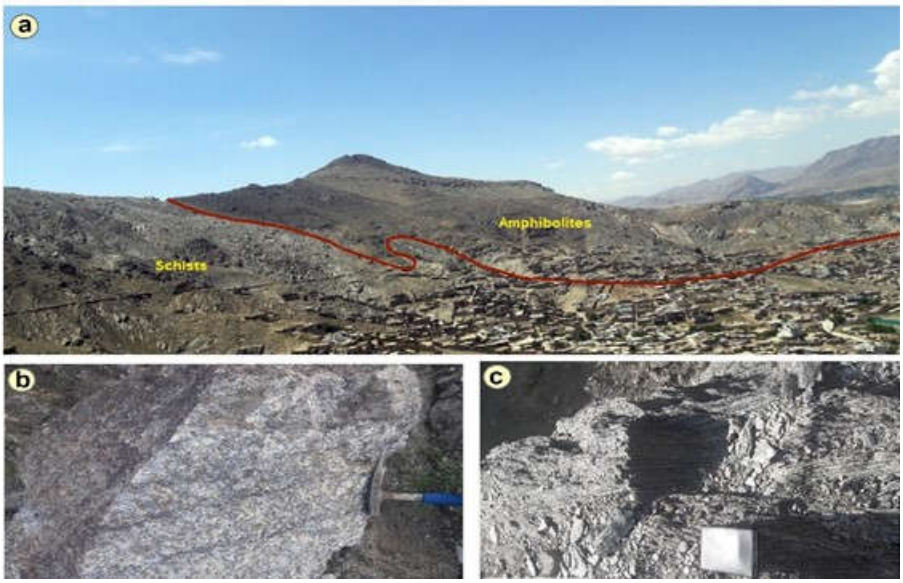

Fig. 18. a) Amphibolites and schists observed in the Welayeti formation, a) Amphibolite, b) Garnet-staurolite-schists, c) Micaschists. Location: Chehelston mountains

Amphibolite

Amphibolites are very common in the formation, and observed in the Chehelston Mountains as garnet amphibolites and amphibolschists. It is in contact with amphibolite schists (Fig. 18). The amphibolites associated with this formation can be divided into three groups. These are; amphibolites, garnet amphibolites and amphibole gneiss.

Garnet is not observed in some amphibolites. The mineral assemblage is amphibole dominated by plagioclase, quartz and opaque phases at the lower level. In some places, amphibole is partially replaced by chlorite or epidote.

These amphibolites make up 90% of Hornblende, including quartz and plagioclase, and are among the rare minerals like, epidote, rutile and magnetite observed.

Plagioclase forms lenticular or long xenoblastic grains. Quartz crystals have a very fine uniformity that seen in the matrix and inclusions. These amphibolites have a foliated structure and their texture is nematoblastic.

Garnet Amphibolite

Garnet-amphibolite samples are significantly coarser-grained than normal amphibolite ones. Garnets are usually observed as sub-idioblastic and hexagonal octagonal porphyroblasts. The garnet in amphibolite is highly eroded and has been partially replaced by chlorite and sometimes calcite. It contains abundant quartz and small feldspar inclusions showing poor alignment. Hornblende values go up to 80% and are mostly seen in prismatic form.

Amphibole Gneiss

The distinction between amphibolite and amphibole gneiss is made by the relative abundance of quartz and amphibole, with more quartz-rich called amphibole gneiss.

Schists

It is commonly observed in the Welayati formation. It is compatible with quartzites. In this formation, kyanite garnet staurolite schist, garnet-mica schist, kyanite garnet micaschist, garnet muscovite schist, chlorite schist, and mica-quartz schist were observed (Fig 19. c and d).

Kyanite garnet-staurolite schists are grey in colour and garnet porphyroblasts are very prominent. These schists are quite common in the formation.

Kyanite-Garnet-Staurolite Schist

Mica can be seen in field samples and brown garnet grains can also be seen. These rocks have a foliated structure and a granolipidoblast texture.

Staurolites are distinctly yellow in color and prismatic in shape and sometimes contain quartz and plagioclase inclusions (Fig.). in these schists, their ratio is up to 15%. They are usually seen as porphyroblasts. Generally, the presence of staurolite is seen together with kyanite.

Garnets are colourless to pale brownish yellow. These appear as xenoblastic sub-idioblastic and prismatic crystals. These garnets are observed as very large porphyroblasts. kyanite usually occurs in these schists as sub-idioblastic and prismatic crystals.

The Kyanite-Garnet-Staurolite Schist specimens are characterized by the presence of garnet and staurolite porphyroblasts, white mica and minor biotite (Fig 19. a and b).

The main minerals are quartz with accessory amounts of apatite, ilmenite and monazite. It is seen that porphyroblasts composed of plagioclase and biotite grow inordinately in foliation. Epidote is found in the inclusion phase of garnets and usually replaces plagioclase.

Garnet-Mica Schist and Kyanite-Garnet-Mica Schist

The matrix of the garnet-mica schist consists of quartz and plagioclase with minor amounts of apatite and tourmaline. Biotite occurs in green to dark green colours, most of them seen as prismatic and sup-idoblasts. In some cases, biotite has changed to chlorite. Feldspars are seen as plagioclase. Quartz, muscovite, biotite, garnet, sphene, rutile and opaque mineral inclusions are seen in plagioclase. Garnets are pale brownish yellow (Fig 19-c, d, e and f).

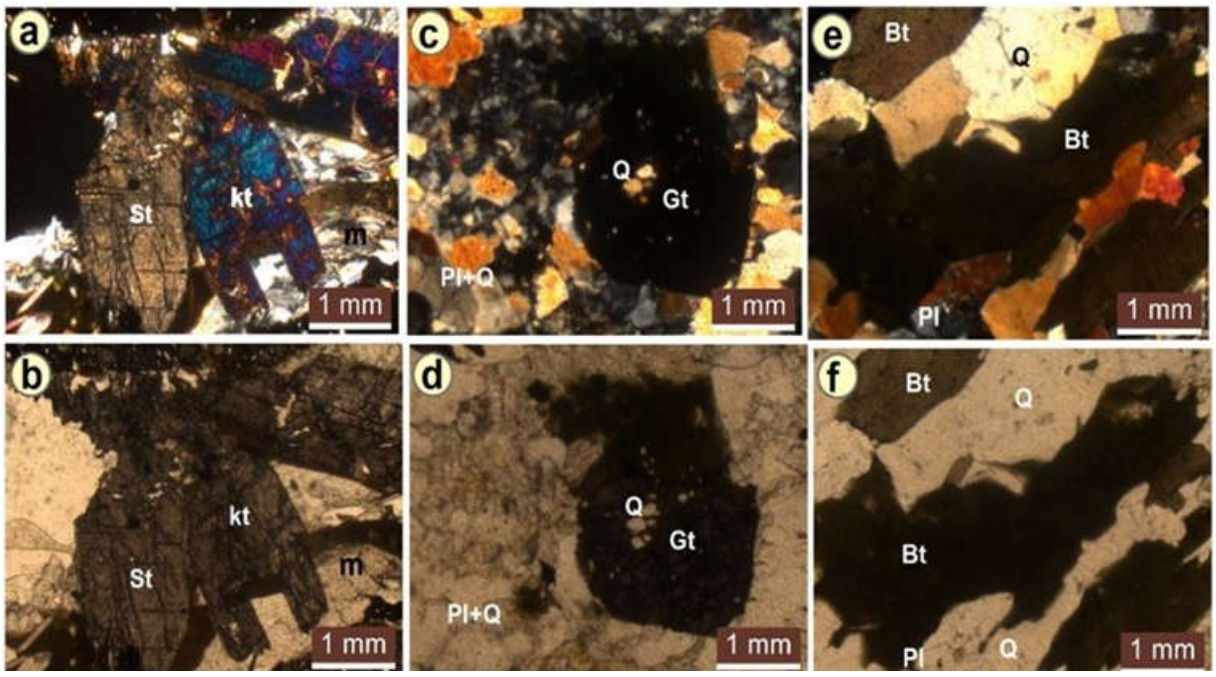

Fig 19. The microscopic view of different schist ralted to Welayeti formation, garnet perfiroblsts and kyanite and staurolite are seen, a, b) kyanite-garnet-staurolite mica schist, c, d) garnet mica schist, e, f) mica schist, a, c, e) //nicol, b, d, f) / nicol. St: staourolite, Gt: garnet, Pl: plagioclase, Q: quartz, Bt: biotite, kt: kyanite

These appear as xenoblastic sub-idioblastic and prismatic crystals. These garnets are sometimes very abundant and are observed as very large porphyroblasts. Garnet porphyroblasts are bordered by biotite, quartz chlorite and feldspar. Rutile seen as inclusions in both garnet and is often interbedded with or bordered by ilmenite.

Garnet-Muscovite Schist

Biotite is not seen in these schists, they contain up to 90% muscovite, quartz and plagioclase are also observed in their composition, garnet porphyroblasts are observed in the form of fabric, the spaces of which are usually filled with muscovite. These rocks have foliated structure and granolepidoblastic texture. Prismatic - short prismatic crystals consisting of tourmaline, apatite and zircon are observed.

V. DISCUSSION

Ref. [12] stated that the Kabul Block is composed of the lower Welayati formation and the overlying Sherdarwaza formation, and the Sherdarwaza formation with a thickness of about 5.5 km is predominantly composed of marble, amphibolite, quartzite, gneiss and migmatite. However, field and laboratory studies show that Sherdarwaza formation also has schist layers in its composition and is usually seen together with biotite-gneiss layers. In most cases, the schist structure has been preserved in biotite-gneiss layers and also granite masses with different dimensions up to 40 meters can be seen in this formation, which indicates the granitization process. Most of this granite is in contact with magmatites, which indicates that these granites are palingenetic formation and locally formed under the anatexis process.

Ref. [19] and [18] in their study on Kabul block stated that this Block is an elongate crustal fragment which cuts across the Afghan Central Blocks, adjoining the Indian and Eurasian continents. The granulite-facies assemblages are overprinted by a younger amphibolite-facies event that is characterized by the growth of garnet at the expense of the granulite-facies phases, but here we can also point out that granulite in Kabul Block are together with granite gneisses and it can be separated under one formation, granulites have been mineralized with different mineral composition, in some cases they are without garnet. The amount of plagioclase is higher in them. In the vast majority of them, orthopyroxenes are observed. Granulites is usually seen alternately with green and light layers. In some cases, the composition of granulites is very similar to that of quartz mangarites.

VI. CONCLUSION

Precambrian aged Kabul Block including metamorphic rocks take places at the base of the study area. The Neo-Proterozoic Welayati formation overlies the Paleo-Proterozoic Sherdarwaza formation with a tectonic contact, and they both overlay Khair Khana formation. In the region, Alghoi meta granitoid intruded into both Khair Khana and Sherdarwaza formations. Therefore, metamorphic rocks in the study area are divided in to four formations which are Khair Khana formation, Sherdarwaza formation, Alghoi meta granitoid and Welayeti formation. The Khair Khana formation consists of granulite, granitic gneiss, marble, amphibolite and amphibole gneiss. The Sherdarwaza formation consists of migmatite, biotite gneiss, marble, quartzite, amphibole gneiss, amphibolite and micashist. The Welayati formation consists of the lower part, which is generally composed of quartzites and their intercalation with schists and amphibolites (micaschist, garnet schist, quartzite, chlorite schist, amphibolite, amphibole schist, amphibole gneiss) and the upper part, which is commonly composed of schists (granite-staurolite schist, micaschist) be divided two sections. Algoi metagranitoid is composed of metagranites. The presence of granulites and granitic gneisses in Khair khana formation indicates the oldest formation in the study area. It shows the formation of granulite facies in the Kable Block, which is located under high temperature and pressure of the metamorphism process and also shows that this block is related to a segment of Columbia

and Rodinia supercontinents during Paleo-Proterozoic collisional events. On the other hand, migmatites indicate the melting process in the form of anataxis, which shows that the area has undergone the process of ultra-metamorphism and the granitization process has taken place.

Authors' Contributions

The authors' contributions to the paper are equal.

Statement of Conflicts of Interest

There is no conflict of interest between the authors.

Statement of Research and Publication Ethics

The authors declare that this study complies with Research and Publication Ethics

REFERENCES

[1] A. Kh Kafarsky, V. M., Chmyriov, K. F., Stazhilo-Alekseev, Sh. Abdullah, and V. S., Saikovsky, "Geological map of Afghanistan, scale 1:2,500,000," pp. 1-50, 1975.

[2] R. G. Bohannon, and K. J. Turner, "Geologic Map of Quadrangle 3468, Chak Wardak-Syahgerd (509) and Kabul (510) Quadrangles, Afghanistan," U.S. Geological Survey.pp. 1-10, 2007.

[3] N. H. Hayden, "The Geology of Northern Afghanistan," *Mern geol. Surv. India*, Calcutta, 39, 1, pp. 1-97, 1911.

[4] V. I. Slavin, *Structure of Afghanistan*, V knige: Mezhdunar sessiya redaktsionnikh komitetov tectonicheskikh kart Evropi, Blizhnego i Srednego Vostoka, Baku, 1945.

[5] J. Fischer, "Zur Geologie des Kohe-Safi bei Kabul (Afghanistan)," *N.Jb.Geol. Pal*., Stuttgart, 139, 3, 1971.

[6] G. Mennessier, "Nouvelles observations sur l'âge de la série de Kotagaé et les ultrabasites qui la surmontent, incidence sur la structure du fossé de Kaboul (Afghanistan occidental)," *Comptes rendus hebdomadaires des séances de l'Académie des sciences. Série D: Sciences naturelles,* vol. 282(17), pp. 1581–1583, 1976.

[7] H. Wittekindt, D. Weippert, S. Gratsch, L. L. Hentschke, F. R. Nezam, H. J. Nicksch, and E. Z. Wintzscher, "Geological map of Central and Southern Afghanistan," Deutsche Geologische Mission in Afghanistan, Bundesanstalt für Bodenforschung, pp.12-23, 1969.

[8] J. Ilavský, and J. Kantor, "Prispevok ku geochronologii sirsieho okolia Kabilu (Afghanistan)," *Geologické Prace*, vol. 37, pp. 65–90, 1965.

[9] V. G. Silkin, and I. A. Gusev, "Geology and minerals in the northern part of the Kabul Massif," Report of the Andreskan team on the work in 1975, Kabul. Rec. Off DGMS, 1976.

[10] V. I. Slavin, T. O. Federov and N. M. Feruz, "The geology and age of the metamorphic complex in the Kabil district," *Vestnik Moskovskogo Universiteta*, Moscow, pp. 123-340, 1972.

[11] J. Boulin, "Hercynian and Eocimmerian events in Afghanistan and adjoining regions," *Tectono-physics*, vol. 148(3), pp. 253–278, 1988.

[12] S. S. Karapetov, Yu. A. Sorokin, Yu. N. Sytov, V. F. Chepela, Sh. Abdullah, and A. Ashmat, "Geological structure of Kabul town region," Report of Logar and Helmand prospecting-mapping group in 1979-1981, Unpublished Report, Afghan Geological Survey, pp. 10-60, 1981.

[13] P. Tapponnier, M. Mattauer, F. Proust, and C. Cassaigneau, "Mesozoic ophiolites, sutures, and Large-scale tectonic movements in Afghanistan," *Earth Planet Sci. Lett.,* vol. 52(2), pp. 355–371, 1981.

[14] P. J. Treloar, and C. N. Izatt, "Tectonics of the Himalayan collision between the Indian plate and the Afghan block: A synthesis," *Geol. Soc. Lond. Spec. Publ.,* vol. 74, pp. 69–87, 1993.

[15] S. G. Peters, S. Ludington, G. J. Orris, D. M. Sutphin, J. D. Bliss, and J. J. Rytuba, "Preliminary Non-Fuel Mineral Resource Assessment of Afghanistan 2007," Geological Survey (US), No: 2007-1214, 045-178, 2007.

[16] R. G. Bohannon, R.G., 2010, "Geologic and Topographic Maps of the Kabil North 30 × 60 Quadrangle. Afghanistan," US Department of the Interior, US Geological Survey, pp.1-110.2010.

[17] S. Collett, S. W. Faryad, and A. M. Mosazai, "Polymetamorphic evolution of the granulite facies Paleo-Proterozoic basement of the Kabil Block, Afghanistan," *Mineralogy and Petrology*, pp. 1-22, 2015.

[18] S. Collett, S., and S. W. Faryad, "Pressure-temperature evolution of Neoproterozoic metamorphism in the Welayati Formation (Kabil Block), Afghanistan," *Journal of Asian Earth Sciences*, vol. 111, pp. 698–710, 2015.

[19] S. W. Faryad, S. Collett, F. Finger, S. A. Sergeev, R. Čopjaková, and P. Siman, "The Kabul Block (Afghanistan), a segment of the Columbia Supercontinent, with a Neoproterozoic metamorphic overprint," *Gondwana Research*, vol. 34, pp. 221–240, 2016.

[20] J. Boulin, "Neocimmerian events in central and western Afghanistan," *Tectonophysics,* vol. 175(4), pp. 285–315, 1990.

[21] A. C. Şengör, "The Cimmeride orogenic system and the tectonics of Eurasia," *Geological Society of America Special Papers*, vol. 195, pp. 1–74, 1984.

[22] J. Boulin, "Structures in Southwest Asia and evolution of the eastern Tethys," *Tectonophysics,* vol. 196, pp. 211–268, 1991.

[23] M. E. Brookfield, and A. Hashmat, "The geology and petroleum potential of the North Afghan platform and adjacent areas (northernAfghanistan, with parts of southern Turkmenistan, Uzbekistan and Tajikistan)," *Earth Sci. Rev.,* vol. 55(1), pp. 41–71, 2001.

[24] G. Andritzký, "Bau und Entstehungsgeschichte des Altkristallin-Keils von Kabil (Afghanistan) und seiner Randzonen," *Geol. Jahrb.,* vol. 84, pp. 617–636, 1967.

[25] S. H. Abdullah, and V. M. Chmyriov, *Geologiya I poleznye iskopaemye Afganistana*, Kniga 1. *Nedra, Geologiy*, Moscow, 535 p., 1977.

[26] Beck, R.A., Burbank, D.W., W.J., Sercombe, M.A. Khan, and R.D., Lawrence, "Late cretaceous ophiolite obduction and Paleocene India-Asia collision in the western most Himalaya". *Geodinamica,* pp.12-27, 1996.

[27] N. Ambraseys, and R. Bilham, "Earthquakes in Afghanistan," March 2003, Seismological Researc Letters, 74(2), 107-123.

[28] J., Crone, Earthquakes Pose a Serious Hazard in Afghanistan. USGS Fact Sheet*,* 2007–3027, pp.1-4. 2007.

[29] H., Moiny, S.W., Faryad, R. Čopjakova, and R., Jedlicka, "Multi-stage metamorphism by progressive accretion of continental blocks, example from the Western Hindu Kush." *Journal of Metamorphic Geology*, 1-25. 2020.

[30] Lawrence, R.D., Khan, S.H. and Nakata, T., "Chaman fault, Pakistan-Afghanistan," In: Major active faults of the world—Results of IGCP project 206. *Special Issue Supplement to Annales Tectonicae*, 6, pp. 196–223, 1992.

[31] S. W. Faryad, S. Collett, M. Petterson, and S. A. Sergeev, "Magmatism and metamorphism linked to the accretion of continental blocks south of the Hindu Kush, Afghanistan," *Lithos*, 175–176, 302–314, 2013.

[32] J., Stocklin, "Structural correlation of the Alpine ranges between Iran and Central Asia." *Memoire Hors-Serve,* 8, pp.333–353, 1977.

[33] F. Debon, H. Afzali, P. Le-Fort, and J. Sonet, "Major intrusive stages in Afghanistan: Typology, age and geodynamic setting," *Geol Rundschau,* vol. 76, pp. 245–264, 1987.

[34] S. Collett, "Crustal evolution in the Paleoproterozoic of Afghanistan: Insights from the Sherdarwaza gneiss of the Kabil Block," Masters Dissertation, University of Leicester, 2011.

[35] T. H. Torsvik, M. A. Smethurst, J. G. Meert, R. VanderVoo, W. S. McKerrow, M. D. Brasier, B. A. Sturt, and H. Walderhaug, "Continental breakup and collision in the Neoproterozoic and Phanerozoic-A tale of Baltica and Laurentia," *Earth-Science Reviews,* vol. 40, pp. 229–258, 1996.

[36] P. F. Hoffman, A. J. Kaufman, G. P. Halverson, and D. P. Schrag, "A Neoproterozoic snowball earth," *Science,* vol. 281(5381), pp. 1342–1346, 1998.

[37] J. Meert, "Paleomagnetic Evidence for a Paleo-Mesoproterozoic Supercontinent Columbia," *Gondwana Research,* vol. 5, pp. 207–215, 2002.

[38] J. J. Rogers, M. Santosh, "Configuration of Columbia, a Mesoproterozoic supercontinent," *Gondwana Research,* vol. 5(1), pp. 5–22, 2002.

[39] G. Zhao, P. A. Cawood, S. A. Wilde, and M. Sun, "Review of global 2.1–1.8 Ga orogens: implications for a pre-Rodinia supercontinent" *Earth-Science Reviews,* vol. 59(1), pp. 125–162, 2002.

[40] K. C. Condie, "Supercontinents, superplumes and continental growth: the Neoproterozoic record," *Geological Society*, *Special Publications*, London, vol. 206(1), pp. 1–21, 2003.

[41] S. A. Pisarevsky, K. Thrane, and V. Vernikovsky, "Assembly, configuration, and break-up history of Rodinia: a synthesis," *Precambrian Research,* vol. 160(1), pp. 179–210, 2008.

[42] G. Zhao, M. Sun, S. A. Wilde, and S. Li, "A Paleo-Mesoproterozoic supercontinent: assembly, growth and breakup*," Earth-Science Reviews,* vol. 67(1), pp. 91–123, 2004.

[43] Li, Z.X., Bogdanova, S.V., Collins, A.S., Davidson, A., De Waele, B., Ernst, R.E., Fitzsimons, I.C.W., Fuck, R.A., Gladkochub, D.P., Jacobs, J., Karlstrom, K.E., Lu, S., Natapov, L.M., Pease, V., Pisarevsky, S.A.,

Thrane, K. and Vernikovsky, V., "Assembly, configuration, and break-up history of Rodinia: a synthesis." *Precambrian Research,* 160(1), pp.179–210, 2008.

[44] J. Meert, "Strange attractors, spiritual interlopers and lonely wanderers: The search for pre-Pangean supercontinents," *Geoscience Frontiers,* vol. 5, pp. 155–166, 2014.

[45] G. M. Stampfli, J. F. von Raumer, and G. D. Borel, "Paleozoic evolution of pre-Variscan terranes: from Gondwana to the Variscan collision," *Special Papers-Geological Society of Americapp*., pp. 263–280, 2002.